Course CTB3350

Open Channel Flow

February 2014

Faculty of Civil Engineering and Geosciences

J. A. Battjes
R. J. Labeur

TU Delft Delft University of Technology
Artikelnummer 06917290048

Contents

Chapter 1

Introduction

1.1 Subject

Many natural or technical systems for flow of water, such as rivers and tidal channels or irrigation canals and pipelines, are quite elongated, i.e. they have characteristic lengths that far exceed the lateral dimensions of width, depth or diameter. Such systems can be referred to as 'conduits'. The description and mathematical modeling of the **unsteady flow in conduits** is the subject of this course. The emphasis is on **free surface flow**, mainly in open channels (free surface flows are also common in sewage systems), but occasionally we will deal with **pressurized flow** in closed conduits.

Steady flow in conduits has been dealt with in the introductory course Fluid Mechanics (CTB2110), both free-surface flows and pressurized flows. Such flows occur when the geometry of the conduit is fixed and when the boundary conditions, such as the discharge from upstream or the downstream water level, do not vary in time. Steady flows can locally vary rapidly in space due to local forcing, e.g. flow over a weir. Except for these, steady free-surface flows are uniform or they vary gradually lengthwise; the corresponding longitudinal free surface profiles are the so-called backwater curves. These have been dealt with in the preceding course Fluid Mechanics. The present course extends this to **unsteady flows**.

Flow in a conduit will be unsteady when the boundary conditions are changing in time. One can think of flood waves in rivers, which reflect the temporal variations in the run-off due to rainfall or melting of snow in the catchment area, or the tides in estuaries and lower river reaches in response to the tidal water level variations at sea. The description and mathematical modeling of such unsteady flows in conduits is the main subject of this course (Chapters 2 through 9). Away from local disturbances, these flows are **gradually varying**. Because they are also unsteady, they belong to the category of the so-called **long waves**, which can be considered as the unsteady counterparts of backwater curves. Long waves belong to the category of **gravity waves**, so called because these derive their potential energy, and therefore their restoring force, to the action of gravity.

In order to regulate the water level and/or the discharge in conduits, **control structures** are built such as weirs and gated inlet structures. These cause strong variations in flow depth and velocity over a short distance, in other words, one deals here with **rapidly varying flow**. Control structures divide a conduit in separate compartments, with different values of water level and/or discharge on the upstream side and the downstream side. These values in turn serve as boundary conditions for the adjacent reaches. For the design and operation of control stuctures, one should be able to calculate the flow in/through/over them. This subject is introduced in Chapter 10. The functional and structural design of control structures is covered in follow-up hydraulic engineering courses.

Conduits convey not only water but dissolved or suspended matter, and heat, as well. Knowledge of these **transport processes** is essential for management of water quality, sedimentation or erosion, etc. This subject is introduced in Chapter 11, as the third and last subject to be dealt with in this course.

1.2 Aim

It is important to be aware of the various flow types and associated problems that can be expected in the context of design and operation of hydraulic engineeering works (e.g. construction of control structures, dredging, damming) in tidal areas, rivers, canals etc. The engineer should have insight in these flows and be able to schematize them, quantify them through mathematical modeling and computations, and interpret the results. He or she should be able to foresee consequences of the works being designed, both qualitatively and quantitatively. The present course deals with the description and analysis of these flow phenomena, providing oversight and insight, and it gives an introduction to various solution methods.

Simplified models are well suited to study the overall behavior of water systems. They provide insight in the main features of the flow, which is invaluable in assessing the dynamics of water systems and in predicting their response to construction works or management strategies.

Still, most engineering applications require a higher level of detail than can be provided by these simplified models. In practice, ready-to-use software packages are available for the numerical computation of various kinds of flows in conduits. These models require fewer assumptions and also allow the treatment of complex geometries. Follow-up courses on numerical methods treat the design of the necessary algorithms.

The present course precedes these, by presenting some simple numerical examples in the context of the flow types treated in this course. The examples are based on Python, a high level programming language. The type of numerical model we present holds somewhere between simple analytical models and full fledged computer packages. In this way Python will provide a simple-to-use tool which nevertheless reaches far beyond the possibilities of the traditional pocket calculator.

Irrespective of the type of computer model used, the numbers they provide need further interpretation and analyses. They should therefore be used alongside analytical models in order to obtain insight and to estimate effects in order of magnitude. The overall system behavior should be studied first by analytical modeling and computed in more detail later using a numerical model. The analytical results may be used to verify whether the numerical model preserves the principal dynamics of the flow. This will warrant a critical usage of numerical software packages and a qualitative evaluation and interpretation of the results obtained with these.

In view of the above, the learning goals of this course can be summarized as follows:

- to gain qualitative knowledge of various kinds of unsteady flow in open channels or pipelines that are important in civil engineering practice;
- to acquire insight in the dynamics of these flows;
- to develop an attitude of always making a (qualitative) problem analysis including the estimation of relevant effects;
- to acquire knowledge of various mathematical approximations and solution methods and their limitations;
- to acquire the ability to make schematizations and to perform approximative calculations for the flow phenomena considered;
- to acquire basic programming skills for computing and visualizing solutions of problems dealt with in his course.

1.3 Approach

The main attention is given to unsteady free-surface flows with a characteristic length scale that is far greater than the depth, the so-called **long waves**. Tides, storm surges and flood waves in rivers provide good examples of this category (contrary to ship waves or wind-generated waves, whose lengths are usually not large or even small compared to the depth). Moreover, we restrict ourselves to laterally confined flows in so-called conduits, such as tidal channels and rivers, in which the main flow direction is determined beforehand by the geometry of the boundary, which may be assumed to be given beforehand. (This does not apply to long-term computations including morphological changes to simulate phenomena such as meandering of rivers.) In these cases, the flow direction is known so that only the flow intensity (the discharge, say) is to be solved for, in addition to the water surface elevation.

An example of such a situation is the Western Scheldt estuary, a tidal region in the southern part of The Netherlands. The geometry of this estuary, shown in Figure 1.1, is quiet complex. The main tidal channels (dark blue color tones) are separated by large tidal flats (reddish tones) and connected by numerous short-cut channels (light blue's). Yet, the bulk of the tidal flow is aligned with the orientation of the main channels and therefore leads to an approximately one-dimensional system behavior.

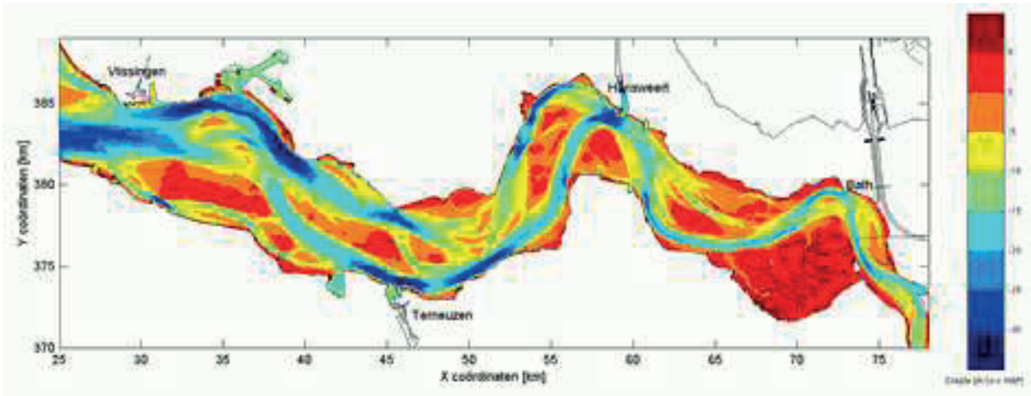

Figure 1.1: Geometry and bottom contours of the Western Scheldt estuary

As expressed by their name, long waves are characterized by length dimensions that far exceed the depths. This implies that the curvature of the streamlines in the vertical plane is negligible, for which reason we can assume a **hydrostatic pressure distribution** in the vertical. Stated another way: all points of a given vertical share a common piezometric level, which - as defined below - lies in the instantaneous local free surface. This greatly simplifies the schematization and the calculations.

In bends, streamlines can have significant curvature in the horizontal plane. The piezometric level and therefore the free surface elevation then vary laterally, being higher at the outer bank and lower at the inner bank. This is essential in detailed computations of the flow in bends, but it is irrelevant for the large-scale computations with which we are concerned. So we will ignore lateral variations in surface elevation. In other words, we assume that the pressure distribution is fully hydrostatic, not only vertically but horizontally as well. This approximation implies that at each instant **all points of a given cross-section have a common piezometric level** coinciding with the local free surface, which is assumed horizontal in the cross-section. The height of this level above the adopted reference plane $z = 0$ is designated as h. This quantity is a function of the downstream coordinate s (measured along the axis of the conduit) and the time t, or $h = h(s, t)$.

Because in this approximation the piezometric level (h) is uniform in the entire cross-section, the same applies to the downstream pressure gradient driving the flow. It is therefore feasible to work with **cross-sectionally integrated flow velocities** (i.e. the total discharge Q), instead of the point values of the velocities within each cross-section.

Summarizing, we have two dependent variables (h and Q) which have to be determined as functions of the longitudinal coordinate and time:

$$\boxed{h = h(s, t) \quad \text{and} \quad Q = Q(s, t)}$$

This requires a so-called **one-dimensional flow model**, typified by the dependence on only one space coordinate.

The assumption of gradually varying flows was at the basis of the one-dimensional flow model. This assumption is not valid for the **rapidly varying flow** near local structures, constrictions etc., where the pressu re is far from hydrostatic and the point flow velocities have unknown and widely varying directions and magnitudes. The calculation of these flows requires **two-dimensional** or even **three-dimensional models**. Because these flows vary rapidly in space, the time variation is usually minor compared to the spatial variatons. This allows the approximation that the flow 'has no memory', i.e. at each instant it is fully adapted to the instantaneous boundary conditions (**quasi-steady approximation**).

Finally, the treatment of **transport processes** rests on the assumption that these are **passive**, i.e. the transported substances or heat do not affect the flow (their possible influence on the (bulk) mass density and viscosity is ignored). This is allowed only for low concentrations and mild temperature variations, respectively.

1.4 Layout

The basic equations for fluid flow which are taken as the starting point for the analysis and calculation of long waves in conduits are presented in Chapter 2. Chapter 3 describes several characteristic long-wave phenomena qualitatively and it presents a quantitative analysis of the major characteristics, making visible which processes are dominant and which ones are relatively weak. This is elaborated in the Chapters 4 through 9 where suitable mathematical approximations are presented for each major class of long waves separately. Corresponding solution techniques and solutions are presented as well. This is done for a sequence of flow types of increasing relative influence of bed friction, varying from the almost frictionless so-called translatory waves (Chapters 4 - 6) to flood waves in rivers, which are friction dominated (Chapter 9). Between these, Chapter 7 deals with oscillations in basins and Chapter 8 with propagation of tides. Tides are of a mixed character in which resistance is important but not dominant. Subsequently, Chapter 10 gives brief considerations on rapidly varying flow in and around control structures. Chapter 11 concludes with an introduction to the modelling of transport processes.

1.5 Prerequisites and course structure

These lecture notes form the basis of the course **Open Channel Flow** (CTB-3350, 4 ECTS). *The sections in these notes dealing with numerical modeling are not a part of the present course CTB-3350. Also, they are not yet complete.*

Shallow water flow has been studied extensively since the inception of the underlying equations by De Saint Venant in 1871, which is reflected in a vast amount of literature on this subject. This course presents a selection of topics that are particularly relevant for civil engineers dealing with flow problems in shallow water environments and pipe systems. For further reading and self study some useful textbooks are listed in the bibliography below.

The treatment of the various subjects in this course relies on a basic understanding of the following topics from calculus and introductory fluid mechanics:

- ordinary - and partial differential equations
- complex algebra
- balance equations for fluids
- free surface flows

In turn, the contents of this course will be useful, if not necessary, for the MSc courses Computational Modeling of Flow and Transport, Wind Waves, Turbulence and Oceanography.

The course comprises the following educational activities:

- lecture series (24×90 min.)
- demonstrations
- MAPLE TA exercises
- written exam

During lectures the theory will be explained and practical applications will be given. Occasionally, theoretical results will be elucidated and verified using the flume in the lecture hall. By means of exercises of increasing complexity, the principal content will be rehearsed systematically during the lectures, in preparation for the exam. Besides this, and with the same purpose, a series of four individual MAPLE TA tests has to be passed before the exam may be attended. After enrollment, they can be activated from Blackboard. The final exam (180 min.) consists of four assignments. Further information (including a time schedule) and various study materials can be found on Blackboard.

Bibliography

[1] M. B. Abbott and D. R. Basco. **Computational fluid dynamics: an introduction to engineers**. Longman, 1989.

[2] H. Chanson. **The hydraulics of open channel flow**. Arnold, Londen, 1999.

[3] M. Chaudry. **Open channel flow**. McGraw-Hill, New York, 1993.

[4] Ven Te Chow. **Open-channel hydraulics**. McGraw-Hill, New York, 1959.

[5] J. J. Dronkers. **Tidal computations in rivers and coastal waters**. North-Holland Publishing Company, 1964.

[6] J. A. Fox. **Transient flow in pipes, open channels and sewers**. Ellis Horwood, Chichester, 1989.

[7] P. Ph. Jansen, L. Van Bendegom, J. Van den Berg, M. De Vries, and A. Zanen. **Principles of river engineering: the non-tidal alluvial river**. Delftse Uitgevers Maatschappij, 1994.

[8] R. S. Johnson. **A modern introduction to the mathematical theory of water waves**. Cambridge University Press, 1997.

[9] B. Le Méhauté. **An introduction to hydrodynamics and water waves**. Springer-Verlag, 1976.

[10] H. H. G. Savenije. **Tides and salinity in alluvial estuaries**. Elsevier, Amsterdam, 2005.

[11] J. J. Stoker. **Water waves**. Interscience Publishers, New York, 1957.

[12] J. M. Tanguy, editor. **Environmental Hydraulics**. 1-5. Wiley, 2010.

[13] Open University Course Team. **Waves, tides and shallow-water processes**. The Open University, 1999.

[14] A. R. D. Thorley. **Fluid transients in pipeline systems**. D and L George, 1991.

[15] C. B. Vreugdenhil. **Numerical methods for shallow water flow**. Kluwer, Dordrecht, 1994.

[16] G. B. Whitham. **Linear and nonlinear waves**. Wiley, New York, 1974.

[17] O. C. Zienkiewicz. **The finite element method for fluid dynamics**. Elsevier Butterworth-Heinemann, 2005.

[18] M. Zijlema. Computational Modelling of Flow and Transport, Course reader CIE4340, 2012.

Problems

1. What is *the* defining property of long waves?

2. Mention several wave types having this property.

3. Also mention several wave types *not* having this property.

4. Which assumptions form the basis of one-dimensional models for long waves?

5. Which are the dependent and independent variables in such models?

6. What can one-dimensional long wave models be used for in practice?

7. Point out some differences between mathematical analyses and numerical modeling.

8. Why is it still important to use simplified mathematical models, despite numerical models being available?

Chapter 2

Basic equations for long waves

This chapter presents the derivation of the basic equations that we will use in analyses and calculations of unsteady flows, first for free surface flows in natural channels, e.g. tidal or fluvial channels, artificial canals, and the like, and subsequently for pressurized flows in closed conduits. In both cases we deal with a mass balance and a momentum balance integrated across the entire flow cross-section, assuming a hydrostatic pressure distribution.

2.1 Free surface flows

Notation and control volume

An important variable in our modelling of the flow is the so-called piezometric level, defined as $h \equiv z + (p - p_{\rm atm})/\rho g$, in which z is the elevation above the chosen horizontal reference plane $z = 0$, p is the fluid pressure at the height z above the reference plane, $p_{\rm atm}$ is the atmospheric pressure at the free surface, assumed to be constant, ρ is the fluid mass density and g is the gravitational acceleration. The assumption of a hydrostatic pressure distribution in each cross-section of the flow implies that at each instant all points in a cross-section share a common piezometric level, which, defined as above, coincides with the local free surface. In other words, under the assumption of hydrostaticity, h also represents the height of the free surface above the reference plane. We use a length coordinate s along a streamwise axis which may be weakly curved and gently sloping. The longitudinal slope of the bed ($\tan\beta$), if nonzero, is assumed to be very small, allowing the approximations $\tan\beta \approx \sin\beta \approx \beta$ and $\cos\beta \approx 1$.

We consider a control volume consisting of a cross-slice of a water course with an arbitray cross-section, with length Δs, containing the entire wet area of the cross-section, from bed to free surface. See Figures 2.1 and 2.2, which also indicate some other symbols such as B for the width of the free surface, P for the length of the wetted perimeter and A for the wet cross-sectional area.

There are situations where only a part of the wetted cross-section contributes significantly to the conveyance. A typical example is provided by a river with a sequence of groins normal

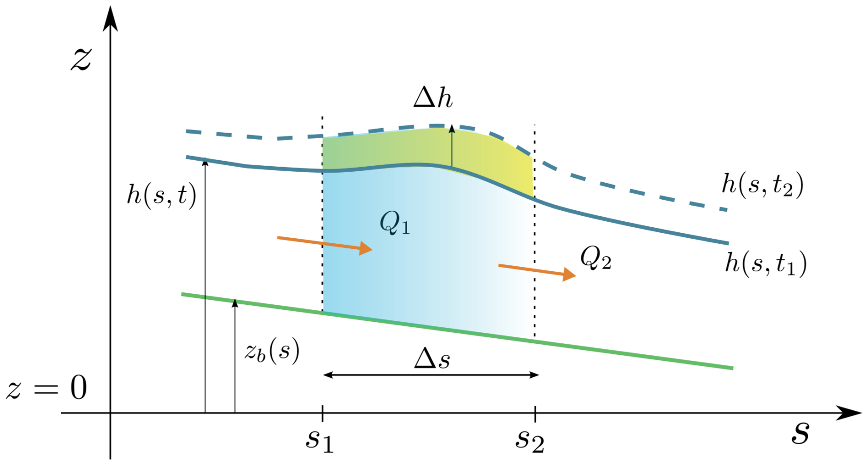

Figure 2.1: Longitudinal transect open conduit

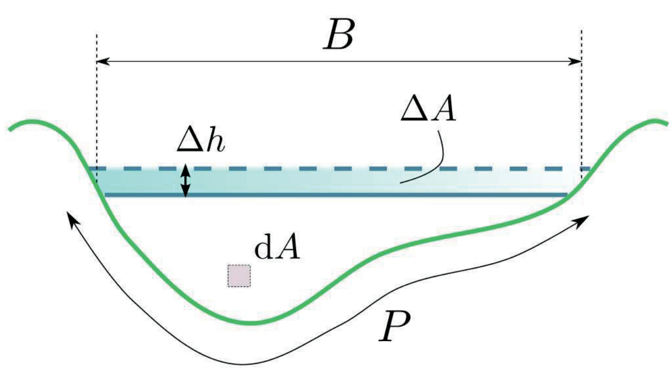

Figure 2.2: Cross-section open conduit

to the flow, where the spaces between adjacent groins do contribute to the storage capacity but - in case of low or moderate water levels - not to the conveyance capacity. In those cases it is necessary to distinguish between these two functions. We designate the surface area, surface width and mean depth of the conveyance cross-section as A_c, B_c and d respectively, where $d = A_c/B_c$. It will be clearly indicated where we use the distinction between the total cross-section and that of the conveyance part.

Conservation of mass

Pressure variations in open channels are very limited because of the presence of a free surface. Therefore, we can neglect pressure-induced density variations. The water can then be considered as **incompressible**. In that case, the mass balance reduces to a **volume balance**, also called the **continuity equation**. To derive it, we consider the change in the volume of water in the control volume in a short time interval from $t = t_1$ to $t = t_2 = t_1 + \Delta t$.

The flux or discharge Q is defined as the volume of water passing a given cross-section in a unit of time:

$$Q = \int_{A_c} u_s \, \mathrm{d}A \tag{2.1}$$

in which u_s is the streamwise velocity in a point. We also define the mean velocity $U = Q/A_c$, i.e. the streamwise velocity averaged over the conveyance cross-section.

The net influx of volume into the control volume in the considered short time interval with duration Δt is

$$Q_1 \, \Delta t - Q_2 \, \Delta t = (Q_1 - Q_2) \, \Delta t = -\Delta Q \, \Delta t \tag{2.2}$$

Suppose this is positive, i.e. there is more inflow than outflow. The difference is stored in the control volume, giving rise to an increase of the stored volume equal to $\Delta V = \Delta A \Delta s$ (see Figure 2.1). Equating this storage to the net inflow yields $\Delta A \, \Delta s = -\Delta Q \, \Delta t$. Dividing by Δt and Δs, and taking the limit for $\Delta t \to 0$ $U = Q/A_c$ and $\Delta s \to 0$, yields

$$\boxed{\frac{\partial A}{\partial t} + \frac{\partial Q}{\partial s} = 0} \tag{2.3}$$

Using the width B of the free surface (not only that of the conveyance area) gives $\Delta A = B \Delta h$ (Figure 2.1), with which Equation (2.3) can be written as

$$\boxed{B \frac{\partial h}{\partial t} + \frac{\partial Q}{\partial s} = 0} \tag{2.4}$$

For given geometry of the cross-section, which may vary with the downstream location s, the free surface width B varies with time in a known manner through the time variation of h: $B = B\,(s, h\,(s,t))$. Therefore, Equation (2.4), expressing mass conservation for the water (considered incompressible), is our first equation linking variations of the two unknowns Q and h. The second one, to be derived in the following, expresses momentum conservation.

Conservation of momentum

The formulation of Newton's second law for a slice of water in the conduit leads to an equation for the dynamics of the flow, a so-called **equation of motion**. This can vary in appearance, partly because the formulation can be cast in acceleration form or in conservation form (see the Appendix to this chapter). Below, we start with the acceleration form.

Apart from the differences in appearance referred to above, different physical processes can play a role. However, in all cases there is a **balance between inertia, forcing and resistance**, where each of these in turn can consist of a number of contributions. It is important to be aware of this, and to check the meaning of the various terms when writing or reading an equation of motion. It is also important to check whether one or more terms is negligible compared to another (in an equation consisting of three or more terms). We return to this extensively in Chapter 3.

We start from Euler's equation for the acceleration in the flow direction ($\mathrm{D}u_s/\mathrm{D}t$) of a fluid particle of an ideal (inviscid) fluid of constant density (ρ) under the action of gravity (with potential gz) and pressure (p):

$$\frac{\mathrm{D}u_s}{\mathrm{D}t} = -\frac{\partial\left(gz + p/\rho\right)}{\partial s} \tag{2.5}$$

in which u_s is the streamwise particle velocity at an arbitrary point in the cross-section. In terms of the piezometric level h, Equation (2.5) becomes

$$\frac{\mathrm{D}u_s}{\mathrm{D}t} = -g\frac{\partial h}{\partial s} \tag{2.6}$$

The right-hand side of Equation (2.6) is the **forcing** in the s-direction per unit mass as a result of the **slope of the free surface**. It expresses the combined effect of gravity and the fluid pressure gradient. It is important to realize that this gradient, and therefore the forcing, is uniform in the cross-section, within the hydrostatic pressure approximation. This is illustrated in Figure 2.3, showing a slice of water. At a given elevation, the slope of the water surface gives rise to different pressures at both sides of the slice, but in case of hydrostatic pressure, the difference δp is constant over the vertical. Expressed mathematically: $\partial\left(\delta p\right)/\partial z = 0$. This implies that the right hand side of Eq. (2.6) is vertically uniform. Neglecting centrifugal effects in bends, it is also laterally uniform. Because the forcing is

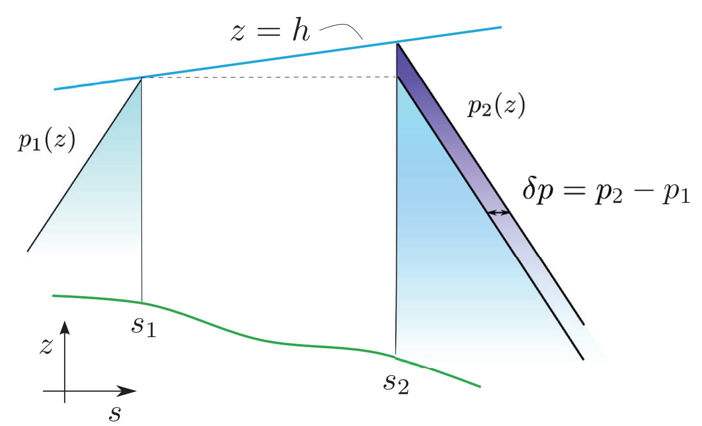

Figure 2.3: Hydrostatic pressure and net horizontal forcing

uniform across the cross-section, so is the local particle acceleration, except for the effect of internal flow resistance, which was ignored in Equation (2.6). To account for this, we are going to apply Equation (2.6) to the cross-sectionally averaged flow velocity U, with the addition of a boundary resistance term.

We express the **resistance** experienced by the water in the slice considered in Figure 2.1 as $\Delta W = \tau P \Delta s$, in which Δs is the length of the slice, P is the perimeter of the cross-section that contributes to the resistance, and τ is the corresponding averaged resistance per unit area of wetted boundary (comparable but not equal to a boundary shear stress, as we will see below). The resistance per unit mass then equals $\Delta W/(\rho A_c \Delta s)$ or $\tau/\rho R$, in which $R = A_c/P$ is the so-called **hydraulic radius** of the conveyance cross-section. Adding this to the right-hand side of Equation (2.6), written for the cross-sectionally averaged velocity U, yields the following **balance between inertia, forcing and resistance**:

$$\frac{\mathrm{D}U}{\mathrm{D}t} + g\frac{\partial h}{\partial s} + \frac{\tau}{\rho R} = 0 \tag{2.7}$$

We will elaborate on this equation. The total acceleration ($\mathrm{D}U/\mathrm{D}t$) is expanded into the local contribution ($\partial U/\partial t$) and the advective contribution ($U\partial U/\partial s$), and the averaged resistance per unit area is written as

$$\tau = c_f \rho |U| U \tag{2.8}$$

in which c_f is a dimensionless resistance coefficient (representing not only bed shear stress as such but also net effects of form resistance due to dunes or other abrupt profile variations). Substituting this in Equation (2.7) yields

$$\frac{\partial U}{\partial t} + U\frac{\partial U}{\partial s} + g\frac{\partial h}{\partial s} + c_f\frac{|U|U}{R} = 0 \tag{2.9}$$

This **acceleration equation** can be expressed in terms of the discharge Q instead of the flow velocity U, by substituting $U = Q/A_c$ and Eq. (2.3) in Equation (2.9). In case the entire cross-section contributes to the conveyance ($A = A_c$ and $B = B_c$), we obtain

$$\frac{\partial Q}{\partial t} + \frac{\partial}{\partial s}\left(\frac{Q^2}{A_c}\right) + gA_c\frac{\partial h}{\partial s} + c_f\frac{|Q|Q}{A_c R} = 0 \tag{2.10}$$

Except for a factor ρ, Equation (2.10) is a **momentum balance equation**. The first term is the rate of increase of the momentum per unit length ($\rho U A_c$ or ρQ), the second is the net outflow of momentum as a result of longitudinal advection, given by $\rho U^2 A_c$, or $\rho Q^2/A_c$, the third is the forcing due to the water surface slope and the fourth is the resistance, all of them divided by ρ.

In the above, the momentum balance has been derived from an acceleration equation. It could also have been established directly by considering the balance of momentum for the entire cross-section (see the Appendix to this chapter).

In the transformation of Equation (2.9) into Equation (2.10), it was assumed that the entire cross-section contributes to the conveyance, such that $A = A_c$ and $B = B_c$. If this is not the case, an additional term arises in Equation (2.10), which (if inserted in the left-hand side) is given by $\rho U(B - B_c)(\partial h/\partial t)$. It arises as a result of the lateral exchange of mass and streamwise momentum between the conveyance cross-section and the adjacent shallow flood plains, which takes place in case of a time-varying water level, as explained in the accompanying text box.

In practice, this additional term is often ignored, particularly in case of flow from the flood plains back into the main channel ($\partial h/\partial t < 0$), it being assumed that this outflowing water carries no streamwise momentum. In some numerical models, the additional term is taken into account only for rising water, and ignored when the water falls.

A note on lateral momentum exchange

The nature of the additional term $\rho U(B - B_c)(\partial h/\partial t)$ is most easily understood in the context of the momentum balance. Consider a river with a main channel bordered by shallow flood plains, which contribute a negligibly small amount to the conveyance. The total width of the flood plain (summed over both river banks) is written as $B - B_c$. When the water rises, at the rate $\partial h/\partial t$, water is stored on the flood plain at the rate $(\partial h/\partial t)(B - B_c)\triangle s$, which is the result of a lateral volume flow from the main channel to the flood plain. This lateral flow carries streamwise momentum. Let us say that this amounts to ρU per unit volume. This implies a net lateral outflow of streamwise momentum from the conveyance cross-section at a rate $\rho U(B - B_c)(\partial h/\partial t)$ per unit length. This comes in addition to the net outflow of streamwise momentum which results from the streamwise motion, given as $\partial(\rho Q^2/A_c)/\partial s$ in Equation (2.10), and so explains the nature of the additional term noted above. However, because the streamwise velocity at the transition between the main channel and the shallow flood plain is usually (much) less than U, the flow velocity averaged over the relatively deep main channel, the expression given here is an overestimate.

Summary of equations for free surface flows

The continuity equation (Equation (2.4)) and the equation of motion (Equation (2.10)) together form the basis for analyses and computations of one-dimensional long-wave phenomena. They are known as the **equations of De Saint-Venant** (1871) or as the (one-dimensional) **shallow-water equations** (because the depth has been assumed to be very small compared to typical length dimensions). They consist of the **continuity equation**

$$\boxed{B\frac{\partial h}{\partial t} + \frac{\partial Q}{\partial s} = 0} \tag{2.11}$$

and the **momentum balance equation**

$$\boxed{\frac{\partial Q}{\partial t} + \frac{\partial}{\partial s}\left(\frac{Q^2}{A_c}\right) + gA_c\frac{\partial h}{\partial s} + c_f\frac{|Q|Q}{A_c R} = 0} \tag{2.12}$$

These equations form a coupled set of hyperbolic partial differential equations (PDE's) for the two unknowns h (water level) and Q (discharge) as functions of location (s) and time (t). The geometric parameters A_c, R and B as well as the resistance coefficient c_f are supposed to be known functions of location (s), water level (h) and discharge (Q), so that mathematically speaking they are known, variable coefficients. The set of PDE's can be integrated if proper initial conditions and boundary conditions are provided.

Reduced equations

It depends on the circumstances whether all contributions to the momentum balance are important or whether one or two are negligible. In the latter case the equation may be reduced to a simpler form. In general, one can say that resistance is less and less important as the motions vary more and more rapidly. On the other hand, inertia becomes negligible when the variations are very slow. Following chapters present different categories of long waves (tides, flood waves in rivers, etc.) with corresponding simplifications of the equations resulting from the neglect of relatively small terms. Here, we present a few cases of even stronger simplification where we can no longer speak of wave propagation. the surface area

Steady flow: backwater curves

A trivial simplification occurs for **steady flow**, for which $\partial h/\partial t = 0$ and $\partial Q/\partial t = 0$. It follows from the continuity equation that in that case Q is also constant in space: $\partial Q/\partial s = 0$, leaving $h(s)$ as the one unknown. Equation (2.12) then reduces to a first-order **ordinary differential equation** (ODE):

$$Q^2 \frac{\mathrm{d}A_c^{-1}}{\mathrm{d}s} + gA_c \frac{\mathrm{d}h}{\mathrm{d}s} + c_f \frac{|Q|Q}{A_c R} = 0 \tag{2.13}$$

As pointed out above, the profile parameters A_c and R and the resistance coefficient c_f are supposed to vary in a known manner with h for given Q, so that (2.13) can be integrated to find the longitudinal profile of $h(s)$ if the value of h is known at some cross-section.

To put this equation in a more compact form, which brings out the physics of the flow more concisely, we use some shorthand by introducing a few new parameters. We write the area of the conveyance cross-section (A_c) as the product of its width (B_c), assumed constant, and its average depth (d), the latter being our new unknown. Further, we write $h = z_b + d$, in which z_b is the average bed elevation above the reference plane $z = 0$. With this, the surface slope can be written as $\mathrm{d}h/\mathrm{d}s = \mathrm{d}z_b/\mathrm{d}s + \mathrm{d}d/\mathrm{d}s = \mathrm{d}d/\mathrm{d}s - i_b$, in which $i_b = -\mathrm{d}z_b/\mathrm{d}s$ is the bed slope, taking the positive s-direction pointing downstream. Furthermore, for easy recognition, we revert to the cross-sectionally averaged velocity $U = Q/A_c$. With these substitutions, and following a few mathematical manipulations, Equation (2.13) can be rewritten into

$$\frac{\mathrm{d}d}{\mathrm{d}s}\left(1 - \frac{U^2}{gd}\right) = i_b - c_f \frac{|U|U}{gR} \tag{2.14}$$

Finally, we introduce the Froude number through the definition

$$Fr^2 \equiv \frac{Q^2}{gA_c^2 d} = \frac{U^2}{gd} \tag{2.15}$$

and the friction slope i_f, defined as

$$i_f \equiv c_f \frac{|Q|Q}{gA_c^2 R} = c_f \frac{|U|U}{gR} \tag{2.16}$$

Using these definitions, and assuming $Fr^2 \neq 1$ (flow not critical), the differential equation (2.14) can be written in the compact form

$$\boxed{\frac{\mathrm{d}d}{\mathrm{d}s} = \frac{i_b - i_f}{1 - Fr^2}} \tag{2.17}$$

This is the so-called **equation of Bélanger for backwater curves**.

If the flow is not only steady but also uniform, the surface slope, the friction slope and the bed slope are equal, and $\mathrm{d}d/\mathrm{d}s = 0$. In this case the left hand side of equation (2.14) equals zero which reduces this differential equation into the **algebraic equation**

$$\boxed{Q = A_c\sqrt{gRi_b/c_f}} \tag{2.18}$$

Using this and the definition (2.15) of the Froude number for an arbitrary flow, uniform or not, the Froude number in uniform flow (Fr_u) can be seen to obey $Fr_u^2 = i_b/c_f$. Depending on whether the bed slope is adverse ($i_b < 0$), horizontal ($i_b = 0$), mild ($0 < i_b < c_f$, or $Fr_u < 1$), critical ($i_b = c_f$, or $Fr_u = 1$) or steep ($i_b > c_f$, or $Fr_u > 1$), and on whether the actual flow is subcritical ($Fr^2 < 1$) or supercritical ($Fr^2 > 1$), the longitudinal profile of the depth (the so-called backwater curve) can take on different forms. We will not eleborate on this here but refer to the preceeding course Fluid Mechanics (CTB2110).

Small-basin approximation

A second simplification occurs when the flow is unsteady but the domain in which it occurs is small, as in a short basin connected by a restricted opening to an exterior water body with a time-varying (e.g. tidal) surface elevation, see Figure 2.4. Because the basin is closed (except for the opening to the exterior) and short, the velocities in its interior are quite small so that inertia and resistance play no role whatsoever. It follows from Equation (2.12) that

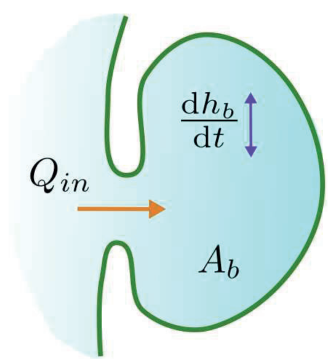

Figure 2.4: Small basin with restricted opening

the surface slope then is negligible inside the domain. The interior water surface goes up and down but it is nearly horizontal at all times, and will in fact be approximated as such. In other words, the surface elevation in the basin, $h(x, y, t)$, is assumed to be a function of time only, written as $h_b(t)$. This type of response is called the **Helmholtz mode** or **pumping mode**.

This simplification implies that the surface elevations in all interior points are considered to be in phase. A condition for this to be allowable is that the time scale of the variations of the exterior forcing be far greater than the time it takes for the resulting disturbances to traverse the basin. Stated another way, the length of the basin should be small compared to the wavelength of the disturbances.

Because the surface elevation in the basin is assumed to be horizontal at all times, the volume balance for the water inside the basin is trivial. Writing A_b for the free surface area inside the basin, the rate of change of the interior water level is linked to the discharge through the connecting opening or channel (Q_{in}, positive for flow into the basin) through

$$\boxed{Q_{in} = A_b \frac{\mathrm{d}h_b}{\mathrm{d}t}} \tag{2.19}$$

Despite its simplicity, the small basin approximation is useful for a number of practical situations, as demonstrated in Example 2.1. We will elaborate more extensively on these approximations in Chapter 7, where we derive explicit relationships for the forced tides in a basin.

Schematizations

So far we have tacitly assumed that the geometry of the channel being considered is known and relatively simple, such that a cross-section can be sufficiently described through only a few geometric parameters, viz. B, A_c and R. Likewise we have assumed that the resistance factor c_f is known, perhaps as a function of the depth (in relation to some roughness value). In practice, life is not that simple, particularly when dealing with natural channels which can have poorly defined and highly variable geometric characteristics. In those cases it is necessary to schematize this complicated geometry to a simpler one that can be handled in our mathematical models while maintaining the main features that determine the overall flow characteristics, both with respect to **storage** and **conveyance**. These main functions should be distinguished and both should be properly represented in the schematization.

The storage capacity (i.e. the free surface area available for storage) plays a dominant role in damping and slowing down of flood waves in rivers: water that is (temporarily) stored does not need to flow downstream at once, thereby lessening the height and rate of progression of the flood wave. Therefore, these storage areas should be accounted for, regardless whether they convey water or not. We mention three situations that can occur in this respect.

1. In The Netherlands and elsewhere, it is common practice to build a sequence of groins in lowland rivers, extending laterally from the banks towards the main channel in order to fix the alignment and the width of the latter and maintain its depth. In those

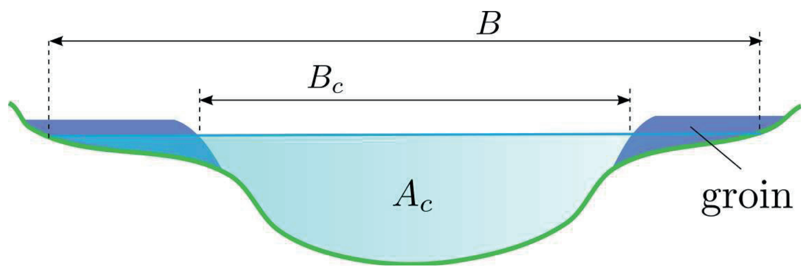

Figure 2.5: River cross-section with groins

cases, only the channel between the heads of the groins contributes to the downstream conveyance of water. The spaces between adjacent groins do not, but they do take part in the storage of water in case of rising water. The width B in the continuity equation therefore should be the width between the banks, which can be far larger than the conveyance width B_c, which is the lateral distance between the heads of the groins (Figure 2.5).

2. The same holds for basins that are connected laterally to the river reach or tidal channel, such as dead river branches, harbours etc. (see Figure 2.6). They can store water, but do not convey it. Their surface area which is available for storage must be accounted for in the continuity equation, but these basins can be ignored in the momentum equation.

3. In periods of high water, the flood plains are covered and contribute to storage as well as conveyance, but the depth of flow over the flood plains is much less than it is in the main channel, and the resistance is usually much greater (due to vegetation, buildings etc.). This must be accounted for in the schematisation by dividing the cross-section into two or more subsections, each of them with its own characteristic width, depth and roughness.

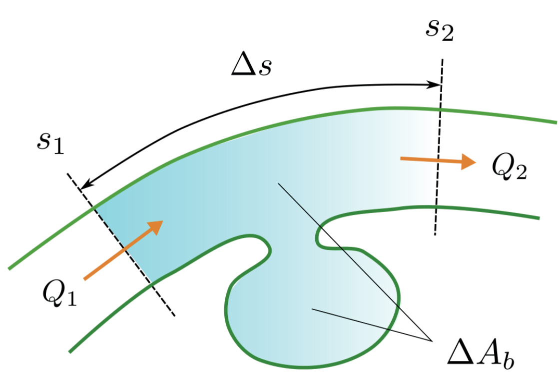

Figure 2.6: Top view of river reach with discrete storage in a lateral basin

Another problem of schematization is the determination of suitable values for the resistance.

This consists of bed ‘shear stress’, which in turn consists partly of form resistance due to grains, ripples and dunes, and form resistance due to abrupt large-scale profile variations, bends, groins, bridge piers etc. The bulk effect of these is modelled through Equation (2.8), with the single coefficient c_f. It is obvious that this is a gross simplification. It is therefore very difficult to assign proper values to this coefficient *a priori*. Calibration in the target area is necessary. This must be done using the chosen profile schematization because c_f, A_c and R occur together in the single resistance term $c_f|Q|Q/(A_cR)$, so that errors in the geometric profile parameters are compensated by errors in the calibrated value of c_f. Typical values of c_f are in the range of 0.003 to 0.006.

Example 2.1. *Small basin (Scheveningen harbour)*

Situation

The harbor of Scheveningen is a semi-enclosed basin with a surface area $A_b = 0.25$ km^2. The tide at sea leads to a time varying water level $h_b(t)$ within the harbor and a corresponding discharge $Q(t)$ in the entrance of the harbor, where inflow is defined positive. The small basin approximation can be applied.

Questions

1. Compute the discharge Q for $\mathrm{d}h_b/\mathrm{d}t = 0.1$ mm/s.
2. Derive an expression for $Q(t)$ if h_b is given by $h_b(t) = \hat{h}_b \sin \omega t$ ($\hat{h}_b$ and ω denote the tidal amplitude and frequency, respectively).
3. Determine the discharge amplitude $\hat{Q}$ if $\hat{h}_b = 0.9$ m and $\omega = 1.4 \times 10^{-4}$ rad/s (corresponding to a so-called M_2-tide with a period of 12 hrs 25 min).

Solution

Since the small basin approximation applies to the tidal water motion in the harbour, the water level in the harbor and the discharge in the entrance are related through Eq. (2.19).

1. Substitution of $A_b = 0.25 \times 10^6$ m^2 and $\frac{\mathrm{d}h_b}{\mathrm{d}t} = 0.1 \times 10^{-3}$ m/s in Eq. (2.19) gives a corresponding discharge $Q = 25$ m^3/s.
2. Differentiation of the given expression for $h_b(t)$ with respect to t and substitution in Eq. (2.19) gives: $Q(t) = A_b\, \omega\, \hat{h}_b \cos \omega t$.
3. From the previous answer it follows that the discharge varies periodically with an amplitude $\hat{Q} = A_b \omega \hat{h}_b = 31.5$ m^3/s.

Comment

Besides giving results in terms of numbers, analytical modelling provides insight in the behavior of a system as a whole. In this simple example we have established a relation between the tidal water level in a small basin and the discharge in the opening proving that these are 90° out of phase.

2.2 Pressurized flow in closed conduits

Introduction

Equations for pressurized flow of a liquid (water, oil, ...) in closed conduits, mainly pipelines, are treated here as a follow-up to the equations for free surface flows because of the great similarity between them. In both cases we deal with balance equations integrated across the entire cross-section, which in both cases yields one-dimensional equations which belong to the category of hyperbolic PDE's, with solutions representing propagating waves.

In free surface flows, storage takes place through variations of the free surface elevation. This is accompanied by pressure variations of a few meters of water column at most, too small to cause appreciable changes in density. The water can therefore be treated as incompressible.

Pressurized flows do not have a free surface so that a corresponding storage cannot occur. In these cases, storage can take place only through **elasticity of the pipe wall**, allowing profile variations, and **compression of the liquid**, allowing variations in mass in a given volume.

The actual magnitudes of the variations in cross-sectional area and density are quite small, resulting in an almost rigid reponse. In fact, if the flow varies gradually, the pressure variations are mild, and these storage effects can be neglected, leading to the so-called **rigid-column approxiation**, in which the liquid moves axially as a rigid body. In these cases the conservation of mass is fulfilled *a priori* so that we have to deal with the conservation of momentum only.

The abrupt closure or opening of a valve or the abrupt switching on or off of a pump in a pipeline for irrigation, hydropower, drinking water supply, etc., either purposefully or as the result of a failure or an accident, results in rapid variations in flow velocity, accompanied by large pressure variations. This phenomenon is called '**waterhammer**' because it can sound as if the pipewall is struck by a hammer. Too large pressures should be avoided, or at least reduced in view of the limited strength of the materials. Modelling of these effects requires the use of the **constitutive equations** for the elasticity of the pipe wall and the compression of the liquid in addition to the equations of conservation of mass and momentum. This is elaborated in the following.

Waterhammer induces negative pressure variations as well. When the pressure reduces to the vapour pressure of the water, vapour bubbles are formed, the so-called process of **cavitation**, resulting in a two-phase system of water and bubbles. This mixture is far more compressible than pure water, so that the speed of propagation of the pressure waves through the pipe/liquid/bubbles system is drastically reduced. Locally, a zone with a free surface of the liquid can develop. These processes are not considerd in this chapter.

Constitutive equations

Here, we restrict ourselves to liquids (water, oil, ...) for which the density varies exclusively as a result of compression, ignoring possible variations of the density due to differences in salinity or temperature. We need to establish so-called constitutive equations for the liquid and for the pipe wall, providing the connection between the pressure p and

- the liquid density (ρ) and
- the cross-sectional area (A).

We will use linear, elastic models for this purpose.

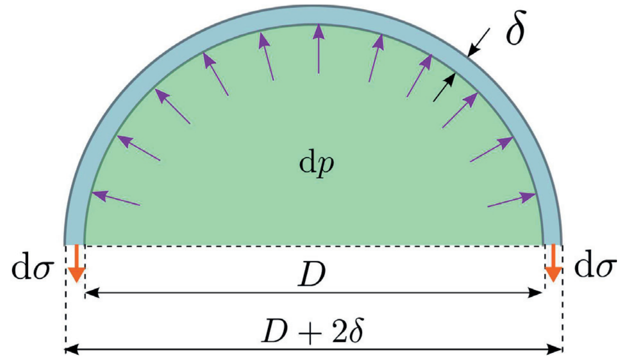

Figure 2.7: Cross-section closed pipe

Liquid compressibility

The modulus of compression (K) of a liquid is defined through the relation

$$\frac{\mathrm{d}\rho}{\mathrm{d}p} = \frac{\rho}{K} \tag{2.20}$$

Under normal operating conditions, the modulus of compressibility of water is K= 2.2 GPa approximately, virtually independent of pressure or temperature. (In case the liquid contains gas or vapour bubbles, even in minute amounts, the bulk value of K is reduced drastically because of the high compressibility of the gas or vapour in the bubbles.)

We will need the partial derivatives of ρ with respect to t and s in the conservation equations. Using (2.20), these can be expressed as follows in terms of the derivatives with respect to the pressure p:

$$\frac{\partial \rho}{\partial t} = \frac{\mathrm{d}\rho}{\mathrm{d}p}\frac{\partial p}{\partial t} = \frac{\rho}{K}\frac{\partial p}{\partial t} \tag{2.21}$$

$$\frac{\partial \rho}{\partial s} = \frac{\mathrm{d}\rho}{\mathrm{d}p}\frac{\partial p}{\partial s} = \frac{\rho}{K}\frac{\partial p}{\partial s} \tag{2.22}$$

Pipe elasticity

Consider a pipeline with a circular cross-section with inner diameter D and a uniform, relatively thin wall thickness δ (so $\delta << D$; see Figure 2.7, in which the relative wall thickness has been exaggerated). Suppose now that a small increase in pressure (dp) causes an increase in hoop stress in the pipewall equal to dσ. Neglecting the inertia of the fluid (radially) and of the wall, equilibrium relations can be used, from which it follows that

$$2\delta \times \mathrm{d}\sigma = D \times \mathrm{d}p \tag{2.23}$$

(The meaning of i_f is that it represents the ratio of the flow resistance to the fluid weight.) Because of the elasticity of the pipe wall, with modulus E, an increase in hoop stress dσ

causes an increase in the circumference ($P = \pi D$) and therefore also of the pipe diameter, which according to Hooke's law can be expressed by

$$\frac{\mathrm{d}D}{D} = \frac{\mathrm{d}P}{P} = \frac{\mathrm{d}\sigma}{E} \tag{2.24}$$

Since the cross-sectional area A is proportional to D^2, and using (2.23), it follows that

$$\frac{\mathrm{d}A}{A} = 2\frac{\mathrm{d}D}{D} = \frac{D}{\delta}\frac{\mathrm{d}p}{E} \tag{2.25}$$

so that

$$\frac{\mathrm{d}A}{\mathrm{d}p} = \frac{D}{\delta E}A \tag{2.26}$$

Using this, the partial derivatives of A with respect to t and s can be expressed as

$$\frac{\partial A}{\partial t} = \frac{\mathrm{d}A}{\mathrm{d}p}\frac{\partial p}{\partial t} = \frac{D}{\delta E}A\frac{\partial p}{\partial t} \tag{2.27}$$

$$\frac{\partial A}{\partial s} = \frac{\mathrm{d}A}{\mathrm{d}p}\frac{\partial p}{\partial s} = \frac{D}{\delta E}A\frac{\partial p}{\partial s} \tag{2.28}$$

Conservation of mass

The mass balance for the liquid under pressure in a pipeline reads

$$\frac{\partial}{\partial t}(\rho A) + \frac{\partial}{\partial s}(\rho A U) = 0 \tag{2.29}$$

This can be expanded into

$$A\frac{\partial \rho}{\partial t} + \rho\frac{\partial A}{\partial t} + \rho U\frac{\partial A}{\partial s} + \rho A\frac{\partial U}{\partial s} + UA\frac{\partial \rho}{\partial s} = 0 \tag{2.30}$$

We substitute Eqs. (2.21), (2.22), (2.27) and (2.28), and divide by A, with the result

$$\left(\frac{\rho}{K} + \frac{\rho D}{E\delta}\right)\frac{\partial p}{\partial t} + \left(\frac{\rho}{K} + \frac{\rho D}{E\delta}\right)U\frac{\partial p}{\partial s} + \rho\frac{\partial U}{\partial s} = 0 \tag{2.31}$$

Defining a quantity c through

$$\frac{1}{c^2} = \frac{\rho}{K} + \frac{\rho D}{E\delta} \tag{2.32}$$

and substituting this into Equation (2.31) brings the latter in the following compact form that will be used in waterhammer computations:

$$\frac{\partial p}{\partial t} + U\frac{\partial p}{\partial s} + \rho c^2\frac{\partial U}{\partial s} = 0 \tag{2.33}$$

We will see in Chapter 6 that c represents the propagation speed of axial pressure waves through the pipeline with the pressurized liquid. In an infinitely rigid pipe ($E \to \infty$), we have $c = \sqrt{K/\rho}$, which is the classical expression for the propagation speed of compression waves (the speed of sound) in a liquid, which for water (without bubbles!) is about 1400 m/s. The elasticity of the pipe wall causes the actual speed in the coupled system to be less than this, often in the order of 1000 m/s in case of steel pipes, see also Example 2.2.

In the approximation of an incompressible liquid and a rigid pipe, $c \to \infty$. This implies that in this approximation a pressure perturbation would be felt instantly over the entire pipe length. This also follows from the mass balance (2.31), which in this case ($K \to \infty$ and $E \to \infty$) reduces to $\partial U/\partial s = 0$, i.e. the fluid behaves as a rigid column. As we will see below, this approximation applies when the flow varies slowly compared to the time it takes for a pressure wave to travel the length of the pipe.

Conservation of momentum

The mass balance must be supplemented with an expression for conservation of momentum. We use the acceleration form, Equation (2.9), which is repeated here for convenience:

$$\frac{\partial U}{\partial t} + U\frac{\partial U}{\partial s} + g\frac{\partial h}{\partial s} + c_f\frac{|U|U}{R} = 0 \tag{2.34}$$

The equations for free surface flows contain the fluid pressure in the equation of motion only, where it occurs next to gravity. Their combined influence could be expressed through the piezometric level, represented by a single quantity h. This is unlike the case for pressurized flow, for which the pressure occurs in both equations, in contrast with gravity. Therefore, using the piezometric level is not meaningful in this case. (We could, but it would not eliminate the pressure.) Assuming that the positive s-axis (along the pipe axis) makes an angle β with the vertical, we have

$$g\frac{\partial h}{\partial s} = \frac{1}{\rho}\frac{\partial p}{\partial s} - g\cos\beta \tag{2.35}$$

Using this, Equation (2.34) is transformed into

$$\frac{\partial U}{\partial t} + U\frac{\partial U}{\partial s} + \frac{1}{\rho}\frac{\partial p}{\partial s} - g\cos\beta + c_f\frac{|U|U}{R} = 0 \tag{2.36}$$

Summary of equations for pressurized flow in a pipe

The **mass balance** for the liquid in the pipe is (re)written as

$$\boxed{\frac{\partial p}{\partial t} + U\frac{\partial p}{\partial s} + \rho c^2\frac{\partial U}{\partial s} = 0} \tag{2.37}$$

The **momentum balance** for the liquid in the pipe, in acceleration form, is written as

$$\boxed{\frac{\partial U}{\partial t} + U\frac{\partial U}{\partial s} + \frac{1}{\rho}\frac{\partial p}{\partial s} - g\cos\beta + c_f\frac{|U|U}{R} = 0} \tag{2.38}$$

The parameter c in Equation (2.37) is the **speed of propagation** of axial waves through the coupled pipe/liquid system. It is defined by

$$\boxed{\frac{1}{c^2} = \frac{\rho}{K} + \frac{\rho D}{E\delta}} \tag{2.39}$$

Equations (2.37) and (2.38) form a coupled set of hyperbolic PDE's for two unknowns, the fluid pressure p and the flow velocity U, as functions of location s and time t. They form the basis of so-called water hammer computations (excluding the occurence of cavitation). Examples are given in Chapter 6.

Example 2.2. *Wave speed in pressurized flow*

Situation

Consider the pressurized flow of water ($\rho = 1000$ kg/m^3) in a pipeline. The bulk modulus (compressibility) of water (K) amounts to 2.2×10^9 Pa.

Questions

Compute the speed of pressure waves in the pipeline in case of:

1. a pipeline with an inifinitely rigid wal;
2. a steel pipeline (tensile modulus $E = 220 \times 10^9$ Pa) with a pipe diameter of 50 times the wall thickness;
3. a glass reinforced plastic (GRP) pipeline ($E = 17 \times 10^9$ Pa), also with a pipe diameter of 50 times the wall thickness.

Solution

To calculate the speed of pressure waves in a pipeline use Equation (2.39).

1. For an inifinitely rigid pipewall $E \to \infty$ reducing Eq. 2.39 to $1/c^2 = \rho/K$ (second right hand side term is zero) from which it follows that $c = \sqrt{K/\rho} = 1483$ m/s.
2. Using the full expression for c and setting $D/\delta = 50$ gives $c = 1211$ m/s.
3. Carrying out the same steps as in question 2. leads to $c = 543$ m/s.

Comment

Provided the wall thickness does not change relative to the pipe diameter,cancels increasing elasticity of the pipewall slows down the speed of pressure waves. For materials commonly used in civil engineering this decrease can be considerable.

2.3 Numerical modeling

In this course we will take a first step into the realm of numerical computing by working out some simple examples using the Python programming language. Our first endavour concerns a simple model of a small basin. Despite its simplicity, this model will illustrate some basic concepts of numerical modeling.

A numerical bay

We consider a tidal bay which is connected to the sea by a narrow entrance. The tidal motion at sea leads to a time varying water level in the bay (h_b) which is independent of the position in the bay area. Apparently, under the action of the tide the bay behaves as a small basin. The bay has some shallow areas which become exposed at low water. The wet surface area of the bay (A_b) which is connected to the sea therefore depends on the water level (h_b). The corresponding discharge in the entrance is given by Eq. (2.19) which for a variable surface area is restated as follows,

$$Q = A_b\,(h_b)\,\frac{\mathrm{d}h_b}{\mathrm{d}t} \tag{2.40}$$

The water level (h_b) is supposed to be known from measurements, giving the water level in the bay at regular time intervals. A bathymetric survey of the bottom level in the bay is available to determine the wet surface area (A_b) as a function of the water level (h_b).

Our task is to compute for some time interval $I = [t_0; t_N]$ the discharge (Q) in the entrance of the bay, given the water level (h_b) in the bay as a function of time (t). The problem bears some resemblance with Example 2.1 but has the additional difficulties of a variable surface area and arbitrary water level variations.

Discretization

In order to simulate the above situation by means of a computer model, the ordinary differential equation (2.40) must be transformed into an **algebraic equation**. To that end, instead of treating the various parameters as continous functions, we represent them as series of discrete values on which we perform our computations.

First, the time interval of interest I is represented as a sequence of $N+1$ discrete time levels: $I = [t_0, t_1, \cdots, t_{N-1}, t_N]$, where N is the number of time steps. This is called a partitioning of the time domain I. In this case the range of time levels $t_0, t_1, \cdots$ is chosen to match those from the water level measurements. We may collect these time levels in an array $[t_i]_{i=0}^{N}$ where i is an index number giving the corresponding order within the array.

Next, to each time level (t_i) we assign the corresponding water level ($h_{b,i}$) as available from the measurements. Once the discrete water levels ($h_{b,i}$) are known, we can compute the corresponding free surface areas ($A_{b,i}$) by using the information from the bathymetric survey.

If we succeed in constructing the sequence $[Q_0, \cdots, Q_N]$ we have solved our problem in the sense that we have obtained a discrete representation of the discharge (Q). It follows from Eq. (2.40) that computation of the discrete discharge (Q_i) at time level (t_i) involves the time derivative of the water level (h_b) at time level (t_i). Since only the water level was measured and not its time derivative we need to estimate the latter. Using for instance the **forward Euler method** we can express the derivative of the water level (h_b) in terms of the discrete water levels ($h_{b,i}$) as follows

$$\left.\frac{\mathrm{d}h_b}{\mathrm{d}t}\right|_i = \frac{h_{b,i+1} - h_{b,i}}{t_{i+1} - t_i} + \mathcal{O}\left(t_{i+1} - t_i\right) \tag{2.41}$$

Due to the approximation we have made an error proportional to the time step size ($t_{i+1} - t_i$), which can be proven by a Taylor series expansion. The discrete dicharge (Q_i) can now be computed as

$$\begin{aligned} Q_i &= A_{b,i} \left.\frac{\mathrm{d}h_b}{\mathrm{d}t}\right|_i \\ &\approx A_{b,i} \frac{h_{b,i+1} - h_{b,i}}{t_{i+1} - t_i} \end{aligned} \tag{2.42}$$

In applying this algorithm we make an error, but Eq. (2.41) shows that the approximation gets better as the time step size decreases, or equivalently, the number of time steps (N) on the given time interval of interest (I) increases. Generally, increasing the numerical accuracy requires more work to be done by the computer.

Implementation

We will code the foregoing into a simple Python program. For this purpose some basic knowledge of Python will be practical (see for instance Hetland [1] or Langtangen [2]), which may also be learned as we proceed along the examples in this book.

The program first needs to process the water level measurements and surface data. To this end the water level data is stored in a file `water-level.dat` containing two columns where the first one gives the time levels and the second one the corresponding water levels. The wet surface area is prescribed for a cancels range of water levels (in increasing order) and interpolated for intermediate water levels. After computing the discharge using Eq. (2.42) the water level and discharge will be plotted as functions of time.

A Python script carrying out these tasks is given in Listing 2.1. The script can be executed by running Python in the directory containing the file `bay.py` and typing `import bay.py`. We will now examine Listing 2.1 in some more detail.

In lines 2 and 3 the modules `numpy` and `pylab` are loaded containing array computing methods and plotting tools, respectively, which are not available in plain Python. Line 6 reads the input file and splits it into separate character strings which, after executing line 7, yields an array of numbers containing the input data. The free surface area of the basin as a function of the water level is specified in lines 10 and 11 by prescribing it for a number of water levels. This information is passed to a function `A(h)` defined in line 14 which calculates the free surface area for arbitrary water levels by means of interpolation. The function `interp` is available from `numpy`. This line concludes the input section.

```
1  # import modules
2  from numpy import *
3  from pylab import *
4
5  # read water level data
6  data = open('water-levels.dat').read().split()
7  data = array([float(p) for p in data])
8
9  # bathymetry basin
10 level = array([-3.0,-1.0, 0.0, 2.0, 5.0, 7.0])      # water level                 [m]
11 area  = array([ 1.0, 1.8, 2.3, 2.5, 2.8, 3.0])      # corresponding surface area  [km2]
12
13 # function := water level [m] -> basin area [m2]
14 def A(h): return interp(h, level, area)*1.E6
15
16 # time partitioning
17 t = data[0::2]                                      # discrete time levels        [s]
18 N = size(t) - 1                                     # number of time steps        [-]
19
20 # water levels
21 hb = data[1::2]                                     # measured water levels       [m]
22
23 # compute discharge Q(t)
24 Q = []
25 for i in range(N):
26     Ab = A(hb[i])                                   # basin area at time i        [km2]
27     dh = hb[i+1] - hb[i]                            # water level increment       [m]
28     dt = t[i+1] - t[i]                              # time increment              [s]
29     Q.append(Ab*dh/dt)                              # discharge                   [m3/s]
30
31 # plot water level
32 subplot(2, 1, 1)
33 plot(t/3600, hb, '-oc')
34 xlabel('time [hrs]', fontsize=14)
35 ylabel('$h_b$ [m wrt datum]', fontsize=14)
36
37 # plot discharge
38 subplot(2, 1, 2)
39 plot(t[:N]/3600, Q, '-ob')
40 xlabel('time [hrs]', fontsize=14)
41 ylabel('$Q$ [m$^3$/s]', fontsize=14)
42
43 show()
```

Listing 2.1: bay.py

The computation proceeds by first initializing some parameters. The time levels, which are stored at uneven index numbers in the array `data`, are assigned to a new array `t`, for convenience, in line 17. The number of time steps (N) equals the size of array `t` minus one (line 18). The water level, stored at even index numbers in `data` is assigned to a new variable `hb` in line 21. The computation of the discharge commences in line 24 by initializing the variable `Q` as an empty list. The list is filled repetitively in a loop defined in line 25. For subsequent time indices `i`, where `i` runs from `0` to `N-1`, the surface level `Ab` (line 26) is computed by using the pre-defined function `A(h)`. Together with the increments of water level (line 27) and time (line 28) this determines the new value of `Q` which is appended to the list in line 29.

What remains is to plot the results. By means of `subplot` (lines 32 and 38) we first create a plot window of two figures, stacked vertically. The arguments of the `plot` function (lines 33 and 39) are the values on the horizontal and vertical axes, respectively, and a format specifier; `'-oc'` for the cyan bullet line of the water level and `'-ob'` for the blue bullet line of the discharge, respectively. The `plot` function in line 39 must only contain list numbers up to `N` since Q_N could not be computed with the algorithm using Eq. (2.42). The plots are shown in Figure 2.8.

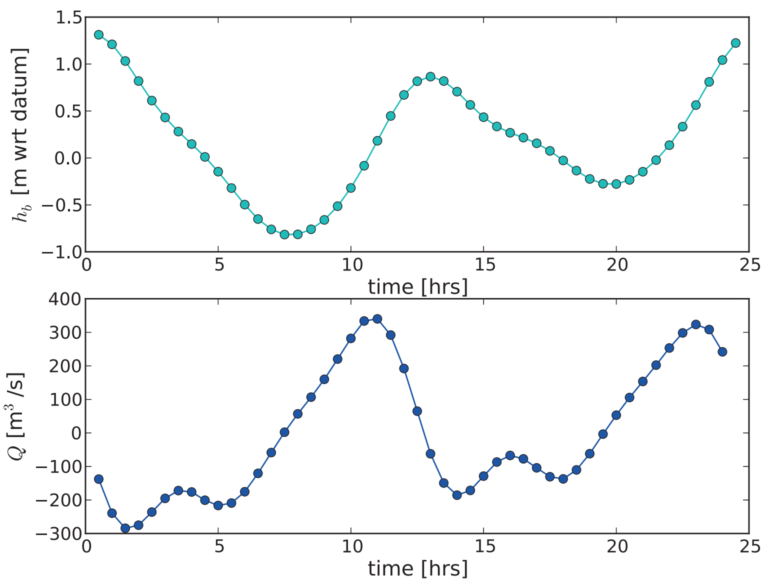

Figure 2.8: Surface elevation (top) and computed discharge (bottom)

Interpretation

We will briefly examine the results to see whether they make sense. Figure 2.8 shows that the discharge is about zero when the water level in the bay attains a maximum or minimum, as expected for a small basin. A maximum of the dicharge occurs around 11 hrs. at which time the water level rises with approximately 0.5 m/hr. Together with a water level h_b of about 0 and a corresponding bay area of 2.3 km^2, this gives an estimated discharge Q of $(2.3 \times 10^6$ m$^2) \times (0.5$ m/hr$) \times (1$ hr/3600 s$) \approx 320$ m^3/s. Both findings are in good agreement with the result computed by the model, giving confidence in the Python program. Advanced testing, by for instance comparing the model results with analytical solutions, could provide a more quantitative assessment of the numerical error (see Problem 14).

Bibliography

[1] Magnus Lie Hetland. **Beginning Python**. Apress, 2005.

[2] Hans Petter Langtangen. **Python scripting for computational science**. Springer Verlag, 2009.

Problems

1. What is the discharge through a conduit? What is its dimension?
2. Where is storage in free surface flows taking place (mainly)?
3. Same, now for pressurized flow.
4. Point out an important consequence of the difference in character and magnitude of the storage in both cases.
5. Derive the volume balance equation for the flow in a river stretch that is laterally connected to a basin.
6. Derive the volume balance equation for the flow in a river stretch provided with a sequence of groins; cast it in differential form.
7. Derive the volume balance equation (in differential form) for the flow in a river for which seepage of water into the subsoil (at a rate of q volume units per unit area of bottom and per unit time) has to be taken into account.
8. Derive an expression for the downstream force per unit volume in a flow with a sloping free surface.
9. Which contributions to this force can be distinguished?
10. Describe situations in which either one of these is zero.
11. Check the dimensions of the individual terms in Equation (2.7).
12. Derive the mass balance equation for pressurized flow in a pipe.
13. Modify the Python program of Listing 2.1 such that it computes the water level as a function of time from a given initial water level and varying discharge in the entrance.
14. Verify that the error in Eq. (2.42) is proportional to the time step size by computing the discharge for a sinusoidal water level variation with constant basin area and comparing the result with the exact solution for different values of the time step size (see also Example 2.1).
15. Write a Python script to compute and plot the wave speed in a pipe relative to the sound speed in water as a function of D/δ, for some realistic values of E/K.

Appendix

Origin and meaning of the advective terms in the equations of motion

The equations of motion can take on different forms, in particular:

- an **equation for the acceleration** of a particle or an ensemble of particles (**Lagrangian description**), in which among others the so-called **advective acceleration** occurs;
- a **balance equation for the momentum** contained in a spatially fixed control volume (**Eulerian description**), containing among others the **advective transfer of momentum** through the surface bounding the control volume.

The difference and the connection between the two can be clarified with the simple example of a mass m with velocity $\vec{v}$ subject to a net force $\vec{F}$. Its momentum is $m\vec{v}$, and the momentum balance can be written as $\mathrm{d}(m\vec{v})/\mathrm{d}t = \vec{F}$. Using $\mathrm{d}m/\mathrm{d}t = 0$, expressing conservation of mass, the momentum conservation equation can be rewritten as the acceleration equation $\mathrm{d}\vec{v}/\mathrm{d}t = \vec{F}/m$.

We now apply this approach to free surface flow in a conduit, considering the water in a slice of length Δs. For simplicity, we assume that the entire cross-section contributes to the conveyance, thus making no distinction between A and A_c. We start with the Eulerian description.

Eulerian mass balance

Stored mass $$\Delta M = \rho A \Delta s \tag{2.43}$$
Mass flux $$S = \rho U A \tag{2.44}$$
Mass balance $$\frac{\partial \rho A}{\partial t} + \frac{\partial \rho A U}{\partial s} = 0 \tag{2.45}$$

Eulerian momentum balance

Stored momentum $$U \Delta M = \rho U A \Delta s \tag{2.46}$$
Momentum flux (by advection) $$\rho U^2 A = \rho Q U = \rho Q^2 / A \tag{2.47}$$
Momentum balance $$\frac{\partial \rho U A}{\partial t} + \frac{\partial \rho U^2 A}{\partial s} = \Sigma F_s = -\rho g A \frac{\partial h}{\partial s} - c_f \frac{\rho |Q| Q}{A R} \tag{2.48}$$

The second term in this **momentum balance equation** represents the difference between inflow and outflow of momentum through two cross-sections a unit length apart. It is the **advective contribution to the change of momentum** in the control volume. (The contribution of the fluid pressure to the total momentum flux through a cross-section is included as part of the external force in the right-hand side.)

From Eulerian momentum balance to an acceleration equation

Applying the product rule of differentiation to the left hand member of Equation (2.48), we expand this equation into

$$U\frac{\partial \rho A}{\partial t} + \rho A\frac{\partial U}{\partial t} + U\frac{\partial \rho A U}{\partial s} + \rho A U\frac{\partial U}{\partial s} = \sum F_s \tag{2.49}$$

The sum of the first term and the third term is zero in view of the mass balance, Equation (2.45). (This is equivalent to the use of $\mathrm{d}m/\mathrm{d}t = 0$ in the momentum balance of a discrete particle, written above.) It follows that

$$\rho A\frac{\partial U}{\partial t} + \rho A U\frac{\partial U}{\partial s} = \Sigma F_s \tag{2.50}$$

Dividing by ρA, the mass per unit length (equivalent to dividing the momentum balance of a particle by its mass m) yields the **acceleration equation**:

$$\frac{\partial U}{\partial t} + U\frac{\partial U}{\partial s} = \frac{\Sigma F_s}{\rho A} = -g\frac{\partial h}{\partial s} - c_f\frac{|Q|Q}{A^2 R} \tag{2.51}$$

The second term is the **advective contribution to the total acceleration** (the result of the motion of a fluid particle through a region with spatially varying particle velocity).

Chapter 3

Classification and analysis of long waves

This chapter deals with the following items:

- types of long waves
- a condition for waves to be classified as 'long'
- estimation of magnitudes of terms in the equaton of motion
- overview of solution methods
- analyses of results of observations or simulations

3.1 Types of long waves

The category of long waves encompasses different wave types, each with a different origin and with different dynamics, in the sense that the relative importance of the different physical processes, as expressed by the different terms in the equation of motion, can vary. In general, one can say that the faster the flow varies, the more important will be the inertia relative to the resistance, and the more it will be in balance with the net driving force. We return to this in following chapters.

Before dealing with the dynamics we give short descriptions of the origin and typical characteristics of different types of long waves:

- translatory waves in open and closed conduits
- tsunamis (waves following earth quakes in deep oceans)
- seiches (standing oscillations in lakes, bays, harbors etc.)

- tides in oceans, shelf seas, estuaries and lowland rivers
- flood waves in rivers

Translatory waves

As a result of rapid manipulation (or breakdown!) of pumps or valves in the operation of locks, sluices, hydropower plants, etc., rapid variations in discharge (δQ) can occur. These are accompanied by rapid variations in water surface elevation (δh) or pressure (δp), respectively, see Figure 3.1.

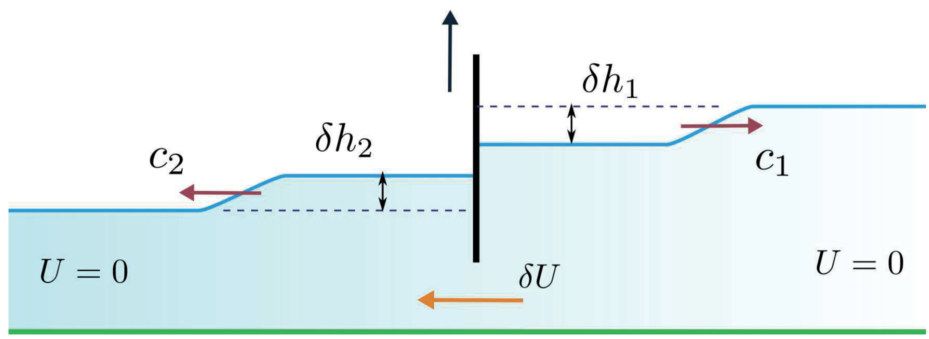

Figure 3.1: Translatory waves after opening a gate

The figure on the cover shows an example from the river Rhine, with an abrupt lowering of the water level near the city of Amerongen on January 24, 1995; this was the result of the raising of a movable weir at a smalll distance downstream. Such disturbances travel as so-called **translatory waves** into the adjacent reaches of a channel or pipeline. The passage of such wave induces a rise in elevation or pressure in case of an increase in discharge, and vice versa. The resulting particle velocities are in one direction only (either forward or backward), which explains the name 'translatory waves', as opposed to 'oscillatory waves', in which the particles move back and forth.

Where translatory waves reach a closed end or another major change in the conveyance capacity of a conduit, they are wholly or partially reflected. Repeated reflections can give rise to a sequence of rapid variations of flow properties. Figure 3.2 shows an example of such intense and rapid variations in pressure in a closed conduit, known as **water hammer**. Notice the scales of pressure (1 MPa corresponds to 100 m water column approximately) and time (1 ms = 1 millisecond = 10^{-3} second). Because translatory waves cause rapid variations, the effect of resistance during its passage is usually unimportant, so that the dynamics are predominantly determined by a (near-)balance between inertia and driving force. On a longer time scale, the cumulative effect of resistance manifests itself, and the motion dies down.

Translatory waves in navigation locks and navigation canals can cause hindrance to shipping as well as large forces in the mooring lines of moored ships, in some case causing

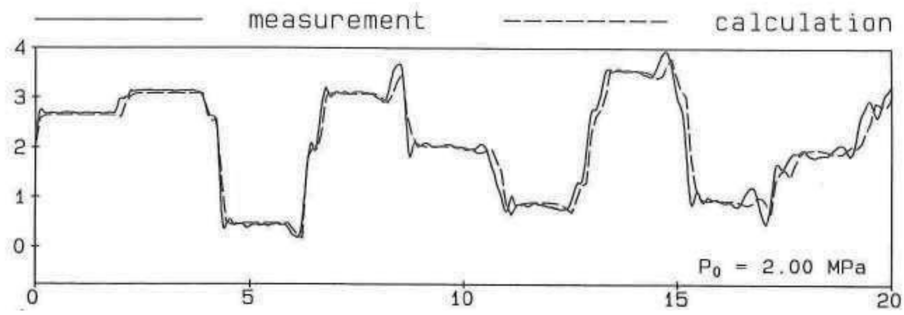

Figure 3.2: Pressure waves in a pipe (from: Tijsseling [2]). The pressure (in MPa) is plotted against the time (in ms)

breaking. Such effects can be reduced through a more gradual operation of pumps or valves. We will return to this matter in Chapter 6.

Tsunamis

Tsunamis are impulsively generated waves in oceans, shelf seas or (large) lakes, most commonly due to subsea earthquakes. Subsea vulcanic eruptions or landslides are other possible causes of tsunamis. Due to its impulsive generation, a tsunami is in essence a transient sequence of oscillations, a so-called wave train. The period of these oscillations is usually of the order of five to twenty minutes.

Figure 3.3 shows a plot of the depth variation, made by an echo sounder on board a yacht anchored at some distance off the coast of Thailand in the early morning of December 26, 2004, when the Indian Ocean tsunami struck. The oscillations in this plot have a period of about 20 minutes.

One can distinguish four stages in the life time of tsunamis: the generation, the propagation in relatively deep water from the source region to a coastal region, the enhancement and deformation in shoaling water, possibly up to breaking, and finally the run-up onto land.

Earthquakes causing tsunamis often occur in the subduction zones along the rims of tectonic plates. The accompanying sea bed motion has a plus-minus signature, generating a negative wave (a depression) traveling landward, and a positive wave (elevation) traveling seaward. This is why the leading wave in most coastal areas is one of depression (as in Figure 3.3). This manifests itself in an initial withdrawal of the sea waters from the coast, exposing vast stretches of what is normally a subsea bottom. This should be a strong warning sign to humans who happen to be present on the site to seek high ground as fast as they can, but unfortunately it also triggers the curiosity of some, who venture seaward, unknowingly towards their almost certain death.

Depending on the distance involved, the propagation from the source region to a coastal area may last several hours, giving time to issue warnings to coastal populations. However, this is not the case when the source region is relatively close to land, as in the Indian Ocean

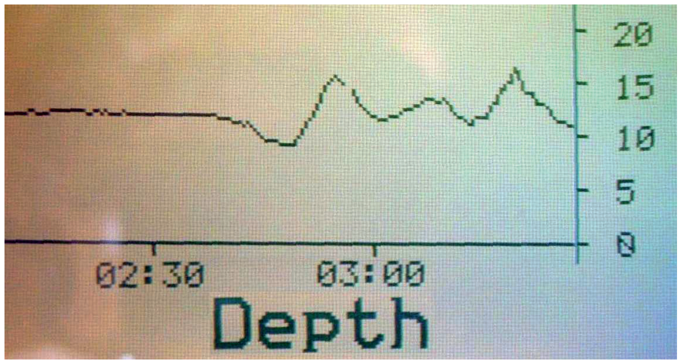

Figure 3.3: Record of depth variation measured offshore of the Thailand coast on December 26, 2004. The horizontal scale indicates the time (hrs), the vertical scale the depth (m)

tsunami of December 2004 and the Tohoku (Japan) tsunami of March 11, 2012.

In deep water, the individual waves in a tsunami wave train are typically a hundred km or more in length. This fact, combined with the relatively moderate wave heights offshore, often less than a meter, makes the steepness of tsunami waves in the deep ocean very low, causing them to pass unnoticed by ships in the deep ocean.

As the tsunami enters water of decreasing depth, the wave lengths shorten, the wave heights increase and the wave fronts steepen, possibly up to the point of breaking. This gives the tsunamis their often massive destructive power. In the fourth and final stage, the tsunami waves may overflow low-lying coastal areas, causing victims and material damage, or they may run up against coastal mountain slopes, locally up to heights in excess of 35 m in the two recent major tsunamis mentioned above.

Seiches

Oscillations of water or other liquids in a drinking glass, a bath tub or other 'closed basins' are easily observable for everyone. They are called 'standing oscillations', as opposed to progressive, oscillatory waves. Similar standing oscillations occur in all kinds of natural water systems and at widely different scales, in closed basins as well as basins that are closed at one end and open at the other, comparable to an open organ pipe. Such oscillations have been first systematically observed in Lake Geneva, by Forel (1892), who called them 'seiches', a name whose origin is obscure but which has nevertheless been rooted in the scientific literature ever since, referring to standing oscillations in lakes, harbour basins, and the like.

Seiches are **free** or **natural oscillations**, i.e. their periods are determined by the geometry of the system, rather than by external forcing. A weak periodic forcing may be sufficient to generate a significant response, provided the excitation contains energy at the natural frequencies of the system. In such cases the system response is **resonant**. In this manner, the water in coastal harbour basins can oscillate with significant amplitude in response to low waves at sea, hardly discernable offshore, which in turn can be the result of oscillations in wind speed and atmospheric pressure during the passage of cold fronts. Figure 3.4 gives an example for the port of IJmuiden in The Netherlands. The record for the offshore surface elevation in the upper panel shows minor disturbances, no more than about 0.1 m in height, superimposed on the astronomic tide. The lower panel shows a similar record in the outer harbour with resonantly enhanced oscillations, with crest-to-trough heights up to 1.2 m and a period of about 35 minutes, which is the natural period of the semi-closed outer harbour basin.

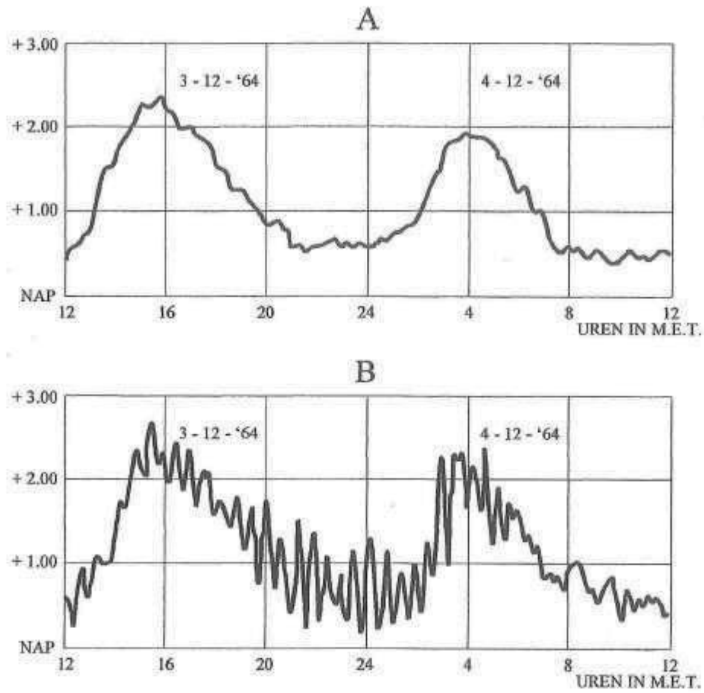

Figure 3.4: Simultaneous records of the surface elevation (in m above NAP, or MSL) offshore (upper panel) and in the outer harbour of IJmuiden (lower panel)

As will be seen, friction is usually unimportant for harbour seiches because of their relatively short period and the large depths in which they occur. The largest contribution to the damping of harbour seiches is the seaward radiation of energy through the harbour mouth.

Seiches can have undesirable or even harmful effects. They can be a nuisance to shipping, and occasionally cause breaking of mooring lines of moored ships. They also affect the tidal window of passage of deep-draught ships through their influence on the instantaneous available depth.

In contrast to human-caused translatory waves, nothing can be changed in the cause of harbour seiches, i.e. the low, long waves incident from the sea. Some alleviation of harmful effects can be achieved by reducing the resonance response factor, e.g. by optimising the geometry of the harbour mouth, but navigational demands put a limit to this. (It can even happen that narrowing the entrance results in higher seiches, because such narrowing may reduce the seaward radiation of seiche energy more than it hampers the excitation; this is the so-called 'harbour paradox'.) Another option is adaptation of the geometry of the interior basins. This can also shift the natural frequencies, but this is an improvement only in case the shift is away from the energetic frequencies in the excitation, which is usually not known *a priori*.

Tides

Tides are caused by the variations in time and space of the gravitational force exerted by the moon and the sun, in combination with the effects of the rotation of the earth. On a global scale, tides are oscillations in the ocean basins. On a smaller scale, the same is true for shelf seas such as the North Sea. From the oceans or shelf seas, tidal waves enter estuaries and bays where they may be damped or be resonantly enhanced, depending on the length and depth of the estuary or the bay. The tide in the Bay of Fundy (Nova Scotia, Canada) is an extreme example of strong enhancement, with a tidal range at the closed end up to 16.3 m, world's highest.

In most locations, the semi-diurnal lunar tide (M_2) is dominant; its period equals the duration of half a moon-day, about 12 hours and 25 minutes. In some areas, a.o. south-east Asia, the diurnal solar tide is dominant, due to resonance characteristics of adjacent ocean basins favouring these longer-period waves. See Figure 3.5. Bed friction is relatively weak (compared to inertia) in ocean tides, because of the large depths, and can there be neglected in a first approximation, but in shelf seas and shallow tidal bays it is of equal significance as the inertia and cannot be neglected.

Tides are very important for coastal engineers. Therefore, a good understanding of their origin and their dynamics is necessary. It is important to be able to understand, anticipate and assess *a priori* the effects of engineering measures in tidal areas such as dredging, closures, etc. To this end, tidal calculations are indispensible.

Flood waves in rivers

Enhanced precipitation and/or melting of snow in the catchment area of a river gives an enhanced discharge downstream, with some delay, and an associated rise in water level, a so-called **flood wave**. Figure 3.6 shows examples of the water surface elevation at several locations along two branches of the river Rhine, during a flood wave of January/February 1995. In each panel, the uppermost plot is for the most upstream location, and so on. All elevations are shown relative to the same reference elevation (NAP, roughly equal to Mean Sea Level, MSL). Tidal activity is visible in the most downstream locations. The record at Amerongen also shows the effect of a sudden raising of a downstream weir, which was necessary to allow free passage of the flood waters, which caused a sudden lowering of the upstream water surface elevation. Flood waves in rivers can last for several days or even weeks (see the example of Figure 3.6). Therefore, the corresponding variations in flow

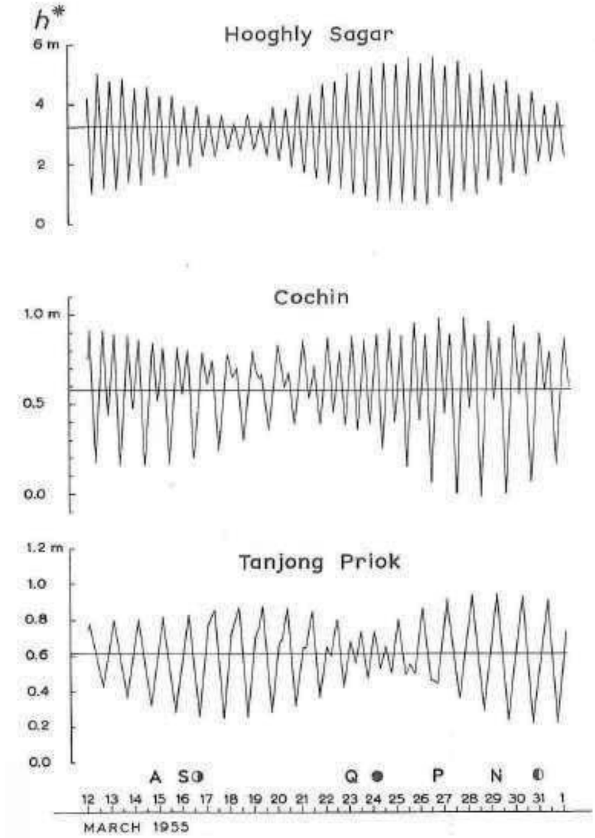

Figure 3.5: Semi-diurnal tides (upper panel), mixed tides (middle panel) and diurnal tides (lower panel) at three locations in south-east Asia (from: Dronkers [1])

velocity are far slower than in translatory waves and even significantly slower than in tides. In a first approximation, inertia can be neglected relative to resistance.

3.2 A condition for the long-wave approximation

By definition, 'long waves' have a wave length far greater than the depth in which they occur. As a consequence, the vertical particle accelerations are negligible, so that the pressure distribution can be considered to be hydrostatic. We shall derive a quantitative criterion for the validity of this basic assumption in the mathematical modelling of long waves.

It would not be sufficient to require that the vertical wave-induced acceleration be small relative to that of gravity (g). An additional requirement is that the wave-induced pressure variation be almost uniform in the entire vertical.

Consider a situation where the local water level is raised by an amount ζ from an undisturbed situation. If the pressure were hydrostatic, the piezometric level would be raised by the same

Bovenrijn / Waal

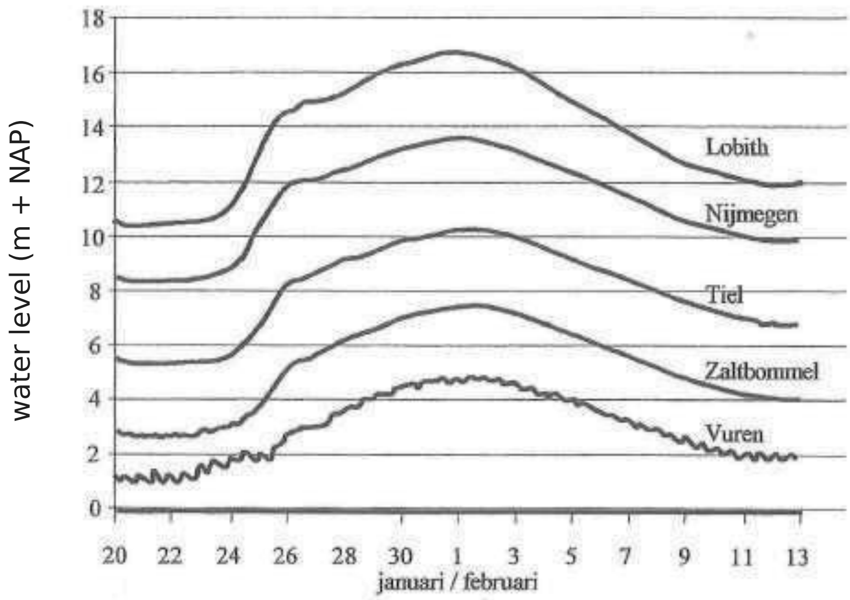

Nederrijn / Lek

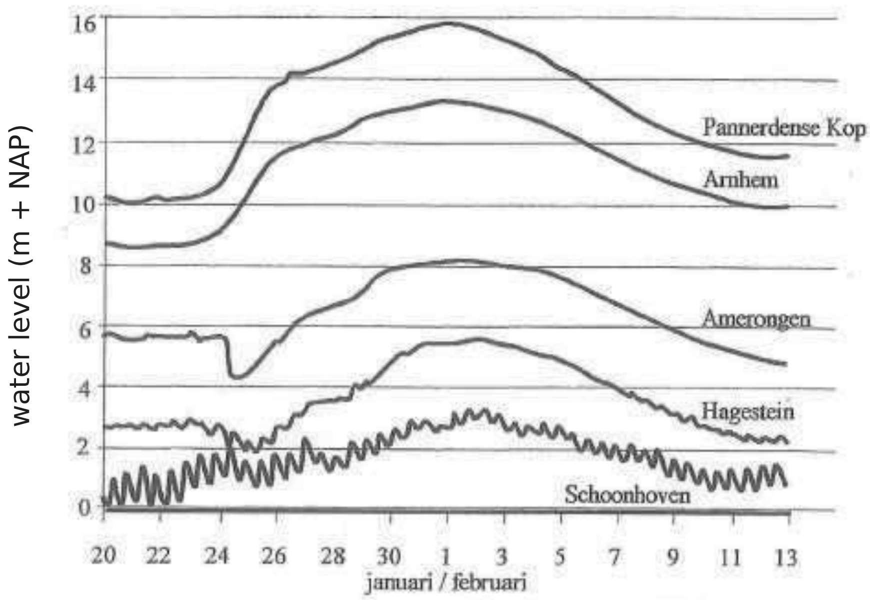

Figure 3.6: Water level records along the northern (upper panel) and the southern (lower panel) branch of the Rhine during high water of January/February 1995

amount in all points of the vertical (see Figure 3.7). Vertical accelerations ($a_z = \mathrm{D}w/\mathrm{D}t$,

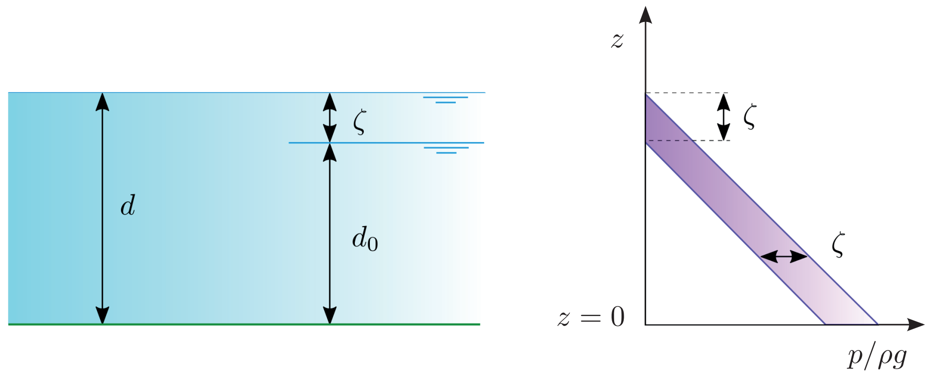

Figure 3.7: Hydrostatic pressure distribution

in which w is the vertical particle velocity) cause deviations from this hydrostatic pressure distribution. To quantify this, we use Euler's equation for the vertical motion:

$$a_z = -g\frac{\partial h}{\partial z} \tag{3.1}$$

It follows that the variation of the piezometric level from the bottom to the free surface ($\triangle h$) can be expressed as

$$\triangle h = \int_0^d \frac{\partial h}{\partial z}\,\mathrm{d}z = -\frac{1}{g}\int_0^d a_z\,\mathrm{d}z \tag{3.2}$$

The approximation of hydrostatic pressure is valid if this difference is negligible compared to the wave-induced variation ζ, or $|\triangle h| << |\zeta|$.

To elaborate this further, we assume a sinusoidal motion of the vertical free surface displacement with amplitude $\hat{\zeta}$ and (angular) frequency ω, as in $\zeta = \hat{\zeta}\cos\omega t$. Expressed in terms of amplitudes, the above inequality becomes

$$\int_0^d \hat{a}_z\,\mathrm{d}z << g\hat{\zeta} \tag{3.3}$$

The vertical motion dies out downward. Therefore, the left-hand side is smaller than $\hat{a}_{z,o}\,d$, in which $\hat{a}_{z,o}$ is the amplitude of the vertical acceleration at the surface, equal to $\omega^2\hat{\zeta}$. Therefore, a sufficient condition for the validity of (3.3) is

$$\hat{a}_{z,o}\,d \;<<\; g\hat{\zeta} \tag{3.4}$$

Because $\hat{a}_{z,o} = \omega^2\hat{\zeta}$, we finally obtain the following **condition for the validity of the approximation of hydrostatic pressure**:

$$\frac{\omega^2 d}{g} << 1 \tag{3.5}$$

A note on the length of a 'long' wave

As we shall see below, long waves in water with a free surface and depth d have a speed of propagation (c) approximately equal to $\sqrt{gd}$. If we substitute this with $c = L/T = L\omega/2\pi$ into Eq. (3.5) we obtain the condition for hydrostatic pressure in the following form:

$$L >> 2\pi d$$

In other words: the wavelength should be much larger than the depth. This explains and justifies the name 'long waves'. A commonly used criterion is $L \tilde{>} 20\,d$.

Let us now investigate the implications of the condition (3.5) for the most important categories of long waves.

Tsunami waves have much shorter periods (higher frequencies) than the tides. Nevertheless, most of the energy contained in them corresponds to periods long enough to treat them as long waves. Taking a period of 10 minutes as an example, and a typical ocean depth of 4000 m, the $\omega^2 d/g$ value is about 0.04, small enough to justify the long-wave approximation, even in the deep ocean. However, tsunamis may also contain some energy in higher frequencies, for which the long-wave approximation is not valid in ocean depths, requiring non-hydrostatic modeling.

Seiches have much shorter periods than the tides, but these are only important in much shallower waters than the oceans. For a seiche with a typical period of about 10 minutes ($\omega \simeq 0.01$ rad/s) in water of about 20 m deep, $\omega^2 d/g \simeq 2 \times 10^{-4}$, so that also for these oscillations the long-wave approximation is very well justified.

For the **tides**, we consider the semi-diurnal tide M_2 in the deepest ocean trough on earth, with a depth of approximately 10^4 m. The period of the M_2 tides is 12 hours and 25 minutes, corresponding to an angular frequency $\omega = 1.405 \times 10^{-4}$ rad/s. For these conditions, $\omega^2 d/g = 2 \times 10^{-5}$, so that even for these extreme depths the pressure in the tidal motion hardly deviates from being hydrostatic. Needless to say, this is even less the case in waters of more moderate depth. Therefore, the long-wave model is very well justified in tidal calculations.

Flood waves in rivers can vary on the time scale of days, in any case more slowly than tides, at least in the lower river reaches, and the depths are relatively small, so that the approximation of hydrostatic pressure is even better justified in these cases than it is for the tides.

Translatory waves which result from slow manipulations (in order to avoid damage) with weirs, valves, pumps etc. behave gradually, so that in those cases too the pressure can be assumed to be hydrostatic. However, in some cases, e.g. when they are the result of an accident, a sudden power outage, etc., they vary more rapidly, even as a shock wave. In such cases the long-wave assumption is locally invalid, but it can still be used in the stretches on either side. This is sufficient for the calculations if locally the shock conditions are used to connect the motions on either side of the shock wave.

Finally, it is obvious from (3.5) that this condition cannot be fulfilled by high-frequency (short-period) waves in waters of moderate or large depth. Examples are ship-generated waves and wind-generated waves, with periods of the order of seconds rather than minutes or hours. Take an example of wind-generated waves with a period of 6 s in water of 10 m depth. In that case, $\omega^2 d/g \simeq 1$, so that the pressure is not even approximately hydrostatic. Waves for which (3.5) is not (nearly) fulfilled are called **short waves**. These are the subject of a different class of theory than that for long waves. They are not considered here.

3.3 Estimation of terms

We are now going to investigate the relative importance of the different terms in the long-wave equations, in particular the equation of motion because that contains up to four terms which may bear ratios to each other of different orders of magnitude. This estimation does not have to be precise. What matters is to gain insight in the parameters determining which contributions (resistance, inertia, ..) are important in any given situation and which ones are so unimportant that they can be neglected in a first approximation.

We start from the equation of motion in acceleration form as derived in the previous chapter:

$$\frac{\partial U}{\partial t} + U\frac{\partial U}{\partial s} + g\frac{\partial h}{\partial s} + c_f\frac{|U|U}{d} = 0 \tag{3.6}$$

Here, we have replaced the hydraulic radius R by the cross-sectionally averaged flow depth d, which is justified for relatively flat cross-sections.

Advective acceleration term

We first consider the **advective acceleration** ($U\partial U/\partial s$) in relation to the **local acceleration** ($\partial U/\partial t$), initially for a conduit whose cross-section does not vary longitudinally (a prismatic conduit). Let $\mathcal{U}$ be a characteristic flow velocity and $\mathcal{L}$ a characteristic length scale, possibly a wave length if it exists, see also Figure 3.8. In that case, $U\partial U/\partial s$ is of the order of magnitude $\mathcal{U}^2/\mathcal{L}$. Likewise, $\partial U/\partial t$ is of the order $\mathcal{U}/\mathcal{T}$, where $\mathcal{T}$ is a characteristic time scale of the motion, such as a wave period (if it exists). In that case, the ratio of the advective acceleration to the local acceleration is of the order $(\mathcal{U}^2/\mathcal{L})/(\mathcal{U}/\mathcal{T})$, or $\mathcal{U}\mathcal{T}/\mathcal{L}$. The ratio $\mathcal{U}\mathcal{T}/\mathcal{L}$ can be interpreted geometrically as the ratio of the longitudinal particle displacement (of order $\mathcal{U}\mathcal{T}$) to the length scale of the flow ($\mathcal{L}$).

For waves in a prismatic conduit, the length scale $\mathcal{L}$ is determined by the flow, and coupled to $\mathcal{T}$ through the relation $\mathcal{L} = c\mathcal{T}$, in which c is the wave propagation velocity, see Figure 3.8, in which case $\mathcal{U}\mathcal{T}/\mathcal{L} = \mathcal{U}/c$. As we will see furtheron, $c = \sqrt{gd}$ for long waves, in which case $\mathcal{U}/c$ equals $\mathcal{U}/\sqrt{gd}$, the Froude number Fr. (Similarly, in compressible flows for which

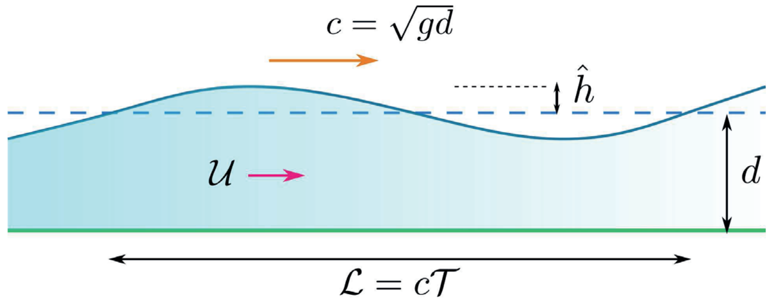

Figure 3.8: Schematic of scaling parameters

c is the speed of sound, U/c is the Mach number.) Therefore, we can say that the lower the Froude number, the smaller is the relative magnitude of the advective acceleration.

The preceding considerations apply in like manner to the momentum balance, Equation (2.10), implying that the term arising from the advection of momentum, $\partial(Q^2/A_c)/\partial s$, is negligible if $Fr^2 \ll 1$.

The ratio $\mathcal{UT}/\mathcal{L}$ also has an interesting link to the surface level amplitude ($\hat{h}$) which follows from scaling the continuity equation:

$$B\frac{\partial h}{\partial t} + \frac{\partial Q}{\partial s} = 0 \tag{3.7}$$

The terms $B\partial h/\partial t$ and $\partial Q/\partial s$ have orders of magnitude of $B\hat{h}/\mathcal{T}$ and $\mathcal{U}Bd/\mathcal{L}$, respectively, where B is the width of the channel. Since these terms equate it follows that $\hat{h}/\mathcal{T} = \mathcal{U}d/\mathcal{L}$ and, consequently, $\hat{h}/d = \mathcal{UT}/\mathcal{L} = Fr$.

For a given depth, therefore a given value of $\sqrt{gd}$, the Froude number (Fr) decreases with decreasing wave height. The ratio of the advective acceleration to the local acceleration decreases in like proportion. Therefore, **for relatively low waves ($\hat{h}/d \ll 1$) in a prismatic conduit,** $\mathcal{UT}/\mathcal{L} \ll 1$, implying that **the advective acceleration is relatively small and can be neglected in a first approximation**.

In harbour oscillations and offshore tidal currents, the flow velocity is seldom more than 0.5 m/s. If the depth there exceeds 10 m, the Froude number is below 0.05, implying that the advective acceleration can be neglected in a good approximation. In tidal entrances, estuaries etc., flow velocities typically exceed 1 m/s, so that in these flows the advective acceleration is of some importance. The same holds for tides in shallow water, such as over tidal flats, where the flow velocities may be less than in the channels but the depths are smaller. In such flows, the advective acceleration is still not dominant but at the same time not negligible.

Category	T (min)	ω (rad/s)	d (m)	$\hat{U}$ (m/s)	σ
Tsunami	10	1.0×10^{-2}	2000	0.1	2×10^{-5}
Tide in the ocean	745	1.4×10^{-4}	4000	0.3	2×10^{-3}
Seiche	20	5.0×10^{-3}	20	0.5	2×10^{-2}
Tide in shelf sea	745	1.4×10^{-4}	50	0.5	3×10^{-1}
Tide in channel	745	1.4×10^{-4}	15	1.0	2×10^{0}
Tide over flats	745	1.4×10^{-4}	2	0.7	1×10^{1}
River flood wave	7000	1.5×10^{-5}	5	2.0	1×10^{2}

Table 3.1: Estimation of terms for different long-wave types

A note on varying geometries

The preceding estimates were restricted to waves in prismatic conduits, in which the length scale is determined by the time scale and the propagation velocity through $\mathcal{L} = c\mathcal{T}$. In non-prismatic conduits, local variations in the geometry can force small length scales, such that $\mathcal{U}^2/\mathcal{L} \gg \mathcal{U}/\mathcal{T}$, or $\mathcal{U}\mathcal{T}/\mathcal{L} \gg 1$. In such conditions, the balance tips to the other side: the advective acceleration is locally dominant. Flows through or over control structures are good examples of this. In such cases, the local acceleration ($\partial U/\partial t$) is unimportant. Neglecting it causes the time variation to vanish from the equation of motion: the flow is being modelled as quasi-steady, which means that at any instant it has fully adapted to the instantaneous boundary conditions, as if these were not changing in time.

Resistance term

We now turn to the importance of the flow **resistance** relative to the local acceleration. We first consider oscillatory motions, as in tides and seiches, in which the flow velocity varies in time with amplitude $\hat{U}$ and frequency ω. The local acceleration ($\partial U/\partial t$) is of the order of $\omega\hat{U}$ whereas the resistance per unit mass in (3.6) is of order $c_f\hat{U}^2/d$. This yields the following result for the ratio of the resistance to the local acceleration, here denoted as σ:

$$\sigma = c_f \frac{\hat{U}}{\omega d} \tag{3.8}$$

The fraction $\hat{U}/(\omega d)$ allows for a simple physical interpretation: $\hat{U}/\omega$ is the amplitude of the horizontal displacement of the water particles, so that said fraction expresses how far the particles move back and forth relative to the flow depth.

Some typical, rounded values of σ have been collected in Table 3.1, using arbitrary but realistic value for the parameters, including $c_f = 0.004$. The entries have been placed in the order of ascending values of σ (see the exponents of σ in the rightmost column of the table).

In addition to periodic motions, flood waves in rivers have been included in the table. Although these are not periodic, they do have a characteristic time scale, which for major lowland rivers is of the order of several days. The time scale chosen in the table for a river flood wave corresponds to five nights and days, or about 9 times the period of the M_2 tide.

It is clear from the σ-values in Table 3.1 that resistance plays no role whatsoever in the instantaneous dynamics in tsunamis and seiches, while it is dominant for flood waves in rivers. For tides, the relative importance of resistance depends mainly on the water depth.

It is negligible in the oceans. Civil engineers mainly deal with tides in coastal waters, for which in general resistance is not negligible or (over tidal flats) even dominant compared to the local acceleration.

Translatory waves are not included in the table. These typically have a time scale of the order of minutes or even less, so that here resistance is unimportant for the instantaneous dynamics. However, because its effects is always to resist motion, its influence can and will be important in the long run. Therefore, when dealing with such motions over long durations, compared to the time scale of the primary variations, resistance should be included in the modeling.

Example 3.1. *Estimating terms*

Situation

A tidal wave in an estuary has a length scale (wave length) $\mathcal{L}$ of 500 km, a time scale (wave period) $\mathcal{T}$ of 12 hrs 25 min ($\approx$ 45,000 s) and a characteristic flow velocity $\mathcal{U}$ of 0.5 m/s. The depth d is about 20 m and the resistance coefficient c_f equals 0.004. See also Figure 3.8.

Questions

Give order of magnitude estimates for:

1. the local acceleration term: $\partial U/\partial t$
2. the advective acceleration term: $U\partial U/\partial s$
3. the resistance term: $c_f|U|U/d$

What can you conclude regarding the importance of the various terms?

Solution

Velocity variations are of order $\mathcal{U}$ over a time interval $\mathcal{T}$ and a spatial interval $\mathcal{L}$, respectively, yielding the following estimates:

1. local acceleration term: $\mathcal{U}/\mathcal{T} = (0.50 \text{ m/s})/(45{,}000 \text{ s}) \approx 1.1 \times 10^{-5} \text{ m/s}^2$.
2. advective acceleration term: $\mathcal{U}^2/\mathcal{L} = (0.50 \text{ m/s}) \times (0.50 \text{ m/s})/(500{,}000 \text{ m}) \approx 5.0 \times 10^{-7} \text{ m/s}^2$.
3. resistance term: $c_f\mathcal{U}^2/d = 0.004 \times (0.50 \text{ m/s}) \times (0.50 \text{ m/s})/(20 \text{ m}) \approx 5.0 \times 10^{-5} \text{ m/s}^2$.

Comment

The resistance term is most important in this case, but the local accelaration term cannot be neglected. The advective acceleration however is two orders of magnitude smaller than the resistance term and can be safely omitted at first.

3.4 Solution methods

Complete equations

The complete long-wave equations, Equations (2.11) and (2.12), are the basis of a large number of numerical codes for the calculation of unsteady flows in open channels or closed conduits, such as DuFlow (used by the Dutch water boards), SOBEK (Delftares) and MIKE11 (Danish Hydraulics). Here, 'complete' refers to the fact that the equations have not been simplified by neglecting *a priori* terms which are expected to be small in a given application. Therefore, such codes are suited, in principle, for all kinds of long-wave phenomena, provided these can be modelled as one-dimensional, which of course in itself is an approximation. Where this is not justified, one must resort to the long-wave equations in two horizontal dimensions.

In the codes referred to, the long-wave equations are integrated in discretized form. Those techniques, the problems that may be encountered, and the accuracy that can be achieved are dealt with in the introductory numerical modeling examples throughout this book. Reference is made to the master course 'Computational Modelling of Flow and Transport' (CIE4340) for a more extensive treatment of this subject [3].

Simplified equations

Based on the complete set of long-wave equations, various simplified forms have been developed and solved in order to obtain insight through simple calculations or analytical solutions. Each of those is tuned to a specific subset of long-wave problems for which certain terms in the equations of motion are estimated beforehand to be small, as was done in Section 3.3. By neglecting them, a simplified model results, which may allow analytical, preferably explicit solutions. The present course focusses on these simplified models and their solutions because the primary purpose is to obtain insight in the dynamics of various long-wave phenomena that may be encountered in engineering practice. If and when more accurate quantitative answers are needed, one must resort to a validated numerical code.

The following subjects of wave propagation are dealt with in the remaining chapters:

- elementary wave equation, applicable to low, rapid phenomena: advective acceleration and flow resistance are neglected (Chapter 4).
- translatory waves: advective acceleration can be included; resistance neglected (Chapter 5).
- method of characteristics, showing fundamentals of wave propagation: particularly suited to high translatory waves; advective acceleration not neglected; resistance can be included but that is cumbersome (Chapter 6).
- harmonic method, suited for low-amplitude oscillatory progressive or standing waves such as seiches and tides: advective acceleration neglected, resistance included in linearized form (Chapter 8).
- flood waves in rivers: various approximations, inertia neglected (Chapter 9).

In addition, two chapters deal with highly reduced cases: storage in a short basin, in which inertia is negligible (Chapter 7), and flow through or over control structures in which storage is negligible (Chapter 10). In both cases the motion is unsteady but not wavelike.

Bibliography

[1] J. J. Dronkers. **Tidal computations in rivers and coastal waters**. North-Holland Publishing Company, 1964.

[2] A. S. Tijsseling. **Fluid-structure interaction in case of waterhammer with cavitation**. PhD thesis, 1993.

[3] M. Zijlema. Computational Modelling of Flow and Transport, Course reader CIE4340, 2012.

Problems

1. What are 'long waves'?
2. Derive a condition for the validity of the long-wave approximation.
3. Mention a few categories of wave phenomena that belong to the class of long waves.
4. Check for each of these to which extent the long-wave approximation is justified.
5. For each of these, choose some characteristic, realistic values of the most relevant parameters such as depth, flow velocity and time scale, and estimate the corresponding values of the ratios of various terms in the equation of motion.
6. What are so-called translatory waves?
7. Do these occur in open channels as well as in closed conduits?
8. Are they normally the result of natural processes or human intervention?
9. Argue why resistance is relatively unimportant in translatory waves.
10. What are seiches?
11. What is in general the cause of seiches?
12. Do seiches in essence belong to the class of progressive waves or to the class of standing waves?
13. Seiches in a given basin cannot have arbitrary frequencies. Why not?
14. Which mechanism is the major cause of energy loss of seiches?
15. Mention a few effects of seiches that may be a nuisance in practice, possibly causing damage.
16. Is resistance important in all kinds of tidal phenomena? In which subclass is it not? In which is it important, possibly even dominant?

17. The major tide in the North Sea is the semi-diurnal tide M_2, with a period of approximately 12 hours and 25 minutes. Do the major tides in all seas and oceans on earth have the same period? If not, why not?

18. Under which condition(s) is the so-called advective acceleration negligible?

Chapter 4

Elementary wave equation

The considerations and analyses in this chapter are based on a strongly reduced set of equations, viz. those for the modelling of **low, long waves without resistance**. We assume a horizontal open channel without longitudinal variations in the channel geometry. Theoretically, the channel does not have to be straight, but for simplicity we refer to it as a prismatic channel. We account for storage and (local) inertia while neglecting advective accelerations (consistent with the restriction to low waves) and resistance (restricting the validity of the results to rapid variations).

4.1 Elementary wave in open water

Before dealing with the introduction of a general wave equation, we consider a relatively simple elementary case, viz. the transition between two regions with a uniform flow in each, different in the two regions. We assume that the transition travels without change with a constant propagation velocity c. The fact that this is possible (within the assumed model equations) is proven below. We choose a mathematical formulation in terms of the disturbance δh of the initially horizontal free surface level (h_0) in the undisturbed region: $h(s,t) = h_0 + \delta h(s,t)$. Similarly, we have $Q(s,t) = Q_0 + \delta Q(s,t)$.

We start with a qualitative description of the disturbances resulting from the partial opening of a gate between two reaches of a prismatic channel in which initially the water is at rest, with different free surface levels on either side of the gate, see Figure 4.1. The gate is raised gradually over a certain height after which the opening is held constant.

As a result of the head difference across the gate, a discharge develops through the gate as soon as the gate is (partially) opened. Water is withdrawn from the high-water side, resulting in a lowering of the free surface adjacent to the gate, and added to the low-water side, where it causes a rise in the water surface on that side of the gate. These disturbances travel away from the gate into the adjacent channel reaches with velocity c, growing in height with increasing opening of the gate. Once the opening is constant, the discharge and the water levels adjacent to the gate remain constant.

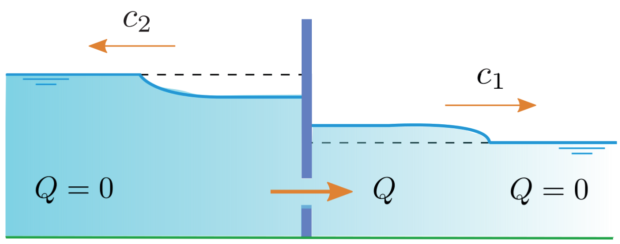

Figure 4.1: Disturbances in a canal resulting from the partial opening of a gate

Propagation of a disturbance

Let us now consider the propagation of the disturbance into a channel reach, starting with the low-water side, which experiences inflow and a rise in water level. We recognize three regions: an undisturbed region, a region of established uniform flow adjacent to the gate, and a traveling transient or wave front between them (Figure 4.2).

Thanks to the slope of the free surface in the wave front, a pressure gradient exists there which causes an acceleration of the water particles in the direction from the high-water side to the low-water side, indicated in the figure with a double arrow. At a given location, the water is initially at rest, while it accelerates during the passage of the wave wave front. Once the front has passed that location, the local free surface is again horizontal, the pressure gradient is zero, and the flow velocity is constant (we ignore flow resistance). As a result

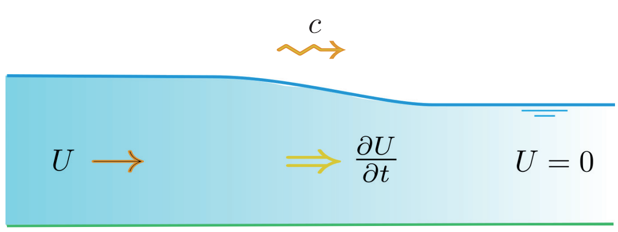

Figure 4.2: Accelerations ($\Rightarrow$), flow velocities ($\rightarrow$) and propagation velocity ($\rightsquigarrow$) in a positive wave

of the difference in flow velocity across the transient, the passage of the transient causes a longitudinal compression of the water beneath it. Since water is almost incompressible, this longitudinal compression is compensated by a rise of the free surface. Because the wave considered here causes a rise in water level at a fixed point, we call it a positive wave. (In the analogous case in gas dynamics, we refer to a compression wave.)

On the upstream side of the gate, water is withdrawn, resulting in a lowering of the free surface: a negative wave. Notice that here the acceleration is again to the right, but now this is against the direction of wave propagation (Figure 4.3). Passage of this transient causes the particle velocities to go from zero to positive, opposite to the direction of wave propagation.

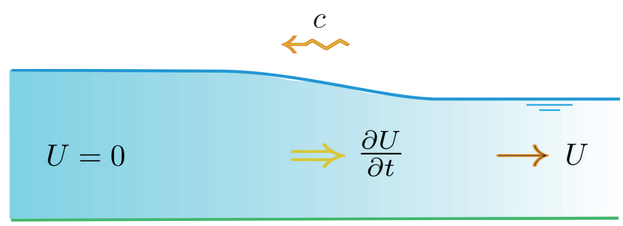

Figure 4.3: Accelerations (⇒), flow velocities (→) and propagation velocity (⇝) in a negative wave

Balance equations

Following the qualitative description given above, we will now quantify the arguments. We could start from the long-wave equations, which form a set of Partial Differential Equations (PDE's), but at this stage we prefer an algebraic formulation based on balance equations for a finite control volume between two fixed cross-sections on either side of the transient. We restrict ourselves to a low disturbance which causes small variations in the elevation of the free surface (δh), the discharge (δQ) and the flow velocity (δU).

We consider the balances of mass and momentum during a time interval with duration Δt (Figure 4.4). We neglect compressibility of the water, so that the mass balance reduces to a volume balance. We further assume that the transient travels without change in shape (to be validated afterwards).

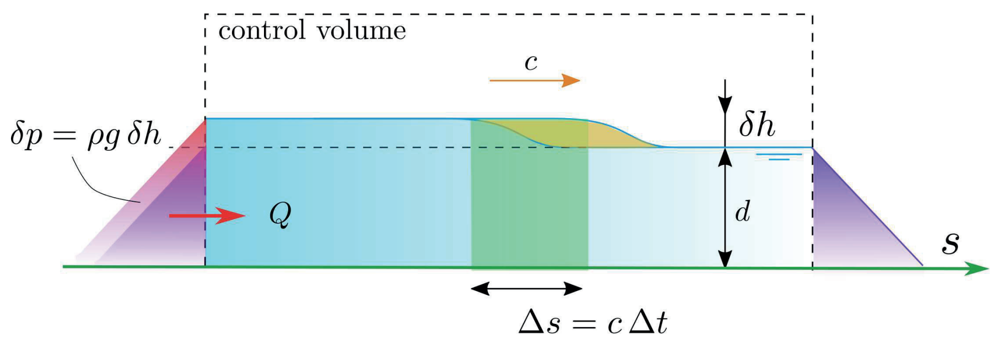

Figure 4.4: Control volume containing the transient

Volume balance

This balance equates the net inflow of water, due to the difference in discharge δQ, to the storage at the free surface (the yellow area in Figure 4.4) over a (storage) width B and a rise in surface elevation δh, occurring in a finite time interval Δt:

$$\text{net inflow} = \delta Q \Delta t = \text{storage} = B \delta h \Delta s = B \delta h \, c \Delta t$$

or

$$\boxed{\delta Q = Bc\,\delta h} \tag{4.1}$$

Momentum balance

The rise of the free surface (δh) gives rise to a pressure difference across the control volume given by $\rho g\,\delta h$, resulting in a net horizontal force on the flowing mass in the control volume equal to $\rho g A_c\,\delta h$. Here, we have neglected the small contribution at elevations above the undisturbed free surface (the small triangle in the figure).

Because of the restriction to a low disturbance, the advection of momentum, which is proportional to the square of the flow velocity, is negligible compared to the contribution by the wave-induced hydrostatic pressure.

During the time interval with duration $\triangle t$, the momentum inside the control volume (initially zero) increases with the amount $\rho\,\delta U A_c \Delta s = \rho\,\delta Q\,c\,\Delta t$ (see the green area in the figure, extending from the bottom to the free surface). The momentum balance becomes:

$$\text{momentum delivered} = \rho g A_c\,\delta h \Delta t = \text{momentum gained} = \rho\,\delta Q\,c\,\Delta t$$

or

$$\delta Q = \frac{gA_c}{c}\delta h \tag{4.2}$$

Elimination of δQ from these equations yields the following important result for the long wave propagation speed:

$$\boxed{c = \sqrt{\frac{gA_c}{B}}} \tag{4.3}$$

Since $\delta Q = A_c\,\delta U$, Equation (4.2) can be expressed in terms of the flow velocity as

$$\boxed{\delta U = \frac{g}{c}\,\delta h} \tag{4.4}$$

If the total cross-section contributes fully to the conveyance, $A_c/B = A_c/B_c = d$, in which case the expression for the propagation speed reduces to

$$\boxed{c = \sqrt{gd}} \tag{4.5}$$

The expression for the flow velocity can then be written as

$$\boxed{\delta U = \frac{c}{d}\,\delta h} \tag{4.6}$$

This also follows directly from Equation (4.1).

The results derived here are valid only for (very) low waves ($Fr \ll 1$). They are used frequently in the following.

Example 4.1. *Translatory wave following gate openening*

Situation	Solution
As the result of a gate having been raised, a positive wave, with a rise in surface elevation (δh) of 0.15 m, propagates in a canal with an initial depth (d) of 5 m, a storage width (B) of 135 m and conveyance width (B_c) of 100 m, where the water is initially at rest. **Questions** 1. compute the wave speed c 2. compute the discharge Q through the gate 3. compute the flow velocity U behind the wave 4. compute the ratio of the advective momentum transfer ($\rho U^2 A_c$) relative to the pressure force ($\rho g A_c\, \delta h$)	Because the water is initially at rest, the total discharge following the passage of the transient (Q) equals δQ. For brevity, we will use the notation Q in the following. 1. wave speed: $c = \sqrt{gA_c/B} = \sqrt{gdB_c/B}$ 6.0 m/s 2. discharge: $Q = Bc\,\delta h = 122$ m^3/s 3. flow velociy: $U = Q/A_c = 0.24$ m/s; this result also follows from $U = (g/c)\,\delta h = 0.24$ m/s. 4. ratio of the advection of momentum relative to the pressure force: $U^2/g\,\delta h = 0.04$. **Comment** In the derivation given above, the advection of momentum was neglected relative to the pressure force. With the ratio of these respective terms being equal to 0.04 this assumption is indeed justified in this example.

4.2 Elementary wave equation

In this section, we derive and analyse an equation for long, low, frictionless waves in a prismatic conduit. It will appeare that the simple wave of the preceding section is an important building block in the solution of this wave equation.

Open channel flow

The continuity equation is given by Equation (2.11), which for easy reference is repeated here:

$$B\frac{\partial h}{\partial t} + \frac{\partial Q}{\partial s} = 0 \tag{4.7}$$

It is important to note that B is the full width of the free surface, available for storage, not the width of only the conveyance cross-section.

On account of the simplifying assumptions mentioned above, the equation of motion, Equation (2.12), reduces to

$$\frac{\partial Q}{\partial t} + gA_c\frac{\partial h}{\partial s} = 0 \tag{4.8}$$

In view of the assumption of low waves, the influence of a varying free surface elevation on the parameters B and A_c will be neglected. Mathematically speaking, we then deal with **a**

set of two first-order linear partial differential equations (PDE's) with constant coefficients. These allow relatively simple solutioins, compared with nonlinear equations with variable coefficients.

We now eliminate Q by differentiating Equation (4.7) with respect to t and (4.8) to s, with the result

$$\frac{\partial^2 h}{\partial t^2} - \frac{gA_c}{B}\frac{\partial^2 h}{\partial s^2} = 0 \tag{4.9}$$

Note that this equation is of second order as a result of including storage (through Equation (4.7)) and inertia (through Equation (4.8)). The interplay of these allows wave propagation, as we will see.

Next, we ignore temporarily the findings of the preceding section, in particular the results for the propagation speed, and for brevity *define* a quantity c by

$$c \equiv \sqrt{\frac{gA_c}{B}} \tag{4.10}$$

Substitution of this into Equation (4.9) yields

$$\boxed{\frac{\partial^2 h}{\partial t^2} - c^2\frac{\partial^2 h}{\partial s^2} = 0} \tag{4.11}$$

Elimination of h instead of Q would have given a similar PDE for the variable Q.

Pressurized pipe flow

In this case, we start from the mass balance (2.37) and the momentum balance (2.38) derived in Chapter 2. We neglect the advective terms and the resistance. A similar operation as given above for free-surface flows leads again to (4.11), now with p instead of h:

$$\frac{\partial^2 p}{\partial t^2} - c^2\frac{\partial^2 p}{\partial s^2} = 0 \tag{4.12}$$

with c defined by

$$\frac{1}{c^2} = \frac{\rho}{K} + \frac{\rho D}{E\delta} \tag{4.13}$$

General wave equation

A PDE with the form of (4.11) or (4.12) is known as 'the' wave equation because it is the most elementary form of all wave equations. Although it applies to pressurized flows as well as free-surface flows, we deal exclusively with the latter in the following. The methods and solutions are transferable to pressurized flows. Notice that the wave equation (4.11) is linear, so that linear superposition applies: **a sum of solutions is also a solution**.

4.3 General solution

Without derivation, we now state that the general solution $h(s,t)$ of (4.11) consists of the sum of an arbitrary function h^- of $(s+ct)$ and an arbitrary function h^+ of $(s-ct)$:

$$\boxed{h(s,t) = h^+(s-ct) + h^-(s+ct)} \tag{4.14}$$

See for instance [1]. A similar expression applies to Q in terms of Q^+ and Q^-.

The wave equation (4.11) is linear. Therefore, in order to prove that the sum given by (4.14) is a solution, it is sufficient to prove this for h^+ and h^- separately. We begin with h^+. This function depends on s and t exclusively through the combination $s-ct$, which quantity we will represent as S^+, so $S^+ = s - ct$. Therefore, $h^+ = h^+(S^+)$, and because $\partial S^+/\partial s = 1$ and $\partial S^+/\partial t = -c$, it follows that

$$\frac{\partial h^+}{\partial s} = \frac{\mathrm{d}h^+}{\mathrm{d}S^+}\frac{\partial S^+}{\partial s} = \left(h^+\right)' \quad \text{and} \quad \frac{\partial h^+}{\partial t} = \frac{\mathrm{d}h^+}{\mathrm{d}S^+}\frac{\partial S^+}{\partial t} = -c\left(h^+\right)' \tag{4.15}$$

in which the prime on h^+ indicates an ordinary derivative of h^+ with respect to S^+. Continuing likewise, we obtain

$$\frac{\partial^2 h^+}{\partial s^2} = \left(h^+\right)'' \quad \text{and} \quad \frac{\partial^2 h^+}{\partial t^2} = c^2\left(h^+\right)'' \tag{4.16}$$

Substitution of these two expressions into the wave equation (4.11) shows that the latter is satisfied by any function $h^+ = h^+(S^+) = h^+(s-ct)$. The same applies to h^- and therefore also to their sum, which was to be proven.

We will now investigate the meaning of the solution, first for h^+ only. The latter depends on s and t solely through S^+, or through $s-ct$. Therefore, we will observe no change in the local value of h^+ if we keep $s-ct$ constant in time, i.e. $\mathrm{d}s/\mathrm{d}t = c$, i.e. if we move in the positive s-direction with speed c. Stated another way: a point of constant h^+ moves with speed c in the positive s-direction. That is why the subscript + was chosen for this function. Because c is a constant in the present approximationin, all points of the disturbance h^+ move with the same speed: the disturbance propagates without change of shape with velocity c, whose value is given by Equation (4.10).

Likewise, it can be shown that the function h^- represents a wave moving at speed c in the negative s-direction without change of shape.

It follows from the above that Equation (4.14) obeys the wave equation (4.11). It can be shown also that it represents **the general solution** to this equation, which therefore consists of **two waves, propagating in opposite directions at a constant speed c without change in shape**. Needless to say, where both are present simultaneously, their sum does vary in shape. Whether such superposition actually occurs depends on the initial conditions and boundary conditions.

Total derivative

The property of propagation without change in the local value of a disturbed quantity (for the + and - waves separately) can be formulated differently, in a manner that we shall use more in the following. To this end, the concept of the total derivative is important.

Suppose an observer travels with a velocity V in the s-direction, observing the local values of a quantity h. The change in h which he observes in a time interval with duration Δt can be expressed as

$$\Delta h = \frac{\partial h}{\partial t}\Delta t + \frac{\partial h}{\partial s}\Delta s = \frac{\partial h}{\partial t}\Delta t + \frac{\partial h}{\partial s}\, V \Delta t \tag{4.17}$$

The observed change per unit time, in the limit as $\Delta\, t$ goes to zero, is the so-called **total derivative** of h:

$$\frac{\mathrm{d}h}{\mathrm{d}t} = \frac{\partial h}{\partial t} + V\frac{\partial h}{\partial s} \tag{4.18}$$

Now consider h^+. It follows from Equation (4.15) that it obeys

$$\frac{\partial h^+}{\partial t} + c\,\frac{\partial h^+}{\partial s} = 0 \tag{4.19}$$

Comparison with Equation (4.18) shows that the left-hand side of Equation (4.19) is the total derivative of h^+ for an observer moving with velocity c, which is zero according to Equation (4.19). Therefore, this observer sees no change in the local value of h^+. Since this reasoning applies to all points of the disturbance, and the value of c is common to all of them (in the present approximation for low waves!), we conclude that Equation (4.19) implies that the disturbance h^+ travels in the positive s-direction at speed c without change in shape.

Another representation, equivalent to Equation (4.19), is

$$\boxed{\frac{\mathrm{d}h^+}{\mathrm{d}t} = 0 \quad \text{provided that} \quad \frac{\mathrm{d}s}{\mathrm{d}t} = c} \tag{4.20}$$

In this formulation, the *partial* differential equation (4.19), for a single dependent variable h^+ and two independent variables s and t, is replaced by a set of two *ordinary* differential equations for the two dependent variables h^+ and s and one independent variable t. Likewise, the following is valid for h^-:

$$\boxed{\frac{\mathrm{d}h^-}{\mathrm{d}t} = 0 \quad \text{provided that} \quad \frac{\mathrm{d}s}{\mathrm{d}t} = -c} \tag{4.21}$$

This kind of formulation will be used extensively in Chapter 6, dealing with the so-called method of characteristics.

4.4 Relation between discharge and free surface elevation in a progressive wave

Variations in discharge and related variations in the free surfae elevation have been considered in section 4.1, using algebraic balance equations for mass and momentum in a finite control volume. Here, we return to that matter using the wave equation, applied to an arbitrary but low wave propagating in the positive s-direction into a region of uniform flow with depth d and discharge Q_0, a so-called simple wave. The corresponding water level h^+ obeys Equation (4.19). Substitution of this equation into the continuity equation (4.7) yields

$$-Bc\,\frac{\partial h^+}{\partial s} + \frac{\partial Q^+}{\partial s} = 0 \tag{4.22}$$

Integration of this with respect to s for constant Bc gives $Q^+ - Bc\,h^+ = \text{constant} = Q_0 - Bc\,h_0$. Expressed in terms of the changes with respect to the undisturbed situation, namely $\delta h^+ = h^+ - h_0$ and $\delta Q^+ = Q^+ - Q_0$, this becomes:

$$\boxed{\delta Q^+ = Bc\,\delta h^+} \tag{4.23}$$

A similar result applies to h^-:

$$\boxed{\delta Q^- = -Bc\,\delta h^-} \tag{4.24}$$

We can express these results in terms of flow velocity rather than discharge. Since $Q = A_c\,U$, we also have $\delta Q = A_c\,\delta U$, neglecting variations in A_c, as is justified for sufficiently low waves. Using this result in (4.23) and (4.24) we obtain

$$\boxed{\delta U^\pm = \pm\frac{Bc}{A_c}\,\delta h^\pm \quad \text{or} \quad \delta U^\pm = \pm\frac{g}{c}\,\delta h^\pm} \tag{4.25}$$

If $B = B_c$, this reduces to

$$\delta U^\pm = \pm\frac{c}{d}\,\delta h^\pm \quad \text{or} \quad \delta U^\pm = \pm\sqrt{\frac{g}{d}}\,\delta h^\pm, \tag{4.26}$$

respectively. Note the resemblance between these results and those obtained in Section 4.1.

4.5 Solution for arbitrary initial situation

Because the wave equation is of second order in time, two initial conditions are needed for a well-posed problem. Here, we use the initial values of the disturbances in surface elevation (δh) and discharge (δQ) at all points of the channel considered, relative to an undisturbed state with uniform water level and discharge.

In section 4.1, a disturbance traveling in the positive s-direction was considered. In the present section we consider the more general case of given arbitrary (low) values of δh and δQ as functions of s for some initial instant $t = t_0$:

$$\delta h_0\left(s\right) = \delta h\left(s; t_0\right) \quad \text{and} \quad \delta Q_0\left(s\right) = \delta Q\left(s; t_0\right) \tag{4.27}$$

In order to determine the time evolution of this arbitrary disturbance, not necessarily traveling in one direction only, we separate it into two contributions that each do travel in one direction only:

$$\delta h = \delta h^+ + \delta h^- \quad \text{and} \quad \delta Q = \delta Q^+ + \delta Q^- = Bc\left(\delta h^+ - \delta h^-\right) \tag{4.28}$$

It follows from these equations that

$$\delta h^+ = \frac{1}{2}\left(\delta h + \frac{\delta Q}{Bc}\right) \quad \text{and} \quad \delta h^- = \frac{1}{2}\left(\delta h - \frac{\delta Q}{Bc}\right) \tag{4.29}$$

At the initial instant $t = t_0$, the values in the right-hand sides of (4.29) are known as functions of s. The same then holds for the initial values of δh^+ and δh^-. By translating the initial profile of δh^+ with speed c in the positive s-direction, and the initial profile of δh^- with speed c in the negative s-direction, and adding the results at each position for a chosen instant, the free-surface profile at that instant is found. The same method applies to the discharge.

If the water is at rest at the initial instant, the initial values of δh^+ and δh^- at each location are equal to half the local value of $\delta h_0(x)$, as follows from Equation (4.29). Figure 4.5 gives an example for this case.

The preceding results are restricted to low waves, described by the linear wave equation, which allows linear superposition of elementary waves travelling in opposite directions to find the total solution. If the restriction to low waves is relaxed, linear superposition no longer applies, but we can still construct the total solution by considering component-waves traveling in opposite directions, using the so-called method of characteristics. This is the subject of Chapter 6.

In the above, we have tacitly assumed that the disturbances can travel unimpeded in a prismatic channel, as if this were infinitely long. If and when the disturbance reaches a location where the channel geometry changes, reflection occurs. This is considerd below.

4.6 Boundary conditions

Because the wave equation is of second order in space (s), two boundary conditions are needed for a well-posed problem.

Where the canal has a **closed end**, at $s = s_c$ say, the discharge must be zero at all times.

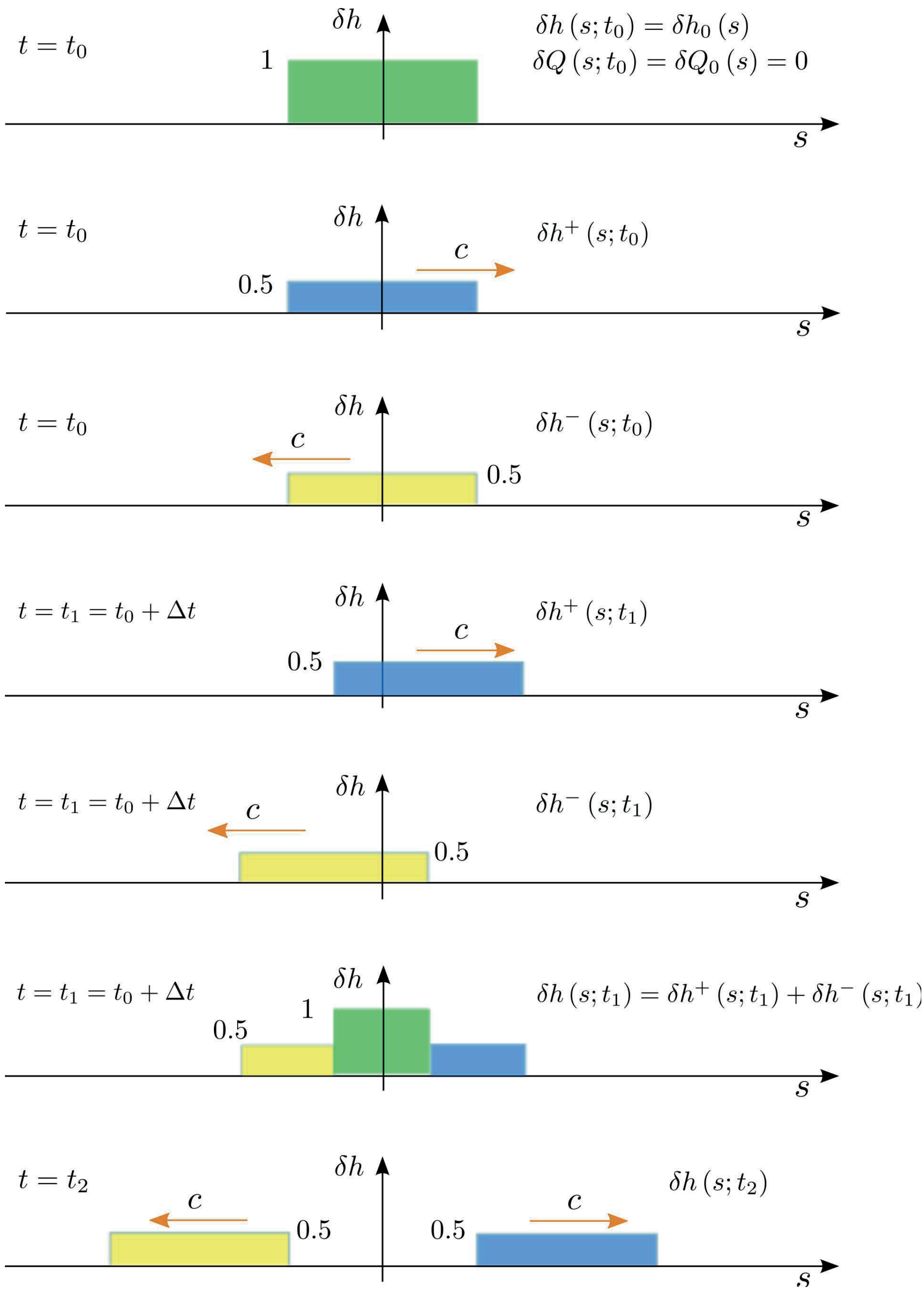

Figure 4.5: Elementary wave solution for an initial discharge $\delta Q_0 = 0$ and an initial water level elevation δh_0 over a finite length

Mathematically, this is expressesd as the boundary condition $Q(s_c, t) = 0$ for all times. In view of (4.28), this implies that $\delta h^- = \delta h^+$ at that location. In words: where an incident wave (δh^+), travelling in the positive s-direction, meets a closed end, a backward propagating wave (δh^-) is generated whose height at the closed end equals that of the incident wave at that location at all times. At the closed end, the free surface elevation is doubled. We say that **at a closed end, total positive reflection occurs**. (The qualification 'positive' refers to the free surface elevation. The discharge is in fact negatively reflected because $\delta Q^- = -\delta Q^+$ at the closed end.)

The opposite situation occurs if the canal at some point, at $s = s_0$, say, has an **open end** where it connects to a large, deep sea or reservoir in which the water level is not affected by inflow into or outflow from the canal. This means that $\delta h(s_0, t) = 0$ at all times, implying that $\delta h^-(s_0, t) = -\delta h^+(s_0, t)$: **at an open end, total negative reflection occurs**. It follows from (4.28) that at such open end, $\delta Q^- = \delta Q^+$, so that there the discharge is positively reflected. Thus, the discharge at an open end is doubled.

Partial reflection of translatory waves at transitions in channel geometry is considered in Chapter 5.

A note on non-reflective boundaries

Numerical or physical models of flow in canals or rivers are often cut-off at some distance from the study area, even when in reality the system extends further. Such cut-off creates an artificial, **open model boundary**. The condition to be imposed there is that disturbances approaching that boundary from within the study area should not be reflected, so as to simulate reality in which the disturbances continue unimpeded. Thus, if the positive s-direction is from within towards the open boundary, δh^- should be zero at the open boundary at all times, implying the boundary condition $\delta Q - Bc\,\delta h = 0$, see Equation (4.29).

4.7 Periodic progressive and standing waves

This section deals with low, sinusoidal waves in a prismatic canal or basin. For brevity, we denote the elevation of the free surface above its mean value as ζ. Its amplitude is written as $\hat{\zeta}$, the wave period is T, and the angular frequency (i.e. the phase change per unit time) is $\omega = 2\pi/T$. The wave length is L and the wave number (i.e. the phase change per unit propagation distance) is $k = 2\pi/L$.

If the wave is progressive, we have $L = cT$ in which c is the speed of propagation. Since we deal with free long waves, $c = \sqrt{gA_c/B}$ (or $\sqrt{gd}$ in two-dimensional motion), so that $L = \sqrt{gA_c/B}\,T$. Written in terms of frequency and wave number, this becomes

$$\boxed{\frac{\omega}{k} = \sqrt{\frac{gA_c}{B}} \; (= c)} \qquad (4.30)$$

This is the so-called **dispersion equation**, linking frequency and wave number for the system considered. Note that it also applies to the superposition of two waves with the same frequency and wave number, as in the case of standing waves, even though the notion of a propagation speed does not apply to the latter category.

Infinitely long canal

In a prismatic canal of infinite length (in practice: in a long canal, away from the influence of boundaries), waves can propagate indefinitely in either direction without reflection, so-called **progressive waves**. We assume a sinusoidal wave to be propagating in the positive s-direction with speed c. The free surface elevation above the mean water level can then be written as

$$\zeta = \hat{\zeta} \cos\left(2\pi \frac{s - ct}{L}\right) \tag{4.31}$$

Written in terms of frequency and wave number, this becomes

$$\zeta = \hat{\zeta} \cos\left(ks - \omega t\right) \tag{4.32}$$

The corresponding discharge is given by

$$Q = Bc\hat{\zeta} \cos\left(ks - \omega t\right) \tag{4.33}$$

Note that for an observer moving at a speed $\mathrm{d}s/\mathrm{d}t = \omega/k$, the phase $ks - \omega t$ is constant. That is why this speed ω/k is called the **phase speed**. An observer moving at this speed sees no variation in the local value of ζ and that of Q.

In a progressive wave as described above, the surface elevation and the discharge (reckoned positive in the propagation direction) are in phase, i.e. at each location they reach their maximum values at the same time.

For a wave progressing in the negative s-direction, we have

$$\zeta = \hat{\zeta} \cos\left(ks + \omega t\right) \tag{4.34}$$

and

$$Q = -Bc\hat{\zeta} \cos\left(ks + \omega t\right) \tag{4.35}$$

In this case, the surface elevation and the discharge are 180 degrees out of phase (in opposite phase), i.e. at each location the maximum of one occurs at the same time as the minimum of the other. In other words, under the crests of the wave, where the surface elevation has its maximum, the discharge is minimal (maximal in an absolute sense, but in the negative s-direction).

When both waves, with equal frequency and amplitude, but propagating in opposite directions, are present simultaneously in the same canal, the resulting motion is given by superposition of the preceding expressions, with the result

$$\zeta = 2\hat{\zeta} \cos ks \cos \omega t = \hat{\zeta}_{st} \cos ks \cos \omega t \tag{4.36}$$

This expression represents a **standing wave** because as time goes on the resulting profile does not move foreward or backward; it merely breathes up and down (see Figure 4.6 b). The maximum amplitude of its surface elevation, $\hat{\zeta}_{st}$, is twice the amplitude of the two opposing component progressive waves of which it consists.

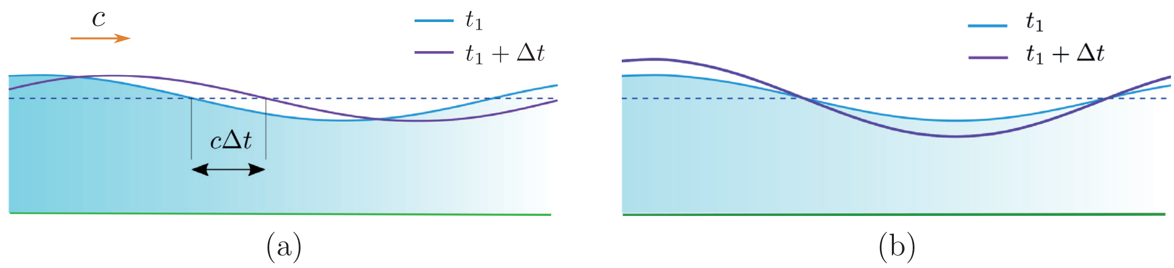

Figure 4.6: Progressive (a) and standing (b) periodic waves in infinitely long canal

The corresponding discharge is given by

$$Q = 2Bc\hat{\zeta} \sin ks \sin \omega t = Bc\hat{\zeta}_{st} \sin ks \sin \omega t \tag{4.37}$$

We see that in a standing wave, the surfac elevation and the discharge are 90 degrees ($\pi/2$ radians) out of phase, both in s and in t (they are in quadrature).

At the locations where $\cos ks = 0$, the surface elevation is zero at all times. Those points are called **nodes**. The distance between adjacent nodes is one half wave length. At these locations, the local amplitude of the discharge is maximal.

At the locations where $\cos ks = \pm 1$, the local amplitude of the surface elevation is maximal, but the discharge is zero at all times. These points are called **antinodes**. The distance between adjacent antinodes is one half wave length.

In an infinitely long canal, progressive waves and standing waves can exist without constraints on the frequency and wave number or (in case of standing waves) on the locations of the nodes and antinodes. This changes when the canal (or basin) is semi-infinitely long, or has a finite length, as considered in the following.

Semi-infinitely long canal with one closed end

In a canal with a closed end, progressive waves cannot exist for an unlimited duration because sooner or later they either vanish towards infinity or they are reflected at the closed end. In the latter case, a standing wave develops with zero discharge, thus an antinode, at the closed end and at all points at a distance of an integer number of half wave lengths away from it. If we choose $s = 0$ at the closed end, the motion is described by Eqs. (4.36) and (4.37). There are no restrictions on the allowable values of the frequency or the wave number.

Closed basin

In a finite-length basin, extending from $s = 0$ and $s = \ell$, say, closed at both ends, the boundary conditions $Q = 0$ at $s = 0$ and $Q = 0$ at $s = \ell$ have to be fulfilled at all times. Thus, we have a **standing wave** with an antinode at both ends, and possibly one or more antinodes between them. Therefore, the basin contains a whole number of half wave lengths. Conversely, this implies that only a discrete set of wave numbers and wave lengths is permitted: $L_n = 2\ell/n$ or $k_n = n\pi/\ell$ for $n = 1, 2, \ldots$. Figure 4.7 shows the surface profile in the standing wave for $n = 3$. The value of n equals the number of nodes in the closed basin. Because we deal with free oscillations, $\omega_n/k_n = \sqrt{gA_c/B}$ for all

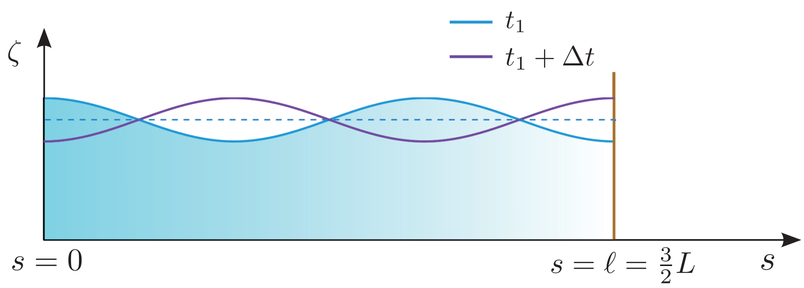

Figure 4.7: Standing wave in a closed basin ($n = 3$)

n. Thus, the discrete set of wave numbers k_n corresponds to a discrete set of frequencies given by $\omega_n = \sqrt{gA_c/B}\,k_n, n = 1, 2, \ldots$, referred to as the set of **natural frequencies**, corresponding to the natural oscillations of the water mass in the closed basin. Of these, ω_1 is the fundamental frequency; the frequencies corresponding to $n = 2, 3, \ldots$ are harmonics.

Semi-closed basin connected to a reservoir or tideless sea

Consider now a basin closed at one end, where $s = 0$, say, and connected to a large reservoir of constant elevation at the other end (the open end), where $s = \ell$, say. This corresponds to the boundary conditions $Q = 0$ at $s = 0$ and $\zeta = 0$ at $s = \ell$ for all times. These conditions are fulfilled in a standing wave with an antinode at the closed end and a node at the open end, requiring $\cos k\ell = 0$ or $k_n\ell = \pi/2 + n\pi$ for $n = 0, 1, 2, \ldots$. Written another way: $\ell = (2n + 1)L/4$: the basin contains an odd number of quarter wave lengths. The value of n equals the number of nodes *inside* the basin, not counting the node at the open end. See Figure 4.8. As above, there is a set of natural frequencies, here given by

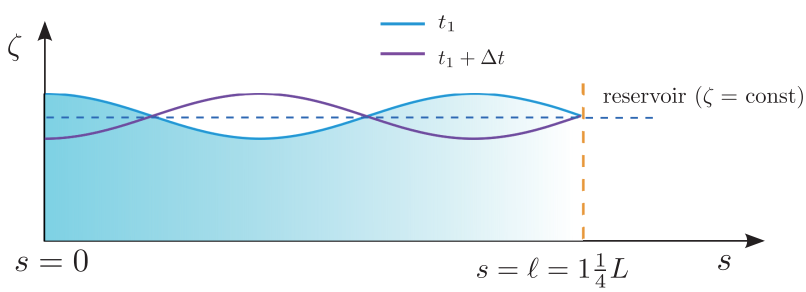

Figure 4.8: Standing wave in a semi-closed basin connected to a reservoir ($n = 2$)

$\omega_n = (\pi/2 + n\pi)\sqrt{gA_c/B}/\ell$ for $n = 0, 1, 2, \ldots$. The fundamental frequency ω_0 applies to the case where there is just one quarter wave in the basin.

Example 4.2. *Basin connected to a reservoir*

<table>
<tr>
<td>

Situation

A prismatic basin, closed at one end, is connected at its open end to a reservoir. The basin dimensions are B = 600 m, B_c = 300 m (the width of the conveyance cross-section), d = 6 m (the depth of the conveyance cross-section) and ℓ = 6 km. There is a natural oscillation in the basin with one node in the interior. The amplitude of the water surface elevation at the closed end ($\hat{\zeta}_{st}$) is 0.5 m.

Questions

Calculate:

1. the period (T) of the oscillation
2. the amplitude of the discharge at the mouth ($\hat{Q}(\ell)$)
3. the amplitude of the flow velocity at the mouth ($\hat{U}(\ell)$)

</td>
<td>

Solution

It follows from the given number of nodes that the basin length equals 3/4 wave length, or $L = cT = 4/3\times$ 6000 m = 8000 m.

1. the wave speed $c = \sqrt{gA_c/B} = \sqrt{gdB_c/B}$ =5.42 m/s, from which the wave period $T = L/c$ = 8000 m / 5.42 m/s = 1475 s
2. $\hat{Q}(\ell) = Bc\hat{\zeta}_{st}\,|\sin k\ell|$. Since $\ell = 3L/4$, we have $k\ell = 3\pi/2$ and $\sin k\ell$ = -1, it follows that $\hat{Q}(\ell)$ = (600 m)×(5.42 m/s)×(0.5 m) = 1627 m^3/s
3. $\hat{U}(\ell) = \hat{Q}(\ell)/A_c = \hat{Q}(\ell)/(dB_c)$ = (1627 m^3/s)/(1800 m^2) = 0.90 m/s

Comment

For a natural oscillation in a semi-closed basin connected to a reservoir, the discharge amplitude is maximum in the entrance and the surface elevation amplitude is maximum at the closed end.

</td>
</tr>
</table>

Semi-closed basin connected to a tidal sea

Instead of a semi-closed basin connected to a reservoir or tideless sea, with a constant water level, we now consider such a basin connected at its open end to a tidal sea. The tide-induced up-and-down motion at the basin mouth generates oscillations of the water mass inside the basin at the tidal frequency, not necessarily related to any of the natural frequencies of the basin. In such cases we speak of a **forced oscillation** of the water mass inside the basin.

As before, Q must be zero at the closed end. A standing wave with an antinode at the closed end can fulfill this condition. Its amplitude is such that ζ at the mouth equals the value being forced by the tide (Figure 4.9). The ratio of the amplitude of ζ at the closed end to that at the open end equals $1/|\cos k\ell|$. This goes to infinity as $|\cos k\ell|$ goes to zero, i.e. the basin contains a whole number of quarter waves. In such cases we speak of **resonance**, occurring if the frequency of the forcing equals one of the natural frequencies of the basin.

As opposed to the case of (near) resonance, with strongly amplified motions in the interior of the basin, we now consider a **short basin**, i.e. one whose length is small compared to the wave length. This implies a very small phase difference from the mouth to the closed end (if there were a progressive wave in the basin), so that the water level responds almost in unison to the tidal forcing at the mouth, rising and falling with the tide but being virtually horizontal at all times. Dynamics play no role inside such a short basin, only storage. The wave character of the motion in the basin can then be disregarded. We refer to such response

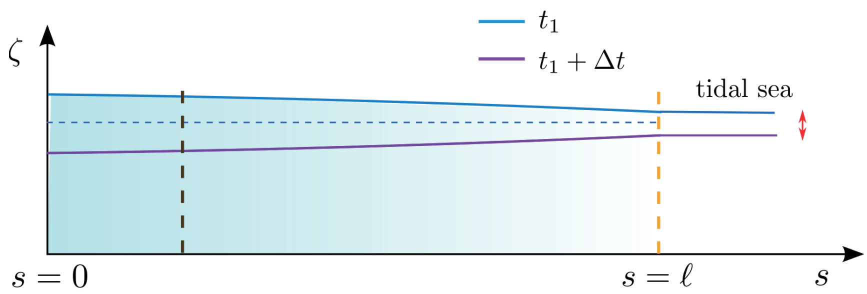

Figure 4.9: Standing wave in a semi-closed basin connected to a sea

as the **pumping mode**, already considered in Chapter 2.

We can quantify this argument as follows. The basic assumption is that $\ell \ll L$, or $k\ell \ll 2\pi$, so that cos $k\ell \simeq 1$. This means that the amplitude of the surface elevation is nearly constant throughout the length of the basin. (See Figure 4.9, the portion of the basin from the closed end to the nearby dashed vertical.) As an example, consider a basin whose length is 1/20th of the tidal wave length in its interior; we then have cos $k\ell \simeq 0.95$, so that the amplitude rises with only 5% from the open end to the closed end. In such cases, we obtain a reasonable first approximation by neglecting these variations, i.e. by assuming the water level in the basin to be horizontal at all times. We will elaborate on this in Chapter 7.

Example 4.3. *Basin connected to a tidal sea*

Situation

Consider the same (prismatic) basin as in Example 4.2, now connected at its open end to a tidal sea with an M_2-tide with a surface elevation amplitude of 1.5 m The period of the M_2-tide is T = 12 hours and 25 minutes, or 44700 s, so the tidal frequency $\omega = 1.4 \times 10^{-4}$ rad/s.

Questions

1. determine the response of the basin in terms of the surface elevation amplitude
2. calculate the discharge amplitude in the open end of the basin
3. calculate the discharge amplitude halfway between the open end and the closed end

Solution

The value of c is the same as in Example 4.2, or 5.42 m/s, and the wavelength $L = cT = 242$ km, which is more than twenty times the basin length (ℓ): the pumping mode approximation applies.

1. in view of the open connection between the basin and the sea, we can equate $\hat{\zeta}_{st}$ to the amplitude of the offshore tide (1.5 m)
2. the discharge amplitude in the entrance $\hat{Q}(\ell) = B\ell\omega\hat{\zeta}_b$ = (600 m)(6000 m)(1.4 × 10^{-4} rad/s)(1.5 m) = 756 m^3/s
3. in a short, prismatic basin the discharge varies linearly with the distance of the cross-section to the closed end. Therefore, the discharge halfway the length of the basin is half of that in the mouth

Comment

The pumping mode approximation neglects the influence of resistance which usually needs to be accounted for in tidal calculations (Chapter 7).

4.8 Exact numerical solutions

In this example we consider a canal with a finite length. In its respective ends either the water level or the discharge may be imposed as boundary conditions. The canal has a constant storage width (B) and conveyance area (A_c), so consideration of linear wave problems leads to Equation (4.9) for the water level. The general representation of solutions to this equation, given in Equation (4.14), is used here to construct exact numerical solutions of that equation (which in itself is not exact!).

Discretization

We first describe the water level (h) and discharge (Q) in the canal in terms of finite sets of discrete numbers. This can be achieved by partitioning the spatial domain of the canal (S) using a sequence of discrete coordinates $S = [s_0, s_1, \cdots, s_{M-1}, s_M]$, where M is the number of spatial intervals. In this example the intervals must be equal in size in which case the partitioning is called *uniform*.

For time stepping, the time interval of interest I is partitioned into N equal time intervals, $I = [t_0, t_1, \cdots, t_{N-1}, t_N]$, where t_0 and t_N are the start time and end time of the numerical simulation, respectively, see also Section 2.3. The time intervals are constant in this example.

The water level in node number i at time level n is now denoted with h_n^i. All discrete water levels at time level n may be stored in an array $[h_n^i]_{i=0}^M$ representing the water level in the canal at time t_n. Similarly, the discharge at time t_n is represented by an array $[Q_n^i]_{i=0}^M$. See Figure 4.10. The numerical solution of the wave problem in the canal involves the computation of these arrays for all time levels n.

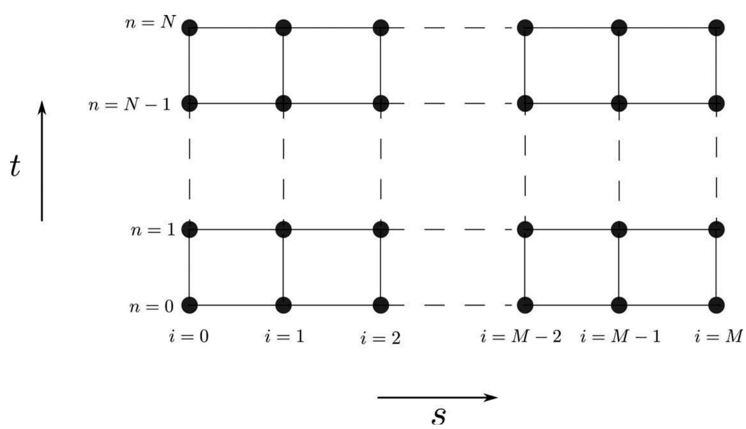

Figure 4.10: Discretization in space and in time

Solution algorithm

Initially, at time level $n = 0$, the water level and discharge in the canal need to be specified. This also determines the discrete water level components h^+ and h^- at time $t = t_0$,

$$\left(h^+\right)_0^i = \frac{1}{2}\left(h_0^i + \frac{Q_0^i}{Bc}\right) \qquad \text{and} \qquad \left(h^-\right)_0^i = \frac{1}{2}\left(h_0^i - \frac{Q_0^i}{Bc}\right) \tag{4.38}$$

where $c = \sqrt{gA_c/B}$ is the wave speed and B and A_c are the constant storage width and conveying cross-section of the canal, respectively.

According to the general solution, given by Equation (4.14), the respective components travel in opposite directions with constant speed c. If the time step size is chosen such that the distance traveled during one time step equals the distance between neighbouring nodes the value for h^+ in a particular node is transferred to the right neighbour node when advancing one step in time and, simultaneously, the value for h^- is transferred to the left neightbour node. This results in the following time stepping procedure for interior nodes

$$\left(h^+\right)_{n+1}^i = \left(h^+\right)_n^{i-1} \qquad \text{and} \qquad \left(h^-\right)_{n+1}^i = \left(h^-\right)_n^{i+1} \tag{4.39}$$

which is commonly referred to as **point to point transfer**. The solutions for the water level (h) and discharge (Q) in interior nodes, that is for $i = 1, M-1$, are obtained afterwards by applying Equation (4.28) node wise

$$h_{n+1}^i = \left(h^+\right)_{n+1}^i + \left(h^-\right)_{n+1}^i \qquad \text{and} \qquad Q_{n+1}^i = Bc\left(\left(h^+\right)_{n+1}^i - \left(h^-\right)_{n+1}^i\right) \tag{4.40}$$

In boundary nodes Equation (4.39) will only update the wave component traveling out of the domain, but it leaves undetermined the ingoing component (the required neighbour node is missing). Instead, the nodal value of the incoming component is determined such that application of Equation (4.40) results in the specified boundary condition. In the left boundary node ($i = 0$) the ingoing component is h^+, the nodal value of which is determined by imposing the water level (h_L) or the discharge (Q_L) leading to, respectively,

$$\left(h^+\right)_{n+1}^0 = h_L - \left(h^-\right)_{n+1}^0 \qquad \text{or} \qquad \left(h^+\right)_{n+1}^0 = Q_L/Bc + \left(h^-\right)_{n+1}^0 \tag{4.41}$$

Similarly, in the right boundary node ($i = M$) the nodal value of the ingoing component h^- is found by imposing the water level (h_R) or the discharge (Q_R) leading to, respectively,

$$\left(h^-\right)_{n+1}^M = h_R - \left(h^+\right)_{n+1}^M \qquad \text{or} \qquad \left(h^-\right)_{n+1}^M = -Q_R/Bc + \left(h^+\right)_{n+1}^M \tag{4.42}$$

Note that in each of the boundary nodes either the water level or the discharge may be imposed as boundary condition. This is related to the fact that the outgoing component is already determined by Equation (4.39) while completion of Equation (4.40) to find the ingoing component requires only one piece of additional information per boundary node.

Starting from the initial time level $n = 0$, Equations (4.39) and (4.40) and the boundary conditions given in Equations (4.41) and (4.42) are now applied successively until the end time t_N at time level $n = N$.

Implementation

A Python script in which the above solution procedure is implemented is given in Listing 4.1.

```
1  # import modules
2  from numpy import *
3  from pylab import *
4
5  # physical parameters
6  g = 9.81                                  # gravitation                    [m/s2]
7
8  # canal dimensions
9  Ac = 75                                   # conveyance area                [m2]
10 B  = 25                                   # storage width                  [m]
11 L  = 500                                  # length                         [m]
12
13 # wave speed [m/s]
14 c = sqrt(g*Ac/B)
15
16 # spatial domain
17 M = 800                                   # number of spatial intervals    [-]
18 s = linspace(0,L,M+1)                     # horizontal coordinates         [m]
19
20 # time stepping
21 dt = L/(M*c)                              # time step size                 [s]
22 N  = 800                                  # number of time steps           [-]
23
24 # initial conditions
25 t = 0                                     # initial time                   [s]
26 h = .2*(sign(s-200)-sign(s-300))          # initial water level            [m]
27 Q = 0*s                                   # initial discharge              [m3/s]
28
29 # initial wave components
30 h1 = .5*(h + Q/B*c)                       # compute initial h'+'           [m]
31 h2 = .5*(h - Q/B*c)                       # compute initial h'-'           [m]
32
33 # time loop
34 ion()
35 for i in range(N):
36     t += dt                               # new time level                 [s]
37     h1[1:M+1] = h1[0:M]                   # shift h'+' one step right
38     h2[0:M]   = h2[1:M+1]                 # shift h'-' one step left
39     # boundary conditions
40     h1[0] =  h2[0]                        # left  boundary condition (QL=0)
41     h2[M] = -h1[M]                        # right boundary condition (hR=0)
42     # plot
43     hold(None)
44     plot(s,h1+h2,'b',linewidth=2)         # plot water level
45     axis([0,L,-.25,.5])                   #
46     xlabel('$s [m]$',size='20')           # define axis and labels
47     ylabel('$\delta h [m]$',size='20')    #
48     draw()
```

Listing 4.1: elementary-wave.py

In the first few lines some necessary modules are loaded. Next, gravity (line 6) and some parameters defining the canal geometry (lines 9-11) are specified from which the wave celerity is computed in line 14.

The partitioning of the spatial domain is performed in lines 17 and 18 by defining first the number of spatial intervals (`M`) after which an array containing the spatial coordinates (`s`) is constructed using the numpy function `linspace`. (This function takes as input arguments, in respective order, the lower and upper bounds of the interval and the number of *points*, which is the number of intervals plus one.) The time step size `dt` for point-to-point transfer is calculated in line 21 and the number of time steps (`N`) for the simulation is set in line 22.

In lines 25 to 26 the initial time, water level and discharge are specified. In this example the `sign` function is used to set the initial water level to 0.4 m over a reach of 100 m in the center of the canal while being zero elsewhere. The initial discharge is set to zero in this example. The initial water levels of both wave components, denoted with `h1` and `h2`, respectively, are computed in lines 30 and 31. Note that `numpy` allows performing these operations on entire arrays.

Time stepping commences in line 35 after the plot screen has been set to interactive mode in the preceding line, using `ion()`, to enable continuous plotting. After calculating the new time level `t` (line 36) the wave components are updated by raising the indices of `h1` with one (line 37) and by lowering the indices of `h2` with one (line 38), except in the boundary node where the respective component is *ingoing*. To complete the solution in these nodes the boundary conditions are applied in lines 40 and 41 using the already computed nodal value of the *outgoing* component. In this example, a zero discharge is prescribed in the left boundary node and a zero water level elevation in the right boundary node.

What remains is to plot the results for which we use the pylab module. First, the previous plot is released using `hold(None)` in order to give way to the new plot. The solution for the water level, obtained by adding the respective components, is plotted in line 45. Some axes- and label properties are set (lines 45-47) after which `draw()` activates the plot on screen.

Listing 4.1 may be modified to compute and visualize all previous examples in this chapter.

Result

Figure 4.11 shows snapshots of the computed water level in the canal at different time levels.

The initial water level elevation (upper left panel) splits in two equal parts (zero initial discharge) which propagate in opposite directions. In the upper right panel (time $t = 20.5$ s) these parts have travelled just over 100 m implying a wave speed c of roughly 5 m/s. This is in agreement with the exact wave speed $c = \sqrt{(9.81 \text{ m/s}^2) \times (75 \text{ m}^2)/(25 \text{ m})} = 5.42$ m/s.

The lower left panel shows the situation just after the waves have reached their nearest boundary. In the left boundary the incoming wave is reflected positively, doubling the local wave height, and in the right boundary the incoming wave is reflected negatively, keeping the local wave height zero.

The lower right panel shows the reflected waves moving away from the boundaries towards the middel of the canal with a height equal to that of the incoming wave (left wave, positive reflection) or a height of minus one times the incoming wave height (right wave, negative reflection).

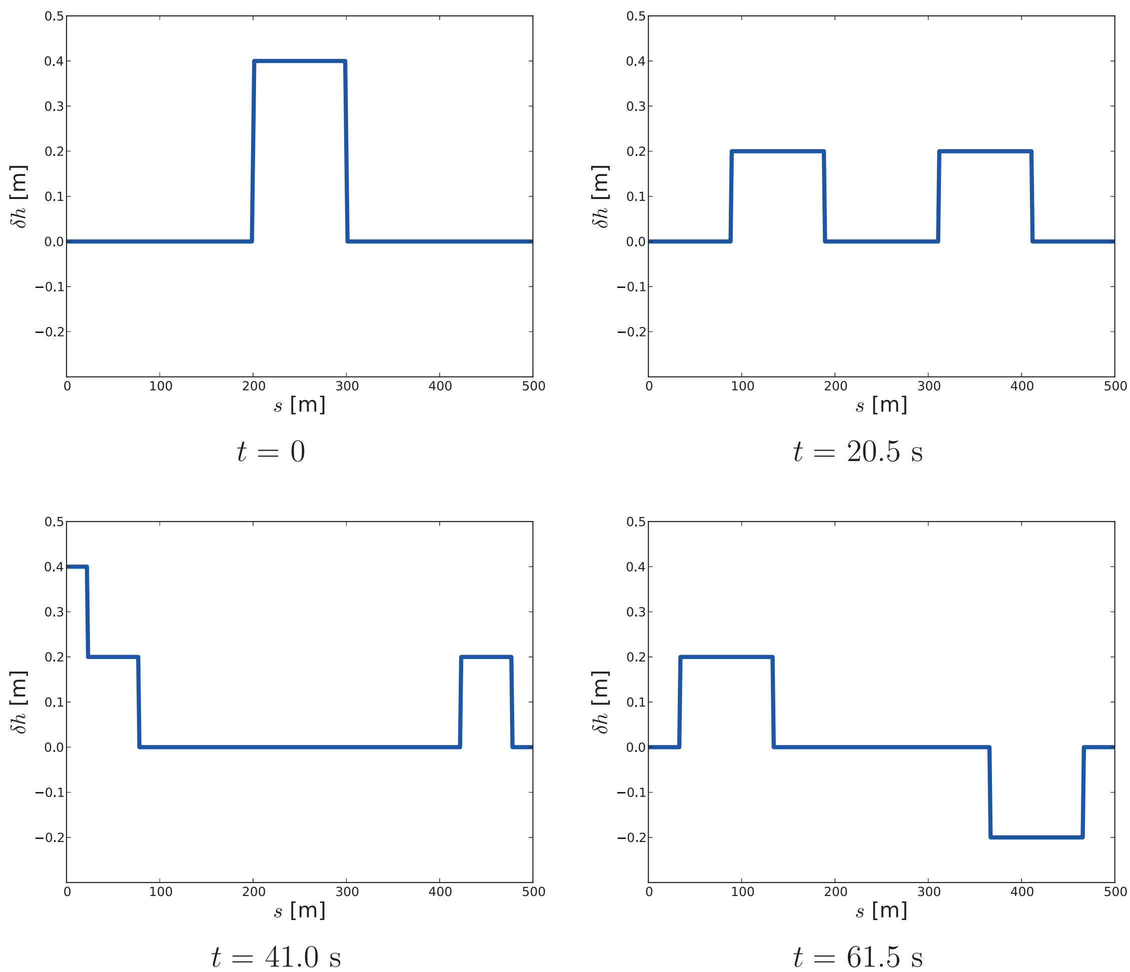

Figure 4.11: Snapshots of the computed solution

The numerical algorithm nicely shows how the information is passed within the domain (by opposing motions) and into the domain (by the action of the boundary conditions) as it is in real waves.

Bibliography

[1] W. A. Strauss. **Partial differential equations**. John Wiley & Sons, Inc., 1992.

Problems

1. What does it mean to linearize the equation of motion? How can this be achieved? What is a condition for its validity?

2. Verify why a small storage capacity in a river leads to an enhanced speed of propagation of flood waves.

3. Calculate the speed of propagation of low waves without resistance in water with a depth of 4000 m (ocean), 50 m (shelf sea) and 5 m (estuary). (Answers: 198 m/s, 22.1 m/s, 7.00 m/s)

4. Calculate the corresponding wave length for an M_2-tide and for a tsunami with a period of 10 minutes. First verify whether the latter can be regarded as a long wave in the given depths. (Answers: 8855 km, 988 km and 313 km for the tide and 119 km, 13.3 km and 4.2 km for the tsunami.)

5. Derive a relation between the variations in water level and discharge for a long wave propagating without change in shape in open water.

6. Derive a relation between the variations in fluid pressure and particle velocity for a wave propagating without change in shape in a closed conduit (pressurized flow).

7. A pumping station begins discharging water at a rate of 40 m^3/s onto an evacuation canal with a depth of 4 m and a width of 50 m. Calculate the speed of the resulting translatory wave propagating into the canal and the associated rise of the free surface and particle velocity. (Answers: c = 6.26 m/s, ζ = 0.13 m and U = 0.20 m/s.)

8. The following values of the flow velocity and surface elevation are given for an initial disturbance (at $t = 0$) in an infinitely long, 5 m deep canal: $s < 0 : \zeta = 0.50$ m, $U = 0$, $s > 0 : \zeta = 0, U =$ 0.50 m/s Calculate and plot the values of ζ and U as functions of s at $t = 10$ ss. (Answers: $s <$ - 70 m: $\zeta = 0.50$ m, $U = 0$; - 70 m $< s <$70 m: $\zeta = 0.07$ m, $U = 0.60$ m/s; $s >$ 70 m: $\zeta = 0$, $U = 0.50$ m/s.)

9. Same as in question 8, now with the following initial values: - 100 m$< s < 0 : \zeta$ = 0.50 m, $U = 0$, $0 < s <$ 100 m: $\zeta = 0$, $U = 0.50$ m/s, elsewhere: $\zeta = 0$ and $U =$ 0 Calculate and plot the values of ζ and U as functions of s for the instants $t = 10$ s and $t = 20$ s.

10. Sketch the two functions $\cos(\omega t - ks)$ and $\cos \omega t \cos ks$ for ks between -2π and 2π

and $\omega t = 0$, $\pi/6, \pi/2, \pi$ and 2π. Verify that the first of these two functions represents a progressive wave advancing at a speed ω/k.

11. Can a periodic, progressive wave exist continually in a basin closed at one end or at both ends?

12. Argue why a free periodic oscillation in a closed basin is possible for a countable set of frequencies only. Same for a semi-closed basin.

13. Verify how the natural frequencies of a prismatic basin are affected by the width of the free surface, the width and depth of the conveyance cross-section, and the length. Which of these has the most influence?

14. Calculate the three longest natural periods of a semi-closed prismatic basin with a length of 30 km, a conveyance cross-sectional area of 6 x 10^3 m^2 and a width of the free surface of 600 m. (Answers: T_1 = 12116 s, T_2 = 4038 s, T_3 = 2423 s.)

15. Continuing with the second of the three modes of the previous question: sketch a longitudinal profile of the surface elevation and the discharge at the instant $\omega t = \pi/4$ (using the phases as in Eqs. (4.36) and (4.37)). Check the relation between surface elevation and discharge in a qualitative sense, including their signs.

16. Same as in the two preceding questions, now for a basin closed at both ends. (Answers: $T_1 = 6058$ s, $T_2 = 3029$ s, $T_3 = 2019$ s.)

17. A semi-closed basin with the dimensions as in question 14 is subjected to a forced oscillation. Sketch the longitudinal profiles of the surface elevation and calculate the ratio (r) of the amplitude of the surface elevation at the closed end to that at the open end, for the periods $T = 3$ hrs and $T = 6$ hrs, respectively. (Answers: $r = 5.26$ and $r = 1.57$, respectively.) Interpret these results considering the periods of the forced motion in relation to the natural periods of the basin.

18. Consider the situation of the preceding question for $T = 6$ hrs, with the additional information that the amplitude of the surface elevation at the closed end is 1 m. Calculate and plot the amplitudes of the discharge at the following distances from the closed end: $x = 1$ km, 2 km, 3 km, 5 km and 10 km. (Answer: $\hat{Q}$ increasing from 175 m^3/s at $x = 1$ km to 1720 m^3/s at $x = 10$ km.) Interpret the results in relation to the approximation of the pumping mode.

19. Modify Listing 4.1 such that it computes the water level and discharge in a semi-closed basin of constant width and depth connected to a tidal sea.

Chapter 5

Translatory waves

5.1 Introduction

This chapter deals with translatory waves, i.e. more or less pulse-like, progressive disturbances of discharge and water level. A simple translatory wave forms the transition between two different states of (more or less) uniform flow. Throughout this chapter we assume that the transition takes place sufficiently rapidly so that we can neglect resistance, yet sufficiently slowly for the long wave approximation to apply.

We first restrict ourselves to the category of weak disturbances (low waves), as in the preceding chapter. This allows linearization of the equations. The constraint of low waves is relaxed in the second half of this chapter.

5.2 Low translatory waves in open water

Basic model

Examples of the generation of low translatory waves in free-surface flows are provided by the operation of gates, locks, pumps etc. in navigation canals. To avoid hindrance to shipping, the operation is such that only acceptably low variations in water level and weak currents are produced. The advection of momentum ($\rho U^2 A_c$) (and the advective acceleration ($U\partial U/\partial s$) can be neglected for such low waves. The linear theory of the preceding chapter can be applied, with the important results that the propagation speed is given by

$$\boxed{c = \sqrt{\frac{gA_c}{B}}} \tag{5.1}$$

and that the variations in surface elevation and discharge for a purely progressive wave are related by

$$\boxed{\delta Q = Bc\,\delta h} \tag{5.2}$$

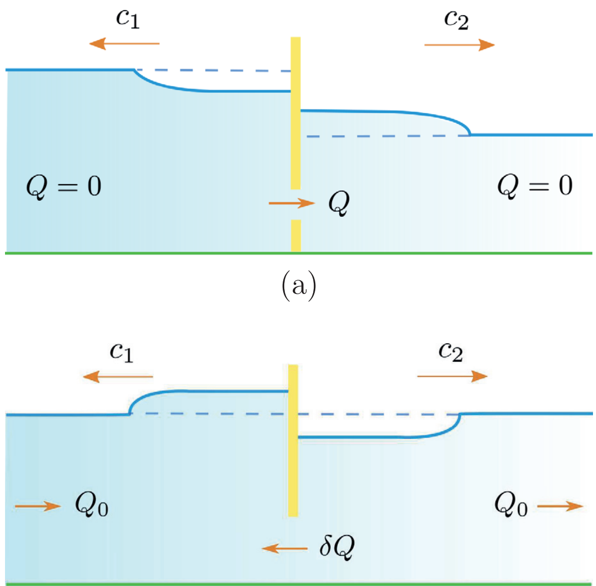

Figure 5.1: Translatory waves resulting from the opening of a gate in tranquil water (a) and resulting from closure of a gate in flowing water (b)

If $B = B_c$, these relations reduce to

$$c = \sqrt{gd} \tag{5.3}$$

and

$$\delta U = \frac{c}{d}\,\delta h = \sqrt{\frac{g}{d}}\,\delta h = \frac{g}{c}\,\delta h \tag{5.4}$$

Generation of translatory waves

Figure 5.1 shows two cases of the generation of translatory waves.

The upper panel (a) is for the partial opening of a gate between two reaches of a canal in which initially the water is at rest ($Q = 0$) but with different water levels on either side. In this case, the opening allows a flow through the gate with a discharge Q, causing water level variations on the two sides which propagate away from the gate into the two canal reaches on either side with speeds c_1 and c_2, respectively (see Chapter 4). Notice that following the negative wave (inducing a lowering of the surface elevation) the flow velocity is directed opposite to the direction of wave propagation.

The second panel (b) concerns the case of a partial closing of a gate in flowing water with an initial discharge Q_0. The partial closing obstructs the flow to a certain extent, causing a reduction in the discharge by δQ, leaving a net discharge $Q = Q_0 - \delta Q$ where the wave has passed.

In both cases, the height of the wave can be controlled by the height of the resulting opening, and the steepness of the front can be controlled by the rate at which the operation is performed.

Because of the rapid spatial variations of the flow through the gate opening, local inertia ($\partial U/\partial t$) can be neglected for this flow. The instantaneous discharge then depends on the instantaneous opening and on the instantaneous head difference, $h_1 - h_2$, say, in which h_1 and h_2 are the water levels on the upstream side and the downstream side, respectively:

$$Q(t) = \mu A\,(t)\,\sqrt{2g\,(h_1\,(t) - h_2\,(t))} = \mu A\,(t)\,\sqrt{2g\Delta h\,(t)} \tag{5.5}$$

Operation of the gate changes the values of the head difference across it, due to the height(s) of the issuing wave(s), which must be taken into account in the calculations, see Example 5.1.

Example 5.1. *Opening of a gate in a barrier*

Situation

A movable gate in a barrier between a canal (A_c = 80 m^2, B = 30 m) and a large reservoir is partially opened to an effective flow cross-section μA of 4 m^2. Initially, the water in the canal is at rest, and the surface level is 3 m below that in the reservoir.

Questions

Calculate:

1. an estimate of the discharge through the gate opening (Q_0), neglecting the influence of the wave height on the discharge
2. the discharge (Q) through the gate opening, taking into account the influence of the wave height on the discharge
3. the resulting wave height (δh) in the canal

Solution

The discharge $Q = \mu A\sqrt{2g\,\Delta h}$. Initially, $\Delta h = \Delta h_0 = 3$ m, changing to $\Delta h = \Delta h_0 - \delta h$, once the gate is being opened, where $\delta h = Q/Bc$ is the height of the wave propagating into the canal (the water level in the reservoir is not affected).

1. neglecting the influence of the wave height on the discharge gives the estimate $Q_0 = \mu A\sqrt{2g\,\Delta h_0} = 30.7$ m^3/s
2. substitution of $\Delta h = \Delta h_0 - Q/Bc$ into the discharge relation gives a second-degree algebraic equation for the discharge whose solution (rounded) is $Q = 29.7$ m^3/s
3. the resulting wave height $\delta h = Q/Bc = 0.20$ m (using $c = \sqrt{gA_c/B} = 5.11$ m/s)

Comment

The wave height δh is about 7% of Δh_0. The estimated discharge Q_0 is therefore approx. 3.5% too high, since the discharge varies in proportion to the square root of the head difference.

Let us now investigate how the time varying conditions at a control structure, resulting from its operation, manifest themselves in the adjacent canal reaches. We take the example of a pumping station which delivers a time-varying discharge, from a time $t = 0$ until $t = T$, with a peak value Q_p, as shown in the left panel of Figure 5.2 (a hypothetical, nonrealistic variation). As soon as the discharge starts, a disturbance propagates into the canal reach, in the positive s-direction, say. At a time $t = t_1$, after the pumps have been switched off ($t_1 > T$), its front and its end have advanced through a distance of ct_1 and $c(t_1 - T)$, respectively. This is shown in the longitudinal profile of the discharge at time $t = t_1$, in the right panel of Figure 5.2. It can be seen that this spatial profile is in a sense the mirror image of the time variation in the left hand panel. This corresponds to the fact that for propagation in the positive s-direction, the variations depend on $s - ct$, in which s and t have opposite signs.

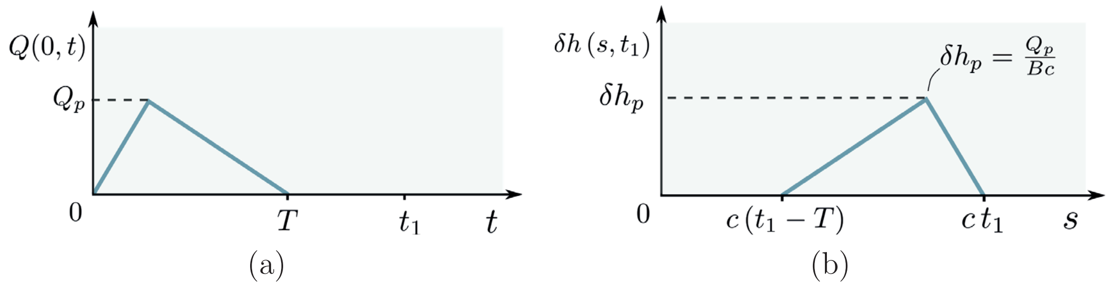

Figure 5.2: Translatory waves in a canal resulting from discharge variations; discharge variation (a) and wave height (b)

Partial reflection at transitions

Consider a transition in canal geometry between two prismatic reaches 1 and 2, such that the conveyance cross sectional area and the width of the free surface change from $(A_{c,1}, B_1)$ into $(A_{c,2}, B_2)$, see Figure 5.3. How does this affect the propagation of a translatory wave? We expect an effect on the ongoing wave as well as reflection to a certain extent. Therefore, we suppose that we have to deal with three waves: incident (from reach 1), transmitted (into reach 2) and reflected wave (back into reach 1), with the following parameters:

- incident wave: $\delta Q_i, \delta h_i$ in reach 1 with $A_{c,1}, B_1$
- reflected wave : $\delta Q_r, \delta h_r$ in reach 1 with $A_{c,1}, B_1$
- transmitted wave : $\delta Q_t, \delta h_t$ in reach 2 with $A_{c,2}, B_2$

(See Figure 5.3.) We assume low waves and neglect wave-wave interactions and their effect on the propagation speed, which in this approximation has the constant values $c_1 = \sqrt{gA_{c,1}/B_1}$ in reach 1, common to the incident wave and the reflected wave, and $c_2 = \sqrt{gA_{c,2}/B_2}$ in reach 2.

Because of continuity of discharge and elevation at the transition (neglecting differences in velocity head), we have

$$\delta h_i + \delta h_r = \delta h_t \tag{5.6}$$

and

$$\delta Q_i + \delta Q_r = \delta Q_t \quad \text{or} \qquad B_1 c_1 (\delta h_i - \delta h_r) = B_2 c_2\, \delta h_t \tag{5.7}$$

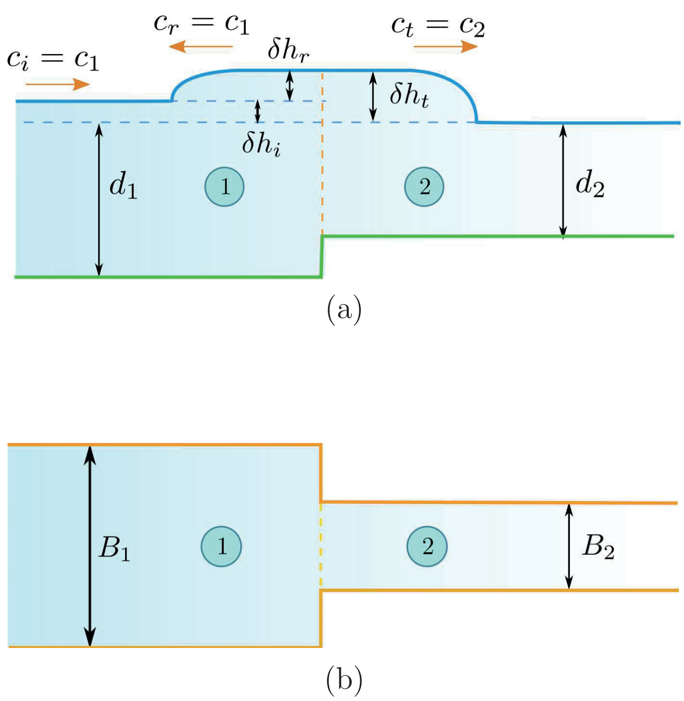

Figure 5.3: Translatory waves at a transition in canal geometry.

(Note that Q is reckoned positive in the direction of wave incidence.) We now define the following dimensionless ratios:

$$\gamma \equiv \frac{B_2 c_2}{B_1 c_1} = \sqrt{\frac{A_{c,2} B_2}{A_{c,1} B_1}} \qquad r_t \equiv \frac{\delta h_t}{\delta h_i} \quad \text{and} \quad r_r \equiv \frac{\delta h_r}{\delta h_i} \tag{5.8}$$

With these definitions, Eqs.(5.6) and (5.7) are transformed into the following dimensionless versions:

$$1 + r_r = r_t \qquad \text{and} \qquad 1 - r_r = \gamma r_t \tag{5.9}$$

which yields the following expressions for the ratios of the heights of the reflected wave and the transmitted wave to the height of the incident wave:

$$\boxed{r_r = \frac{1-\gamma}{1+\gamma} \qquad \text{and} \qquad r_t = \frac{2}{1+\gamma}} \tag{5.10}$$

The following points are noted with respect to this result:

1. There is no reflection at transitions for which the product Bc remains constant ($\gamma = 1$).
2. Waves experiencing a reduction in the value of Bc are positively reflected.
3. If $B_2 c_2 \ll B_1 c_1$, the reflection is almost 100%, and the transmitted wave height is almost twice the incident wave height (though the discharge in the transmitted wave is relatively small because it is proportional to $B_2 c_2$).

4. In case of a strong enlargement of the cross-section ($B_2c_2 \gg B_1c_1$), as in the case of waves in a canal approaching a lake or reservoir, the reflection is negative and almost 100% in absolute value, whereas the transmitted wave height is quite small, going to zero in the limit as γ goes to zero. This property was already used in the preceding chapter.

In cases of a connection of three or more canal reaches, the reflection and the transmission of a wave approaching the transition through one of these can be calculated by lumping the others into one equivalent canal, having a Bc-value equal to the sum of the Bc-values of the constituent canals which are being approached by the incident wave.

This is illustrated with the situation in the Julianakanaal, a canal parallelling the river Meuse in the Dutch province of Limburg. Figure 5.4 gives a sketch of the situation. Point A represents the location of the lock. Some distance downstream, at point B, a lateral harbour connects to the Julianakanaal. The (positive) waves originated at the lock are transmitted along the canal as well as into the harbour. The Bc-value of the harbour (about 500 m^2/s)

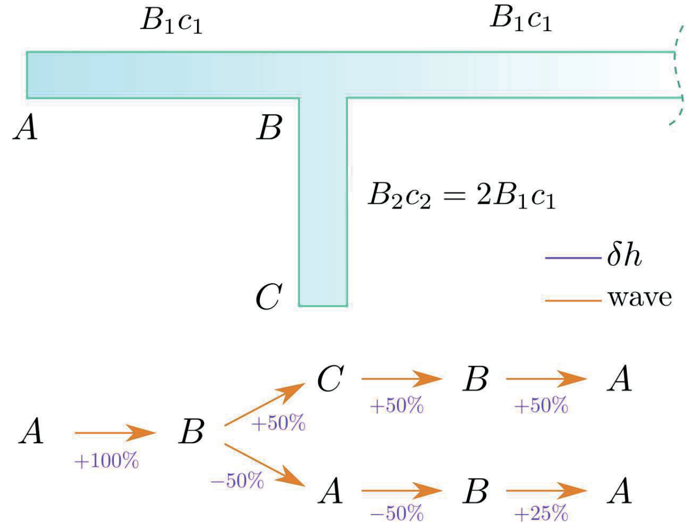

Figure 5.4: Wave reflection near shipping lock Born, The Netherlands

is roughly twice that in the canal (250 m^2/s). The total Bc-value of these is three times that of the canal itself, so the waves approaching the harbour mouth from the side of the canal experience a γ-value of 3. This gives r_r = - 0.5, or 50% negative reflection back to the lock, and $r_t = 0.5$, or 50% transmission down the canal and into the harbour. (Note that $\gamma = 1$ for reflected waves approaching the harbour mouth from the closed end of the harbour, so these waves are not reflected at the mouth but fully transmitted into both canal reaches.)

We see that the presence of the harbour causes the height of the (first) wave transmitted down the canal to be only 50% of the original height in the upstream canal reach. Of course, in the long run the total volume of water discharged from the lock must flow down the canal. The remaining 50% is temporarily stored in the harbour and in the upstream canal reach, between the harbour and the lock, undergoing multiple reflections and being released onto the canal going downstream in smaller portions, spread out over time.

Example 5.2. *Partial reflection*

Situation

At a transition between two prismatic canal reaches, the values of A_c and B change from 150 m^2 and 50 m to 250 m^2 and 80 m, respectively. A translatory wave with a height $\delta h_i =$ 0.35 m approaches the transition from the side of the narrower canal reach.

Questions

Calculate:

1. the height of the reflected wave (δh_r)
2. the height of the transmitted wave (δh_t)
3. the discharge (Q) at the transition shortly after reflection of the incoming wave

Solution

The wave speeds ($c = \sqrt{gA_c/B}$) in the narrow and wide reaches are 5.43 m/s and 5.54 m/s, respectively. This gives a Bc ratio $\gamma = 1.63$ (from narrow towards wider reach).

1. reflected wave: $r_r = (1-\gamma)/(1+\gamma) = -0.24$ giving $\delta h_r = -0.24 \times 0.35$ m = -0.08 m
2. transmitted wave: $r_t = 2/(1+\gamma) = 0.76$ giving $\delta h_t = 0.76 \times 0.35$ m $= 0.27$ m
3. discharge: $Q = Q_i(1-r_r)$, where Q_i is the discharge of the incoming wave (95 m^3/s). So $Q = 95$ m^3/s $\times$ 1.24 = 118 m^3/s

Comment

Since the discharge is continuous at the transition it equals the discharge of the transmitted wave $Q_t = Bc\,\delta h_t$ (using Bc of the wide canal reach).

5.3 High translatory waves in open water

We will now abandon the assumption of (very) low waves, and do not make the associated simplifying approximations of neglecting the advective acceleration and the effects of a variable surface elevation on the channel cross-section geometry (the instantaneous values of A and B). Because the resulting equations are nonlinear, their mathematical treatment is much more complicated than it is for low waves described by linear equations, as dealt with in the preceding chapters. In the present chapter, we will mention only a few characteristic consequences of the inclusion of nonlinear terms. A more complete treatment is presented in Chapter 6 (method of characteristics).

Wave deformation

Within the framework of the linear theory in the preceding chapters, the effects of the presence of a (low) disturbance on the velocity of propagation were neglected. As a consequence, propagation in a prismatic channel without change in shape is possible (in case of absence of resistance). In case of higher waves, their effect on the instantaneous depth and thereby on the velocity of propagation is no longer negligible. Various theories have been developed to account for this, all having in common that **the waves deform as they propagate**.

The occcurrence of wave deformation can be made plausible, without a formal mathematical derivation, using the relation $c = \sqrt{gA_c/B} = \sqrt{gd_B}$, in which d_B is the average depth of the entire cross-section. This relation was derived for low waves propagating without change in shape, but it should by approximation also be valid for slowly varying waves, using the instantaneous local depth. This implies that higher portions of a wave propagate at greater speed than lower portions.

Furthermore, the given expression for c applies to the wave speed relative to the water mass ahead of it. The effect of the wave-induced (as opposed to pre-existing) flow velocity of this mass on the wave propagation speed was neglected in the preceding chapters. By taking it into account, the wave speed relative to the bottom becomes $U \pm c$ with c the wave speed relative to the water as given above, the + and - signs being applicable to waves propagating in the positive and the negative x-direction, respectively. For a positive wave propagating in

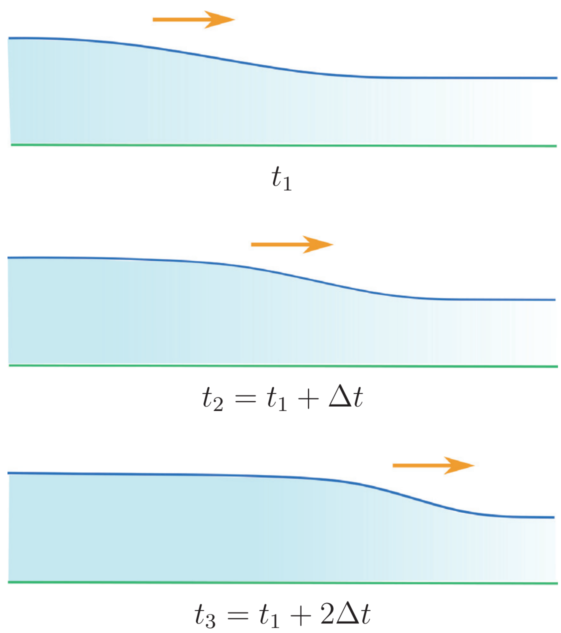

Figure 5.5: Steepening of a positive wave

the positive $s-$direction, the wave-induced flow velocity U is positive, enhancing the velocity of propagation relative to the bottom for the higher parts of the wave even further. It follows that the wave deforms: positive waves steepen (see Figure 5.5), negative waves flatten out. Because a positive wave steepens, it will eventually develop into a shock wave or bore.

In the preceding considerations, friction was not considered. This implies on the one hand that (bed) friction is not a causative factor in the formation of a shock wave, but on the contrary it might prevent a shock wave from developing if the rate of friction-induced damping outweighs the rate of inherent steepening. Another reason why a steepening wave does not necessarily develop into a bore is due to the fact that as the waves become steeper,

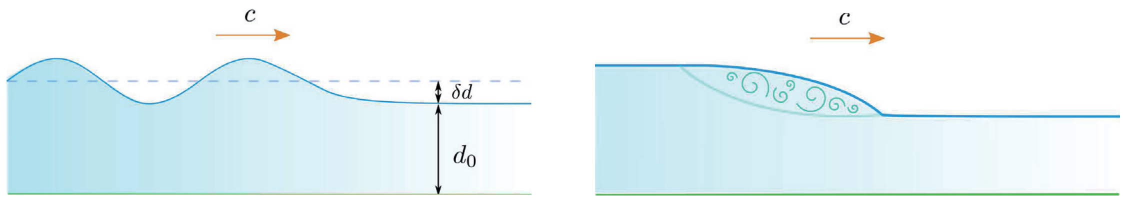

Figure 5.6: Undular bore (a) and turbulent bore (b)

vertical accelerations increase more and more, so that the pressure deviates more and more from being hydrostatic. This effect, not included in the long-wave approximation, delays the formation of a shock wave. (In fact, it allows the presence of certain nonlinear waves that do not deform at all.)

There are two types of bores. For sufficiently low bores (relative bore height $\delta d/d_0$ less than about 0.28), the bore is undular; its surface is smooth and wavy (left panel in Figure 5.6). Higher bores are turbulent; in fact, they are traveling hydraulic jumps (right panel in Figure 5.6).

Tidal bores

Shock waves in free-surface flows can develop as a result of human manipulation of control structures, pumping stations etc., but also as the result of natural processes. Within the latter category, the so-called **tidal bores** are the most common and best known. They occur at a number of coastal bays or estuaries on earth at rising tide, particularly spring tide, appearing as an undular or as a turbulent front moving inland, causing a significant rise in the local surface elevation in a short time. An overview of all tidal bores occurring around the world is given in Chanson [1]. As an illustration, we will present some details of the bores occurring in the estuary of the river Severn in Great Britain.

The Severn discharges into Bristol Channel. The tides, approaching from the Atlantic Ocean, where they already have a significant amplitude, are enhanced in this Channel with a factor of about 3 as a result of its funnel shape, narrowing in the inland direction. As a result, the tides in the Severn estuary are quite strong, reaching more than 10 m tidal range (HW - LW) at spring tides.

The incoming, rising tide front is steepened as it propagates inland. For sufficiently high (spring) tides, a tidal bore develops somewhere in the estuary. This happens about 250 times a year. Most of the time, the bore occupies the entire width of the estuary, advancing at a speed of a few meters per second. Depending on the height of the tide and the local depths, the bore may be undular or turbulent. Figure 5.7 shows a situation where both occur at the same time: undular in the deeper parts and turbulent in the shallower water near the banks. An individual bore in the Severn estuary exists for about two hours and traverses a distance of about 30 km, after which it vanishes.

The highest tidal bores on earth occur in the Qiangtang River in Hangzhou, in the south-

Figure 5.7: Bore in the Severn river (UK), from: Rowbotham [2]

east of China, which can reach a height exceeding four meters. They travel at a speed of some 40 km/hour, spanning the entire width of the estuary of several km's. Their approach, accompanied by a strong roar, can be heard from a great distance. A number of spectacular videos and photographs can be seen on YouTube (where there is also some erroneous information, such as that the bore height can reach 9 m, and that it would be an annual phenomenon; the latter misinformation is probably due to a mix-up with the fact that it is common for Chinese people to gather at the site of the bore on the occasion of one of the annual Chinese festivals.) An exceptionally spectacular bore occurred on August 23, 2013 (see footage on YouTube).

Whether or not a tidal bore develops depends on the strength of the tide and on the longitudinal profile of the width and depth of the estuary. A funnel shape in plan and decreasing depths are conducive to bore formation. Due to dredging, several tidal bores have disappeared from the scene. An example is the bore in the Seine River in France, which was a regular phenomenon well into the 20th century, prior to major dredging works, even reaching Paris where its rushing between the river banks, in the heart of this metropole, was a popular sight for residents and tourists.

Shock wave propagation

In this section, we derive an expression for the velocity of propagation of a shock wave in open water, with height Δd, which forms a moving transition between two regions of uniform flow with depths d_0 and $d_1 = d_0 + \Delta d$, respectively. Ahead of the wave, the water is at rest ($U_0 = 0$), behind it the flow velocity is U_1. We ignore the fact whether the shock is undular or turbulent. Contrary to the derivation presented in Chapter 4, using low-wave approximations, we will here include the advection of momentum and use a more exact expression for the total pressure force. The long-wave theory does not apply to the flow in

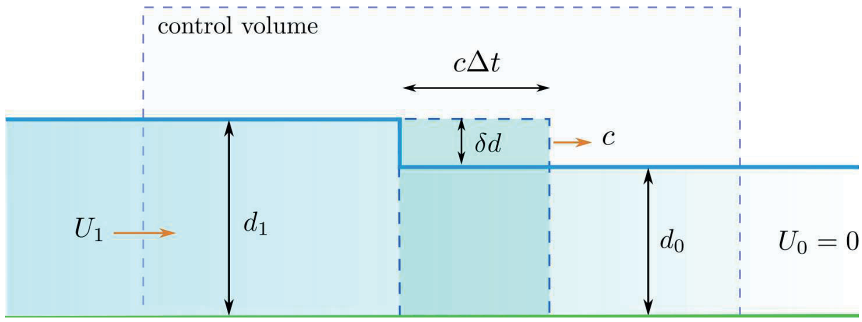

Figure 5.8: Control volume shock wave

the shock region. Instead, we use balance equations for the mass and momentum inside a control volume encompassing the shock, see Figure 5.8.

The volume balance per unit width reads

$$U_1 d_1 = c\,\Delta d = c\,(d_1 - d_0) \tag{5.11}$$

and the momentum balance

$$\frac{1}{2}\rho g {d_1}^2 + \rho {U_1}^2 d_1 - \frac{1}{2}\rho g {d_0}^2 = \rho U_1 d_1 c \tag{5.12}$$

Elimination of U_1 from these two equations yields after some algebraic manipulation

$$\boxed{c = \sqrt{g\frac{d_0 + d_1}{2}\,\frac{d_1}{d_0}}} \tag{5.13}$$

This is the propagation speed of a shock wave entering quiescent water. More generally, we can say that this is the propagation speed relative to the water ahead of the wave. If the initial velocity U_0 is nonzero, the wave speed relative to the fixed bed is $U_0 + c$.

Because $d_1 > d_0$, it follows that $c > \sqrt{gd_0}$ (and even $c > \sqrt{gd_1}$). We see that the inclusion of the effects of a finite wave height causes the wave propagation speed to exceed the linear-theory value of $\sqrt{gd_0}$. (The latter is the limiting value in case Δd goes to zero.)

Bibliography

[1] H. Chanson. **Tidal bores**. World Scientific, 2012.

[2] F. Rowbotham. **The Severn bore**. David & Charles, London, 1983.

Problems

1. What are translatory waves?
2. A control structure connects an irrigation canal ($A_c = 100$ m$^2, B = 30$ m) with a reservoir. At an initial head difference of 4 m, a gate is abruptly opened to an effective flow area $\mu A = 5$ m^2. Calculate the discharge and the height of the resulting translatory wave in the canal for two cases: (a) neglecting the effect of the wave on the head difference, and (b) taking that effect into account. (Answers: (a) $Q =$ 44.3 m^3/s, $\delta h = 0.258$ m and (b) $Q = 42.9$ m^3/s, $\delta h = 0.250$ m).
3. Verify the percentages in the scheme in Figure 5.4.
4. Answer the questions in Example 5.2 for waves approaching the transition from the other side. (Answers: $r_r = 0.24$ and $r_t =$ 1.24, $Q_i = 155$ m^3/s and the discharge at the transition $Q = 118$ m^3/s).
5. Mention a few theoretical consequences of the distinction between so-called low translatory waves and high translatory waves.
6. Why do (high) translatory waves deform?
7. What is a characteristic difference between the deformation of positive translatory waves and of negative ones?
8. How does resistance affect the deformation of translatory waves?
9. Mention some factors favouring the formation of tidal bores.
10. Why are there fewer tidal bores at present than in older days?
11. Derive an expression for the velocity of propagation of a bore entering a region with depth d_0 and flow velocity U_0.

Chapter 6

Method of characteristics

A general feature of wave phenomena is the transmission of information and energy through a physical system at a finite speed. A disturbance brought about somewhere in the system, e.g. due to operation of a control structure in an irrigation system, reaches other locations after a finite time. Insight in this phenomenon is important both for the purpose of effective control of water levels and discharges in the system, and for performing the required computations. The so-called method of characteristics lends itself particularly well for this purpose because it makes visible how the disturbances travel through the system, and it enables their computation.

6.1 Introduction

In this chapter, we use the complete version of the mass balance and the momentum balance, without the low-wave approximations. Flow resistance is not included except for a minor reference.

As before, we restrict ourselves to one-dimensional systems (pipes, canals, ...), schematically represented by the $s-$axis, and consider the varying position of a disturbance in the course of time. This can be represented as a curve in the s, t**-plane** whose slope $\mathrm{d}s/\mathrm{d}t$ equals the local propagation speed of the disturbance. Such curves are called **characteristics**. They portray how information travels through the system.

The balance equations for mass and momentum for one-dimensional wave phenomena form a set of two partial differential equations (PDE's) for two dependent variables, such as the depth and the discharge (d, Q), as functions of two independent variables (s, t). The two dependent variables are called **state variables**. The instantaneous values of these can be represented as a point in the **state diagram**, a plane with the two state variables as coordinates.

Given a set of sufficient initial and boundary conditions, the solution of the set of PDE's is determined. Expressed in terms of (d, Q), this solution is a set of values $d\,(s, t)$ and $Q\,(s, t)$ which can be represented as a surface in the (d, s, t)-space and the (Q, s, t)-space, respectively, the so-called **integral surfaces**, depicted schematically in Figure 6.1.

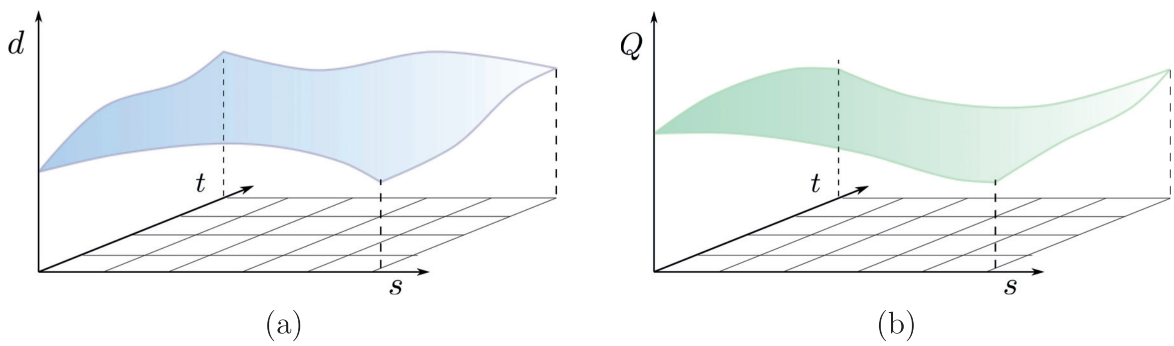

Figure 6.1: Integral surfaces for d (a) and Q (b)

In finite-difference methods for the integration of the PDE's, the values of (d, Q) are determined in a set of points in the (s, t)-plane chosen beforehand, for instance according to a rectangular grid with finite differences $\Delta s, \Delta t$. In the method to be dealt with in this chapter, the computations proceed along specific paths in the s, t-plane, the characteristics. The advantage of this is that (as we will see) the set of two PDE's in s, t (the balances of mass and momentum) is replaced by a set of ordinary differential equations (ODE's) in t, simplifying the solution. Note that a similar operation was carried out on h^+ in Section 4.4, where the PDE given by Equation (4.19) was replaced by the ODE's given by Equations (4.20).

As stated above, the slope of a characteristic ($\mathrm{d}s/\mathrm{d}t$) equals the local propagation speed, which depends on the depth and the flow velocity, which are not known beforehand. That is why the position of the characteristics has to be determined as part of the solution. For low waves, the propagation speed does not depend on the disturbance, in which case the slope of the characteristics is determined beforehand. Needless to say, this simplifies the solution greatly. This low-wave approximation has already been used extensively in preceding chapters.

The introductory remarks made above have given a broad indication of the essence of the method of charactristics. The formal mathematical formulation and examples of applications of the method are given in subsequent sections, first for free-surface flows and then for pressurized flow in pipes.

6.2 Mathematical formulation for free-surface flows

For simplicity, we restrict the formulation to two-dimensional motions (i.e., no lateral variations) over a horizontal bottom. We describe it in terms of the state variables U and d.

We recapitulate the long-wave equations from Chapter 2. The continuity equation reads

$$\frac{\partial d}{\partial t} + \frac{\partial U d}{\partial s} = 0 \tag{6.1}$$

whereas the equation of motion (without resistance) reads

$$\frac{\partial U}{\partial t} + U\frac{\partial U}{\partial s} + g\frac{\partial d}{\partial s} = 0 \tag{6.2}$$

(Because the bottom has been assumed to be horizontal, we can replace $\partial h/\partial s$ by $\partial d/\partial s$.) Instead of using d as one of the two state variables, we replace it temporarily as such by c, defined by $c \equiv \sqrt{gd}$. This simplifies the algebra without loss of information. Note that it is not necessary to assign a physical meaning to this quantity at this stage (doing as if we have no prior knowledge about it from preceding chapters).

By substitution of $d = c^2/g$ into Equation (6.1) and division of the result by c/g, and substitution of $d = c^2/g$ into Equation (6.2), we obtain

$$\frac{\partial c}{\partial t} + c\frac{\partial U}{\partial s} + 2U\frac{\partial c}{\partial s} = 0 \tag{6.3}$$

and

$$\frac{\partial U}{\partial t} + U\frac{\partial U}{\partial s} + 2c\frac{\partial c}{\partial s} = 0 \tag{6.4}$$

Adding these two equations yields

$$\frac{\partial (U+2c)}{\partial t} + (U+c)\frac{\partial (U+2c)}{\partial s} = 0 \tag{6.5}$$

For brevity, we define

$$R^+ = U + 2c \tag{6.6}$$

Using this shorthand notation, Equation (6.5) becomes

$$\frac{\partial R^+}{\partial t} + (U+c)\frac{\partial R^+}{\partial s} = 0 \tag{6.7}$$

The left-hand side of this equation represents the total derivative of R^+ with respect to t for an observer moving at a speed $\mathrm{d}s/\mathrm{d}t = U + c$ in the positive s-direction (see Section 4.3). Therefore, such observer sees no change in the value of R^+. Stated another way: a constant value of the state variable $U + 2c$ is propagated at speed $U + c$ along the $s-$axis. Therefore, a formulation equivalent to Equation (6.7) is

$$\boxed{\frac{\mathrm{d}R^+}{\mathrm{d}t} = 0 \qquad \text{provided that} \qquad \frac{\mathrm{d}s}{\mathrm{d}t} = U + c} \tag{6.8}$$

Next, we perform the same operations with change of sign. Subtracting Equation (6.4) from Equation (6.3), the result is

$$\frac{\partial (U-2c)}{\partial t} + (U-c)\frac{\partial (U-2c)}{\partial s} = 0 \tag{6.9}$$

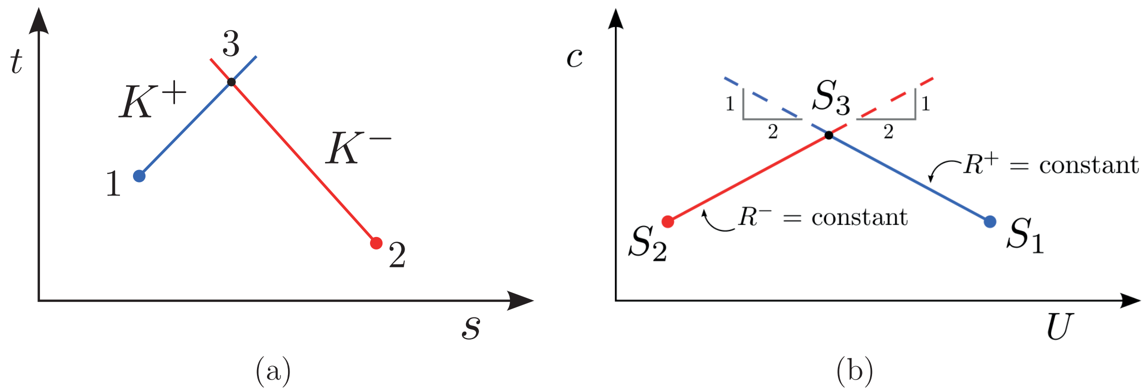

Figure 6.2: s, t-diagram (a) and state diagram (b)

Defining

$$R^+ = U - 2c \tag{6.10}$$

we obtain the following equivalent of Equation (6.9):

$$\boxed{\frac{dR^-}{dt} = 0 \qquad \text{provided that} \qquad \frac{ds}{dt} = U - c} \tag{6.11}$$

The velocities $U \pm c$ are called the **characteristic velocities**, and curves in the (s, t)-plane for which $ds/dt = U \pm c$ are called **positive characteristics** and **negative characteristics**, to be labeled as K^+ and K^-, respectively. (These are labels, not quantities.) The so-called **characteristic relations** (6.8) and (6.11) imply that R^+ is constant along K^+ and that R^- is constant along K^-. The quantities R^+ and R^- (in some places taken together as $R^\pm$ for brevity) are called **Riemann invariants**. Notice that the condition that $R^\pm$ = constant, or $U \pm 2c$ = constant, corresponds to straight lines in the (U, c)-plane.

It follows from the preceding results that information is transmitted through the system at speeds $U \pm c$, or with speeds $\pm c$ relative to the fluid. This gives a physical meaning to the quantity c, which formally was only a short hand way of writing $\sqrt{gd}$ (ignoring knowledge from previous chapters).

6.3 Principle of application

The essence of the manner in which the characteristic method is applied is as follows.

Suppose that the state of motion is known in two closely neighbouring points in the (s, t)-plane, say the points 1 and 2 in the left panel of Figure 6.2, meaning that the values of U and c (or U and d) are known in these points, shown as points S_1 and S_2 in the (U, c)-plane in the right panel of Figure 6.2. Because the values of the state variables U and c are known in the points 1 and 2, so are the characteristic velocities $ds/dt = U \pm c$ in these two points. These are velocities along the s-axis, but they are also directions or slopes in the (s, t)-plane.

Now draw a short straight line segment in the (s, t)-plane, starting in point 1 in the direction given by $\mathrm{d}s/\mathrm{d}t = U_1 + c_1$ (assumed positive, which will always be the case for subcritical flow, regardless of the sign of U_1). That is by definition a portion of a positive characteristic K^+. Likewise, we draw a line segment starting in point 2 with slope $\mathrm{d}s/\mathrm{d}t = U_2 - c_2$ (assumed negative). This is a segment of a negative characteristic K^-. Strictly speaking, the characteristics are curved in general, but this can be ignored over sufficiently short intervals, which can be achieved by starting at closely neighbouring points.

Along the characteristics K^+ and K^-, the Riemann invariants R^+ and R^- are constant, respectively. Physically, this means that information about the state of motion in points 1 and 2 is carried to point 3, which determines the state of motion in that point:

$$R_3{}^+ = R_1{}^+ \quad \text{and} \quad R_3{}^- = R_2{}^- \tag{6.12}$$

or, in terms of the state variables U and c:

$$U_3 + 2c_3 = U_1 + 2c_1 \quad \text{and} \quad U_3 - 2c_3 = U_2 - 2c_2 \tag{6.13}$$

The values of U_3 and c_3 are easily calculated from these two linear algebraic equations:

$$U_3 = \frac{1}{2}(U_1 + U_2) + (c_1 - c_2) \quad \text{and} \quad c_3 = \frac{1}{4}(U_1 - U_2) + \frac{1}{2}(c_1 + c_2) \tag{6.14}$$

The various states of motion and the connections between them can be portrayed graphically in the (U, c)-plane: the point S_3, representing the state in point 3, can be found from the states S_1 and S_2 as the point of intersection of the straight line $R^+ = U + 2c =$ constant, starting in point S_1, and the straight line $R^- = U - 2c =$ constant, starting in point S_2.

The computation can proceed in like manner as for point 3, by starting in an additional point 4 with given state of motion, which yields a new point 5 where the state of motion follows from that in points 2 and 4. This can be continued for many more points, so covering the (s, t)-plane with a network of positive and negative characteristics, as shown in Figure 6.3. The state of motion in the nodes of this network are determined from those in the starting points. This is elaborated in following paragraphs.

Instead of using the (U, c)-state diagram, in which lines of constant $R^\pm$ or constant $U \pm 2c$ are straight, we can use a (U, d)-diagram. In that case, the Riemann invariants are $R^\pm = U \pm 2\sqrt{gd}$, and lines of constant $R^\pm$ are parabolas, as shown in Figure 6.4b.

Changes in the state of motion correspond to displacements along the parabolas of constant R^+ or R^-, i.e. a curved path in the (U, d)-plane. For weak disturbances of an undisturbed state (U_0, d_0), these displacements are small and follow approximately the local tangent to the parabola, given by $\mathrm{d}U/\mathrm{d}d = \mp\sqrt{g/d_0}$. Thus, for small steps along these local tangents, the small variations in U and d are related by

$$\boxed{\delta U = \mp\sqrt{\frac{g}{d_0}}\,\delta d = \mp\frac{g}{c_0}\,\delta d = \mp\frac{c_0}{d_0}\,\delta d} \tag{6.15}$$

in which $c_0 = \sqrt{gd_0}$.

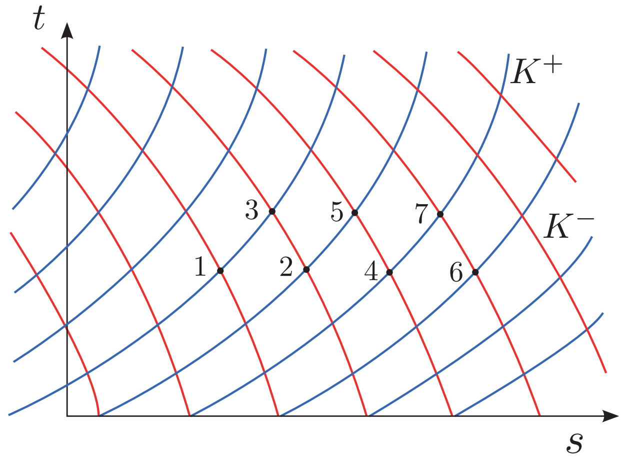

Figure 6.3: The s, t plane with several characteristics

6.4 Characteristics

As we have seen above, **characteristics are paths in the (s, t)-plane along which the information travels.** This is of great importance for a good understanding of wave propagation, as is needed for a proper operation of control structures, pumping stations etc. to obtain a certain discharge or water level. (It makes little sense to open a gate or start a pump if the effect is not there where and when it it is needed.)

The slope of a characteristic ($\mathrm{d}s/\mathrm{d}t$) equals the characteristic velocity ($U \pm c$).

In **subcritical flow**, for which $|U| < c$, the sign of $\mathrm{d}s/\mathrm{d}t = U \pm c$ equals that of $\pm c$, so the slopes of the positive and the negative characteristics have opposite signs. Stated another way: $\mathrm{d}s/\mathrm{d}t > 0$ for K^+, and $\mathrm{d}s/\mathrm{d}t < 0$ for K^-. This means that in subcritical flow, **information is transmitted downstream as well as upstream**.

In **supercritical flow**, $|U| > c$, and the sign of $\mathrm{d}s/\mathrm{d}t = U \pm c$ equals that of U, for the positive as well as for the negative characteristics. Therefore, in supercritical flow, **information is transmitted in the downstream direction only.**

It is important to be aware of the fact that the *position* of the points in the (s, t)-plane (where? when?) is determined by the *characteristics*, whereas the *state of motion* (what?) is determined in the (U, c)-plane using the *Riemann invariants*. Different points in the (s, t)-plane can very well have the same state of motion (steady, uniform flow), represented by a single point in the (U, c)-plane.

In case of weak disturbances entering a region with uniform depth d_0 and flow velocity U_0, the characteristic velocity can be approximated as $\mathrm{d}s/\mathrm{d}t \simeq U_0 \pm c_0 = U_0 \pm \sqrt{gd_0}$. In this approximation, the characteristics are straight and independent of the solution. We will use this approximation in following graphical representations and elaborations

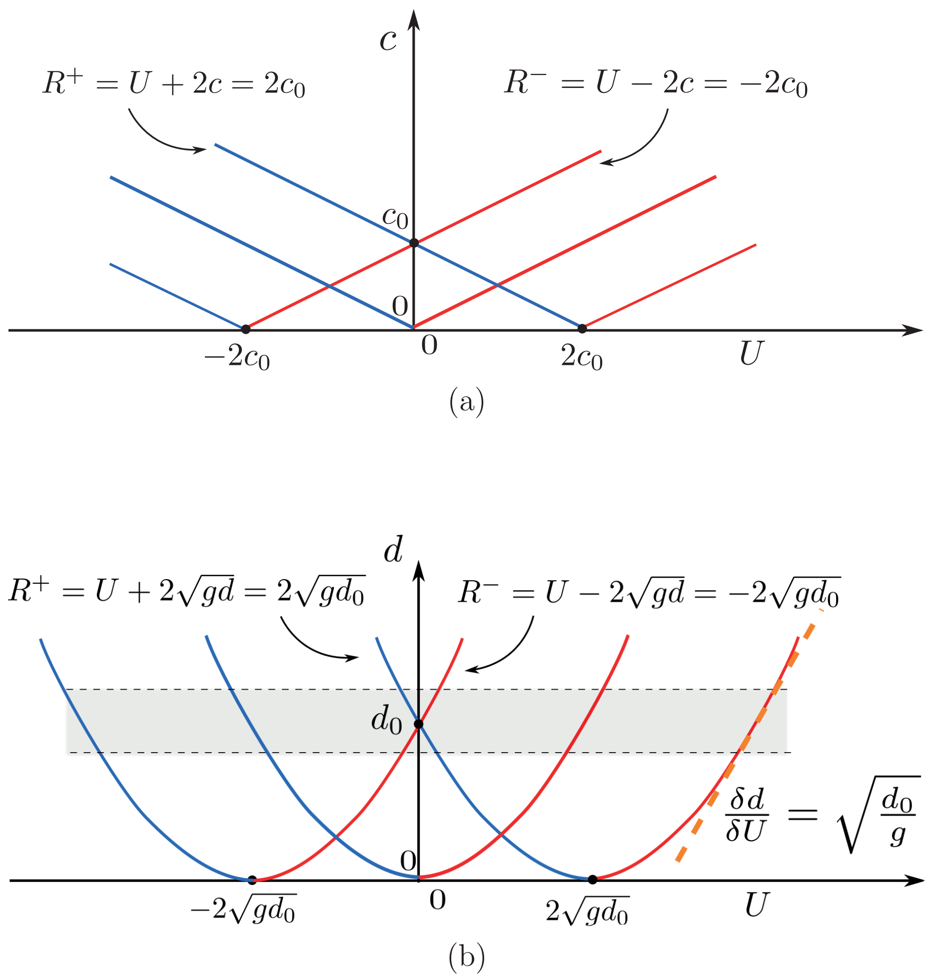

Figure 6.4: State diagrams: (U, c) diagram with straight lines $R^{\pm} = U \pm 2c = \text{constant}$ (a) and (U, d) diagram with parabolas $R^{\pm} = U \pm 2\sqrt{gd} = \text{constant}$ (b)

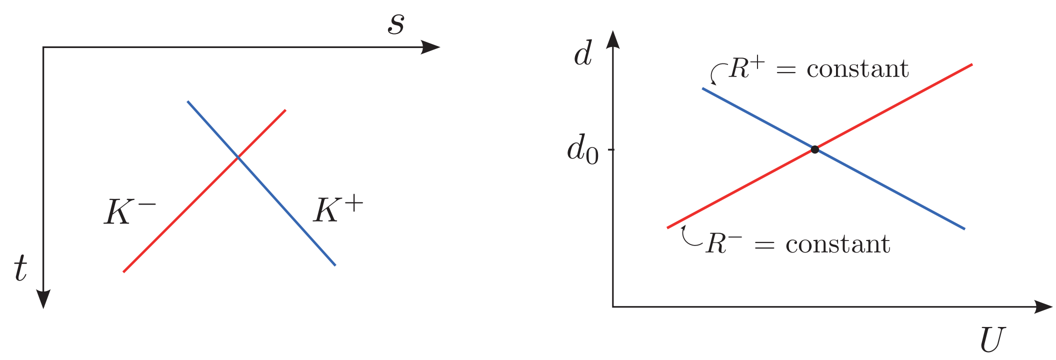

Figure 6.5: Orientation s, t-diagram and U, d diagram

Also, we will draw the (s, t)-diagram 'upside down', compared to Figure 6.2, i.e., we plot the direction of increasing time downwards, as in Figure 6.5. The advantage of this is that the positive characteristics K^+ in the (s, t)-plane are more or less parallel to the lines R^+ = constant in the (U, c)-plane, and similar for K^- and the lines of constant R^- (except for supercritical flow).

A note on curved characteristics

Since the characteristic velocities depend on the instantaneous, local depth and flow velocity, they are not known beforehand but must be determined as part of the solution, which therefore proceeds in consecutive small steps. Moreover, in regions where U and d vary, so does $U \pm c$. In those cases, the characteristics are curved. Using straight-line segments instead is an approximation valid for weak disturbances and/or small steps in s and t. This is in contrast with the (U, c) state diagram: the condition of constant Riemann invariants is graphically represented as straight lines in the (U, c)-plane, no matter how large the variations. See Figure 6.4 a.

6.5 Initial value problem

The long-wave equations (6.1) and (6.2), or their equivalent characteristic relations (6.8) and (6.11), require a set of two conditions in t and two conditions in s for a well-posed problem.

In order to be able to march forward in time with the integration of the basic equations, we impose **two initial conditions** which specify the state of motion through two independent state variables at some initial instant $t = t_0$ in the entire s-domain of calculation.

As an example, we consider the evolution of an initial disturbance of finite length in a long canal, such that the canal boundaries do not (yet) affect the solution. We start with the same initial conditions as in the example presented in Section 4.5, i.e. a state of rest everywhere with an undisturbed depth d_0 and a small rise of the free surface (to a depth d_1) over a finite interval from $s = s_1$ to $s = s_2$, say (Figure 6.6). The undisturbed state is labelled as I, the disturbed state as II. These have been plotted in the upper panel of Figure 6.7. The initial conditions have also been indicated along the s-axis at $t = 0$ in the uppermost line

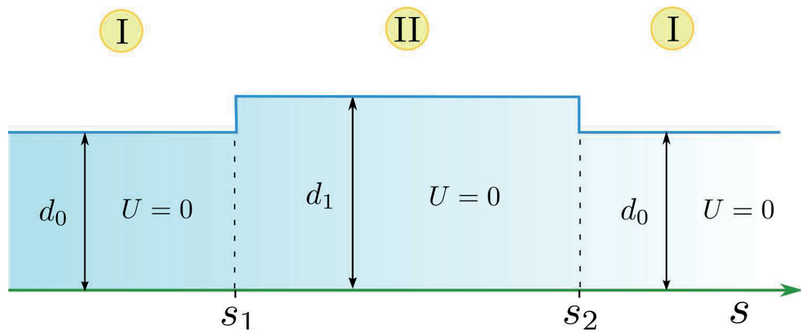

Figure 6.6: Example: initial condition

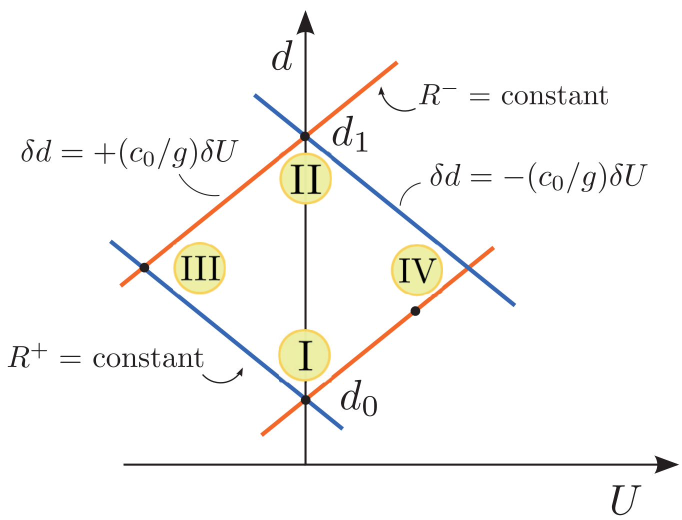

Figure 6.7: Example: (U, d)-state diagram

in Figure 6.8. Because the disturbance is assumed to be weak, and there is no pre-existing flow, we use the approximations $\mathrm{d}s/\mathrm{d}t \simeq \sqrt{gd_0}$, implying that in this approximation the characteristics are straight. For the same reason, we use the approximations expressed in Equation (6.15).

We introduce the initial conditions step by step, beginning with the construction of a small network of characteristics issuing at $t = 0$ from points a, b and c in the undisturbed region where $s < s_1$ (upper panel in Figure 6.8). Because these points share the same undisturbed state of motion (I, actually a state of rest), the corresponding lines of constant $R^{\pm}$ in the (U, c)-diagram all pass through the point I, so that same state (I) exists in the points d, e, f, etc. Therefore, this undisturbed state (I) exists in the entire domain to the left of the negative characteristic ${K_1}^-$. The disturbance issuing from $s = s_1$ just has not yet arrived at those far away points in the restricted time. The same applies to the region to the right of ${K_2}^+$.

A similar consideration, applied to the triangular domain between the s-axis and the two

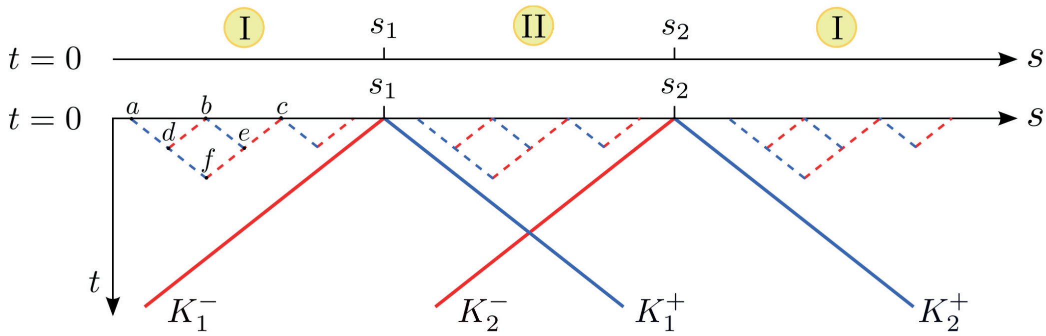

(a)

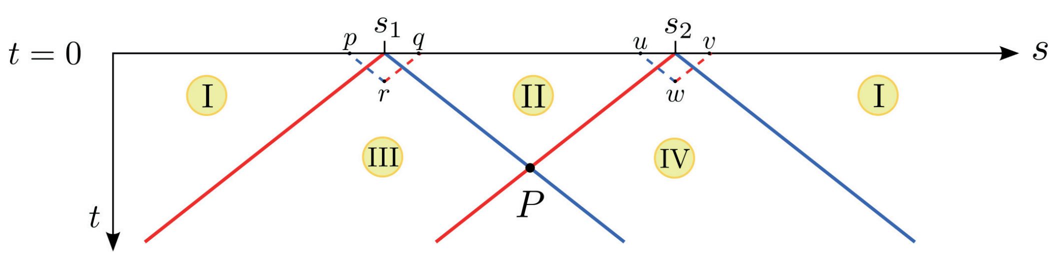

(b)

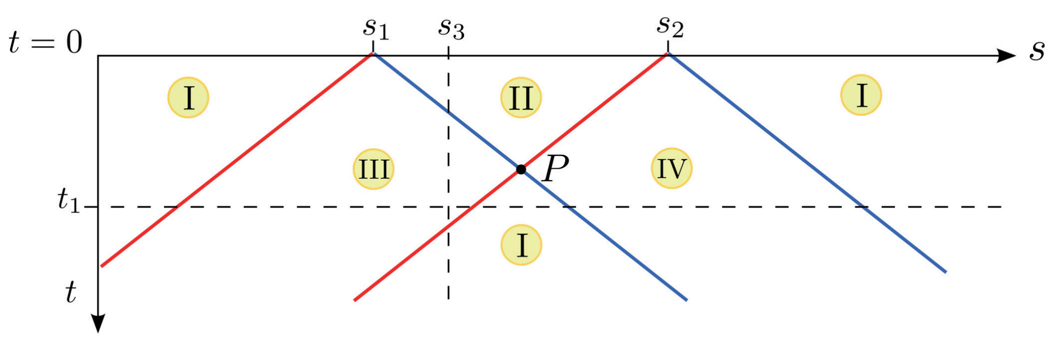

(c)

Figure 6.8: Example: characteristics s, t-plane

characteristics ${K_1}^+$ and ${K_2}^-$, will show that the state II (still) exists in that domain. The disturbances originating at the locations $s = s_1$ and $s = s_2$ have not yet reached the points inside this triangular domain.

Next, we draw a positive characteristic issuing from the left region with initial state I (point p) and a negative characteristic issuing from the region with initial state II (point q) (middle panel in Figure 6.8). They intersect in point r . The state in this point can be found in the state diagram of Figure 6.7 as the intersection of the line R^+ = constant through point I and the line R^- = constant through point II, yielding the state III valid for point r and other nearby points between ${K_1}^-$ and ${K_1}^+$. Likewise, starting in points u and v, we find the state IV for point w and nearby points between ${K_2}^-$ and ${K_2}^+$. At some instant, the characteristics ${K_1}^+$ and ${K_2}^-$ intersect (point P). At that time, a new domain comes into existence in the center, in which the undisturbed state I has returned, as shown in the middle panel of Figure 6.8.

The lowest panel in Figure 6.8 gives an overview of the results. It is clear that the initial disturbance is effectively split into two disturbances, one propagating to the left and the other to the right along the s-axis. At first, these two partial disturbances overlap, but after some time they are separated, after which the undisturbed state is restored in the center, extending over an increasingly long interval of the s-axis as the two disturbances vanish to the left and to the right.

The disturbance propagating to the right causes state IV, with height δd equal to $d_{IV} - d_I = (d_1 - d_0)/2$ (the same as the one going left). The associated flow velocity is $\delta U = \sqrt{g/d_0}\,\delta d$, see the state diagram in Figure 6.7. These results were already obtained in Chapter 4. The same problem was treated here again to illustrate the application of the method of characteristics, which is more powerful because it is not restricted to weak disturbances, as will be seen below.

Using the finalized diagrams, the variation of the flow state in time at a particular location can be found by plotting a *vertical* line in the (s, t)-diagram. Intersection of the line $s = s_3$ in Figure 6.8c with the principal characteristics (those separating the different flow states), gives the time instances at which the state in the point s_3 changes. The alternate flow states (subsequently II, III and I) are obtained from the corresponding state diagram, Figure 6.7. Similarly, a *horizontal* line $t = t_1$ in the (s, t)-diagram will give the spatial variation of the flow state at time t_1.

6.6 Boundary conditions

A boundary condition prescribes the values of a state variable, or a relation between two state variables (such as a dependence of discharge on water level) at one of the boundaries of the computational domain, as a function of time from the moment at which the initial conditions have been prescribed. Two boundary conditions are required. It depends on the flow conditions at which boundary or boundaries these should be imposed, as will be made clear in the following.

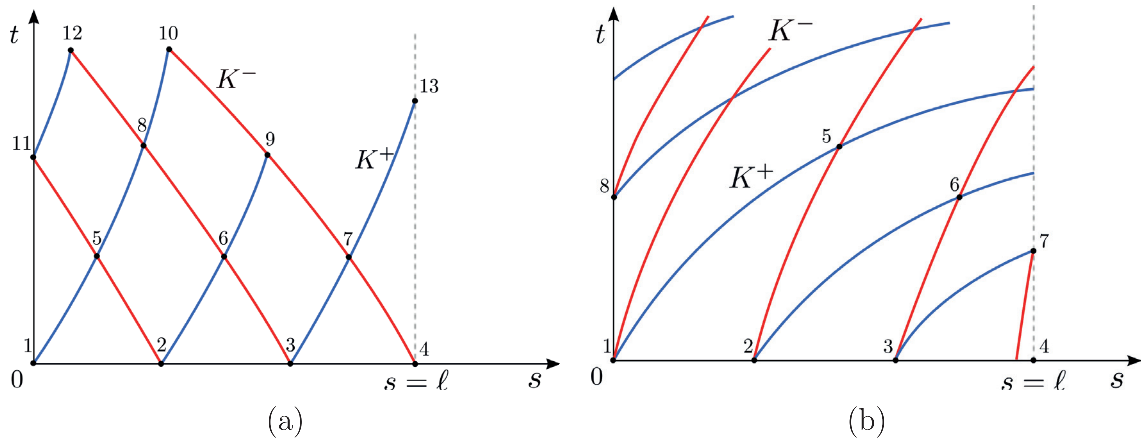

Figure 6.9: Characteristic paths for given initial- and boundary conditions; sub-critical flow (a) and super-critical flow (b)

Flow regimes

Consider a prismatic canal of finite length, from $s = 0$ to $s = \ell$, say, in which the values of U and d, so U and c, are known at time $t = t_0$ (the initial conditions), allowing the start of the construction of a network of characteristics and the determination of the associated values of the state variables. Boundary conditions are specified for $t > 0$ at $s = 0$ and/or at $s = \ell$.

Subcritical flow

Assuming subcritical flow, in which at each point the two characteristic velocities ($\mathrm{d}s/\mathrm{d}t = U \pm c$) have opposite signs (or: the characteristics have opposite slopes), we obtain a network as shown in the left panel of Figure 6.9, in which we have chosen four points (1, 2, 3, 4) in the computational domain to start the computation. (This is just an illustration. In practical applications, it is likely that more points would be required.) In the manner described in Section 6.5, the solution can be obtained successively in the points 5 through 10, in a more or less triangular region bordered by the characteristics K^+ issuing at $t = 0$ from the left boundary $s = 0$ (point 1), and K^- issuing at $t = 0$ from the other boundary $s = \ell$ (point 4).

The values of the Riemann invariants in point 10 equal those in the points 1 and 4, but the characteristics linking these points to point 10 depend also on information in points in between, in fact the entire interval from $s = 0$ to $s = l$. The latter interval is called the **domain of dependence** of point 10. Boundary conditions at $s = 0$ and at $s = l$ for $t > 0$ have no influence in point 10 (or in the triangular domain 1 - 4 - 10).

Conversely, considering an individual location such as $s = s_2$, the initial condition there can only influence the state of motion in the domain between the positive characteristic (2 - 6 - 9) and the negative characteristic (2 - 5 - 11) issuing from that point at $t = 0$, the so-called **domain of influence** of point s_2.

In order to extend the solution beyond the domain of dependence (the triangle 1 - 4 - 10), we continue the negative charateristic issuing from point 2 up to the left boundary, $s = 0$. This yields point 11 and the value of R^- in that point ($R^-_{11} = R_2{}^-$). In order to find the solution, a second relation is required. This cannot be delivered by a positive characteristic, because such characteristic cannot reach point 11 from the region where information is available. That is why a boundary condition is needed at the left boundary, and only one. (With two boundary conditions in $s = 0$, the problem would be overdetermined, with three relations for only two variables.)

Proceeding in this manner, we obtain two relations between the two state variables at the left boundary, viz. the values of R^- obtained from the initial condition, and the other one being provided by the boundary condition. With this information, positive characteristics issuing from the left boundary can be constructed, entering the domain of computation. See e.g. point 12, where R^- is also known, from the negative characteristic through that point $R^-_{12} = R_3{}^-$). Thus, the solution in point 12 is known, etc.

Proceeding in like manner from the other boundary $s = \ell$, we see that there too a boundary condition is required, and only one. We can conclude that in subcritical flow, one boundary condition is required at each of the two boundaries. In other words, **in subcritical flow, one boundary condition is required at the upstream boundary and one at the downstream boundary**. This is consistent with Section 6.4, where it was noted that in subcritical flow, information is transmitted downstream as well as upstream. The influence of the left boundary enters the computational domain along positive characteristics. When the positive characteristic issuing from point 1 reaches the right boundary, the influence of the left boundary condition is felt in the entire domain.

Supercritical flow

Next, we consider supercritical flow, in which the two characteristic velocities at each point ($\mathrm{d}s/\mathrm{d}t = U \pm c$) have the same sign (or: the characteristics are slanting in the same direction), equal to that of U. Assuming $U > 0$, implying also $\mathrm{d}s/\mathrm{d}t > 0$, we obtain a network of characteristics slanting to the right, as shown in the right panel of Figure 6.9.

In contrast to the situation for subcritical flow, the left boundary (the upstream boundary) cannot be reached by negative characteristics issuing from the domain $s > 0$, where information is available from the initial conditions. If we want to know the solution at the left boundary for some time $t > 0$, as in point 8, the required information must be delivered entirely by the (two) boundary conditions there. Thus, **in supercritical flow, two boundary condition are required at the upstream boundary** (e.g. depth and flow velocity). This is consistent with Section 6.4, where it was noted that in supercritical flow, information is transmitted downstream only.

Now consider the downstream boundary. The positive characteristic issuing from point 3, for example, reaches the downstream boundary in point 7. But that point can also be reached by a negative characteristic issuing closer to the downstream end because such characteristics also slope to the right (downstream). Thus, the values of both Riemann invariants in point 7 are known, and the state of motion there is fully determined. A downstream boundary condition is not necessary. In fact, it would make the problem overdetermined.

Transcritical flow

Suppose now that, in supercritical flow conditions, after some time a gate at the downstream boundary is closed. Then what? Closing a gate effectively imposes a downstream boundary condition $Q = 0$ in $s = \ell$. In that case, the local flow becomes subcritical, and negative characteristics issuing from the closed downstream end enter the computational domain. At some point these reach the region of supercritical flow, which point is also reached by a positive charactaristic and by a negative one issuing in the region of supercritical flow. The solution is overdetermined at that point. It becomes multi-valued, i.e. two values of the surface elevation exist simultaneously at the same location, implying the existence of a shock wave or bore.

At the location of the shock, there are five unknowns: the two state variables on either side, and the velocity of the shock. An equal number of relations is available for their determination: three Riemann invariants obtained from the three characteristics intersecting at the location of the shock, and two equations for the balances of mass and of momentum across the shock (as derived in the preceding chapter). Together, the available information is just sufficient to obtain a unique solution.

Graphical solution

We will now illustrate in detail how the boundary conditions are introduced, first at one boundary only, at $s = 0$. For simplicity, we do as if the characteristic velocities are known beforehand, as is the case for low disturbances entering a region of rest with constant depth d_0, so that $\mathrm{d}s/\mathrm{d}t = U \pm c \simeq \pm c \simeq \pm\sqrt{gd_0}$.

General procedure

Consider three points 1, 2 and 3 (left panel of Figure 6.10) with different but arbitrary initial conditions, indicated in the state diagram (right panel of Figure 6.10) as the states S_1, S_2 and S_3. At $t = 0$, a gate at $s = \ell$ is suddenly closed. This gives the boundary condition $U = 0$ at $s = \ell$ for $t > 0$. A positive characteristic (K^+) issuing from point 1 reaches the closed gate in a point (actually, an instant) A, say. Therefore, the state of motion in A, as yet unknown, must ly somewhere on the line $R^+ =$ constant in the state diagram going through S_1. The intersection of this line with the line $U = 0$ yields the state of motion in A, indicated as S_A. The same applies to point B, starting in point 2.

Proceeding in this manner, we can determine the state of motion at the closed end in points like A, B, $\cdots$. This allows us to construct negative characteristics issuing from these points, with known values of R^-, to determine the motion in the interior computational domain. These negative characteristics intersect positive characteristics, issuing from points like 2, 3 .... at $t = 0$, with known values of R^+, in points like C, D, ..., so that the state of motion in these interior points is known as well.

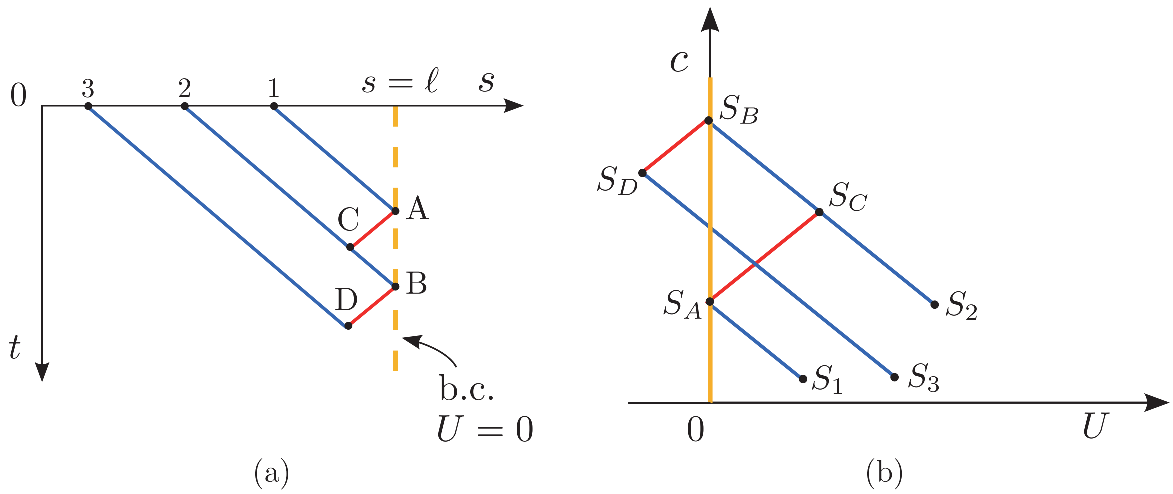

Figure 6.10: Boundary conditions: graphical solution procedure boundary; s,t-plane (a) and state diagram (b)

We can proceed in this manner until a positive characteristic starting at the left boundary at $t=0$ reaches the right boundary. For later times, the positive characteristics reaching $s=\ell$ obtain their R^+-values from the boundary condition at $s=0$.

Boundary types

The above procedure can be used for any type of boundary by plotting in the state diagram the relation holding for U and/or h at the boundary. In this way, a *vertical line* $U=U_B$ prescribes the velocity U_B while a *horizontal* line $h=h_B$ prescribes the water level h_B.

When the boundary represents a control structure (weir, orifice), a **discharge relation** has to be specified as boundary condition. Given that the head loss over such structures is proportional to the local velocity head, the following relation between h and U will hold locally,

$$h = h_B - \xi \frac{|U|\,U}{2g} \tag{6.16}$$

where ξ is the head loss coefficient of the structure and h_B is the surface level in the water system outside the structure (a lake or sea to which it is connected). The notation using the absolute value of the velocity warrants that the difference in head over the structure obtains the correct sign as the flow direction reverses (as with the resistance term in the momentum equation). Equation (6.16) represents two *half parabolas* in the (U,h)-state diagram, yet the graphical solution procedure remains effectively the same, i.e. intersection of the half parabolas with the characteristic relations holding along outgoing characteristics.

Absorbing boundaries

The influence of engineering measures in water systems is often mainly local, diminishing with increasing distance from the site. This is utilized in physical or numerical model studies of the local situation by cutting off the model at a sufficiently remote boundary which can reasonably be assumed to be beyond the influence of the engineering measure concerned.

Because in reality the system extends further, such cut-off creates an artificial, open model boundary. The condition to be imposed there is that disturbances approaching that boundary from within the study area should not be reflected, so as to simulate reality in which they continue unimpeded. In these cases we speak of an **absorbing boundary** (see also Section 4.6). The method of characteristics is particularly helpful in determing the appropriate condition to be imposed at an open boundary in order to make it absorbing.

We start from a situation in which a disturbance, indicated by the bold line segment along the s-axis in Figure 6.11, has entered an initially undisturbed region over some distance in the direction of s-positive. The model is cut off at a point $s = s_r$ while, in reality, the system extends further (lower left panel of Figure 6.11). The state of motion in that exterior domain (i.e. $s > s_r$), possibly varying with location and time, is supposed to be known, e.g. a time-varying discharge from a river with associated water levels. In absence of the cut-off, interior

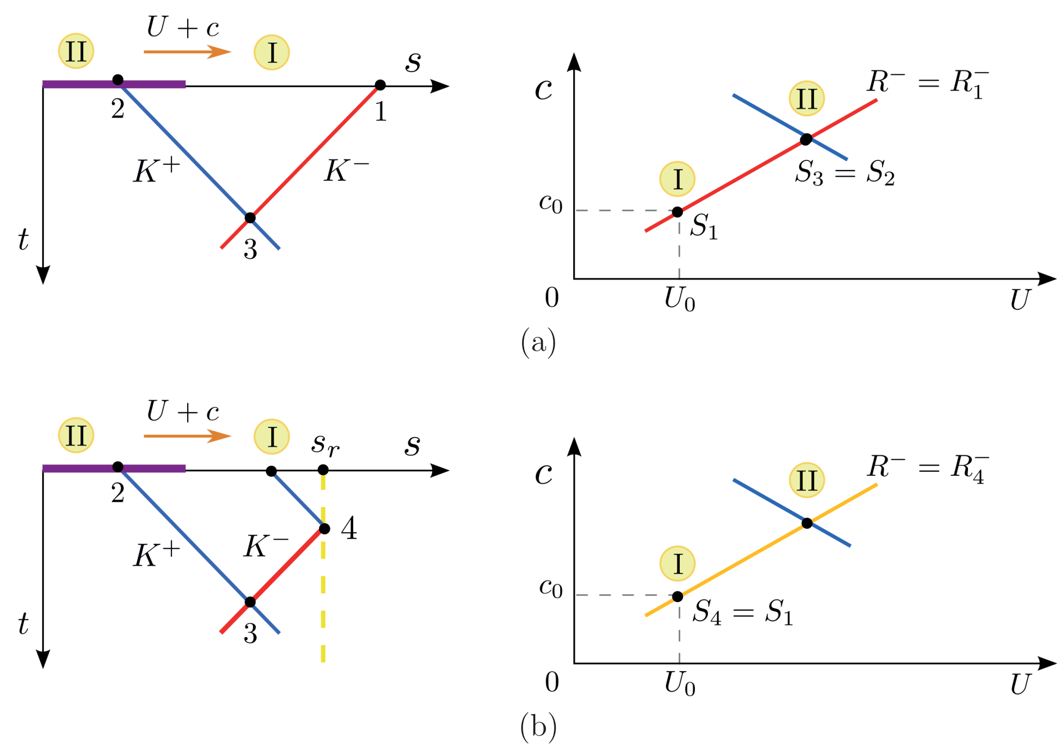

Figure 6.11: Traveling disturbance: (s,t)-plane and state diagram (a), same with the spatial domain truncated at $s = s_r$ (b)

points like point 3 can be reached by a negative characteristic issuing in a point 1, say, in which case $R_3{}^- = R_1{}^- = U_1 - 2c_1$. In the presence of the cut-off, the negative characteristic reaching point 3 should start at the boundary $s = s_r$, in point 4, but this should not affect the state of motion in the interior (computational) domain ($s < s_r$). This implies for point 3 that it should receive the same R^- as in absence of the cut-off, i.e. $R_4{}^- = U_1 - 2c_1$.

In other words, **at the open boundary, the value of the incoming Riemann invariant should be imposed to make it absorbing.** In this manner, the influence from the exterior domain ($s > s_r$) is retained, also in case the state of motion there is varying with location and time, whereas disturbances created by the engineering measure are not reflected at the open boundary.

6.7 External forces

So far, external forces such as resistance or wind action have been ignored, so as to present the method of characteristics in its most elementary form. This restriction is now relaxed.

Let F be the resultant of the external forces per unit mass acting in the positive s-direction. We add this to the right-hand side of Equation (6.2). Repeating the procedure to go from the balance equations of mass and momentum to the characteristic form, we obtain instead of (6.8) and (6.11):

$$\frac{\mathrm{d}R^\pm}{\mathrm{d}t} = F \quad \text{provided that} \quad \frac{\mathrm{d}s}{\mathrm{d}t} = U \pm c \tag{6.17}$$

For finite but small time steps Δt, the differential equation for the rate of change of $R^\pm$ can be approximated in finite-difference form as

$$\Delta R^\pm = \tilde{F} \Delta\, t \tag{6.18}$$

(not $\pm\tilde{F}\Delta\, t$!), where $\tilde{F}$ is the average value of F over the time interval considered. This means that in situations as sketched in Figure 6.12, these variations in $R^\pm$ (which, strictly speaking, are no longer invariants) must be added to the right-hand sides in Equation (6.12):

$$R_3{}^+ = R_1{}^+ + \Delta R_{1,3} \quad \text{and} \quad R_3{}^- = R_2{}^- + \Delta R_{2,3} \tag{6.19}$$

or, in terms of the state variables U and c:

$$U_3 + 2c_3 = U_1 + 2c_1 + \tilde{F}_{1,3} \Delta\, t_{1,3} \tag{6.20}$$

and

$$U_3 - 2c_3 = U_2 - 2c_2 + \tilde{F}_{2,3} \Delta\, t_{2,3} \tag{6.21}$$

in which $\tilde{F}_{1,3}$ and $\tilde{F}_{2,3}$ denote the average values of F between the points 1 and 3 and the points 2 and 3 in the (s, t)-plane, respectively, which can be approximated by using the known values of depth and flow velocity in the respective points.

As before, the algebraic formulation can be carried out graphically in the state diagram,

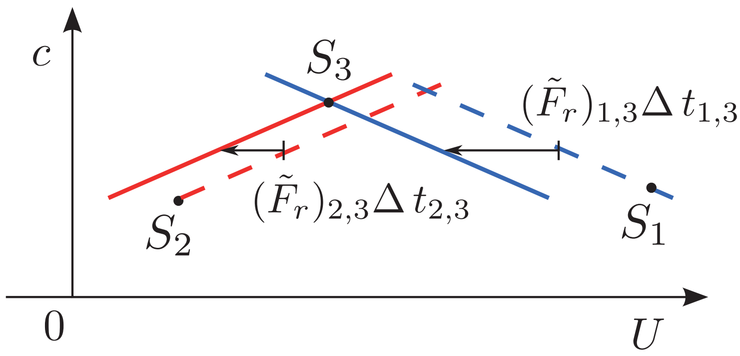

Figure 6.12: Graphical procedure forcing terms in the case of a resistance force (F_r) only

say the (U, c)-plane. To illustrate this, we reconsider the situation in Figure 6.2 where the state of motion in point 3 of the (s, t)-plane (S_3) has to be found. Due to the external force F, S_3 does not ly on the line $R^+ = R_1{}^+$ (dashed in Figure 6.12), but on another (drawn) line parallel to this. This line can be found by shifting the first one such that $\Delta R^+ = \Delta U + 2\Delta\, c = F\Delta\, t$. If we measure this shift along lines of constant c ('horizontally', so $\Delta c = 0$), we have $\Delta U = F\Delta\, t$.

If resistance is the only external force ($F = F_r = -c_f|U|U/d$, say) F opposes U, and the lines of constant $R^\pm$ must be shifted in the direction of $U = 0$, as shown in Figure 6.12. This results in a gradual decrease in absolute value of the flow velocities, or a damping of the motion, as expected for the effect of resistance.

6.8 Simple wave

General solution

This section deals in detail with the important case of a disturbance entering a region of rest or of uniform flow, first considered in Section 4.1 (see Figure 4.2). Such disturbance, traveling in one direction only, is called a **simple wave**. They occur frequently in practice as a result of operation of control structures.

Initially, at $t = 0$, the flow is uniform with depth d_0 (propagation speed $c_0 = \sqrt{gd_0}$ and flow velocity U_0, indicated as state I in the (U, c)-plane of Figure 6.13. Starting at $t = 0$, a time-varying disturbance is imposed at $s = 0$ from where it propagates into the canal, in the direction of s-positive, say ($s > 0$).

We assume that the canal is prismatic and that there are no reflections nor autonomous disturbances propagating in the direction of s-negative.

The disturbance enters the domain $s > 0$ at $t = 0$ with velocity $U_0 + c_0$. Where it has not yet arrived, i.e. in the domain $s > (U_0 + c_0)t$, the initial state of uniform flow is still present. This can be seen formally (as an exercise) by using positive and negative characteristics like $K_a{}^+$ and $K_b{}^-$, issuing at $t = 0$ from two arbitrary points like a and b, and intersecting in a point c, as shown in Figure 6.13 a. Since $R_c{}^+ = R_a{}^+ = R_b{}^+$ and $R_c{}^- = R_b{}^- = R_a{}^-$, the

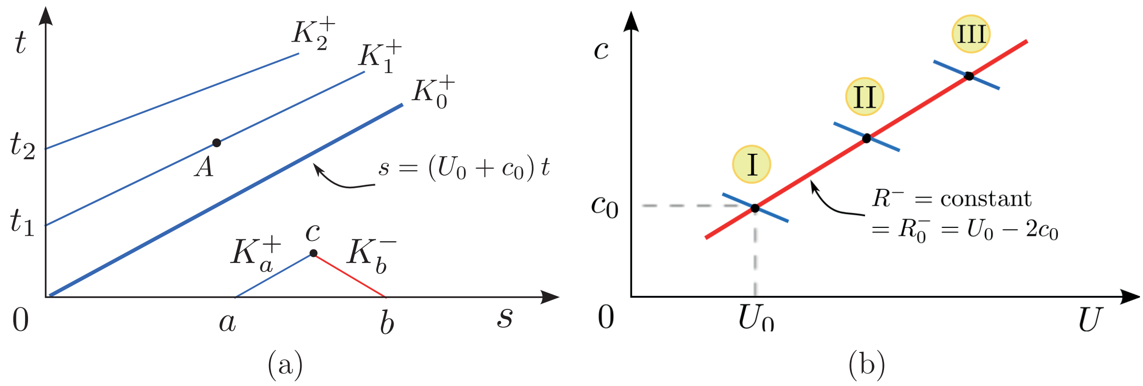

Figure 6.13: Simple wave traveling in positive s-direction; s, t plane with characteristics (a) and state diagram (b)

state in point c is the same as it is in points a and b, i.e. the initial, undisturbed state of uniform flow. This domain is bounded by the characteristic ${K_0}^+$ issuing from $s = 0$ at $t = 0$, indicating the progression of the front of the disturbance.

In order to determine the motion in the region where the disturbance is present, we need (among others) negative characteristics issuing at $t = 0$ from the undisturbed domain. All of these share the same value of R^-, also in the disturbed region. It follows that **in the entire domain, including the disturbed part, all points have the same value of** R^-, given by ${R_0}^- = U_0 - 2c_0$. In other words, in the entire region, the two state variables U and c obey the relation

$$U - U_0 = 2c - 2c_0 = 2\sqrt{gd} - 2\sqrt{gd_0} \tag{6.22}$$

This is a straight line in the (U, c)-plane passing through point I, as shown in the right panel of Figure 6.13. It shows that the flow velocity in the simple wave increases with the local depth, i.e. with the local wave height, and how.

A note on low simple waves

In Chapter 4 relations were derived between variations in flow velocity and surface elevation for a low simple wave, see Equation (4.26). Equation (6.22) is a similar relation, valid for simple waves of arbitrary height. Let us check whether it reduces to Equation (4.26) for low waves, i.e. $\delta d = d - d_0 \ll d_0$. To this end, we make the approximation $\sqrt{gd} = \sqrt{gd_0\,(1 + \delta d/d_0)} \simeq \sqrt{gd_0}\,\left(1 + \frac{1}{2}\delta d/d_0\right)$ and substitute this into Equation (6.22), to obtain $\delta U = U - U_0 \simeq \sqrt{g/d_0}\,\delta d = c_0\,\delta d/d_0$, which is indeed the same as Equation (4.26) (accounting for the difference in notation).

We now consider a positive characteristic ${K_1}^+$ issuing from $s = 0$ at a time $t = t_1$, say (see Figure 6.13, left panel). Along this characteristic, R^+ is constant $= {R_1}^+$. But, as we have seen, all points share the same value of R^-, viz. R_0^- . It follows that both R^+ and R^- are constant along ${K_1}^+$, so that the same is true for the two state variables U and c separately. Since this applies to an arbitrary positive characteristic, it applies to all of them. This in turn implies generally that **in a simple wave, the state of motion is constant along**

any positive characteristic.

Since both U and c are constant along the positive characteristcs, so is their sum $U + c$, i.e. the characteristic direction $(\mathrm{d}s/\mathrm{d}t)$ in the (s,t)-plane. This means that **in a simple wave, the positive characteristics are straight.**

The value of $U + c$ for any positive characteristic depends on the associated value of R^+, which in turn is determined by the boundary condition in $s = 0$ at the time when the characteristic was started. Using Equation (6.22), this can be written as

$$\frac{\mathrm{d}s}{\mathrm{d}t} = U + c = U_0 + 3c - 2c_0 = U_0 + 3\sqrt{gd} - 2\sqrt{gd_0} \tag{6.23}$$

It follows that points of constant U and c (or constant U and d, therefore also of constant discharge $q = Ud$) are moving with a constant speed which is higher for points of the wave with a larger wave height (larger depth) than it is for the lower parts. Stated another way: higher parts of the wave travel faster than lower parts: the wave deforms. This can also be seen from the characteristics, because two positive characteristics with constant but different wave heights (therefore also different values of U and c) diverge or converge, which means that the distance between any two points on the wave with different depths varies linearly in time.

Thus, **the wave deforms as it propagates**. This was already made plausible in the context of high translatory waves in Chapter 5. The difference is that we now have proof, and a method to calculate the rate of deformation.

Expansion wave

In order to investigate the wave deformation further, we choose for simplicity (without losing anything essential) a uniform state of rest ($U_0 = 0$, $d = \text{constant} = d_0$) in a long canal as the initial condition, and a prescribed time variation of the flow velocity in $s = 0$ as one of the boundary conditions. A second boundary condition is provided by the assumed absence of reflected waves from downstream, as in any simple wave.

We first consider a situation with **outflow** at $s = 0$ with an initially increasing outflow velocity, tapering off to a constant value after some time, as sketched in the left panel of Figure 6.14. The starting outflow causes a **negative wave** propagating away from the outflow boundary. Along the characteristic ${K_0}^+$ through the point $s = 0, t = 0$, the wave speed is $U_0 + c_0$ (actually, $U_0 = 0$, but we write it for consistency in the expressions). It separates the disturbed domain from the undisturbed one.

Next consider a characteristic ${K_1}^+$ starting at the left boundary at some time $t = t_1$, when $U = U_1 < 0$, so $d = d_1 < d_0$, and therefore also $U_1 + c_1 < U_0 + c_0$. This implies that ${K_1}^+$ diverges from ${K_0}^+$: the disturbance travels more slowly than those in the undisturbed region. The point on the wave where $d = d_1$ lags more and more behind the front of the wave. The wave, being negative, becomes less and less steep and more and more stretched as time goes on. This type of wave is called an **expansion wave**.

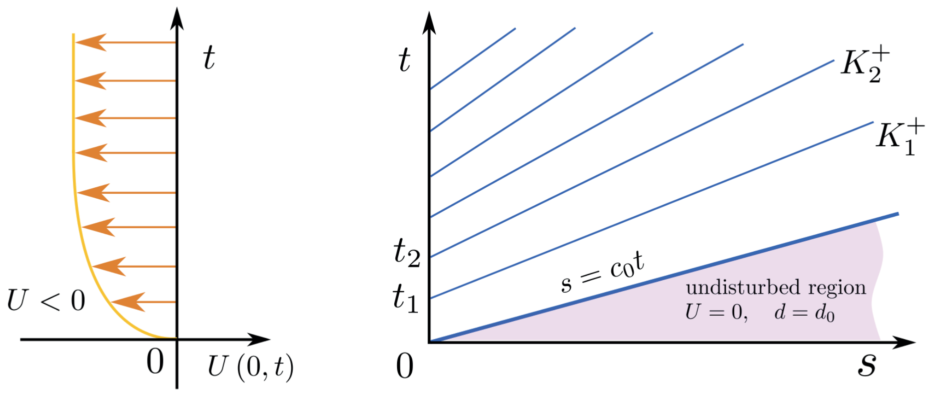

Figure 6.14: Expansion wave traveling in positive s-direction; velocity variation at outflow boundary (left panel) and (s, t) plane with characteristics (right panel)

At some instant, the outflow velocity has become constant. From that moment on, the positive characteristics issuing at $s = 0$ have the same values of U and c; they are mutually parallel, signifying a new state of uniform flow, with a smaller depth than initially, and with a negative flow velocity equal to the velocity finally imposed at $s = 0$.

Example 6.1. *Expansion wave*

Situation	Solution
Consider a semi-infinite canal with initial depth $d_0 = 5$ m and initial velocity $U_0 = 0$. A pumping station at the (left) boundary of the canal starts withdrawing water as a result of which an expansion wave starts traveling along the canal. Consider a point on the expansion wave in which the velocity U_1 = -0.5 m/s.	In the undisturbed region $c_0 = \sqrt{gd_0} = 7.0$ m/s. 1. using Equation (6.22) (with $U_0 = 0$) we obtain $c_1 = c_0 + U_1/2 = 6.75$ m/s, so $d_1 = c_1^2/g = 4.5$ m 2. the propagation speed $\mathrm{d}s/\mathrm{d}t\|_1$ equals $U_1 + c_1 = c_0 + (3/2)\, U_1 = 6.25$ m/s
Questions	**Comment**
1. calculate the water depth (d_1) in this point 2. determine the speed ($\mathrm{d}s/\mathrm{d}t\|_1$) with which this point propagates along the canal	Notice how the smaller value of d and that of U (with respect to the initial state) both contribute to the propagation speed ($\mathrm{d}s/\mathrm{d}t$) being smaller than its undisturbed value.

Compression wave

We now treat a situation of **inflow**, with a flow velocity initially increasing from zero, and finally going to a constant value, as in the left panel of Figure 6.15. The starting inflow causes a **positive wave** propagating into the adjacent canal reach. When in a certain time

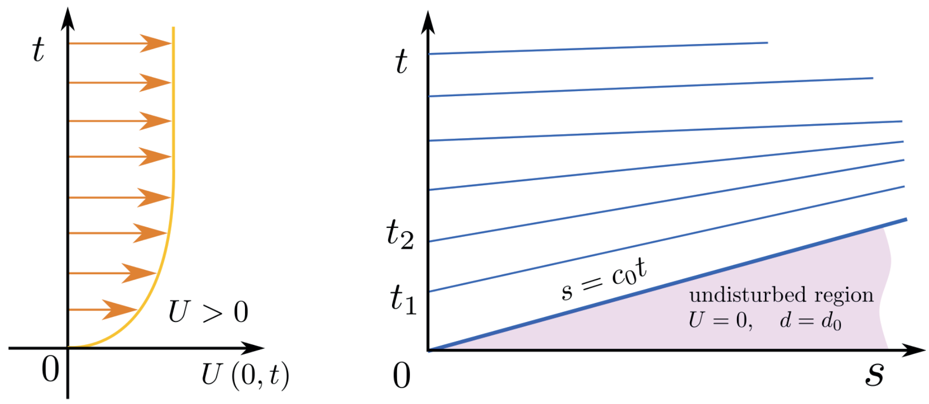

Figure 6.15: Compression wave traveling in positive s-direction; velocity variation at inflow boundary (left panel) and (s,t) plane with characteristics (right panel)

interval the inflow velocity increases, so do the local values of d and c, therefore also that of $U + c$: the positive characteristics converge, the wave becomes steeper in time. This type of wave is called a **compression wave**. At some moment, positive characteristics intersect, at which point (in space and in time) the solution becomes multi-valued, with two different values of the momentary surface elevation at the same cross-section. A discontinuity in surface elevation develops: a bore or **shock wave**.

Consider two positive characteristcs ${K_1}^+$ and ${K_2}^+$, issuing from $s = s_0$ at times $t = t_1$ and $t = t_2 = t_1 + \Delta t$, respectively, such that $\mathrm{d}s/\mathrm{d}t|_2 > \mathrm{d}s/\mathrm{d}t|_1$. Elementary geometry shows that they intersect at a time t_i and a location s_i given by

$$t_i = t_1 + \frac{V_2}{V_2 - V_1}\Delta t = t_2 + \frac{V_1}{V_2 - V_1}\Delta t \tag{6.24}$$

and

$$s_i = s_0 + \frac{V_1 V_2}{V_2 - V_1}\Delta t \tag{6.25}$$

in which we have used the shorthand notation $V = \mathrm{d}s/\mathrm{d}t = U + c$.

In the above, the prescribed time variation of the flow velocity was chosen as the boundary condition, for convenience. In practice, it is more likely that the discharge is given, as at a pumping station, or a relation between surface elevation and discharge, as in a gated control structure. Such conditions make the algebra a bit more complicated without adding insight in the process of wave deformation. Stoker [1] treats in detail the case of a horizontally translating vertical gate, with special attention to the case of withdrawal. When the gate recedes at a sufficiently high velocity, the water cannot keep up with it and the bed falls dry. This is the so-called dambreak problem, which can be solved analytically in closed form using the method of characteristics.

Example 6.2. *Compression wave*

Situation	Solution
As in Example 6.1, but with a discharge of water from the pumping station causing a compression wave traveling along the canal. In a time interval from t_1 to $t_2 = t_1 + \Delta t = t_1 + 60$ seconds the velocity at the pumping station increases from $U_1 = 0.5$ m/s to $U_2 = 1$ m/s.	Using $V = \mathrm{d}s/\mathrm{d}t = c_0 + (3/2)U$ gives $V_1 = 7.75$ m/s and $V_2 = 8.50$ m/s. 1. instant of intersection (Equation (6.24)): $t_i = t_1 + (V_2/(V_2 - V_1))\,\Delta t = t_1 + 680$ s 2. location of intersection (Equation (6.25)): $s_i = s_0 + (V_1 V_2/(V_2 - V_1))\,\Delta t = 5270$ m from the pumping station
Questions	**Comment**
1. determine the instant, with respect to t_1, at which the respective characteristics K_1^+ and K_2^+ intersect 2. determine the location, with respect to the pumping station, where these characteristics intersect	A bore is formed when an intersection of positive characteristics *first* occurs. When and where this happens depends on the time variation of the imposed inflow velocity. The numbers used in the example were chosen arbitrarily; they do not refer to the instant and location of bore formation.

6.9 Pressure waves in pipelines

In this Section, we consider applications of the method of characteristics to presssure waves in closed conduits, in particular pipelines, for which it is highly suitable, as we will see.

Characteristic equations

In Chapter 2, the mass balance for the liquid under pressure in a pipeline was expressed in terms of the state variables U and p as follows (Equation (2.37)):

$$\frac{\partial p}{\partial t} + U\frac{\partial p}{\partial s} + \rho c^2 \frac{\partial U}{\partial s} = 0 \tag{6.26}$$

in which c is defined by

$$\frac{1}{c^2} = \frac{\rho}{K} + \frac{\rho D}{E\delta} \tag{6.27}$$

Neglecting friction, and using p for the dynamic pressure (the deviation from hydrostatic pressure), the equation of motion is written as (Equation (2.38))

$$\frac{\partial U}{\partial t} + U\frac{\partial U}{\partial s} + \frac{1}{\rho}\frac{\partial p}{\partial s} = 0 \tag{6.28}$$

The characteristic relations for U and p can be derived from (6.26) and (6.28) through the same kind of procedure as used for open water, with the result

$$\frac{\mathrm{d}R_p^{\pm}}{\mathrm{d}t} = 0 \quad \text{provided} \quad \frac{\mathrm{d}s}{\mathrm{d}t} = U \pm c \tag{6.29}$$

in which

$$R_p{}^{\pm} = p \pm \rho c U \tag{6.30}$$

Using the piezometric level h and U as the two state variables, we define

$$R_h{}^{\pm} = h \pm \frac{c}{g} U \tag{6.31}$$

and obtain

$$\frac{\mathrm{d}R_h^{\pm}}{\mathrm{d}t} = 0 \quad \text{provided} \quad \frac{\mathrm{d}s}{\mathrm{d}t} = U \pm c \tag{6.32}$$

It follows from these characteristic relations that c is the speed of longitudinal propagation of pressure waves in the coupled fluid-pipe system, relative to the fluid.

Although the pressure-induced variations of the mass density ρ have been accounted for in the mass balance, and so in the expression for the wave speed, the relative magnitude of these is always quite small, and can be neglected where ρ appears in the equations as a multiplying factor. In this approximation, the wave speed c is independent of the actual state of motion, and lines of constant values of $R_p{}^{\pm}$ in the (U, p) state diagram are straight; so are lines of constant values of $R_h{}^{\pm}$ in the (U, h)-plane. This means that variations in U and p or h are proportional, not only for infinitesimal variations but also for finite values. Written in finite difference form, the characteristic relations can be expressed as

$$\boxed{\Delta p^{\pm} = \mp \rho c \Delta U \quad \text{and} \quad \Delta h^{\pm} = \mp \frac{c}{g} \Delta U \quad \text{provided} \quad \frac{\mathrm{d}s}{\mathrm{d}t} = U \pm c} \tag{6.33}$$

These relations are valid for disturbances of arbitrary magnitude, not just infinitesimal ones.

For low disturbances in free-surface flows, the relation $\delta d = \mp(c_0/g)\delta U$ was derived (Equation (6.15)), valid along the $\pm$ characteristics. At the free surface, $\delta p = 0$, so that $\delta d = \delta h$ and $\delta h = \mp(c_0/g)\delta U$ along the $\pm$ characteristics, + the same as for pressurized flow in a pipe. The difference is that for free-surface flows these proportionalities are valid only for weak disturbances, whereas such restriction does not apply in pressurized flows.

Physical behavior

As a result of the very limited storage available in pressurized flow (in contrast to free-surface flow where mass can be stored by a rise in the free surface), the speed of pressure waves in pipe flow is quite high, of the order of 1000 m/s (see Chapter 2). Relative to this, the flow velocity U can be neglected in the characteristic velocities $U \pm c$, which therefore can be approximated as $\mathrm{d}s/\mathrm{d}t = \pm\, c$, in which moreover c can be be considered to be a constant (for pipes of constant cross-section and elastic properties), independent of the actual pressure. This means that the characteristic velocities to a very good approximation can be considered as constant, i.e. the characteristics are straight lines, independent of the state of motion.

It follows from Eq. (6.30) that even moderate variations in flow velocity can cause large variations in pressure, because of the high values of c, such as 100 m water column for a change in flow velocity of only 1 m/s. This phenomenon is called **water hammer**.

The large pressure variations associated with water hammer can be positive as well as negative. When and where the fluid pressure tends to become lower than the vapour pressure, **cavitation** occurs, i.e. vapour bubbles or even complete cavities are formed. When these collapse, an intense sound is generated (which in some houses can be heard when closing the kitchen tap too rapidly), not unlike the sound caused by hammering on steel.

Water hammer and the associated cavitation can cause serious damage, even fracture, to the pipeline system including its appurtenances such as pumps and valves. Therefore, water hammer requires careful consideration in the design, and it imposes restrictions on the allowable operation of pipeline systems.

Examples

Next, some examples are given of application of the method of characteristics to pipe flow involving the operation of valves in pipeline systems. In each case, the solution is determined graphically. It is important to study the example problems and their solutions closely and to rework them.

Abrupt closure

Consider a pipe with length ℓ between two reservoirs. Initially, the flow in the pipe is uniform with velocity U_0. Wall friction and velocity head effects at the upstream end are ignored, so the piezometric level in the pipe at that end is set equal to the free surface level in the adjacent reservoir, which we take as our reference level $h = 0$ (boundary condition in $s = 0$), which is also the initial level in the whole pipe. At $t = 0$, a valve at the downstream end is suddenly closed completely (boundary condition $U = 0$ in $s = \ell$ for $t > 0$). The solution is given in Figure 6.16, showing the (s, t) diagram and the (U, h) state diagram.

At the location of the closed valve, the initial flow (state I) is suddenly brought to a halt and the pressure rises steeply (state II). The front of this transition travels upstream and reaches the open end at time $t = \ell/c$, where it is 100% negatively reflected (state III) because $h =$ constant as a result of the presence of the reservoir. The reflected negative wave arrives at time $t = 2\ell/c$ at the end of the closed valve and is reflected there by 100% (state IV).

At time $t = 4\ell/c$, the front has traveled up and down the pipe once more, after which the original state is restored and the process repeats itself with a period $T = 4\ell/c$. This goes on 'forever' because energy losses (due to wall friction and expansion at the exit) have been neglected.

Ignoring cavitation, the maximum and minimum piezometric level are $\pm c\,U_0/g$ higher/lower than the undisturbed value of zero, corresponding to pressure variations of $\pm \rho c U_0$. The sequence of states I through IV (right panel of Figure 6.16) is indicated in the s, t-diagram as well as in the graphs in Figure 6.18 where they are visible in a sequence of longitudinal profiles.

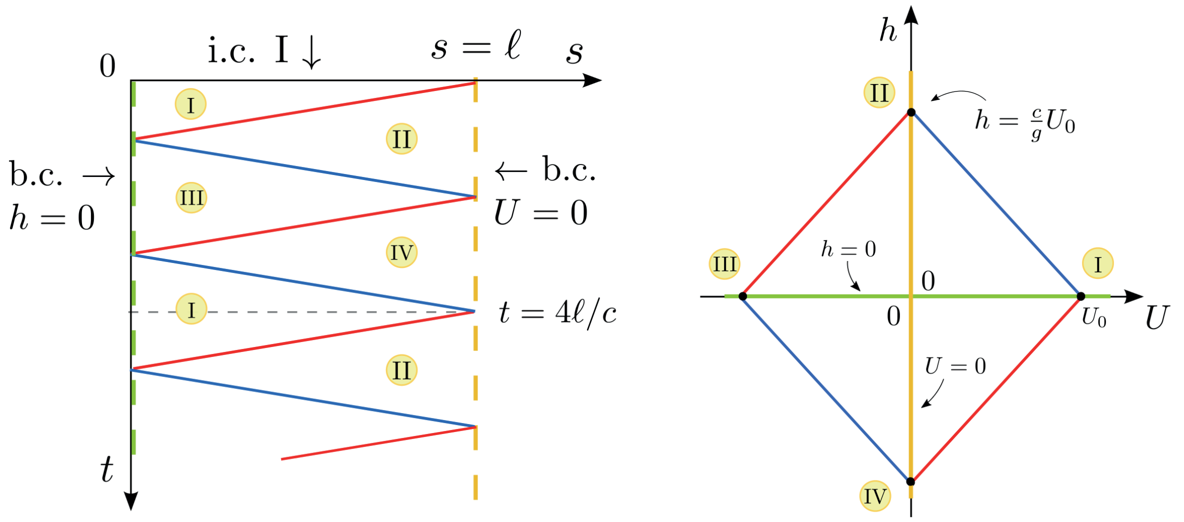

Figure 6.16: Abrupt closure at downstream end of a pipe; (s,t) diagram (left panel) and (U,h) state diagram (right panel)

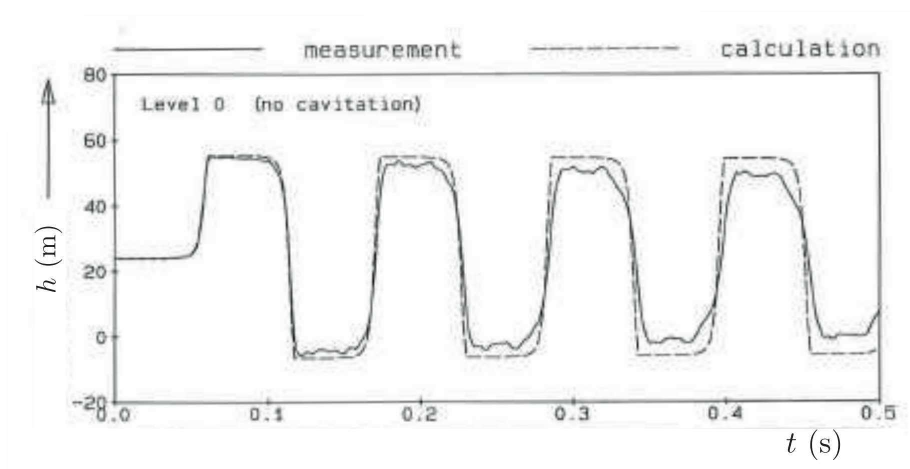

Figure 6.17: Abrupt closure: measured (Simpson, 1986) and computed (Tijsseling, 1993) pressures (from: Tijsseling [2])

At a fixed point, the maximum and minimum pressures alternate as time goes on. Near either end, the durations of maximum and of minimum pressure are unequal (consider some sections $s =$ constant in the (s, t)-plane), but halfway the length of the pipe they last equally long.

Figure 6.17 shows a time sequence of absolute pressure heads measured in a fixed point in the middle of the pipe for the present situation (Figure 3.2 presents a similar plot). The initial pressure was sufficiently high to prevent the occurrence of cavitation (see the minimum pressure head of almost - 10 m water column). The pattern of the pressure variations and the values agree with the theory. The most notable deviation is the gradual decay of the measured oscillations, which is not predicted by this theory in which all losses were neglected. (For a quantitative check, the experimental data listed in Problems 16 and 17 at the end of this chapter can be used.)

Gradual closure

The large pressure variations associated with abrupt closure of a valve (or the sudden start or shut-off of a pump) are undesirable. They can be avoided to a controlable extent by a more gradual closure. This can be seen as follows.

The preceding example shows that the high-pressure wave, originated at the location of the sudden closure, is negatively reflected at the other, open end of the pipe. When this reflected negative wave arrives at the closed end, it can compensate the pressure build-up there, provided the closure was not yet complete by the time of arrival of the reflected, negative wave. This means that the closure should take longer than $2\ell/c$.

In the following elaboration of this idea we assume the same situation and approximations as in the preceding example, except for the presence of a valve at the downstream end. Initially, the valve is fully open ($h = 0$). We assume the following relationship to describe the effect of partial closure of the valve:

$$h = \left(\frac{1}{\mu^2} - 1\right) \frac{|U|U}{2g} \tag{6.34}$$

in which h is the piezometric level and U the flow velocity in the pipe near the valve (U is positive in case of outflow), and μ is the ratio of the effective cross-sectional area of the valve opening to that of the pipe. This relation is shown graphically in the state diagram of Figure 6.19 as two mirrored half-parabolas. For a fully open valve, $\mu = 1$ ($h = 0$ for finite U), and for a fully closed valve, $\mu = 0$ ($U = 0$ for finite h).

Instead of using a truly gradual closure we approximate it as a two-step process, assuming that at $t = 0$ the valve is abruptly but partially closed, such that $\mu =$ constant $= \mu_1$ for $0 < t < 4\ell/c$, with $0 < \mu_1 < 1$, after which it is abruptly fully closed ($\mu = 0$).

The solution is shown in Figure 6.19. It can be seen that the partial closure causes a moderate pressure rise (state II). In the end, after the valve has been closed completely, a periodic state is established (states V, VI, VII and VIII), as in the preceding example, but the maximum

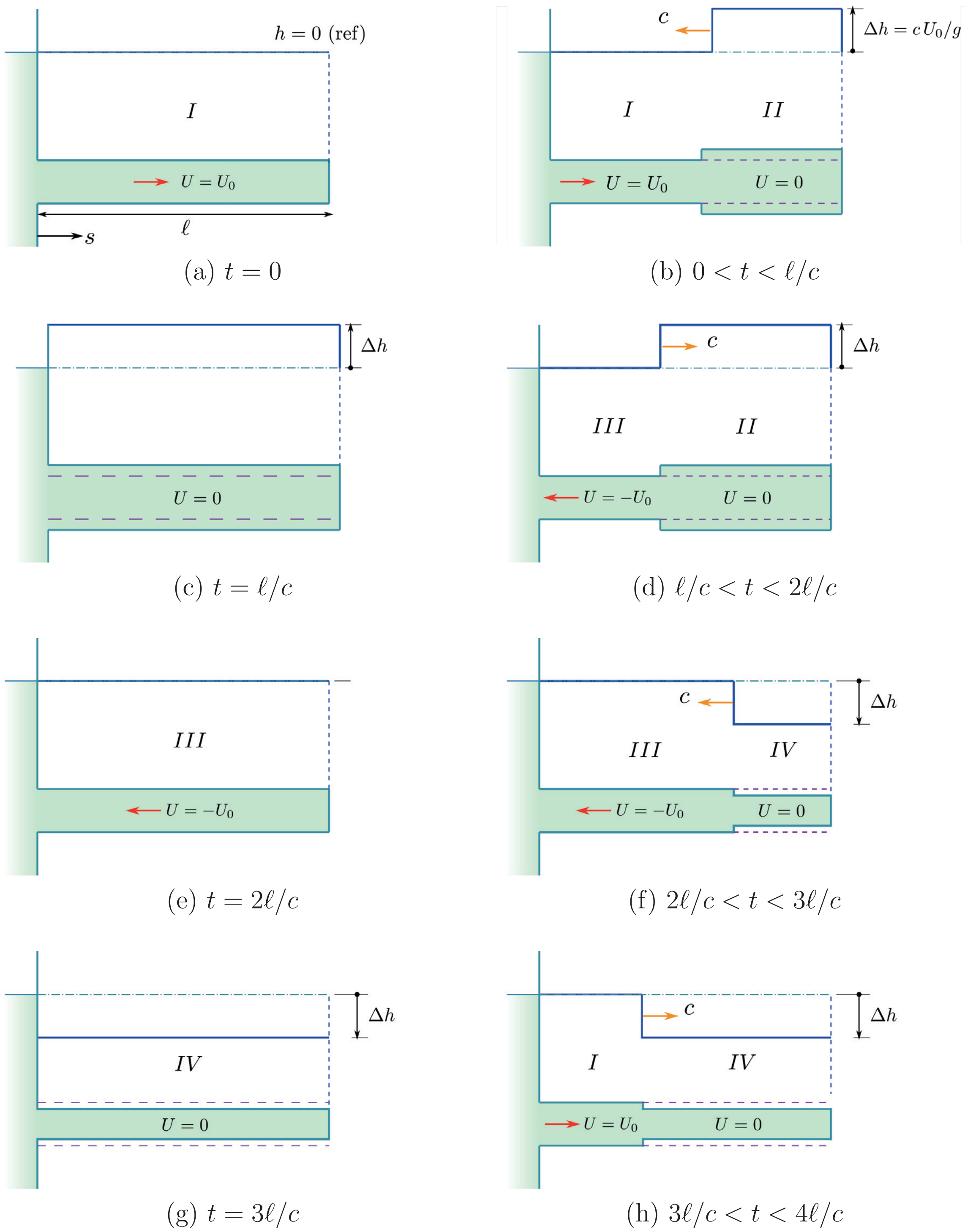

Figure 6.18: Abrupt closure: snapshots of pressure variation and flow velocity in a pipeline; state at $t = 4\ell/c$ equals that at $t = 0$ (a)

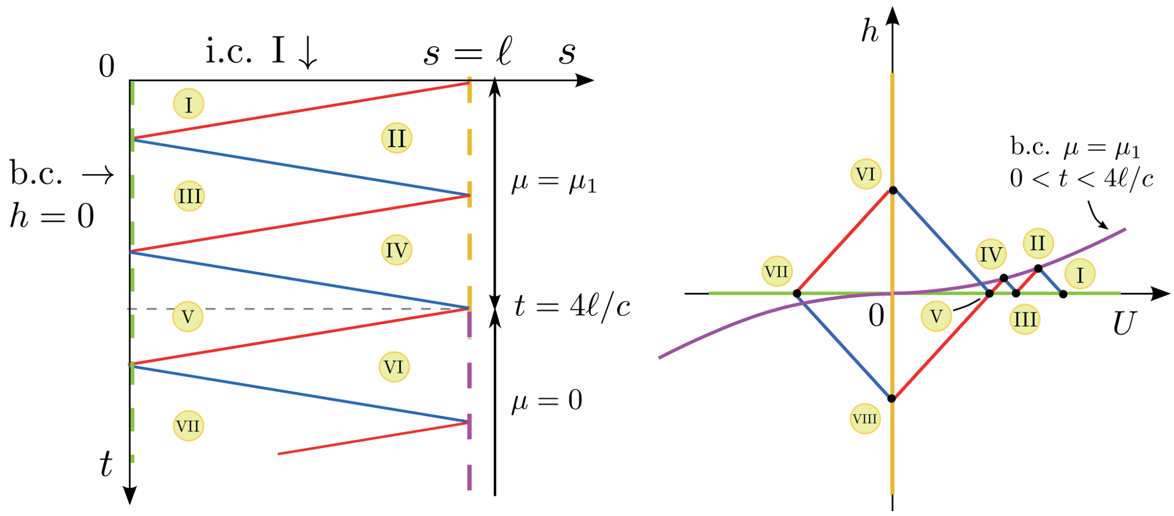

Figure 6.19: Gradual closure at downstream end of a pipe; s, t diagram (left panel) and state diagram (right panel)

and minimum pressures are smaller in absolute magnitude due to the effect of the reflected negative wave arriving at the valve at $t = 2\ell/c$, when the valve was not yet fully closed.

It is obvious from the above that closing the valve in a sequence of small steps, or gradually, can reduce the maximum and minimum pressures (in absolute magnitude) at will, provided the duration is sufficiently long compared to the basic travel time of $2\ell/c$.

Influence of exit losses and/or wall friction

We return to the situation first considered, of initially uniform flow in a pipe which at the downstream end is abruptly closed. The only difference is in the boundary condition at $s = 0$, where we now take velocity head effects into account, leading to $h = 0$ during outflow and $h = -U^2/2g$ during (streamlined) inflow. This results in the following relation to be imposed in $s = 0$:

$$h = \begin{cases} 0 & \text{if } U < 0 \\ -U^2/2g & \text{if } U > 0 \end{cases} \tag{6.35}$$

See the state diagram in Figure 6.20

The solution is presented in Figure 6.20. Again, an oscillation develops with a period equal to $4\ell/c$, but this time the extreme values decrease in time as a result of the assumed exit losses. Formally, the effect of wall friction can be accounted for with the method described in Section 6.7 but this would require a large number of computational points along the length of the pipe, which makes the solution laborious. The overall effect of resistance, i.e. the gradual decay of the oscillations, can be obtained more simply by lumping the overall resistance in one or two endpoints, accounting for it through a modification of the boundary conditions.

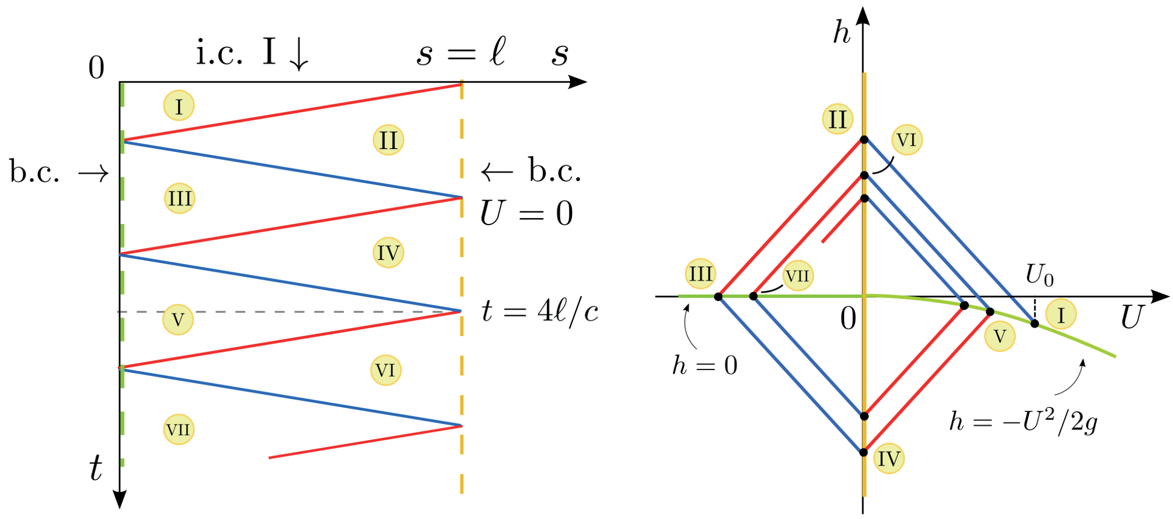

Figure 6.20: Influence of exit losses; s, t diagram (left panel) and state diagram (right panel)

Influence of time scales

The examples presented above clearly show that two time scales are important: the time scale τ_e of external influences, e.g. the duration of closure of a valve, or (at the other extreme) the period of the tide, on the one hand, and the internal system time scale of the travel time of pressure waves over a pipe length (ℓ/c) on the other. Their ratio determines the dynamics of the system:

- for $\tau_e \ll \ell/c$ (relatively fast excitation), dynamic effects are important and compression waves must be taken into acount;
- for $\tau_e \gg \ell/c$, the influence of (slowly varying) boundary conditions is quasi-instantaneously present throughout the pipe length via frequent pressure waves travelling back and forth.

In the latter case, by approximation, the fluid reacts as a rigid column; compression and expansion waves need not be considered.

Bibliography

[1] J. J. Stoker. **Water waves**. Interscience Publishers, New York, 1957.

[2] A. S. Tijsseling. **Fluid-structure interaction in case of waterhammer with cavitation**. PhD thesis, 1993.

Problems

1. Describe the essence of the method of characteristics.
2. What is a characteristic?
3. What is the importance of the characteristics?
4. Which is the physical meaning of the characteristic velocities?
5. Which variables determine these velocities?
6. Considering the characteristic velocities of long waves in open water, what can be said about the relative importance of the flow velocity compared to the wave speed?
7. Same, now for pressurized flow in pipes.
8. Why do the two characteristic velocities in free-surface flows have opposite signs in some cases, and the same signs in others?
9. What is the relevance of the answer to the previous question for the boundary conditions? And for the initial conditions?
10. Is the speed of propagation of a shock wave, relative to the water ahead of it (with depth d_0), larger than $\sqrt{gd_0}$, or smaller, or equal to it?
11. A simple wave, started in $s = 0$ at $t = 0$, propagates into a prismatic canal ($s > 0$) with water at rest, where the undisturbed wave speed is c_0. Is it possible that under certain circumstances it causes disturbances in the domain $s > c_0t$?
12. Verify step by step the graphical solutions for all examples of this chapter by critical analyses of the corresponding s, t-diagram and the state diagram.
13. Elaborate all examples of this chapter by making sketches of the corresponding s, t-diagram and the state diagram.
14. Choose some instants in these solutions and sketch the corresponding longitudinal profiles of the state variables.
15. Choose some fixed locations in these solutions and sketch the corresponding time variations of the state variables in those points.
16. The following data apply to the experiments of Figure 6.17: E = 120 GPa, D

$= 19.05$ mm, $\delta = 1.588$ mm, $\ell = 36$ m, $K = 1.95$ GPa, $\rho = 1000$ kg/m^3. Calculate c and ℓ/c and compare the latter value to the experimental data in the Figure.

17. The pressures shown in Figure 6.17 were measured after the sudden closure of a valve in a flow with initial velocity $U_0 = 0.239$ m/s. Calculate the difference between the maximum and the minimum piezometric level and compare it with the experimental result in the Figure.

18. The following data apply to the situation of a simple wave in a prismatic canal: $d_0 = 5$ m, $U_0 = 0$, and

$$U(0,t) = \begin{cases} U_m \sin^2(\pi t/T) & \text{for } 0 < t < T/2 \\ U_m & \text{for } t > T/2 \end{cases}$$

in which U_m = -0.7 m/s and $T = 60$ s. The following questions should be answered using the method of characteristics.

a Determine the state of motion in the domain $s > c_0 t$.

b Same for the domain $s < c_0 t$, both for some instants $t < T/2$ and for some instants $t > T/2$.

c Calculate and plot the variation of U and d with s for the instants chosen in question (b).

19. Same as Problem 18, now for $U_m = +0.7$ m/s.

20. Same as Problem 18, except that now the discharge per unit canal width ($q = Ud$) is given:

$$q(0,t) = \begin{cases} q_m \sin^2(\pi t/T) & \text{for } 0 < t < T/2 \\ q_m & \text{for } t > T/2 \end{cases}$$

where $q_m = 3.5$ m^2/s. The same questions and assignments apply as in question 19.

21. A canal, initially at rest with $d_0 = 5$ m, $U_0 = 0$, is connected at $s = 0$ by a movable gate to a reservoir whose surface level is 2 m above the undisturbed canal level. Initially, the gate is closed but from time $t = 0$ to $t = T/2 = 30s$, the gate is gradually opened to an effective height $\mu a(t)$ and then brought to a standstill. The discharge per unit canal width (q) is related to the head difference across the gate (Δh) by

$$q = Ud = \mu a \sqrt{2g\Delta h}$$

in which the time variation of the gate opening is given as

$$\mu a = \begin{cases} \mu a_m \sin^2(\pi t/T) & \text{for } 0 < t < T/2 \\ \mu a_m & \text{for } t > T/2 \end{cases}$$

where $\mu a_m = 0.5$ m. The same questions and assignments apply as in Problem 18.

Chapter 7

Tidal basins

7.1 Introduction

In the preceding chapters, the discharge and the surface elevation were treated as continuous functions of s and t. This led to a coupled system of partial differential equations (PDE's) in two unknowns, with wave-like solutions.

Certain flow systems can be schematized in terms of separate but connected basins of finite dimension, in each of which we disregard the spatial variations. In each basin, either storage or transport occurs, but not both, so that the motion within them is not wave-like. In these cases, we speak of a discrete model. One such model is presented in the present chapter.

The disregard of spatial variations in the basins considered is allowed if the dimensions (ℓ) are small compared to a typical length of the (long) waves in the domain. Stated another way, flow systems for which the travel time ('residence time') of long waves through them are short compared to the wave period. In such cases, phase differences within the system are negligible. In other words, the motion loses its wave-like character.

A good example of this category of situations is the tidal motion in a harbour basin. The water level in the basin can to a good approximation be assumed to be horizontal at all times, varying in time only. Its variation can be modelled with an ordinary differential equation (ODE) instead of a PDE, which simplifies the mathematics greatly. This category of flow systems has already been introduced in Section 2.1 under the heading 'Small-basin approximation'. They are treated in detail in the present chapter.

The discrete modelling approach is utilized in the present chapter. It is relevant in itself, because numerous situations occurring in practice lend themselves to this approximation, and it is at the same time a preparation for the theory in the following chapter (on harmonic wave propagation) with respect to the linearized modelling of the flow resistance, and the use of complex algebra in the solution process. The advantage is that these building blocks in the theory of Chapter 8 are introduced in the simpler context of the present chapter.

We focus on flow systems consisting of a nearly closed basin or reservoir, connected through some narrow, short opening or a channel of some length to an external body of water with a time-varying water level. The latter distinction (short vs. long) is relevant because in a short connection, inertia and wall resistance can be neglected, whereas these may be important in a long connecting channel. An artificial, man-made example of such system is the so-called

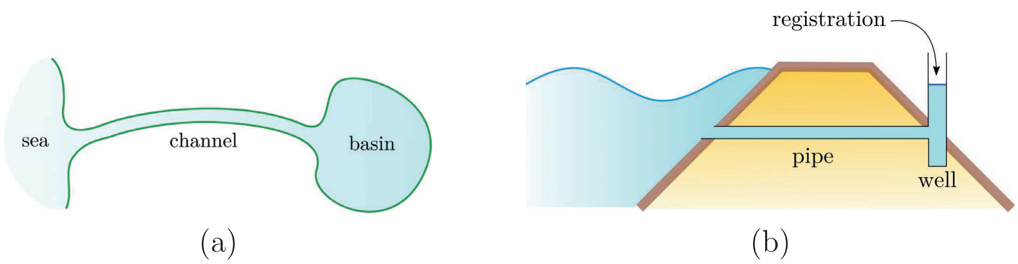

Figure 7.1: Basin with channel (a) and tide well with pipe (b)

tide well, a device used for measuring tides (or river stages), which may consist of a large-diameter tube, placed vertically and connected to an external water with varying water level. The connection may be long, such as a piece of pipe needed to bridge the distance from the external water to the location of the tide well (Figure 7.1b), or it may be quite short, for instance not more than an orifice in the tube wall (Figure 7.2b).

A more common, natural example is the tidal basin, connected to a tidal sea with a a tidal channel (Figure 7.1a), or it may be short, such as an inlet, a breach in a dike or a gap in a barrier (Figure 7.2a). In fact, this is the archetype of the category of systems considered here. Below, we will for brevity use the terminology for such a tidal system, even though the theory applies more generally.

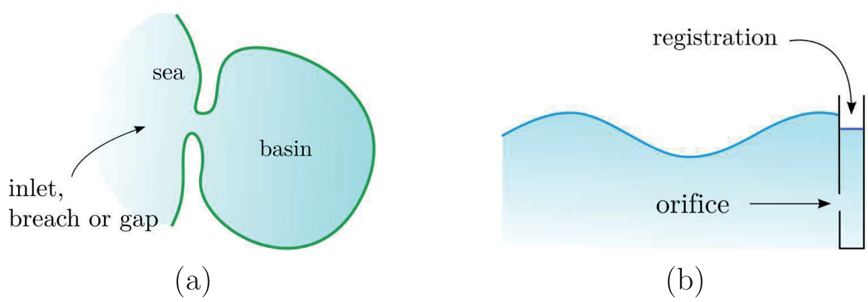

Figure 7.2: Basin with gap (a) and tide well with orifice (b)

In the discrete modelling of the flow systems as described, the only function ('task') of the tidal basin is **storage**; its connection to the tidal sea has only a function of **transport**. In the basin, flow resistance and inertia are neglected, whereas in the connection these may be relevant, certainly head loss due to boundary resistance or expansion loss, but storage is not. Thus, in such discrete model these two functions are separated, in contrast to the continuous-modelling approach in the preceding chapters, in which they were intertwined.

An example of this kind of schematization is the discrete model of a **mass-spring-dashpot system**, well known from classical dynamics, in which kinetic energy is stored only in the mass, neglecting the mass of the spring, and all potential energy is ascribed to the spring, treating the mass as a rigid body.

7.2 Mathematical formulation

Motion in the basin

The basin is assumed to be relatively short, and it is closed except for a connection to the external body of water. There is no throughflow, so that the flow velocities in the basin are quite low. Flow resistance and inertia are negligible. Therefore, the water level in the basin can be assumed to be horizontal at all times. It can be described as a function of time only: $h_b(t)$. This is the so-called **Hemholtz mode** or **pumping mode**.

If we denote the incoming rate of flow (discharge) as Q_{in}, and the area of the free surface in the basin, available for storage, as A_b, the balance equation for the volume of water stored in the reservoir reads

$$\boxed{Q_{in} = A_b \frac{\mathrm{d}h_b}{\mathrm{d}t}} \tag{7.1}$$

Note that A_b may vary in time through its dependence on the time-varying water level: $A_b(t) = A_b(h_b(t))$.

Motion in the channel

For generality, we assume initially that the connection between basin and sea consists of a channel. By letting the channel length go to zero, we cover the case of a short connection, e.g. a gap in a barrier. The main function of the channel is to convey water between the sea and the basin. Within the discrete-modelling approach, storage in the channel is neglected. This is allowable if the free-surface area in the channel is far smaller than that in the basin.

Elaborating on this approximation, we start with the one-dimensional volume balance as derived in Chapter 2:

$$B\frac{\partial h}{\partial t} + \frac{\partial Q}{\partial s} = 0 \tag{7.2}$$

where B is the width of the free surface in the channel. Neglecting storage in the channel implies neglect of the first term in this equation, from which it follows that also $\partial Q/\partial s = 0$. Therefore, in the channel, Q can be considered to be a function of time only: $Q(t)$, which therefore also equals $Q_{in}(t)$.

By definition, $Q = UA_c$. For a prismatic channel, $\partial A_c/\partial s = 0$, in which case the approximation $\partial Q/\partial s = 0$ implies also $\partial U/\partial s = 0$. This in turn implies that the water mass in the channel is moving back and forth as a solid block, with constant distance between the fluid particles. That is why this is called the **rigid-column approximation**.

Our next task is to model the dynamics of the flow. We start with the motion *in* the channel. The transitions at both ends are considered separately. See Figure 7.3. The equation of motion for the flow in the channel (Equation (2.10)) reads

$$\frac{\partial Q}{\partial t} + \frac{\partial}{\partial s}\left(\frac{Q^2}{A_c}\right) + gA_c\frac{\partial h}{\partial s} + c_f\frac{|Q|Q}{A_cR} = 0 \tag{7.3}$$

We integrate this over the channel length, say from $s = 0$ at the sea side to $s = \ell$ at the basin side (not counting the transitions). To do this, we must know how the various terms vary with s.

We set $\partial Q/\partial s$ equal to zero, and, assuming a prismatic channel, do the same with $\partial A_c/\partial s$, so that the second term vanishes. This also makes the resistance term independent of s, and since the same is true for the first term, it must also apply to the last remaining term, proportional to the slope of the free surface. So we obtain upon integration with respect to s:

$$\ell\frac{\mathrm{d}Q}{\mathrm{d}t} + gA_c\left(h\left(\ell\right) - h\left(0\right) + \Delta H_r\right) = 0 \tag{7.4}$$

in which ΔH_r is the head loss due to boundary resistance, given by

$$\Delta H_r = c_f\,\frac{|Q|Q}{g{A_c}^2R}\ell = c_f\,\frac{\ell}{R}\,\frac{|U|U}{g} \tag{7.5}$$

These equations apply to the flow in the channel.

Next, we account for the flow in both transitions. To this end, we distinguish the free surface elevation in the channel ends, $h(0)$ and $h(\ell)$, respectively, from those at sea (h_s) and in the basin (h_b).(Of course, in practice such transitions are always gradual, and the definition of a channel end is subjective, but we must make such schematizations in the framework of a one-dimensional (s, t) model. It would require a two-dimensional (x, y, t) model to account for the transitions in a more realistic way.)

We treat the flow in the transitions as quasi-steady, i.e. at any moment adapted to the instantaneous upstream and downstream water levels, and to be modelled with the methods of classical hydraulics (see also Figure 7.3):

- When and where there is **inflow** (flood at the sea side, ebb at the basin side), the flow in the transition zone is accelerating fairly rapidly and we can apply Bernoulli's law. (Boundary resistance in the short transitions is neglected.) This implies velocity head in the channel ($U^2/2g$). (This drop does not represent an energy loss, but merely a transformation of potential energy to kinetic energy.)

- When and where there is **outflow** (ebb at the sea side, flood at the basin side), the flow is decelerating, and we can assume an expansion loss given by $\Delta H_e = U^2/2g$, implying a horizontal free surface across the transition.

For ebb as well as flood, the total head difference between sea and basin is now given by

$$h_s - h_b = h(0) - h(\ell) + \Delta H_e \tag{7.6}$$

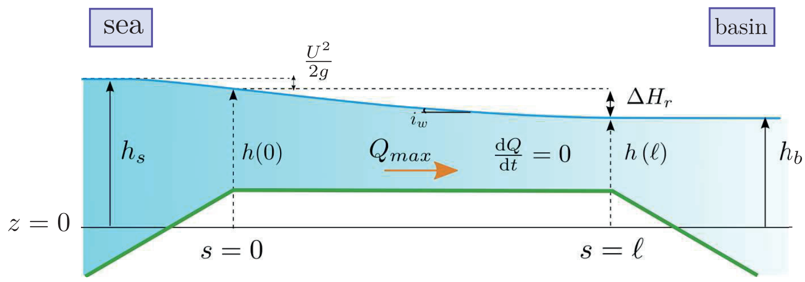

(a) Maximum flood:

$Q = Q_{max}$, $dQ/dt = 0$, $h_s - h_b = W$

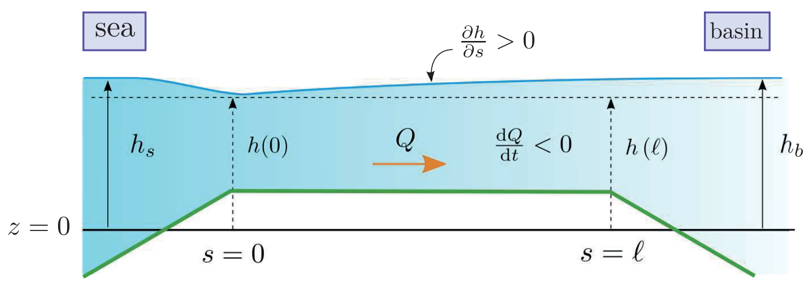

(b) Zero head loss:

$h_s - h_b = 0$, $Q > 0$, $dQ/dt = -gA_cW/\ell$

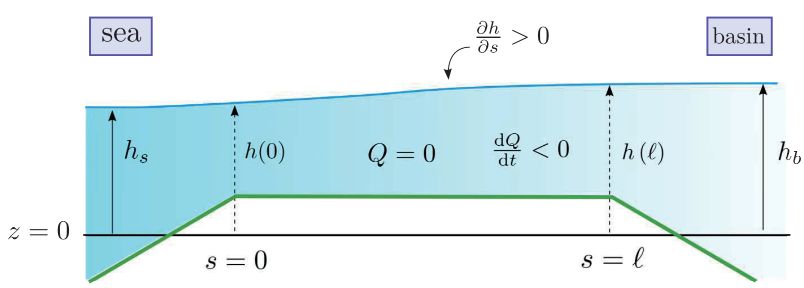

(c) Slack tide:

$Q = 0$, $W = 0$, $dQ/dt = gA_c(h_s - h_b)/\ell$

Figure 7.3: Discharge in the channel

in which $\Delta H_e = |U|U/2g$. Substituting this into Equation (7.4) gives

$$\boxed{h_s - h_b = \frac{\ell}{gA_c}\frac{\mathrm{d}Q}{\mathrm{d}t} + W} \tag{7.7}$$

in which W is the total head loss due to boundary resistance and expansion loss:

$$W = \Delta H_e + \Delta H_r = \frac{|U|U}{2g} + c_f\,\frac{\ell}{R}\frac{|U|U}{g} \tag{7.8}$$

The overall head difference, i.e. the left-hand side of Equation (7.7), accelerates the water in the channel (first term in the right-hand side) and it overcomes the losses (second term in the right-hand side).

Reference is made to Figure 7.3, which shows longitudinal profiles at a few special instants during the flood phase of the tidal cycle. (The subsequent ebb phase follows the same pattern and is not shown separately.)

Figure 7.3a applies to the moment of maximum flood current, so that $\mathrm{d}Q/\mathrm{d}t = 0$. The flow momentarily behaves as a steady flow, in which the available head difference $(h_s - h_b)$ is spent on overcoming the losses (W).

As a result of the inflow, the water level in the basin rises; at some moment it equals the level at sea: $h_s - h_b = 0$ (Figure 7.3b). At that moment there is still flood flow, but it is being decelerated because of the adverse pressure gradient (induced by the surface slope) and the flow resistance. (Needless to say, this situation, with flow against the applied forces, is only possible on account of inertia.)

In the next phase, the water level in the basin has risen above that in the sea, strengthening the opposing pressure forces. The continuing action of the opposing forces causes the flow at some moment to change direction, i.e. slack tide occurs, at which time the flow velocity is momentarily zero, and so are the losses: $W = 0$, as shown in Figure 7.3c. (This applies to the cross-sectionally averaged velocity. The relatively low near-bottom velocities reverse earlier.) Following that moment, the ebb current starts, being accelerated by the seaward-directed pressure force.

Coupled system

Equations (7.1) and (7.7) form a coupled set of two first-order ODE's in h_b and Q as functions of time. These can be integrated with standard numerical routines such as Runge-Kutta, provided the initial values of h_b and Q are known, as well as the tide level at sea (h_s). By eliminating Q, we obtain a second-order ODE in h_b, or vice versa.

First, we simplify the notation by introducing the dimensionless loss coefficient

$$\chi = \frac{1}{2} + c_f\,\frac{\ell}{R} \tag{7.9}$$

with which the expression for W can be written as

$$W = \chi \frac{|U|U}{g} = \chi \frac{|Q|Q}{gA_c{}^2} \tag{7.10}$$

Substituting this in Equation (7.7) and rearranging terms we obtain

$$\frac{\ell}{gA_c} \frac{\mathrm{d}Q}{\mathrm{d}t} = h_s - h_b - W = h_s - h_b - \chi \frac{|Q|Q}{gA_c{}^2} \tag{7.11}$$

Substituting Equation (7.1) in this equation, with $Q = Q_{in}$, and neglecting variations of A_c with h_b, yields

$$\boxed{\frac{\ell}{g} \frac{A_b}{A_c} \frac{\mathrm{d}^2 h_b}{\mathrm{d}t^2} + \frac{\chi}{g} \frac{A_b{}^2}{A_c{}^2} \left|\frac{\mathrm{d}h_b}{\mathrm{d}t}\right| \frac{\mathrm{d}h_b}{\mathrm{d}t} + h_b = h_s} \tag{7.12}$$

This second-order ODE for h_b has the same form as the equation for a quadratically **damped mass-spring-dashpot system**. Such system has **natural oscillations** with a **natural frequency** which in absence of damping ($\chi = 0$) has the value

$$\omega_0 = \sqrt{\frac{g}{\ell} \frac{A_c}{A_b}} \tag{7.13}$$

When such system is excited sinusoidally, it responds at the forcing frequency. Initially, natural oscillations may also be excited (this is the homogeneous part of the general solution, solely dependent on the initial conditions), but these are gradually decaying due to the damping forces. In the end, the response is purely periodic at the forcing frequency (the non-homogeneous part of the general solution), although not sinusoidal due to the nonlinearity of the damping in Equation (7.12). In the following, we will linearize the damping, in order to simplify the mathematics. In that approximation, the response to a sinusoidal forcing is sinusoidal.

7.3 Linearization of the quadratic resistance

The head loss W is proportional to $|Q|Q$. Let us write it for short as $W = \lambda_1 |Q|Q$, in which $\lambda_1 = \chi/gA_c{}^2$ (see Equation (7.10). Suppose that Q varies sinusoidally in time:

$$Q = \hat{Q} \cos \omega t \tag{7.14}$$

Figure 7.4 shows the form of the associated time variation of the resistance, plotted as $|Q|Q/\hat{Q}^2 = |\cos \omega t| \cos \omega t$. The quadratic form, with a modulus operator, causes a deviation from a sinusoidal variation. We want to get rid of that. To do so, we approximate the resistance term as $W = \lambda_2 Q$ instead of $W = \lambda_1 |Q|Q$. In doing so, we accept an error in the time variation, but we will choose λ_2 in such a way that the energy loss in a cycle (with

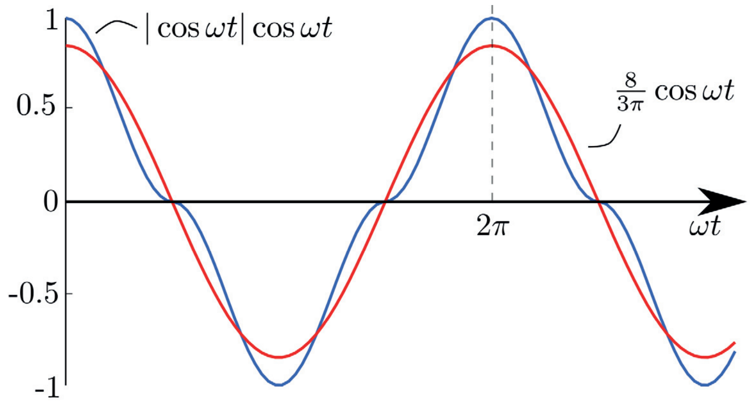

Figure 7.4: Quadratic resistance and linearization

duration T) has the same value in both formulations, so that the damping in the course of time is correctly represented. The rate of energy loss due to the resistance W is proportional to WQ, so that the condition to be imposed on λ_2 can be written as

$$\int_0^T WQ\,\mathrm{d}t = \int_0^T \lambda_1|Q|Q^2\mathrm{d}t = \int_0^T \lambda_2 Q^2\mathrm{d}t \tag{7.15}$$

Substitution of Equation (7.14) and carrying out the integrations yields

$$\frac{\lambda_2}{\lambda_1} = \frac{\int_0^T |\cos\omega t|\,\cos^2\omega t\mathrm{d}t}{\int_0^T \cos^2\omega t\mathrm{d}t}\hat{Q} = \frac{\int_0^{T/4}\cos^3\omega t\mathrm{d}t}{\int_0^{T/4}\cos^2\,\omega t\mathrm{d}t}\hat{Q} = \frac{8}{3\pi}\hat{Q} \tag{7.16}$$

With this result for λ_2, and using the definition $\lambda_1 = \chi/gA_c{}^2$, we obtain the following expression for the linearized resistance:

$$W = \frac{8}{3\pi}\chi\frac{\hat{Q}}{gA_c^2}Q \qquad (= \frac{8}{3\pi}\chi\frac{\hat{U}}{g}U) \tag{7.17}$$

(The same result is obtained by requiring that the difference between the quadratic resistance and the linear approximation be minimal in a least-square sense, or by expanding the quadratic resistance in a Fourier series and retaining only the first term.)

In this approximation, W varies linearly with Q (or U), albeit with a proportionality coefficient that contains $\hat{Q}$, which is not known beforehand. The solution can be determined iteratively by making successive, improved estimates of $\hat{Q}$ (or of $\hat{U}$) and using these as input in the next round of calculation. (It will appear that for the problem of a tidal basin the solution can in fact be determined in closed form. For more complicated situations iteration is indeed necessary; see Chapter 8.)

Using the linear approximation to W (Equation (7.17)) in Equation (7.11), instead of the original, quadratic expression (Equation (7.10)), we obtain the following ODE instead of Equation (7.12):

$$\frac{\ell}{g}\frac{A_b}{A_c}\frac{\mathrm{d}^2 h_b}{\mathrm{d}t^2} + \tau\frac{\mathrm{d}h_b}{\mathrm{d}t} + h_b = h_s \tag{7.18}$$

in which for brevity we have introduced a resistance parameter τ defined by

$$\tau \equiv \frac{8}{3\pi}\chi\frac{A_b}{g{A_c}^2}\hat{Q} \tag{7.19}$$

It appears from the structure of Equation (7.18) that τ is the **time scale** (the relaxation time) of the system response to a varying excitation. Because of the linearization of the resistance, this time scale depends partly on the unknown amplitude of the discharge ($\hat{Q}$) or of the flow velocity ($\hat{U}$).

As stated before, we neglect variations of A_b and A_c with h. In that approximation, Equation (7.18) is linear with constant coefficients. This implies that the response to a sinusoidal excitation is also sinusoidal, with the same frequency.

For completeness and added insight we mention an aspect which so far has not been mentioned at all, i.e. a difference in mean water level between basin and sea.

Treating A_b and A_c as constants, independent of the water level, is an approximation. Strictly speaking, the ebb flow occurs on average at a smaller depth than the flood flow, so that it experiences a higher resistance. The result is that the time-averaged water level in the basin is somewhat above that at sea. This is a nonlinear effect, which we neglect in the present linear approximation. This allows us to write the instantaneous surface elevations as, respectively,

$$h_s(t) = h_0 + \zeta_s(t) \qquad \text{and} \qquad h_b(t) = h_0 + \zeta_b(t) \tag{7.20}$$

in which h_0 is the mean water level, the same in the basin as it is at sea (in the linear approximation), and ζ_s and ζ_b are the fluctuations of the water level, being zero on average. With this substitution, Equation (7.18) is transformed into

$$\boxed{\frac{\ell}{g}\frac{A_b}{A_c}\frac{\mathrm{d}^2 \zeta_b}{\mathrm{d}t^2} + \tau\frac{\mathrm{d}\zeta_b}{\mathrm{d}t} + \zeta_b = \zeta_s} \tag{7.21}$$

In the following paragraphs, we present solutions (ζ_b) to this equation for a given sinusoidally varying water level at sea (ζ_s).

7.4 System with discrete storage and resistance

Before dealing with the full Equation (7.21), we consider the simplified case of a short connection in order to build up the complexity gradually.

Governing equation

Short connections between the basin and the sea (i.e. $\ell \to 0$), such as a gap in a barrier, or a gap in a dike, contain little mass, whose inertia we can neglect. (Moreover, if $\ell \to 0$, boundary resistance in the connection becomes negligible, so that only expansion losses remain: $\chi \to 1/2$.) This reduces the system to one of storage in the basin and head loss in the connection. Equation (7.21) reduces to

$$\tau \frac{\mathrm{d}\zeta_b}{\mathrm{d}t} + \zeta_b = \zeta_s \tag{7.22}$$

From a mathematical point of view, the neglect of inertia reduces the order of the equation from second order to first order.

Physically, it implies that the discharge through the connection responds instantaneously to variations in the head difference across it, being zero as soon as the head difference is zero. Because the discharge is proportional to the rate of change of the water level in the basin, this in turn implies that the maximum and minimum water levels in the basin occur at the instants when the water levels in the basin and in the sea are equal. This of course can also be seen in Equation (7.22) since this shows that $\mathrm{d}\zeta_b/\mathrm{d}t = 0$ when $\zeta_b = \zeta_s$.

Nonhomogeneous solution

We will now derive the nonhomogeneous (forced) solution of Equation (7.22) for a sinusoidal tide at sea with water level given by

$$\zeta_s = \hat{\zeta}_s \cos \omega t \tag{7.23}$$

Since the response is also sinusoidal, with the same frequency, it can be written as

$$\zeta_b = \hat{\zeta}_b \cos(\omega t - \theta) = r\,\hat{\zeta}_s \cos(\omega t - \theta) \qquad \text{in which} \qquad r = \hat{\zeta}_b/\hat{\zeta}_s \tag{7.24}$$

We have introduced the symbol r for the ratio between the two amplitudes. The amplitude $\hat{\zeta}_b$ (or the ratio r) and the phase angle θ are to be determined. Notice that θ is the phase lag of the water level in the basin behind that at sea.

Substitution of Equations (7.23) and (7.24) in Equation (7.22) yields one equation in the two unknowns r and θ, but that is sufficient because it must be fulfilled for all times. Substituting two conveniently chosen phases to simplify the algebra, such as $\omega t = \pi/2$ and $\omega t = \theta$, yields the results

$$\tan\theta = \omega\tau \qquad \text{and} \qquad r = \cos\theta = \frac{1}{\sqrt{1 + (\omega\tau)^2}} \tag{7.25}$$

To help visualize this result, the excitation and the response are shown in Figure 7.5, for an arbitrary value of r. The two curves satisfy the condition that the water level in the basin is at its maximum or minimum when the two curves intersect. Consider the first

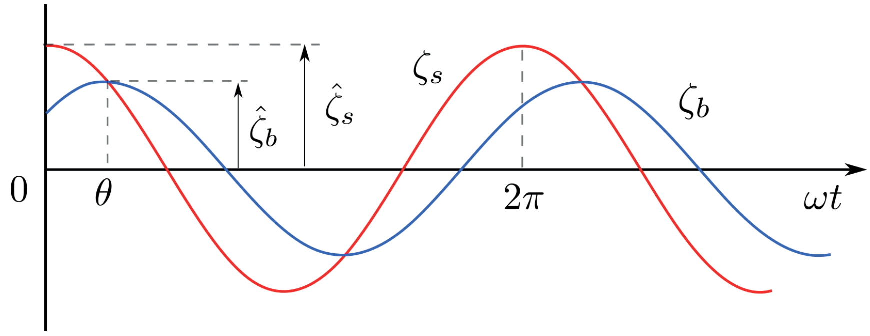

Figure 7.5: Example solution linearized discrete system with storage and resistance

intersection shown in the figure, occurring at time $t = t_1$, say. At that moment, ζ_b reaches its maximum value of $\hat{\zeta}_b$, which implies that $\omega t_1 = \theta$ (see Equation (7.24)), and ζ_s reaches the value $\hat{\zeta}_s \cos \omega t_1 = \hat{\zeta}_s \cos \theta$. Since this must equal $\hat{\zeta}_b$, it follows that $r = \cos \theta$.

It appears that the solution is determined by the dimensionless product $\omega\tau$ or, stated another way, by the ratio τ/T, in which τ is the time scale of the system response and $T = 2\pi/\omega$ is the tidal period. Another interpretation is that $\omega\tau = W/\hat{\zeta}_b$, as follows from the definitions of W and τ (and using Equation (7.26) given below). In other words, this product represents the **relative magnitude of the resistance**.

If τ is small compared to T, or $\omega\tau \ll 1$, resistance is insignificant, so the basin level can more or less follow the relatively slowly varying tide level at sea, or $r \simeq 1$, $\cos\theta \simeq 1$, and $\theta \simeq 0$, in agreement with Equation (7.25).

On the other hand, if the system has a time scale which is long compared to the tidal period ($\omega\tau \gg 1$), it can hardly follow the tides, which in this case vary relatively rapidly, so the response is weak ($r \ll 1$) and the lag is large ($\cos\theta \ll 1$, or $\theta \simeq \pi/2$), again in agreement with Equation (7.25).

Explicit solution

The solution has been expressed in terms of $\omega\tau$, in which τ depends on the amplitude of the discharge or the flow velocity in the connection (see Equation (7.19)), which is not known beforehand. To deal with this problem, we substitute Equation (7.24) in Equation (7.1), with the result

$$\hat{Q} = A_b\, \omega\, \hat{\zeta}_b \tag{7.26}$$

Substituting this in the definition of τ (Equation (7.19)), we obtain

$$\omega\tau = \frac{8}{3\pi}\, \chi \left(\frac{A_b}{A_c}\right)^2 \frac{\omega^2\, \hat{\zeta}_b}{g} \tag{7.27}$$

We replace the unknown $\hat{\zeta}_b$ in the right-hand side by $r\hat{\zeta}_s$ and write the result as

$$\omega\tau = \Gamma r \tag{7.28}$$

in which Γ is defined by

$$\boxed{\Gamma \equiv \frac{8}{3\pi}\,\chi\,\left(\frac{A_b}{A_c}\right)^2 \frac{\omega^2\,\hat{\zeta}_s}{g}} \tag{7.29}$$

Γ is a dimensionless parameter, containing all independent variables playing a role in the present problem. Therefore, except for a scale factor, the solution is determined exclusively and entirely by this parameter. This also follows from Equation (7.28), knowing that r is determined by $\omega\tau$.

If we now substitute (7.28) in (7.25), we obtain a quadratic algebraic equation in r^2, from which we finally obtain the following explicit, closed-form solution for r (therefore also for θ, since $r = \cos\theta$) as a function of the independent parameter Γ:

$$\boxed{r = \cos\theta = \frac{1}{\sqrt{2}\,\Gamma}\sqrt{-1+\sqrt{1+4\Gamma^2}}} \tag{7.30}$$

Figure 7.6 shows this variation of r and θ as a function of Γ. Qualitatively, the influence of Γ on the solution is similar to that of $\omega\tau$, discussed above. Small values of Γ correspond to a rapid ($\theta \simeq 0$) and strong ($r \simeq 1$) system response, and large values to a slow ($\theta \simeq \pi/2$) and weak ($r \ll 1$) response. In these two limiting cases, simple approximations for r can be derived from (7.30):

$$r \simeq 1 - \frac{1}{2}\Gamma^2 \qquad \text{for} \qquad \Gamma < \text{appr. } 10^{-1} \tag{7.31}$$

and

$$r \simeq \frac{1}{\sqrt{\Gamma}} \qquad \text{for} \qquad \Gamma > \text{appr. } 10^{1} \tag{7.32}$$

Example 7.1. *Tidal basin with gap*

Situation	Solution
A tidal basin with length and width of the order of 10 km ($A_b = 100$ km^2), depths varying from 2 m to 3 m, connected to the sea (M_2-tide, $\hat{\zeta}_b = 0.75$ m) by a gap in a barrier under construction with $A_c = 3000$ m^2. **Questions** Demonstrate that the small basin approximation is valid. Next, calculate: 1. the surface amplitude in the basin (ζ_b) 2. the phase lag (θ) 3. the maximum discharge in the gap ($\hat{Q}$)	Tidal wave length (without friction): $L = T\sqrt{gd}$, using $T = 44700$ s (M_2-tide) and $d = 2$ m (lower bound), $L \simeq 200$ km $\gg$ basin dimensions ($\approx$ 10 km), as required for the small basin approximation. Loss coefficient: $\chi = 1/2$ (gap), yielding (using given data) $\Gamma = 0.71$. We now obtain: 1. $r = 0.85 \rightarrow \hat{\zeta}_b = r\hat{\zeta}_s = 0.64$ m 2. $\theta = \arccos r = \arccos 0.85 = 31°$ 3. $\hat{Q} = A_b\omega\hat{\zeta}_b = 9.0 \times 10^3$ m^3/s. **Comment** The parameter $\omega\tau = \Gamma r \simeq 0.6 < 1$, indicating that the influence of resistance is considerable.

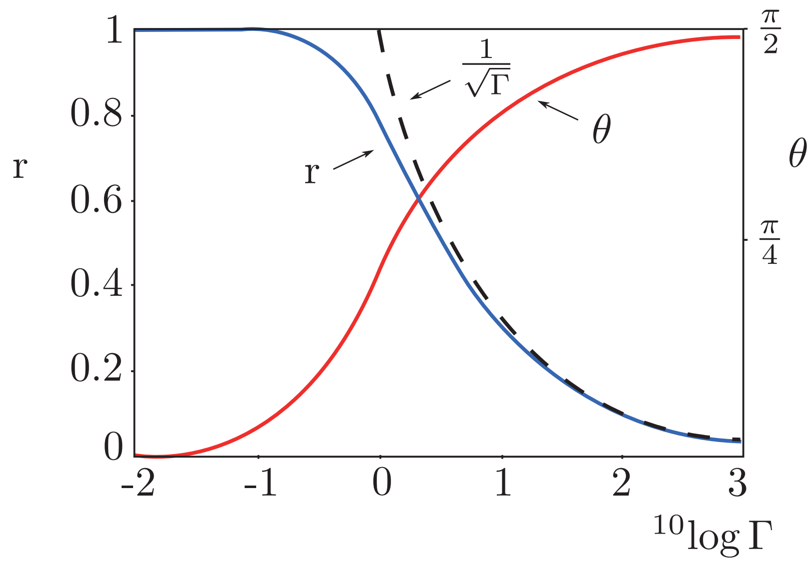

Figure 7.6: Amplitude ratio and phase lag for a discrete system with storage and resistance as functions of the resistance parameter Γ

In the above, incl. Example 7.1, inertia in the connection (a gap with a length virtually equal to zero) was neglected. This may not be valid in case of a channel. However, as we will see, it is possible for a channel of some length to contribute significantly to the overall resistance, through bed friction, while it is at the same time short enough for the inertia of the mass in it to be negligible. We will now formulate a condition to check the validity of the neglect of the inertia in the channel.

In Equation (7.21), inertia is represented by the first term in the left-hand side, with amplitude $(\omega^2\ell/g)\,(A_b/A_c)\,\hat{\zeta}_b$. The third term in the left hand side of Equation (7.21), representing the restoring force, has an amplitude $\hat{\zeta}_b$. Looking at the ratio of these terms, it follows that inertia may be neglected whenever $(\omega^2\ell/g)\,(A_b/A_c) \ll 1$. See also Example 7.2.

7.5 System with discrete storage, resistance and inertia

This section deals with the complete Equation (7.21), representing the effects of inertia, resistance and storage. We repeat it here for convenience:

$$\frac{\ell}{g}\frac{A_b}{A_c}\frac{\mathrm{d}^2\zeta_b}{\mathrm{d}t^2} + \tau\frac{\mathrm{d}\zeta_b}{\mathrm{d}t} + \zeta_b = \zeta_s \tag{7.33}$$

Equations of this form describe a forced, damped linear mass-spring system. As stated above, the natural frequency of this system in absence of damping is

$$\omega_0 = \sqrt{\frac{g}{\ell}\frac{A_c}{A_b}} \tag{7.34}$$

Example 7.2. *Tidal basin with (short) entrance channel*

Situation	Solution
Same as in Example 7.1, except that now the connection consists of a short channel with length $\ell = 600$ m, conveyance cross section $A_c = 3000$ m^2, hydraulic radius $R = 6$ m and friction coefficient $c_f = 0.004$. **Questions** Demonstrate that the inertia term can be neglected. Next, calculate: 1. the surface amplitude in the basin (ζ_b) 2. the phase lag (θ) 3. the discharge in the gap ($\hat{Q}$)	Importance of inertia (relative to the restoring force): $\left(\omega^2 \ell / g\right)(A_b/A_c) \approx 0.04$, acceptably small to neglect it in a first approximation. Including the boundary resistance in the channel, the resistance coefficient $\chi = 1/2 + c_f\,\ell/R = 0.9$. We now obtain: 1. $\Gamma = 1.28 \rightarrow r = 0.73 \rightarrow \hat{\zeta}_b = 0.55$ m 2. $\theta = \arccos 0.73 = 43°$ 3. $\hat{Q} = A_b\,\omega\,\hat{\zeta}_b = 7.7 \times 10^3$ m^3/s **Comment** The channel is sufficiently short to allow the neglect of inertia, yet sufficiently long for the bed resistance to have a significant effect.

Nonhomogeneous solution

For harmonic forcing with frequency ω, the solution depends on $\omega\tau$ (the relative damping, as before) but also on the ratio of the forcing frequency to the natural frequency. It can be found in texts on dynamics, and reads

$$\frac{\hat{\zeta}_b}{\hat{\zeta}_s} = r = \frac{1}{\sqrt{(1 - \omega^2/{\omega_0}^2)^2 + \omega\tau}} \tag{7.35}$$

with

$$\tan\theta = \frac{\omega\tau}{1 - \omega^2/{\omega_0}^2} \tag{7.36}$$

Explicit solution

As before, the solution is implicit because τ depends in part on the unknown amplitude $\hat{Q}$ or $\hat{U}$. Using the same approach as in the preceding section, we can make the solution explicit in terms of the same Γ as before ($\Gamma = \omega\tau/r$), with the result

$$\boxed{r = \frac{1}{\sqrt{2}}\frac{1}{\Gamma}\sqrt{-(1 - \omega^2/{\omega_0}^2)^2 + \sqrt{(1 - \omega^2/{\omega_0}^2)^4 + 4\Gamma^2}}} \tag{7.37}$$

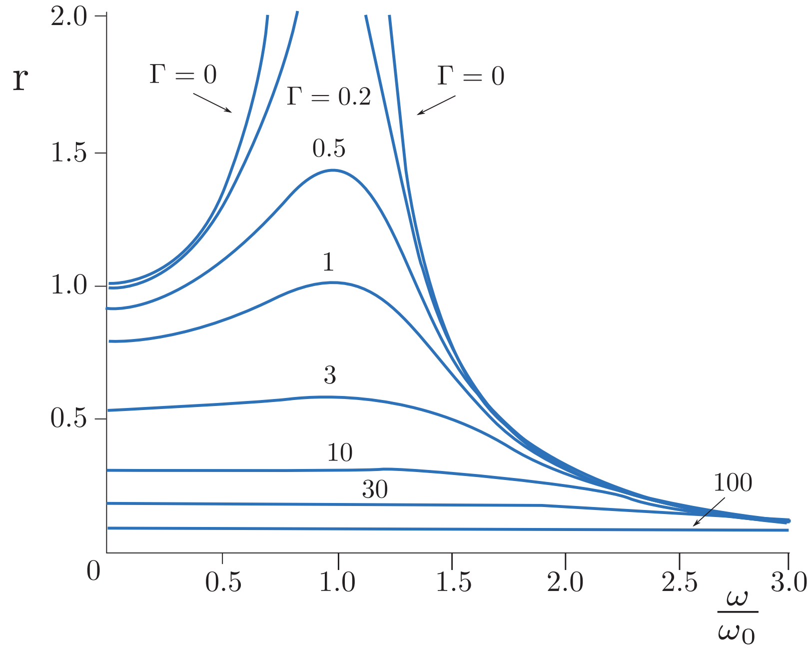

Figure 7.7: Amplitude ratio of a discrete system with inertia, storage and resistance as functions of the resistance parameter Γ and the frequency ratio ω/ω_0

Once r is determined from this equation, the phase lag θ follows from

$$\boxed{\tan\theta = \frac{\omega\tau}{1-\omega^2/{\omega_0}^2} = \frac{\Gamma r}{1-\omega^2/{\omega_0}^2}} \tag{7.38}$$

For $\omega/\omega_0 \ll 1$, i.e. slow excitation, this solution reduces to that in the preceding section, where inertia was neglected *a priori*.

Figure 7.7 shows the variation of r with ω/ω_0 for a chosen set of values of Γ. The most striking feature is the possibility of **resonance**, manifesting itself in high r-values for $\omega/\omega_0 \simeq 1$, for small or moderate values of Γ. For large values of Γ, i.e. a relatively high damping as a result of a narrow connection and/or strong resistance, the effects of resonance are suppressed.

7.6 Solution through complex algebra

In preparation for the following chapter, we are once more going to derive the solution given above for the system with storage and resistance, now using the representation of sinusoidal functions as complex quantities. The advantage of this is that the amplitude and the phase angle are represented in terms of a single variable, that the time variation can be factored out, and that the partial differential equation reduces to an algebraic equation from which the solution can be more easily found and represented graphically.

Complex representation

A real quantity like $A = \hat{A}\cos(\omega t + \alpha)$ can be represented as the real part of a complex quantity $\tilde{A}\, e^{i\omega t}$, in which $\tilde{A}$ is the so-called complex amplitude of A, given by $\tilde{A} = \hat{A}e^{i\alpha}$. The modulus of $\tilde{A}$ equals $\hat{A}$, i.e. the (real) amplitude of A, and its argument is the time-independent part of the phase of A, or $\arg \tilde{A} = \alpha$.

We will apply the complex representation to find the harmonic (i.e., sinusoidal) solution of the model with discrete storage and resistance, described by Equation (7.22), which is repeated here for convenience:

$$\tau \frac{\mathrm{d}\zeta_b}{\mathrm{d}t} + \zeta_b = \zeta_s \tag{7.39}$$

Each time-varying sine function is represented as the real part of a complex quantity:

$$\zeta_s(t) = \mathrm{Re}\left\{\tilde{\zeta}_s\, e^{i\omega t}\right\} \qquad \text{and} \qquad \zeta_b(t) = \mathrm{Re}\left\{\tilde{\zeta}_b\, e^{i\omega t}\right\} \tag{7.40}$$

In view of Equation (7.40), the first term in Equation (7.39) is given by

$$\tau \frac{\mathrm{d}\zeta_b}{\mathrm{d}t} = \mathrm{Re}\left\{i\omega\tau\tilde{\zeta}_b\, e^{i\omega t}\right\} \tag{7.41}$$

We substitute this and Equation (7.39) in (7.40). Each term in that equation is the real part of a complex, time-varying quantity, but the presence of the time factor $e^{i\omega t}$ requires that Equation (7.39) be fulfilled by the corresponding complex, time-independent amplitudes. Moreover, because the time factor is common to all terms, it can be factored out. The result is

$$i\omega\tau\tilde{\zeta}_b + \tilde{\zeta}_b = \tilde{\zeta}_s \tag{7.42}$$

Here, we see two great advantages of using the complex representation: the time dependence is represented as a common multiplyer which can be factored out, and the differential equation (7.39) is replaced by the algebraic Equation (7.42).

Solution

For given $\tilde{\zeta}_s$, we need to find $\tilde{\zeta}_b$. First, we do this graphically because that gives a good insight. After that the solution is determined purely algebraically.

For the graphical solution procedure, we plot $\tilde{\zeta}_b$ in the complex plane as a vector with length $|\tilde{\zeta}_b|$, i.e. the amplitude $\hat{\zeta}_b$, at an angle $\arg\tilde{\zeta}_b$ with the real axis (see Figure 7.8). The modulus and the argument of $\tilde{\zeta}_b$ have been chosen arbitrarily. The quantity $i\omega\tau\tilde{\zeta}_b$ has been plotted in Figure 7.8 as well. It stands at a right angle to $\tilde{\zeta}_b$, because of the factor i, and its modulus is a factor $\omega\tau$ larger than $\hat{\zeta}_b$ (or smaller, as the case may be); in the figure, an arbitrarily chosen value of $\omega\tau$ of about 0.5 was used. (Note that $i = \exp(i\pi/2)$, so multiplying with i means turning over 90^o.)

According to Equation (7.42), the sum of $i\omega\tau\tilde{\zeta}_b$ and $\tilde{\zeta}_b$, i.e. the resultant of the corresponding two vectors in the figure (the hypotenuse), equals $\tilde{\zeta}_s$. The angle enclosed between

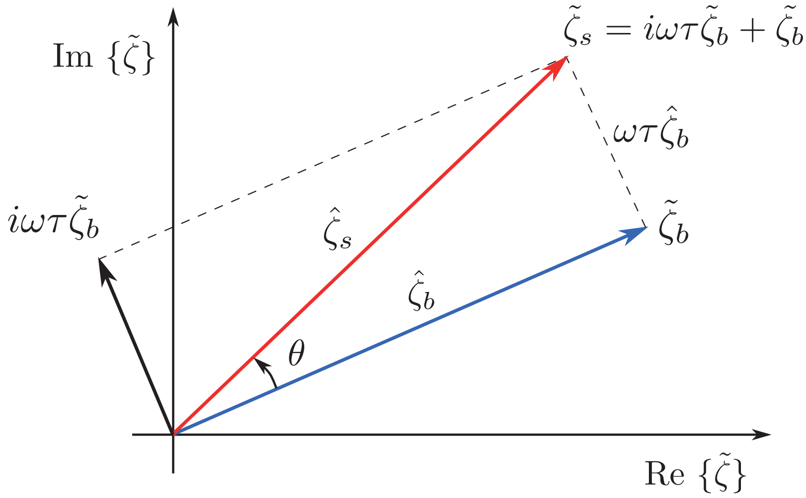

Figure 7.8: Complex amplitudes

this resultant and $\tilde{\zeta}_b$ represents the phase difference between the two, which we had denoted as θ, as indicated in the figure. We see at once in the resulting right triangle that $\tan\theta = \omega\tau$ and that $\cos\theta = \hat{\zeta}_b/\hat{\zeta}_s = r$, the same as was found above.

For the analytical solution method, we define a complex-amplitude ratio $\tilde{r}$ as

$$\tilde{r} \equiv \tilde{\zeta}_b/\tilde{\zeta}_s \tag{7.43}$$

For the real amplitudes, we have $|\tilde{r}| = |\tilde{\zeta}_b/\tilde{\zeta}_s| = |\tilde{\zeta}_b|/|\tilde{\zeta}_s| = \hat{\zeta}_b/\hat{\zeta}_s = r$, and for the phases we have $\arg\tilde{r} = \arg\left(\tilde{\zeta}_b/\tilde{\zeta}_s\right) = \arg\tilde{\zeta}_b - \arg\tilde{\zeta}_s = -\theta$.

It follows from Equation (7.42) and the definition of $\tilde{r}$ that

$$\tilde{r} = \frac{1}{1 + i\omega\tau} \tag{7.44}$$

so that

$$r = |\tilde{r}| = |\frac{1}{1 + i\omega\tau}| = \frac{1}{|1 + i\omega\tau|} = \frac{1}{\sqrt{1 + (\omega\tau)^2}} \tag{7.45}$$

and

$$\arg\tilde{r} = -\theta = -\arctan(\omega\tau) \qquad \text{or} \qquad \tan\theta = \omega\tau \tag{7.46}$$

The preceding simple example illustrates the advantages and the potential of the complex representation for solving a linear problem with sinusoidal forcing and response. This is a good preparation for the application in the following chapter, which deals with one-dimensional propagation of long waves including damping.

Problems

1. What is the so-called small-basin approximation?

2. Under which conditions is this approximation valid?

3. Can a variation in the (undisturbed) depth in the basin affect the behaviour of the system? If so, how (through which mechanism)?

4. Same question, now with respect to the bed friction coefficient c_f.

5. What is the so-called rigid-column approximation?

6. Under which conditions is this approximation valid?

7. Explain why the water in a small basin, connected to a tidal sea by a gap in a barrier, reaches its highest level at the instant when this level equals that at sea.

8. Which physical criterion is applied in the linearization of the quadratic resistance? Why?

9. Which physical process is lost in the linearization of the quadratic resistance?

10. What is the meaning of the dimensionless parameters $\omega\tau$ and Γ as used in this chapter?

11. Derive Eq. (7.30), given Eq. (7.25) and the definition $\Gamma = \omega\tau/r$.

12. Argue why the amplitude ratio r is nearly 1 for small Γ and goes to zero for large Γ (without using the analytical solution: doing that would not be 'arguing').

13. A cylindrical tide well with an inner diameter of 1 m, placed in a harbour, should be able to measure harbour oscillations (seiches) with a period of about 10 minutes and an amplitude of 0.5 m with a damping of at most 1% (r at least 0.99). Calculate the required diameter of the orifice which connects the tide well with the surrounding water (answer: 6.4 cm).

14. For that opening diameter, calculate the damping of wind waves given that these have a period of 8 s and an amplitude of 0.3 m at the location of the tide wel (answer: 95%; $r = 0.05$).

15. Argue for each of the following parameters how a 20% increase in their value could affect the discharge through the channel between basin and sea: A_c, B_c, R_c, c_f, l, A_b, $\hat{\zeta}_s$, ω. Think of possible feedbacks! Verify your estimates through numerical calculation of the discharge for a self-chosen example. (Note that the number of calculations required is less than the number of parameters.)

16. A tidal basin of approximately 10 km x 20 km in plan is connected by a channel to a sea with M_2-tide with a tidal range (HW - LW) of 2 m. The channel is 10 km long and has a cross-sectionally averaged mean depth of about 9 m, a free-surface width of 600 m and a conveyance cross-section of 5 x 10^3 m^2 with $c_f = 0.004$. Ignore inertia at first.

    - Calculate the amplitude of the tidal elevation in the basin. (Answer: $\hat{\zeta}_b$ = 0.27 m.)
    - Calculate the phase lag of the basin tide behind the tide at sea. (Answer: $\theta = 76°$.)
    - Calculate the maximum discharge throught the channel. (Answer: $\hat{Q}$ = 7.6 x 10^3 m$^3/s$.)
    - Sketch in one plot the time variation of the tides at sea and in the basin

as well as the discharge through the channel and interpret the result.

- Now take inertia into account and calculate the natural frequency (Answer: $\omega_0 = 1.58$ x 10^{-4} rad/s.)
- Verify whether the neglect of inertia was allowed.
- Regardless of the answer to the preceding question, take inertia into account and calculate the amplitude of the tidal elevation in the basin (answer: $\hat{\zeta}_b = 0.27$ m, (almost) the same as before) and the phase lag of the basin tide behind the tide at sea (answer: $\theta = 87°$.) Why is this lag greater with inertia taken into account than when it is neglected?

17. Using complex algebra, and starting from Equations (7.33) and (7.34), derive the results of Equations (7.35) and (7.36).

18. Given: $\zeta_s = \hat{\zeta}_s \cos(\omega t - \alpha)$ with $\hat{\zeta}_s = 1$ m and $\alpha = 212^o$. Calculate $\tilde{\zeta}_s$. Plot this in the complex plane and calculate its real part and its imaginary part. (Answer: $\tilde{\zeta}_s$ = (1 m)(exp(2.583 i), Re $\tilde{\zeta}_s$ = -0.85 m, Im $\tilde{\zeta}_s$ = 0.53 m.)

19. Given: $\tilde{\zeta}_s$ = (0.9 - 0.8i)m. Plot this and give the corresponding expression for $\zeta_s(t)$. Calculate ζ_s for $\omega t = 0$ and $\omega t = \pi/2$. (Answer: $\tilde{\zeta}_s$ = (1.20 m)exp(-0.727i), or $\zeta_s(t)$ = (1.20 m) cos(ωt - 0.727 rad), so ζ_s = 0.9 m at $\omega t = 0$ and ζ_s = 0.8 m at $\omega t = \pi/2$. (The latter two answers can be seen at once from the given expression for $\tilde{\zeta}_s$!).

20. Suppose that $\omega\tau = 0.5$. Plot $\tilde{r}$, equal to $1/(1 + i\omega\tau)$, and calculate r and arg $\tilde{r}$. (Answer: $r = |\tilde{r}| = 0.894$ and arg $\tilde{r}$ = -0.464 rad = -26.6^o (equivalent to arg $\tilde{r}$ = (- 0.464 + 2π) rad = 5.819 rad = 333.4^o).)

Chapter 8

Harmonic wave propagation

8.1 Introduction

The chapters 4 and 5 have dealt with propagation of disturbances into a domain. In several of the cases considered, the disturbance consisted of a transition between two states of uniform motion, in some cases starting from rest. Another typical set of situations occurs when an initial state of rest is affected by continual periodic disturbances at a boundary which propagate into the domain considered. Given enough time, a periodic state of motion is established in the entire domain, without memory of the initial situation. In such cases the motion is unsteady within each wave cycle, but the cycles themselves do not vary in time.

This chapter deals with low **periodic long waves and oscillations** (without transients) such as tides. Seiches are somewhat of the same category, but these are not always quasi-periodic but more pulse-like. In line with the analysis in Chapter 3, inertia and resistance are both taken into account. The main aim of this chapter is to provide **insight in the dynamics of wave propagation including effects of resistance**, which were ignored in Chapter 4. Using linear approximations, valid for low waves, simple solutions are obtained in the form of complex exponential functions, representing damped harmonic (sinusoidal) waves or oscillations.

The main features of the variation of amplitudes and phases in tides and seiches can reasonably well be represented with this linear model, but not the deformation of the wave profile, which is the result of nonlinear influences such as the variation of the conveyance cross-section and the width of the free surface as a function of the free-surface elevation. These effects are not considered in the linear approximation. The linear solutions give insight and can be useful in preliminary analyses requiring the simulation of a large number of scenarios. They are not to be used when high accuracy is needed; various (commercial) numerical codes are available for that purpose in one, two or three space dimensions.

The approach in the present chapter is a continuation of the preceding chapter in the use of the linearization of the quadratic resistance and the complex algebra formulation. The difference is that we are now dealing with progressive and standing waves. We start with a description of damped, harmonic progressive waves in terms of the complex formalism, prior to a derivation of the characteristic features of these waves, in particular the propagation speed and the rate of damping.

8.2 Complex representation of damped progressive harmonic waves

We assume a periodic wave progressing in the positive s-direction in a prismatic channel. The wave period is T, the angular frequency (i.e. the phase change per unit time) $\omega = 2\pi/T$, the wave length L, the wave number (i.e. the change of phase per unit distance) $k = 2\pi/L$, the propagation speed (or the phase speed, i.e. the speed of points of constant phase) $c = L/T = \omega/k$. The surface elevation ζ has a location-dependent amplitude $\hat{\zeta}$:

$$\zeta(s,t) = \hat{\zeta}(s)\cos(\omega t - ks + \alpha) \tag{8.1}$$

In complex form, this can be written as

$$\zeta(s,t) = \mathrm{Re}\left\{\tilde{\zeta}(s)\exp(i\omega t)\right\} \tag{8.2}$$

in which

$$\tilde{\zeta}(s) = \hat{\zeta}(s)\exp(i(-ks + \alpha)) \tag{8.3}$$

Notice that in this complex formulation a **separation of variables** has taken place, i.e. the dependences on s and on t occur in separate factors instead of combined as in $\cos(\omega t - ks)$. This simplifies the analysis.

As in Chapter 7, the complex amplitude $\tilde{\zeta}$ contains both the real amplitude and the phase, but instead of being constant, these now vary with s at a rate that will be determined in the next section.

In a fixed point (constant s), the complex amplitude $\tilde{\zeta}$ can be represented as a point in the complex plane (see Figure 8.1 a). Its argument is the phase of $\zeta(s,t)$ at that point at time $t = 0$. According to Equation (8.2), the time variation of ζ is obtained by multiplying $\tilde{\zeta}$ with $\exp(i\omega t)$, i.e. by rotating the corresponding vector in the complex plane over an angle ωt, followed by taking the real part, i.e. the projection on the real axis (Figure 8.1a). This time variation can be carried out at any moment if desired, but it is not necessary to show this in a graph. It is sufficient to know that it can be done, provided $\tilde{\zeta}$ is known. Starting at $s = 0$, $\arg\tilde{\zeta} = \alpha$, i.e. the phase at time $t = 0$, as shown in panel (b) of Figure 8.1. The phase at $t = 0$ in an arbitray other point can be found by multiplication of $\tilde{\zeta}(0)$ with $\exp(-iks)$, i.e. by rotation over an angle $-ks$ (Figure 8.1b).

Choosing a continuous succession of points, i.e. a continuous variation of s, we obtain a continuously varying sequence of values of $\tilde{\zeta}$, generating a smooth curve in the complex plane, a so-called **hodograph**. For constant amplitude, the hodograph is a circle, shown in panel (b).

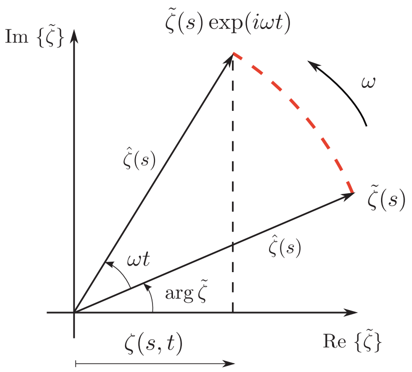

$$
\begin{aligned}
\zeta(s,t) &= \mathrm{Re}\left\{\tilde{\zeta}(s)\exp\left(i\omega t\right)\right\} \\
&= \mathrm{Re}\left\{\hat{\zeta}(s)\exp\left(i\omega t + \arg\tilde{\zeta}(s)\right)\right\} \\
&= \hat{\zeta}(s)\cos\left(i\omega t + \arg\tilde{\zeta}(s)\right)
\end{aligned}
$$

(a) variation in time in a fixed point

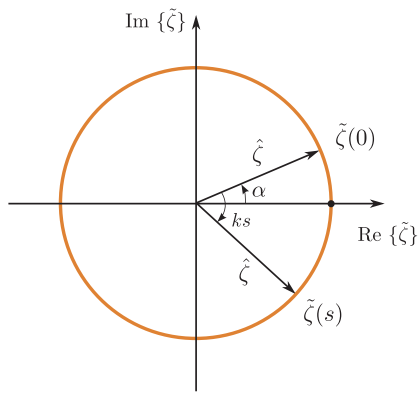

hodograph of $\tilde{\zeta}(s) = \hat{\zeta}\exp\left(i\left(\alpha - ks\right)\right)$
with $\hat{\zeta}$ and k constant

(b) phase shift as function of distance in a progressive wave of constant amplitude

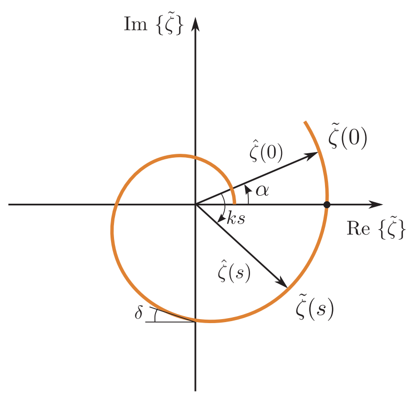

hodograph of $\tilde{\zeta}(s) = \hat{\zeta}(0)\exp(-\mu s)\exp\left(i\left(\alpha - ks\right)\right)$
in which $\tan\delta = \mu/k$ (plotted for $\tan\delta = 0.2$)

(c) variation of amplitude and phase as functions of distance in a damped progressive wave

Figure 8.1: Complex plane with hodographs

A special case of amplitude variation is the exponential decay with s, as occurs in systems with linear(ized) resistance. Denoting the damping modulus with μ, this can be written as $\hat{\zeta}(s) = \hat{\zeta}(0)\exp(-\mu s)$. In this case, Equation (8.3) becomes

$$\tilde{\zeta}(s) = \hat{\zeta}(0)\ \exp(-\mu s)\ \exp(i(-kx+\alpha)) = \tilde{\zeta}(0)\ \exp(-ps) \tag{8.4}$$

in which $\tilde{\zeta}(0) = \hat{\zeta}(0)\exp(i\alpha)$ and we have introduced the complex constant

$$p = \mu + ik \tag{8.5}$$

In the right-hand side of Equation (8.4), $\tilde{\zeta}(0)$ is the initial complex amplitude, and $\exp(-ps)$ describes its spatial variation. The rate of change of the real amplitude is given by μ, and that of the phase is given by k. These two are combined in the single complex parameter p.

In the case of exponential decay, the hodograph of $\tilde{\zeta}(s)$ takes the form of a logarithmic spiral, characterized by a constant angle of convergence (i.e. the angle between the tangent at a point of the spiral and the normal to the radius connecting that point with the origin, designated as δ in panel (c) of Figure 8.1.

A note on the convergence angle of the logarithmic spiral

When propagating over a small distance Δs from s_1 to s_2, a phase change occurs given by $k\Delta s$, corresponding to a rotation of the associated vector in the complex plane over a small angle $k\Delta s$, see Figure 8.1c. The amplitude, represented by the length of the radius to the origin, thereby reduces by a factor $\exp(-\mu s_2)/\exp(-\mu s_1) = \exp(-\mu(s_2 - s_1)) = \exp(-\mu\Delta s)$. The relative amplitude reduction is therefore given by $(1 - \exp(-\mu\Delta s))]$, which for small Δs can be approximated as $\mu\Delta s$. The angle between the tangent and the normal to the radius, i.e. the angle of convergence, is therefore given by $\arctan(\mu/k)$, which is constant along the spiral.

The values of ω, μ and k are not independent because the wave motion must fulfill the balances of mass and momentum. Only one of them can be chosen freely, normally the frequency. Using the balance equations, an expression for $p(\omega)$, the so-called **complex dispersion relation**, will be derived in the following sections. From this we also know $\mu(\omega)$ and $k(\omega)$ and from the latter the phase speed $c = \omega/k$.

8.3 Formulation and general solution

This section will present the basic equations and their solutions for harmonic motion. This method of long wave modelling, called the **harmonic method**, was developed and first used by a committee chaired by the Nobel prize winning physicist Lorentz, for the purpose of predicting the changes that were to be expected in the tides as a result of the construction of an enclosure dam in The Netherlands.

Formulation

We start from the linearized one-dimensional balance equations for mass and momentum. The quadratic resistance is linearized as in Chapter 7, and the advection of momentum is neglected, as is allowed for low waves. The latter restriction also allows us to neglect variations in the cross-section which occur as a result of variations in flow depth. With this, the balance equations for mass and momentum are written as follows (see Equations (2.4) and (2.10)):

$$B\frac{\partial \zeta}{\partial t} + \frac{\partial Q}{\partial s} = 0 \tag{8.6}$$

and

$$\frac{\partial Q}{\partial t} + gA_c\frac{\partial h}{\partial s} + \kappa Q = 0 \tag{8.7}$$

The parameter κ is a shorthand factor (dimension: 1/time) in the expression for the linearized resistance, defined by (see also Equation (7.17)):

$$\kappa = \frac{8}{3\pi}\, c_f\, \frac{\hat{Q}}{A_c R} = \frac{8}{3\pi}\, c_f\, \frac{\hat{U}}{R} \tag{8.8}$$

In the following derivations and applications, κ is assumed to be a known constant. Since it contains the amplitude $\hat{Q}$ or $\hat{U}$, which are not known beforehand, iteration is necessary.

Equations (8.6) and (8.7) form a set of two coupled PDF's in ζ and Q, with constant coefficients (in the linear approximation). Such equations allow (complex) exponential solutions.

For harmonic motion, the first term in the momentum balance is of the order of $\omega\hat{Q}$, and the resistance term is of the order $\kappa\hat{Q}$. It follows that the ratio of resistance to inertia is of the order κ/ω, written as σ for short:

$$\boxed{\sigma \equiv \frac{\kappa}{\omega} = \frac{8}{3\pi}\, c_f\, \frac{\hat{Q}}{\omega A_c R} = \frac{8}{3\pi}\, c_f\, \frac{\hat{U}}{\omega R}} \tag{8.9}$$

Apart from the factor $8/3\pi$ (about 0.85), this is the same σ as in Chapter 3, of which some typical values have been given in Table 3.1.

Eliminating Q between Eqs (8.6) and (8.7), and using the property of a prismatic channel that $\partial A_c/\partial x = 0$, we obtain

$$\boxed{\frac{\partial^2 \zeta}{\partial t^2} - c_0^2\,\frac{\partial^2 \zeta}{\partial s^2} + \kappa\frac{\partial \zeta}{\partial t} = 0} \tag{8.10}$$

in which c_0^2 is the long-wave speed in absence of resistance (see Equation (4.10)):

$$c_0 = \sqrt{\frac{gA_c}{B}} \tag{8.11}$$

Equation (8.10) is the linearized wave equation (see Chapter 4) with (linearized) resistance. Because of this, and with reference to Chapter 4, we expect solutions which in general may consist of two waves, traveling in opposite directions, decaying as they propagate.

General solution

We seek solutions for $\zeta(s,t)$ in the form

$$\zeta(s,t) = \mathrm{Re}\left\{\tilde{\zeta}(s)\ \exp(i\omega t)\right\} \tag{8.12}$$

We substitute this in Equation (8.10), drop the time factor $\exp(i\omega t)$, and obtain

$$\frac{\mathrm{d}^2\tilde{\zeta}}{\mathrm{d}s^2} + \frac{\omega^2 - i\omega\kappa}{c_0^2}\,\tilde{\zeta} = 0 \tag{8.13}$$

Substitution of $\kappa = \sigma\omega$ and of $k_0 = \omega/c_0$, the wave number in absence of resistance, yields

$$\boxed{\frac{\mathrm{d}^2\tilde{\zeta}}{\mathrm{d}s^2} + {k_0}^2\,(1 - i\sigma)\tilde{\zeta} = 0} \tag{8.14}$$

This is an ordinary differential equation (ODE) with constant coefficients. Such equations have exponential solutions. Therefore, we pose

$$\tilde{\zeta}(s) = \exp(Ps) \tag{8.15}$$

and substitute this in (8.14), which results in

$$P^2 + k_0^2\,(1 - i\sigma) = 0 \tag{8.16}$$

This is the so-called **dispersion relation**. For given frequency (contained in k_0) and relative resistance (σ), it determines the propagation constant P, which governs the spatial variation, as expressed in Equation (8.15).

Notice the reduction in mathematical complexity in the various steps: we started with a partial differential equation (PDE), Equation (8.10). Due to the restriction to harmonic solutions and the complex representation, this reduced to an ODE, Equation (8.14). Finally, assuming a (complex) exponential solution, the integration constant P is determined by an algebraic equation ((8.16)).

Equation (8.16) is of second degree. It has two opposite, complex roots P_1 and $P_2 = -P_1$, which will be designated as p and $-p$, respectively, in which

$$p = ik_0\sqrt{1 - i\sigma} \tag{8.17}$$

The general solution for $\tilde{\zeta}(s)$ can then be written as

$$\boxed{\tilde{\zeta}(s) = C^+\exp(-px) + C^-\exp(ps) = \tilde{\zeta}^+(s) + \tilde{\zeta}^-(s)} \tag{8.18}$$

Equation (8.18) is the general solution of Equation (8.14). If we include the time factor $\exp(i\omega t)$, it represents two waves travelling in opposite directions. The two (complex) integration constants C^- and C^+, each containing amplitude and phase information, are to be determined from the (two) boundary conditions, as we will see furtheron. If either C^- or C^+ is zero, the propagation is in one direction only. Usually, there is some reflection somewhere, in which case there is propagation of two wave systems in opposite directions.

Solution of the dispersion equation

Our next task is to derive a more explicit solution of Equation (8.17). The propagation constant p is in general complex. (If $\sigma = 0$ it is purely imaginary.) We write $p = \mu + ik$, in which μ and k are real, representing damping and propagation, respectively (see Section 8.2).

In order to determine μ and k, we have to separate the right-hand side of Equation (8.17) into its real part and its imaginary part, for which we need (among others) the modulus and the argument of $\sqrt{1 - i\sigma}$. The argument of this square root is $-(1/2)\arctan\sigma$. To shorten the notation, we introduce an auxiliary variable, an angle δ, such that

$$\boxed{\tan 2\delta \equiv \sigma = \frac{8}{3\pi}\, c_f\, \frac{\hat{U}}{\omega R}} \tag{8.19}$$

where δ is a dimensionless measure of the resistance/inertia ratio, just as σ. It can be seen as a kind of friction angle. In terms of δ, we have $\arg\sqrt{1 - i\sigma} = -(1/2)\arctan\sigma = -\delta$. Furthermore, $|1 - i\sigma| = \sqrt{1 + \sigma^2} = \sqrt{1 + \tan^2 2\delta} = 1/\cos 2\delta$, so that altogether we have

$$p = ik_0 \frac{\exp(-i\delta)}{\sqrt{\cos 2\delta}} \tag{8.20}$$

or

$$p = i\,\frac{\cos\delta - i\,\sin\delta}{\sqrt{\cos 2\delta}}\,k_0 = \frac{\sin\delta + i\,\cos\delta}{\sqrt{\cos 2\delta}}\,k_0 \tag{8.21}$$

so that finally

$$\boxed{\operatorname{Im} p = k = \frac{\cos\delta}{\sqrt{\cos 2\delta}}\,k_0 \qquad \text{and} \qquad \operatorname{Re} p = \mu = \frac{\sin\delta}{\sqrt{\cos 2\delta}}\,k_0 = k\,\tan\delta} \tag{8.22}$$

The preceding algebraic steps have been visualized in Figure 8.2. It is recommended to analyse this figure closely. Note: it can be seen in the above that $\delta = \arctan(\mu/k)$, which is just equal to the angle of convergence of the logarithmic spiral representing the hodograph of $\tilde{\zeta}$ (see Section 8.2).

Finally, we write the phase speed $c = \omega/k$ in a more explicit form, using the preceding results:

$$\boxed{c = \frac{\omega}{k} = \frac{\omega}{k_0}\,\sqrt{1 - \tan^2\delta} = c_0\,\sqrt{1 - \tan^2\delta}} \tag{8.23}$$

or

$$c = \sqrt{\frac{gA_c}{B}}\,\sqrt{1 - \tan^2\delta} \tag{8.24}$$

Apparently, resistance not only dampens the waves but it is also slowing them down.

$$\boxed{p = ik_0\sqrt{1-i\sigma} = \mu + ik}$$

$$\downarrow$$

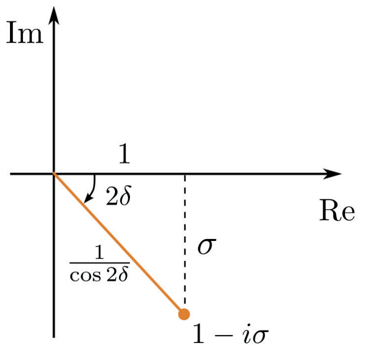

$$\arg(1-i\sigma) \equiv -2\delta \;\Rightarrow\; \sigma = \tan 2\delta$$

$$|1-i\sigma| = \sqrt{1+\sigma^2} = \sqrt{1+\tan^2 2\delta} = \tfrac{1}{\cos 2\delta}$$

$$\Rightarrow 1 - i\sigma = \tfrac{1}{\cos 2\delta}\exp(-2i\delta)$$

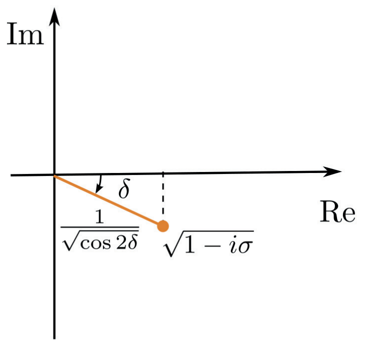

$$\begin{aligned}
\sqrt{1-i\sigma} &= \tfrac{1}{\sqrt{\cos 2\delta}}\exp(-i\delta) \\
&= \tfrac{1}{\sqrt{\cos 2\delta}}(\cos\delta - i\sin\delta) \\
&= \tfrac{1}{\sqrt{1-\tan^2\delta}}\tfrac{\cos\delta - i\sin\delta}{\cos\delta}
\end{aligned}$$

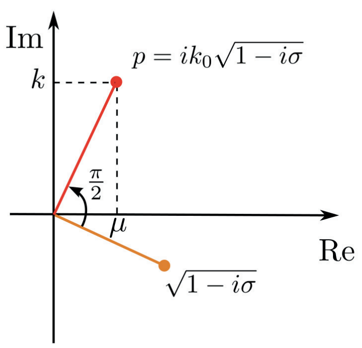

$$\begin{aligned}
ik_0\sqrt{1-i\sigma} &= \tfrac{k_0}{\sqrt{\cos 2\delta}}(\sin\delta + i\cos\delta) \\
&= \tfrac{k_0}{\sqrt{1-\tan^2\delta}}(\tan\delta + i) \\
&\equiv \mu + ik
\end{aligned}$$

$$\downarrow$$

$$\boxed{\begin{aligned}
k &= k_0\tfrac{\cos\delta}{\sqrt{\cos 2\delta}} = \tfrac{k_0}{\sqrt{1-\tan^2\delta}} \\
\mu &= k_0\tfrac{\sin\delta}{\sqrt{\cos 2\delta}} = k\tan\delta
\end{aligned}}$$

Figure 8.2: Solution of the dispersion equation

Solution for the discharge

Subsituting the general solution for $\tilde{\zeta}(x)$ (Equation (8.18)) in the continuity Equation (8.6) yields the following expression for the associated discharge:

$$\tilde{Q}(s) = \frac{i\omega B}{p} \left(C^+ \exp(-ps) - C^- \exp(ps)\right) \tag{8.25}$$

or

$$\tilde{Q}(s) = \frac{i\omega B}{p} \left(\tilde{\zeta}^+(s) - \tilde{\zeta}^-(s)\right) \tag{8.26}$$

The complex factor $i\omega B/p$ can be reworked as follows:

$$\frac{i\omega B}{p} = \frac{i\omega B}{\mu + ik} = \frac{\omega}{k} \frac{B}{-i\mu/k + 1} = \frac{Bc}{1 - i\,\tan\delta} \tag{8.27}$$

Since $\arg(1 - i\tan\delta) = -\delta$, and $|1 - i\tan\delta| = \sqrt{1 + \tan^2\delta} = 1/\cos\delta$, we finally obtain

$$\frac{i\omega B}{p} = Bc\,\cos\delta\,\exp(i\delta) \tag{8.28}$$

Summarizing, the general solution for $\tilde{\zeta}$, Equation (8.18), is

$$\boxed{\tilde{\zeta}(s) = C^+ \exp(-ps) + C^- \exp(ps) = \tilde{\zeta}^+(s) + \tilde{\zeta}^-(s)} \tag{8.29}$$

and the corresponding discharge is

$$\boxed{\tilde{Q}(s) = \frac{i\omega B}{p} \left(C^+ \exp(-ps) - C^- \exp(ps)\right) = Bc\,\cos\delta\,\exp(i\delta)\left(\tilde{\zeta}^+ - \tilde{\zeta}^-\right)} \tag{8.30}$$

This general solution will be interpreted and eleborated in the following sections, first for the simple case of a unidirectional wave system, so as to facilitate the understanding of the meaning of the results, to be followed by various cases of bi-directional waves.

8.4 Unidirectional propagation

The preceding results apply to the spatial variation of the complex amplitudes of the surface elevation and the discharge, the time variation having been set aside temporarily. We are re-introducing it:

$$\zeta(s,t) = \mathrm{Re}\left\{\tilde{\zeta}(s)\,\exp(i\omega t)\right\} \tag{8.31}$$

We will now examine closely the particular form of this expression for progressive waves.

Mathematical interpretation

We restrict the following discussion to ζ^+:

$$\zeta^+(s,t) = \text{Re}\left\{\tilde{\zeta}^+(s)\ \exp(i\omega t)\right\} = \text{Re}\ \left\{C^+\ \exp(-ps)\ \exp(i\omega t)\right\} \tag{8.32}$$

Substituting $p = \mu + ik$ and expanding C^+ into its modulus and argument, we obtain

$$\zeta^+(s,t) = \text{Re}\ \left\{|C_+|\exp(-\mu s)\exp(i(\omega t - ks + \arg C^+))\right\} \tag{8.33}$$

or

$$\zeta^+(s,t) = \hat{\zeta}^+(s)\cos\left(\omega t - ks + \arg C^+\right) \tag{8.34}$$

in which $\hat{\zeta}^+(s) = |C_+|\exp(-\mu s)$. The associated discharge is

$$Q^+(s,t) = Bc\hat{\zeta}^+(s)\ \cos\delta\ \cos(\omega t - ks + \arg C^+ + \delta) \tag{8.35}$$

Inspecting these equations, we note the following items:

- $\arg C^+$ is the initial phase (when $\omega t = 0$) of ζ^+ in $s = 0$.
- The phase varies in s and t as $(\omega t - ks)$, implying that we deal with a wave progressing in the positive s-direction (that is the reason for the superscript + in C^+, ζ^+ and Q^+) with speed $c = \omega/k$, the so-called phase speed, because, observed at this speed, the phase is constant.
- $|C^+|$ is the amplitude of ζ^+ in $s = 0$.
- $|C^+|\exp(-\mu s)$ is the amplitude of ζ^+ as a function of s: exponential damping in the direction of propagation.
- In absence of damping ($\delta = 0$), we would have $Q(s,t) = Bc\zeta(s,t)$, the same as was found in Chapter 4 for purely progressive waves without resistance.
- The discharge is a factor $\cos\delta$ smaller with damping than without, and it is an angle δ ahead in phase relative to the surface elevation. The fact that resistance reduces the discharge for a given surface elevation, i.e. for a given driving force due to the slope of the free surface, is fairly obvious. The advance in phase of the discharge, by an angle δ, is due to the fact that the flow acquires less momentum in the presence of resistance than it does without resistance, and therefore responds faster to the oscillatory driving forces.

The preceding items refer to a purely progressive wave propagating in the positive s-direction, i.e. proportional to C^+, with $C^- = 0$. Needless to say, they are equally applicable to a wave propagating in the negative s-direction, apart from a change of sign in Q^-. As anticipated, **the general solution of the wave equation** (8.10) **consists of two wave systems, propagating in opposite direction, each exponentially decaying in its propagation direction.**

Quantity	Equation	Tide	Seiche
T	(given)	745 min	60 min
$\hat{U}$	(given)	1.2 m/s	0.6 m/s
ω	$\omega = 2\pi/T$	1.405×10^{-4} rad/s	1.745×10^{-3} rad/s
c_0	$c_0 = \sqrt{gA_c/B}$	7.7 m/s	7.7 m/s
k_0	$k_0 = \omega/c_0$	1.8×10^{-5} rad/m	2.3×10^{-4} rad/m
L_0	$L_0 = c_0 T = 2\pi/k_0$	343 km	28 km
σ	$\sigma = \frac{8}{3\pi}\, c_f\, \frac{\hat{U}}{\omega R}$	2.64	0.106
δ	$\delta = (1/2) \arctan \sigma$	34.6°	3.02°
$\tan\delta$	$\tan\delta$	0.69	0.053
$\sqrt{1-\tan^2\delta}$	$\sqrt{1-\tan^2\delta}$	0.72	1.00 (0.998...)
k	$k = k_0/\sqrt{1-\tan^2\delta}$	2.5×10^{-5} rad/m	2.3×10^{-4} rad/m
μ	$\mu = k \tan\delta$	1.8×10^{-5} m^{-1}	1.2×10^{-5} m^{-1}
c	$c = c_0\sqrt{1-\tan^2\delta}$	5.5 m/s	7.7 m/s
L	$L = 2\pi/k = cT$	247 km	28 km

Table 8.1: Example: unidirectional propagation of tidal waves and seiches

Example

Consider an M$_2$-tide (T = 12 hours and 25 minutes = 745 minutes = 44700 s) with $\hat{U}$ = 1.2 m/s, and a seiche with T = 1 hour and $\hat{U}$ = 0.6 m/s, both in a channel in an estuary with $c_f = 0.004$, hydraulic radius R = 11 m, depth d = 12 m, conveyance width B_c = 350 m^2, conveyance area $A_c = B_c d = 4.2 \times 10^3$ m^2, storage width $B = 2B_c$ = 700 m. These input data and their elaborations have been summarized in Table 8.1, assuming a purely progressive wave. (This is not realistic, but the restriction to a single wave propagation direction is preferred to provide insight in the relationships.)

The phase speed of the tide (5.5 m/s) is only about one half of $\sqrt{gd_c}$, which is almost 11 m/s. The difference is due to two factors: the width of the free surface (available for storage) is twice the conveyance width B_c, which slows down the wave speed by a factor $\sqrt{2}$ (since $c = \sqrt{gA_c/B} = \sqrt{gA_c/(2B_c)}$), or about 70%, and resistance reduces it further with a factor $\sqrt{1-\tan^2\delta}$, which is roughly another 70%. The phase speed of the higher-frequency seiches is hardly affected by resistance, in agreement with the general conclusion in Chapter 3 about the relative impact of resistance (Table 3.1).

Although σ (and therefore δ) is far smaller for the seiche than it is for the tide, their μ-values, i.e. the relative damping per unit propagation distance, are comparable. This is because μ is not only proportional to $\tan\delta$, but also to the wave number k, which is almost a factor ten larger (shorter wave length) for the seiches than it is for the tides, which compensates to a high degree for the difference in σ-values. For a propagation distance Δs of 10 km, say, the tidal amplitude is reduced with a factor $\exp(-\mu\Delta s)$ or about 0.84, whereas the seiche amplitude over that same distance is reduced with a factor of about 0.89.

8.5 Bi-directional wave propagation

In the linearization of the resistance, the amplitude of the discharge and that of the flow velocity have been assumed constant. Even in a prismatic channel, this is not the case because of the wave decay due to resistance. In practice, a long channel is subdivided in sections of a limited length, such that in each of them the amplitude does not vary too much. The above equations are applied to each of these sections, while the various solutions are coupled by demanding continuity of discharge and surface elevation at the junctions. In the preceding example, a length of some 10 km appears acceptable in view of the decay numbers given above.

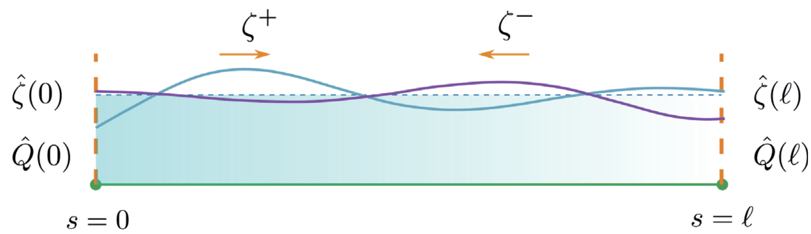

Figure 8.3: Bi-directional wave propagation in a section

In this section, we will derive relationships between the amplitudes and phases of the surface elevation and of the discharge at one end of a prismatic channel section, expressed in terms of those at the other end (Figure 8.3). These relationships should be valid for arbitrary combinations of two wave systems traveling in opposite directions, not necessarily unidirectional waves.

Relation between the amplitudes of surface elevation and discharge

Our starting point is the general solution for the surface elevation and the discharge, given in Equation (8.29) and (8.30), which are repeated here for convenience:

$$\tilde{\zeta}(s) = C^+ \exp(-ps) + C^- \exp(ps) \tag{8.36}$$

and

$$\tilde{Q}(s) = \frac{i\omega B}{p} \big(C^+ \exp(-ps) - C^- \exp(ps)\big) \tag{8.37}$$

For easier algebraic manipulation, we eliminate temporarily the factor $i\omega B/p$ by introducing a new complex variable $\tilde{Z}$, with the dimension of a length:

$$\tilde{Z} \equiv \frac{p}{i\omega B} \tilde{Q}(s) = C^+ \exp(-ps) - C^- \exp(ps) \tag{8.38}$$

It then follows that

$$\tilde{\zeta}_0 = C^+ + C^- \qquad \text{and} \qquad \tilde{Z}_0 = C^+ - C^- \tag{8.39}$$

where we have written $\tilde{\zeta}_0$ for $\tilde{\zeta}(0)$, and likewise for $\tilde{Z}$. These two equations determine the integration constants C^+ and C^- in terms of $\tilde{\zeta}_0$ and $\tilde{Z}_0$:

$$C^+ = \frac{1}{2}\left(\tilde{\zeta}_0 + \tilde{Z}_0\right) \qquad \text{and} \qquad C^- = \frac{1}{2}\left(\tilde{\zeta}_0 - \tilde{Z}_0\right) \tag{8.40}$$

Substituting these integration constants in Equation (8.36) and (8.37), we can express the values of $\tilde{\zeta}$ and $\tilde{Q}$ at $s = \ell$ in terms of those at $s = 0$:

$$\tilde{\zeta}_\ell = \frac{1}{2}\left(\tilde{\zeta}_0 + \tilde{Z}_0\right)\exp(-p\ell) \;+\; \frac{1}{2}\left(\tilde{\zeta}_0 - \tilde{Z}_0\right)\exp(p\ell) \tag{8.41}$$

$$\tilde{Z}_\ell = \frac{1}{2}\left(\tilde{\zeta}_0 + \tilde{Z}_0\right)\exp(-p\ell) \;-\; \frac{1}{2}\left(\tilde{\zeta}_0 - \tilde{Z}_0\right)\exp(p\ell) \tag{8.42}$$

or

$$\tilde{\zeta}_\ell = \tilde{\zeta}_0 \cosh p\ell \;-\; \tilde{Z}_0 \sinh p\ell \tag{8.43}$$

$$\tilde{Z}_\ell = -\tilde{\zeta}_0 \sinh p\ell \;+\; \tilde{Z}_0 \cosh p\ell \tag{8.44}$$

This is the key result of this section, i.e. two equations relating the four complex amplitudes of surface elevation and discharge at both ends of the channel section. Given any two of these, the other two are determined. These relations play an important role in the calculations for a set of channel sections in series or in a network, where it is necessary to transfer information on amplitudes and phases from junction to junction.

Note: although we have referred to channel section 'ends' in the preceding text, no special conditions were imposed there. Therefore, the relations in fact apply to any pair of cross-sections of a prismatic channel. In other words, '$p\ell$' in the equations above might just as well be replaced by 'ps', indicating an arbitrary location.

Example

We present a simple application of this result to a system as considered in Chapter 7, viz. a small basin, closed except for a connection by a channel to a tidal sea. The water in the channel is excited sinusoidally at the channel mouth ($s = 0$, say), while at the other end ($s = \ell$) it in turn excites a Helmholtz mode in the basin with complex surface elevation amplitude $\tilde{\zeta}_b$.

The volume balance for the basin reads $Q(\ell, t) = A_b\,\mathrm{d}\zeta_b/\mathrm{d}t$, implying that $\tilde{Q}_\ell = i\omega A_b \tilde{\zeta}_b$. Ignoring velocity-head effects in the transition between the channel and the basin, we have $\tilde{\zeta}_b = \tilde{\zeta}_\ell$, so that

$$\tilde{Q}_\ell = i\omega A_b \tilde{\zeta}_b = i\omega A_b \tilde{\zeta}_\ell = \frac{i\omega B}{p}\,\tilde{Z}_\ell \tag{8.45}$$

Subsitution of this result in Equation (8.43) and (8.44) yields the following result for the ratio ($\tilde{r}$) of the complex amplitude in the basin to that at the channel mouth:

$$\tilde{r} = \frac{\tilde{\zeta}_b}{\tilde{\zeta}_0} = \left(\frac{pA_b}{B}\sinh p\ell + \cosh p\ell\right)^{-1} \tag{8.46}$$

In Chapter 7, it was assumed that the channel was short so that the storage in it could be neglected. In that approximation, the motion in the channel was not wave-like. Instead, the water was seen to oscillate back and forth as a rigid column. Here, we have gone beyond that approximation by modelling wave propagation in the channel.

A note on hyperbolic functions of complex argument

It can be seen in the preceding equations that the superposition of two exponentially decaying waves, traveling in opposite direction, gives rise to hyperbolic functions (cosh and sinh) of complex argument. To facilitate computations, these are expressed in terms of their real part and imaginary part in the following. By definition, $\cosh ps = (\exp ps + \exp(-ps))/2$. Substituting $p = \mu + ik$ and collecting the real parts and the imaginary parts, we obtain

$$\cosh ps = \cosh \mu s \cos ks + i (\sinh ps \sin ks) \tag{8.47}$$

Likewise, since $\sinh ps = (\exp ps - \exp(-ps))/2$, we find

$$\sinh ps = \sinh \mu s \cos ks + i (\cosh \mu s \sin ks) \tag{8.48}$$

Taking the squares of these expressions, we obtain for the moduli, after some reworking:

$$|\cosh ps|^2 = \sinh^2 \mu s + \cos^2 ks = \cosh^2 \mu s - \sin^2 ks \tag{8.49}$$

$$|\sinh ps|^2 = \sinh^2 \mu s + \sin^2 ks = \cosh^2 \mu s - \cos^2 ks \tag{8.50}$$

in which we have used $\cos^2 ks + \sin^2 ks = 1$ and $\cosh^2 \mu s - \sinh^2 \mu s = 1$.

8.6 Response function of a semi-closed basin

Consider a semi-closed basin, with its mouth at $s = 0$, where it is subjected to harmonic excitation from the sea, and with a closed end at $s = \ell$, see Figure 8.4. We will investigate the variation of the response as a function of the frequency of the harmonic excitation. This yields the so-called **response function**.

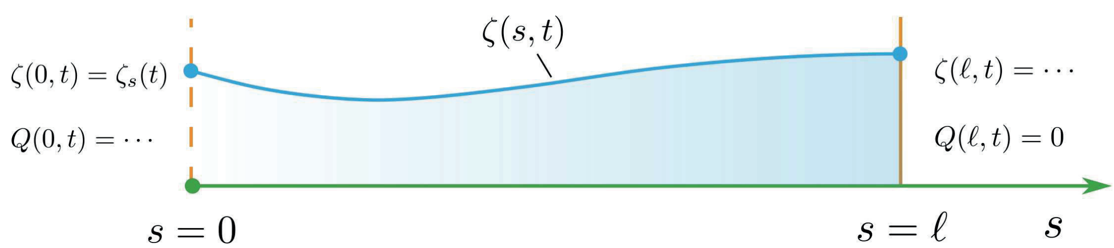

Figure 8.4: Standing wave in a semi-closed basin

At the open end, $\zeta(0,t)$ is prescribed as a sine function with known frequency, amplitude and phase. At the closed end, the boundary condition is $Q(\ell,t) = 0$. Since this is just a special case of the situation considered in the preceding section, we can immediately obtain the required response from those results. Setting $\tilde{Z}_\ell = 0$ in Equations (8.43) and (8.44), and returning to the complete expression for the complex discharge ($\tilde{Q} = (i\omega B/p)\,\tilde{Z}$), we obtain

$$\tilde{\zeta}_\ell = \frac{\tilde{\zeta}_0}{\cosh p\ell} \tag{8.51}$$

$$\tilde{Q}_0 = \frac{i\omega B}{p}\,\tilde{\zeta}_0\,\tanh p\ell \tag{8.52}$$

Note that Equation (8.51) also follows from Equation (8.46) by setting $A_b = 0$.

According to Equation (8.51), the ratio of the amplitude at the closed end to that at the mouth, the so-called **amplification factor**, is given by

$$\boxed{r \equiv \frac{\hat{\zeta}(\ell)}{\hat{\zeta}(0)} = \frac{1}{|\cosh p\ell|} = \frac{1}{\sqrt{\sinh^2 \mu\ell + \cos^2 k\ell}}} \tag{8.53}$$

This amplification factor is determined by two constants for the given channel: $\mu\ell$ and $k\ell$, determining the damping and the phase change of a wave progressing over the length of the basin. These two parameters can for given ℓ be calculated from $k_0\ell$ and σ, which can therefore be used as independent parameters in the calculations. The graph in Figure 8.5 is based on this. It consists of a set of curves, each showing the variation of r as a function of $k_0\ell$ (proportional to the frequency) for constant σ according to Equation (8.53).

The response function shown in Figure 8.5 gives at a glance insight in the dynamics of wave propagation and reflection in a semi-closed basin.

For basins that are very short compared to the wave length ($k_0\ell \ll 1$), the amplitude at the closed end is virtually the same as it is at the mouth, signifying that the water level in the basin rises and falls in unison with the external tide: the so-called Helmholtz mode that we have encountered in Chapter 7. Notice that in this range the value of σ has no influence, as expected, since resistance is negligible in a short, semi-closed basin.

For small to moderate values of σ, the response shows a high peak near $k_0\ell = \pi/2$, signifying quarter-wave resonance. The influence of σ is significant, causing a strong reduction in the response peak with increasing σ and a slight shift in the resonance frequency, which is the result of the influence of σ (or δ) on the phase speed. This is because quarter-wave resonance occurs when $k\ell = \pi/2$, or $k_0\ell = (\pi/2)\sqrt{1 - \tan^2\delta}$, therefore for lower values of $k_0\ell$ when σ increases.

For values of $k_0\ell$ near $3\pi/2$, there is another set of response peaks for small to moderate values of σ, signifying three-quarter-wave resonance. These are less pronounced than those near $k_0\ell = \pi/2$ because damping is more important for these longer basins (and/or shorter waves).

The amplitude of the discharge at the mouth follows from Equation (8.52). Subsitution of Equations (8.49) and (8.50) in this equation yields

$$\frac{\hat{Q}_0}{Bc\,\hat{\zeta}_0\,\cos\delta} = \left|\frac{\sinh k\ell}{\cosh k\ell}\right| = \sqrt{\frac{\sinh^2 \mu\ell + \sin^2 k\ell}{\sinh^2 \mu\ell + \cos^2 k\ell}} \tag{8.54}$$

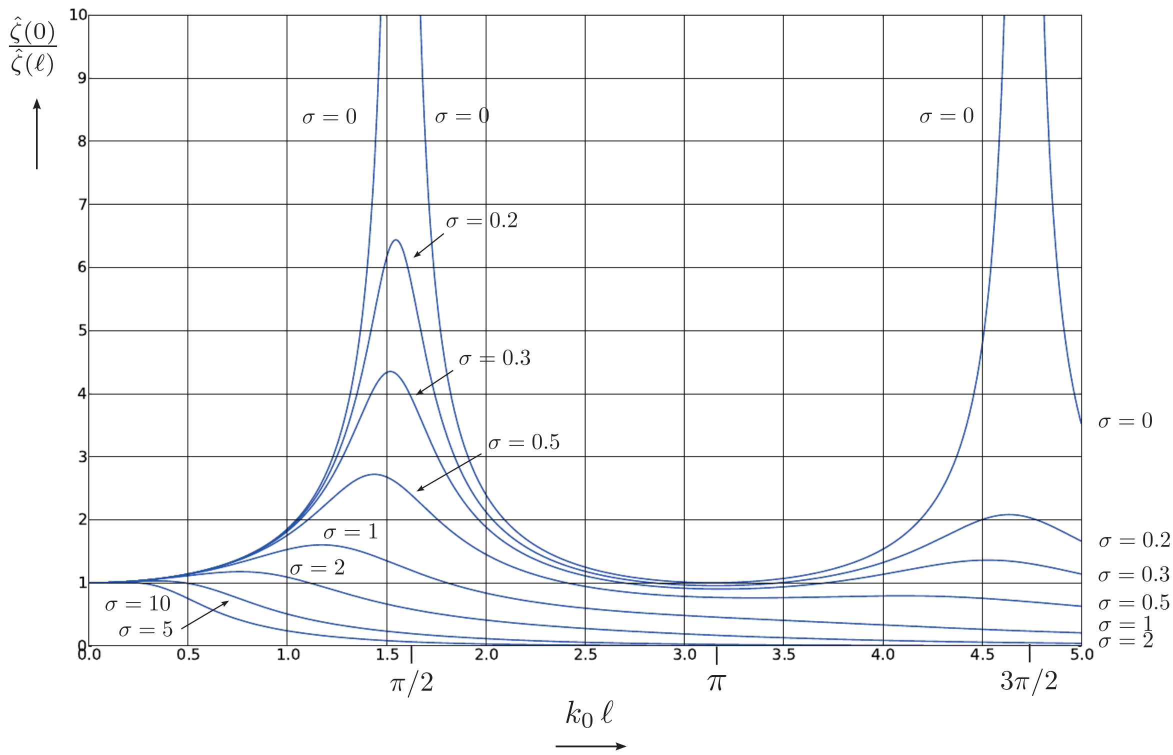

Figure 8.5: Response factor for a basin closed in one side

Because of the sine- and cosine functions of $k\ell$ in this expression, the discharge amplitude at the mouth is not a monotonic function of the relative basin length. Shortening of a basin may therefore increase the discharge at the mouth.

A note on the Zuiderzee closure (1932)

A significant example where the shortening of a tidal basin increased discharge in its mouth occurred when the previous Zuiderzee in the central part of The Netherlands was closed by the construction of an enclosure dam in 1932. This shortened considerably the tidal basin, extending from the North Sea to the closed end of the basin, but counter to intuitive expectations the discharge through the tidal inlets feeding the tides in the basin increased significantly, more than 25% in the most nearby inlet. The reason was that the tide in the shorter, remaining basin was nearer to quarter-wave resonance. This unexpected behaviour was correctly predicted by the Lorentz Committee, using the harmonic method described above (though in a more complicated version, to reflect the netwerk topology of the tidal channels), which was specifically developed for that purpose (see Figure 8.7)

8.7 Partial reflection

In Chapter 5, we considered the partial reflection of low translatory waves at discrete changes in the channel geometry. Here we do the same for harmonic waves, using the same approach. Only the algebra is a bit different.

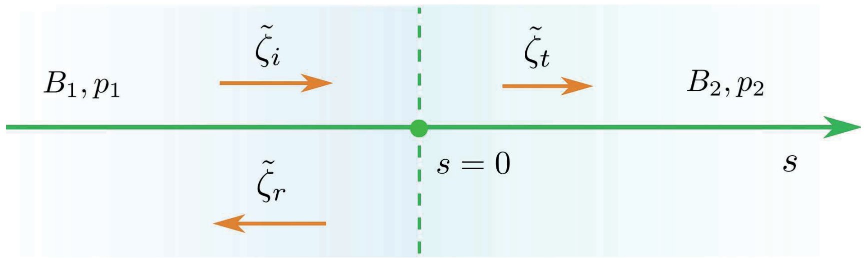

Figure 8.6: Transition in channel geometry

Two long, prismatic channel sections with mutually different geometry are connected at a point $s = 0$ (Figure 8.6). From section 1 ($s < 0$), a wave is approaching the transition and is partially reflected there, as well as partially transmitted into section 2 ($s > 0$), from where it does not reflect back to the transition. For given channel geometry and incident wave parameters at the site of the transition, we have to make a first estimate of the values of $\hat{U}$ or $\hat{Q}$ in both sections near the transition, so that we can start the calculation with an estimated σ or δ. If necessary the calculations can be repeated with improved estimates to obtain better results.

We write the following expressions for the incident waves (sub i) and the reflected waves (sub r) in channel 1:

$$\tilde{\zeta}_i = C_i \, \exp(-p_1 s) \qquad \text{and} \qquad \tilde{\zeta}_r = C_r \, \exp(p_1 s) \tag{8.55}$$

and the following for the tranmsitted waves (sub t) in section 2:

$$\tilde{\zeta}_t = C_t \, \exp(-p_2 s) \tag{8.56}$$

The associated discharges are given by

$$\tilde{Q}_i = (i\omega B_1/p_1)\, C_i \, \exp(-p_1 s) \qquad \text{and} \qquad \tilde{Q}_r = -(i\omega B_1/p_1)\, C_r \exp\left(p_1 x\right) \tag{8.57}$$

and

$$\tilde{Q}_t = (i\omega B_2/p_2)\, C_t \, \exp(-p_2 s) \tag{8.58}$$

At the transition, where $s = 0$, we must have continuity in ζ and in Q, which implies

$$C_i + C_r = C_t \tag{8.59}$$

and

$$\frac{i\omega B_1}{p_1}(C_i - C_r) = \frac{i\omega B_2}{p_2} C_t \tag{8.60}$$

For brevity, we introduce a complex transition ratio

$$\tilde{\gamma} = \frac{i\omega B_2/p_2}{i\omega B_1/p_1} = \frac{B_2 c_2}{B_1 c_1} \frac{\cos\delta_2}{\cos\delta_1} \exp\left(i\left(\delta_2 - \delta_1\right)\right) \tag{8.61}$$

(see Equation (8.28)) as well as a complex coefficient for reflection and one for transmission:

$$\tilde{r}_r = \frac{\tilde{\zeta}_r(0)}{\tilde{\zeta}_i(0)} = \frac{C_r}{C_i} \qquad \text{and} \qquad \tilde{r}_t = \frac{\tilde{\zeta}_t(0)}{\tilde{\zeta}_i(0)} = \frac{C_t}{C_i} \tag{8.62}$$

It then follows from Equations (8.59) and (8.60) that

$$\boxed{\tilde{r}_r = \frac{1-\tilde{\gamma}}{1+\tilde{\gamma}} \qquad \text{and} \qquad \tilde{r}_t = \frac{2}{1+\tilde{\gamma}} = 1 + \tilde{r}_r} \tag{8.63}$$

These results have an identical structure as those obtained in Chapter 5 for low translatory waves, the difference being that here the transition ratio and the coefficients are complex, bearing both amplitude and phase information. They also show that at the transition the reflected wave is not in phase with the incident wave, because $\tilde{r}_r$ is complex. The only exception to this is when the resistance angle δ does not change at the transition, in which case $\tilde{\gamma}$ is real (equal to B_2c_2/B_1c_1, the same as in Chapter 5, Equation (5.10)), and therefore also $\tilde{r}_r$ and $\tilde{r}_t$. In that case, the results are fully identical to those of Chapter 5.

8.8 Propagation in networks

It has been stated at numerous places in the above that a long channel may have to be divided in a number of adjacent sections, forming a one-dimensional chain, with sections in series. In other cases, the tidal channels in the study region form a network structure. In all such cases, there are internal nodes at the channel junctions, and nodes providing a link to the external world, usually a tidal sea or a closed end.

The primary unknowns are the complex amplitudes of the surface elevation and the discharge at the nodes of the system, i.e. four (complex) unknowns for each section, or on average two per node for each section, or $2N$ unknowns per node if there are N sections joined at a node. As we have seen in Section 8.5, there are two algebraic equations for each channel section describing the propagation therein, or (on average) one per node for each section, or N equations per node. For each node there is one more equation describing that the sum of the discharges towards the node is zero (neglecting storage at the node), and $(N-1)$ equations describing that the water levels of the N sections at the node are equal (neglecting velocity-head effects). At external nodes, boundary conditions are imposed. Altogether, the number of available independent equations is equal to the number of unknowns, as required or a well-posed problem, so that the solution is uniquely determined.

The tidal computations of the Lorentz Committee, performed for the prediction of the tides after the construction of the enclosure dam in the previous Zuiderzee, consisted of a network of 26 channels, see Figure 8.7. Boundary conditions were provided by the M_2-tides at the inlets connecting the basin with the North Sea, and the condition of zero discharge was imposed at the southern boundary of the Zuiderzee. As mentioned previously, the Committee

Figure 8.7: Harmonic network model of the Zuiderzee, The Netherlands, as used by Lorentz, from [1]

succesfully predicted the changes in the tides that were the result of the construction of the enclosure dam. The harmonic method has been applied since then in many projects. Needless to say, numerical codes have long since replaced the analytical harmonic method in practical projects, but the method is still useful for insight in the wave dynamics and for preliminary computations.

8.9 Nonlinear effects

In this section, we briefly touch on a few nonlinear effects, which were systematically ignored in the above.

We distinguish two kinds of nonlinearities in the equations describing the flow: terms that are nonlinear in the dependent variables, e.g. quadratic terms, and geometric nonlinearities, in particular the variation of the wet cross-section with the water level.

In contrast to a linear system, the response of a nonlinear system to harmonic forcing is not sinusoidal, altough still periodic. Higher harmonics can be excited, as well as a nonzero mean response.

Let us take the quadratic advective term in the momentum balance, $\partial(Q^2/A_c)/\partial s$, as an example. If Q varies in time as $\cos \omega t$, then Q^2 varies in time as $\cos^2 \omega t = (1 + \cos 2\omega t)/2$. We see that the square introduces both a higher harmonic, at a frequency 2ω, and a nonzero mean value. Likewise, a factor like $U|U|$, occurring in the resistance term, introduces 3d, 5th and higher odd harmonics if U itself varies sinusoidally. The presence of higher harmonics causes deformation of the wave profile.

Nonlinear effects increase with increasing ratio of wave height to water depth. They are strongest in shallow water. That is why the nonlinearly generated higher harmonics of the M_2-tide, i.e. the components M_4, M_6 etc., are called 'shallow-water tides'.

Geometric nonlinearities often play an important role in tidal propagation, because the cross-section available for flow can vary greatly between high water and low water, even to the extent of falling dry. Because of damping, the tide in estuaries is usually mainly progressive, so that the surface elevation and the discharge are in phase for most of the time. This means that for flood flow the cross-section available for conveyance and storage is larger than it is for ebb flow. As a consequence, ebb flow velocities are on average higher than flood flow velocities. This contributes to asymmetries in the tidal curves for surface elevation and flow velocities.

Because the ebb occurs on average at a smaller depth and with larger velocities than the flood, the ebb flow encounters a higher resistance (which is proportional to $U|U|/d$). As a result, the mean water level (MWL) slopes down towards the sea, even in purely oscillatory flow in absence of a net discharge.

Figure 8.8 gives a series of tidal curves, showing the variation in time of the surface elevation at a sequence of stations along the Western Scheldt estuary and river. Station 'V' (Vlissingen) is the most seaward station, 'A' is Antwerp, and 'G' is Gentbrugge, far inland. The increased deformation of the tidal curves for the more inland stations is obvious, as is the gradient of the mean surface elevation.

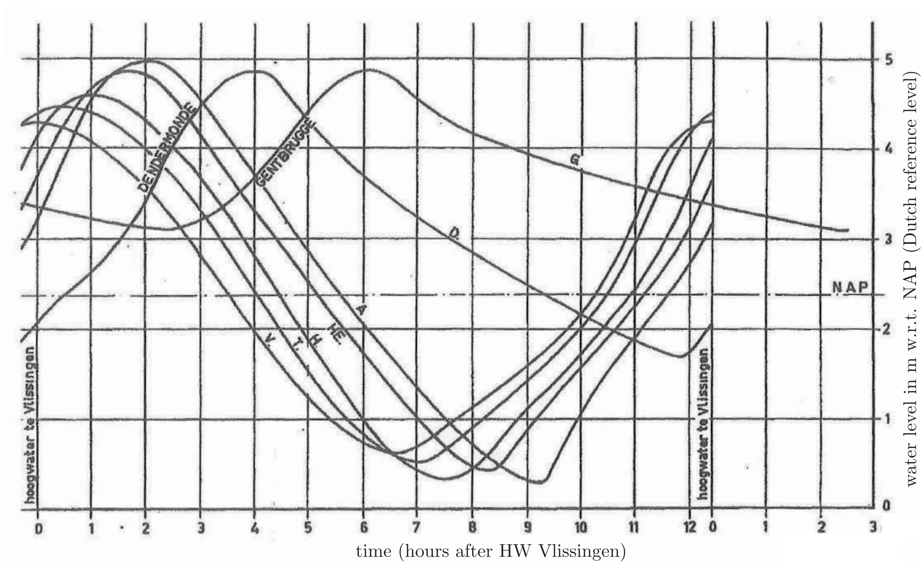

Figure 8.8: Tidal wave propagation in the Western Scheldt, The Netherlands

Bibliography

[1] H. A. Lorentz. Verslag Staatscommissie Zuiderzee. Technical report, 1926. in Dutch.

Problems

1. Mention two effects of resistance on the relation between variations in the discharge and in the surface elevation.

2. An M_2-tide in a channel with a width of the free surface B of 500 m has a damping modulus $\mu = 2 \times 10^{-5}$ /m and a wave number $k = 1.5\mu$. The integration constants are given as $C^+ = (1.2\text{ m})\exp(i\pi/6)$ and $C_- = (0.8\text{ m})\exp(-i\pi/4)$. Plot the values of these constants in the complex plane and construct the corresponding two hodographs of the + wave and of the - wave for a self-chosen sequence of values of s. Construct the hodograph for the total surface elevation. Compare the angle of convergence with the theoretical value.

3. For the data in the preceding question, construct the hodographs for $\tilde{Q}^+$, for $\tilde{Q}^-$, as well as for the total discharge $\tilde{Q} = \tilde{Q}^+ + \tilde{Q}^-$.

4. Using the data listed above Table 8.1, calculate the values of the dependent variables in the left column.

5. Calculate the wave number and the damping modulus for propagation in the channel of Question 17 in Chapter 7. (Answer: $k = 2.51 \times 10^{-5}$ rad/m, $\mu = 1.97 \times 10^{-5}$ /m.)

6. Using this result, verify whether the rigid-column approximation is justified for this case. (Answer: $\cos k\ell = 0.97$, close enough to 1, so that it is justified.)

7. Suppose that this channel is closed at one end and that the M_2-tide at the mouth has a surface elevation amplitude of 1 m. Calculate the surface elevation amplitude at the closed end, estimate it from Figure 8.5 and compare the results. Calculate the value the amplitude of the discharge at the mouth. (Answer: $\hat{\zeta}_\ell \simeq \hat{\zeta}_0 = 1$ m and $\hat{Q} = 843\text{ m}^3/\text{s}$.)

8. Do the same for a seiche with a period of 45 minutes and a surface elevation amplitude at the mouth of 0.3 m. (Answer: $\hat{\zeta}_\ell = 0.36$ m and $\hat{Q} = 00\text{ m}^3/\text{s}$.)

9. The Bay of Fundy, where the world's highest tides occur, has a length of about 270 km. The width does not vary too much, in contrast to the depth, but we will ignore the latter variations for this assignment and put the depth at a constant value of 75 m. We take $c_f = 0.0025$. If the M_2-tide at the mouth has a tidal range (HW - LW) of 5 m, estimate the

tidal range at the closed end, using Figure 8.4. (Answer: appr. 18 m).

10. Using Figure 8.4, estimate the amplification factor for a seiche with a period of 20 minutes in a semi-closed harbour basin with a length of 3 km and a depth of 15 m; the surface elevation amplitude at the mouth is 0.25 m. (Answer: 3.7.) Check the influence of the offshore amplitude on the amplification factor for this case. Do the same for the preceding question and compare both sensitivities.

11. Mention two sources of nonlinearity of the long-wave equations.

12. Explain why a mean slope of the free surface occurs in a purely oscillatory tide (no net discharge).

Chapter 9

Flood waves in rivers

9.1 Introduction

Flood waves are in essence humps of water traveling downriver. Stated in more detail, they are temporary increases and decreases of discharge and water level ('stage') in a river caused by temporarily enlarged run-off in the catchment area due to heavy rainfall or snow melt, which travel downriver as a wave.

The temporal evolution and dynamics of flood waves differ greatly between the upper reaches and the lower reaches of a river.

In the upper reaches, characterized by relatively steep slopes and a small catchment area, the response to an increased run-off can be quite fast, with rapid variations in flow rate and water level, even to the extent that inhabitants along the river border are taken by surprise, sometimes with fatal consequences.

In contrast, flood waves in the lower river reaches are slow processes, in many cases taking place over several days, due to the larger catchment area, the existence of tributaries, and the greater propagation distance from upstream. Run-off peaks in different part of the larger catchment area do not in general occur simultaneously, so that the maxium of their sum is less than the sum of the individual maxima. Moreover, as we will see, the internal dynamics of the flood wave cause it to flatten and to elongate as it propagates. As a result, the variations in flow rate and water level in the lower reaches are gradual, even such that inertia is insignificant (see Table 3.1).

Let us take the lower reaches of the river Rhine for a comparison of the order of magnitude of the inertia in the momentum balance ($\partial U/\partial t$) to the downslope gravity force per unit mass (or the acceleration), $g\,\partial h/\partial x$. A typical rate of rise or fall of the water level is 0.5 m/24 hrs (see Figure 3.6 or 9.1). The increase in flow velocity would be a few dm/s per 24 hrs, corresponding to an acceleration of about $2 * 10^{-6}$ m/s^2. This is roughly a factor 500 less than $g\,|\partial h/\partial x|$, if we equate the slope of the free surface to the bed slope, which for the lower Rhine is about 10^{-4}. The inertia being relatively small implies that the driving force due to the surface slope is approximately in equilibrium with the resistance.

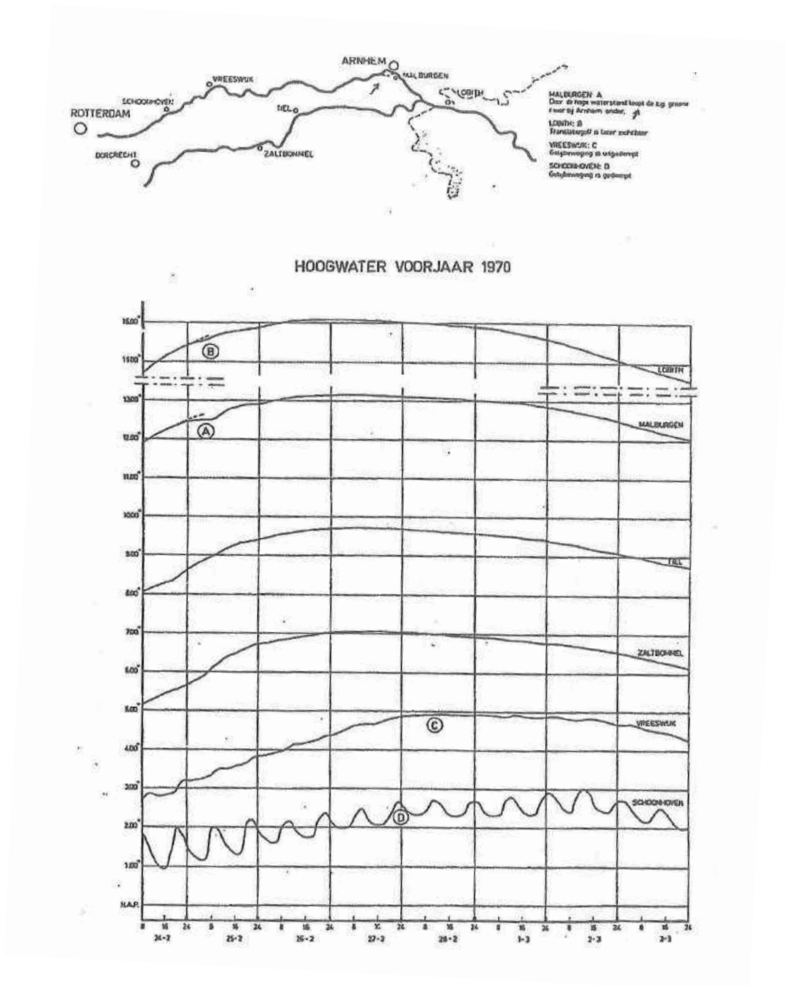

Figure 9.1: Recorded water levels during flood wave in the Rhine (February 26 - March 3, 1970)

In engineering practice, numerical models are used to simulate flood waves. These are based on the complete equations of De Saint-Venant (the long-wave equations, see Chapter 2), including inertia. This is needed in order to cover a wide range of occurrences of flood waves. Moreover, they should be able to cover the estuarine reaches of rivers, where tides penetrate, for which inertia and resistance are of comparable magnitude. Lastly, they should be able to simulate properly the effects of operation of weirs, which can induce rapidly varying translatory waves superimposed on the slowly varying flood waves.

The resistance-dominated flood wave is a new and final category in the progression of wave categories considered so far, ranging from the rapidly varying translatory waves, for which resistance could be neglected, via the intermediate category of tidal waves with their mixed character, to the present case of flood waves, in which resistance is dominant. In order to fully understand the special features of this new category, we will examine it in its most elementary form, in which inertia is neglected and we assume equilibrium between the driving force and the resistance. The remainder of this chapter is based on that assumption.

The neglect of inertia leads to the so-called **quasi-steady approximation**: although the flow is unsteady on a long time scale, the relations between dependent variables are at any time assumed to be the same as for steady flow. In other words, the flow is instantaneously adjusted to (slow) variations in the driving force. It has no memory, as it were.

From a mathematical point of view, the neglect of inertia has important consequences because it reduces the set of coupled balances of mass and momentum from being of second order in time to first order (though still second order in space). This implies that dynamic wave propagation in two directions is no longer possible.

9.2 Governing equations

We use the continuity equation in the form given by Equation (2.11):

$$B\frac{\partial h}{\partial t} + \frac{\partial Q}{\partial s} = 0 \tag{9.1}$$

In the momentum balance (Equation (2.12)), we neglect the inertia terms, in which case it reduces to

$$gA_c\frac{\partial h}{\partial s} + c_f\frac{Q^2}{A_cR} = 0 \tag{9.2}$$

We have replaced $|Q|Q$ by Q^2 because the flow is unidirectional. In a compact notation, Equation (9.2) can be written as

$$\frac{\partial h}{\partial s} + i_f = 0 \tag{9.3}$$

in which i_f is the so-called friction slope (see Chapter 2, Equation (2.16)), defined by

$$i_f \equiv c_f\frac{Q^2}{gA_c^2R} = c_f\frac{U^2}{gR} \tag{9.4}$$

Equations (9.2) and (9.3) are expressions of **equilibrium**: the resistance balances the driving force due to the slope of the free surface.

In previous chapters, dealing with translatory waves, tides etc., there was no preferred flow direction. The undisturbed reference state was one of rest. A bed slope, if present, played no particular role. This is quite different for river flow, where the reference state is one of uniform, downward flow. For that category, it is meaningful to bring the bed slope explicitly into account: $i_b \equiv -\partial z_b/\partial s$, in which z_b is the cross-sectionally averaged bed elevation above the reference plane $z = 0$. Writing d for the average depth in the conveyance cross-section, we have $h = z_b + d$ (see Figure 9.2). Substituting this in Equation (9.2) gives

$$\frac{\partial d}{\partial s} - i_b + c_f\frac{Q^2}{g{A_c}^2R} = 0 \tag{9.5}$$

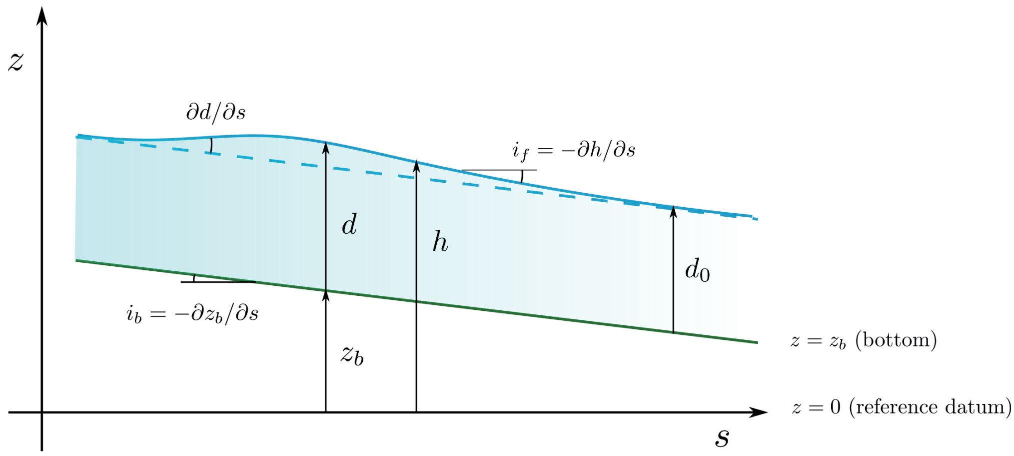

Figure 9.2: Longitudinal profile flood wave

or

$$\frac{\partial d}{\partial s} = i_b - i_f \tag{9.6}$$

This is the so-called **Bélanger equation** for backwater curves (see Chapter 2, Equation (2.17)), if in the latter equation we neglect the term Fr^2, which is consistent with our present neglect of inertia.

Equation (9.5) forms the basis of the analyses in the remainder of this chapter, using approximations of increasing complexity.

9.3 Quasi-uniform approximation

We assume an initial state of uniform flow which is gradually being disturbed by a flood wave.

In **uniform flow**, the free-surface slope and the friction slope both equal the bed slope, and the depth gradient $\partial d/\partial s$ is zero, in which case the discharge and the flow velocity are given by

$$Q = Q_u \equiv A_c\sqrt{\frac{gRi_b}{c_f}} \qquad \text{and} \qquad U = U_u \equiv \frac{Q_u}{A_c} = \sqrt{\frac{gRi_b}{c_f}} \tag{9.7}$$

These equations express two messages: they *define* Q_u and U_u, and they state that in uniform flow the actual discharge Q and flow velocity U equal Q_u and U_u, respectively. The latter does not hold in nonuniform flow, but in that case Q_u and U_u are still given by the expressions in the respective right-hand sides of Equation (9.7).

The occurrence of a flood wave implies **nonuniform flow**, in which the depth gradient is nonzero. The surface slope deviates from its uniform-flow value, which equals the bed slope i_b. However, if the flood wave is sufficiently low and/or elongated, the difference between the two slopes is small. We will initially neglect it. This is a so-called **quasi-uniform approximation**, so named because the flow, though varying in space on a large scale, is treated as if it were uniform as far as the relations between local variables are concerned.

Formulation and general solution

In the quasi-uniform approximation, the value of the discharge is taken to be the value in uniform flow, or $Q = Q_u$ as defined in Eq. (9.7). This is an algebraic equation, describing the dependence of the discharge on the instantaneous values of the local geometric profile variables A_c and R (not their derivatives!).

These (and other) geometric profile variables are monotonic, unique functions of the flow depth d. Therefore, we can consider Equation (9.7) as an implicit relation between the uniform-flow discharge Q_u and the depth d, which is written as $Q_u = Q_u\,(d\,(s,t))$. (The dependence on g, i_b and c_f given in Equation (9.7) is not written explicitly.) Substitution of $Q = Q_u$ and of $Q_u = Q_u\,(d\,(s,t))$ in Equation (9.1), in which we replace $\partial h/\partial t$ by $\partial d/\partial t$ (which is allowed since $h = z_b + d$ and $\partial z_b/\partial t = 0$), yields

$$\frac{\partial d}{\partial t} + \frac{1}{B}\frac{\mathrm{d}Q_u}{\mathrm{d}d}\frac{\partial d}{\partial s} = 0 \tag{9.8}$$

The left-hand side of this equation has the structure of a total derivative of d for an observer moving with a velocity $\mathrm{d}s/\mathrm{d}t = (1/\mathrm{B})\mathrm{d}Q_u/\mathrm{d}d$, and the equation states that an observer moving at this speed sees no change in the local value of d (see Section 4.4 for an introduction of the total derivative). Neither would this observer see changes in the other local geometric variables such as R, A_c or A, nor in the discharge Q (within the quasi-uniform flow approximation $Q = Q_u$). This can be expressed mathematically as follows:

$$\boxed{\frac{\mathrm{d}d}{\mathrm{d}t} = 0, \quad \frac{\mathrm{d}Q}{\mathrm{d}t} = 0 \qquad \text{provided} \qquad \frac{\mathrm{d}s}{\mathrm{d}t} = \frac{1}{B}\frac{\mathrm{d}Q_u}{\mathrm{d}d}} \tag{9.9}$$

It follows from these relations that the specified value of $\mathrm{d}s/\mathrm{d}t$ is the speed of propagation of the flood wave. Denoting this as c_{HW} (HW for High Water), we have:

$$c_{HW} \equiv \frac{1}{B}\frac{\mathrm{d}Q_u}{\mathrm{d}d} \tag{9.10}$$

It is noted that in finite-difference form, Equation (9.10) can be written as $\delta Q = Bc_{HW}\,\delta h$, the same as was found for translatory waves (Equation (4.20), except for the difference in propagation speed.

We see that flood waves can only propagate downstream (at a low speed, as we will see), as a consequence of the neglect of inertia in the momentum balance. For the latter reason, flood waves are said to belong to the category of **kinematic waves**, as distinct from the dynamic waves considered in preceding chapters, which - thanks to inertia - can travel both downstream and upstream.

The high-water wave speed

In order to obtain a more transparent, explicit expression for c_{HW}, we substitute $A_c = B_c d$ in Equation (9.7), as well as the approximation $R = d$, with the result

$$Q_u = B_c\, d \sqrt{\frac{g d i_b}{c_f}} \tag{9.11}$$

so that

$$\frac{\mathrm{d}Q_u}{\mathrm{d}d} = \frac{3}{2} B_c \sqrt{\frac{g d i_b}{c_f}} = \frac{3}{2} B_c U \tag{9.12}$$

With this, we find the following important expression for the propagation speed of the flood wave:

$$\boxed{c_{HW} = \frac{1}{B}\frac{\mathrm{d}Q_u}{\mathrm{d}d} = \frac{3}{2}\frac{B_c}{B} U} \tag{9.13}$$

We see that this speed is of the order of magnitude of the flow velocity. In the lower river reaches, where the Froude number usually is much less than 1, the flow velocity U is much less than the classical long-wave speed of $\sqrt{gd}$, and so is c_{HW}. For $B_c/B < 2/3$, c_{HW} is even less than the flow velocity! When at a high river stage the flood plains are submerged, B can be much larger than B_c, which causes the propagation speed of the flood wave to become considerably less than the flow velocity in the main (conveyance) channel.

For inertia-dominated waves in a channel, the wave speed is also affected by the ratio B_c/B, but to a smaller extent. This can be seen from the expression for that speed, viz. $c = \sqrt{gA_c/B}$ (Equation (4.10)). This can be written as $c = \sqrt{B_c/B}\,\sqrt{gd}$. We see that for a given depth the wave speed is here proportional to the square root of B_c/B, i.e. a lower sensitivity than it is for resistance-dominated flood waves.

A note on the relation between the bed friction formulation and c_{HW}
In the above, we have treated c_f as a constant, independent of the depth, in which case U varies in proportion to the square root of the depth (see Equation (9.7)). Had we used a Strickler- or Manning-type of resistane law, U would vary with the 2/3-power of the depth, and the discharge with the 5/3 power, in which case the coefficient 3/2 in Equation (9.13) would have to be replaced by 5/3.

Kinematic wave behavior

According to the preceding results, it is possible for an observer to follow a point of constant depth or discharge, provided he/she travels at the appropriate speed. This also applies to the point with the highest surface elevation, or river stage, which implies that this maximum remains constant: the flood wave does not diminish in height according to this simple model. Nor does the flood wave lengthen in this model, since two points with equal depth, one upstream of the maximum stage, the other downstream, would travel at the same speed.

The fact that the propagation speed increases with depth (through its proportionality to

U) causes deformation of the wave, since points of larger depth travel faster than points of smaller depth. It follows that the leading part of the flood wave steepens (and the trailing part flattens). If this continues for a sufficient time and distance, the assumption that the change in surface slope is negligible compared to the slope in uniform flow, i.e. the bed slope, becomes untenable. In the following section we will consider the effect of this variation in slope, first qualitatively and thereafter quantified in an extended mathematical model.

9.4 Influence of variable free-surface slope

In the preceding section, the variations in the slope of the free surface, which accompany the passage of a flood wave, were ignored. Actually, the slope varies, being larger than the slope in uniform flow (i_b) in the leading part of a flood wave, i.e. at rising river stage in a fixed point, whereas it is less than i_b in the trailing part, i.e. at falling river stage. Therefore, at a given stage, the discharge is greater when the surface elevation rises than when it falls. This is a manifestation of the phenomenon of **hysteresis**.

The hysteresis is illustrated with a rating curve in Figure 9.3, i.e. a plot of the discharge vs the simultaneously occurring river stage at the same location as a function of time during the passage of a flood wave. It can be seen that the maximum discharge occurs ahead of the maximum stage. This is because the enhanced slope of the free surface ahead of the cross-section of maximum stage enhances the flow rate, which more than compensates for the larger depth at maximum stage, which must do with a smaller slope, viz. i_b.

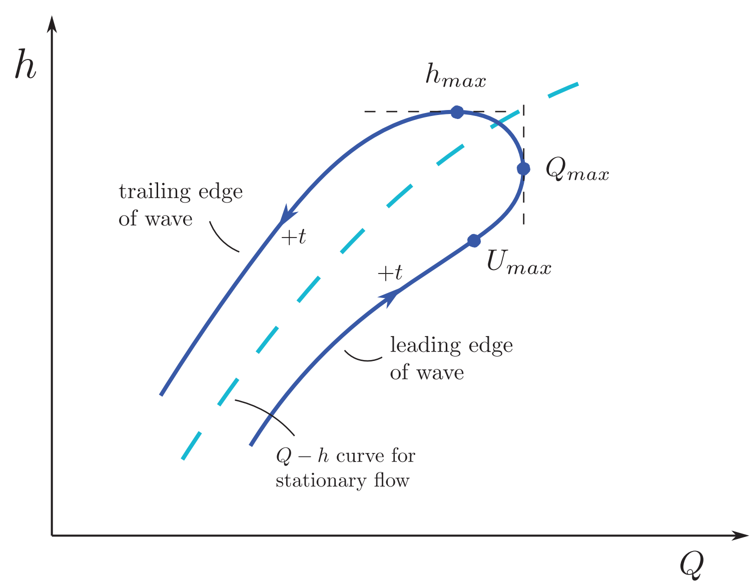

Figure 9.3: Example $Q - h$ curve with hysteresis

The occurrence of hysteresis in a flood wave has important consequences for the evolution of the wave as it travels downriver. As noted above, the discharge is greater ahead of the peak than it is following the peak, if we compare two cross-sections with the same stage. Considering a (moving) control volume between two such sections, we see that mass is flowing out of it at the downstream section at a higher rate than it is flowing into it at the upstream section. In other words, the mass contained between those two cross-sections on either side of the top of the flood wave decreases in time. As a result, the surface elevations between these moving cross-sections decrease as the wave propagates downriver. This means that **the flood wave decreases in height and** (consequently) **increases in length as it propagates downriver.**

Diffusion model for flood waves

In order to model this phenomenon mathematically, we start with Equation (9.5), recasting it into an expression for the discharge:

$$Q = A_c \sqrt{\frac{gR}{c_f}} \sqrt{i_b - \frac{\partial d}{\partial s}} = Q_u \sqrt{1 - \frac{1}{i_b}\frac{\partial d}{\partial s}} \tag{9.14}$$

We have substituted the expression for Q_u, i.e. the discharge for the given depth if the flow were uniform, given by Equation (9.7).

We take account of a variable surface slope on the assumptioin that it deviates by a relatively small amount from the uniform-flow value, i.e. the bed slope i_b. This implies that the depth gradient, though nonzero, is small compared to the bed slope ($|\partial d/\partial s| \ll i_b$). This allows us to approximate the square root as in $\sqrt{1-\epsilon} \simeq 1 - \epsilon/2$ if $\epsilon \ll 1$. Using this approximation, we obtain

$$Q = Q_u \left(1 - \frac{1}{2i_b}\frac{\partial d}{\partial s}\right) \tag{9.15}$$

With this approximation, we have obtained a linearized expression for the effect of the variable free-surface slope on the discharge, with a correction to $Q = Q_u$ which is proportional to the depth gradient $\partial d/\partial s$. Considering the depth of flow as a measure of volume 'concentration', i.e. volume per unit horizontal area, we can say that the correction to the volume transport is proportional to the gradient of the volume concentration. This is typical for **diffusive transport**.

A note on diffusive transport

The classical example of diffusion is heat transport in a continuous medium, which in good approximation is proportional to the gradient of the temperature, the latter being a measure of the heat concentration. Such transport takes place in the direction of decreasing temperature. Differences in temperature are gradually being smeared out as time goes on. That is typical for diffusion. A similar process applies in the case of flood waves, although the physical mechanism behind it is drastically different.

Our next task is to express the effect of diffusion on the flow depth mathematically. In view of the volume balance, Equation (9.1), we need the derivative of Q with respect to s, to be determined from Equation (9.15):

$$\frac{\partial Q}{\partial s} = \frac{\partial Q_u}{\partial s}\left(1 - \frac{1}{2i_b}\frac{\partial d}{\partial s}\right) - \frac{Q_u}{2i_b}\frac{\partial^2 d}{\partial s^2} \tag{9.16}$$

We neglect the small, second term between parentheses, which is consistent with the approximation already made in the transformation of Equation (9.14) into Equation (9.15). Furthermore, since Q_u can be considered a function of d, we can replace $\partial Q_u/\partial s$ by a factor proportional to $\partial d/\partial s$:

$$\frac{\partial Q_u}{\partial s} = \frac{\mathrm{d}Q_u}{\mathrm{d}d}\frac{\partial d}{\partial s} - \frac{Q_u}{2i_b}\frac{\partial^2 d}{\partial s^2} \tag{9.17}$$

Dividing the result by B, in anticipation of the insertion into the volume balance, we obtain

$$\frac{1}{B}\frac{\partial Q}{\partial s} = \frac{1}{B}\frac{\mathrm{d}Q_u}{\mathrm{d}d}\frac{\partial d}{\partial s} - \frac{Q_u}{2i_b B}\frac{\partial^2 d}{\partial s^2} \tag{9.18}$$

The factor multiplying the first-order depth derivative in the right-hand side can be recognised as the propagation speed, c_{HW} (see Equation (9.13)). The factor multiplying the second-order depth derivative is called the **diffusivity**, to be denoted as K:

$$K \equiv \frac{Q_u}{2i_b B} \tag{9.19}$$

Finally, substitution of these results in the volume balance, Eq. (9.1), in which we again replace $\partial h/\partial t$ by $\partial d/\partial t$, yields the following PDE for the flow depth d:

$$\boxed{\frac{\partial d}{\partial t} + c_{HW}\frac{\partial d}{\partial s} - K\frac{\partial^2 d}{\partial s^2} = 0} \tag{9.20}$$

This equation has the classical structure of the so-called (one-dimensional) **advection-diffusion equation**, a standard equation in mathematical physics. The first two terms represent the displacement (advection) of the longitudinal surface profile, with velocity c_{HW}, as in the quasi-uniform approximation. The third term adds the effect of diffusion. It is proportional to $\partial^2 d/\partial s^2$, i.e. the curvature of the free surface, which results in a spatial smoothing of the profile, elongating and flattening the flood wave as time progresses. This can be seen as follows.

Consider a control volume between two cross-sections in a reach where the free surface is concave (hollow) upwards. In that case, the discharge at the most upstream cross-section (inflow) is larger than it is at the downstream cross-section (outflow), causing a net inflow into this control volume and therefore a rise of the free surface.

Where the free surface is convex upward, i.e. concave downward, the opposite occurs, with net outflow and a lowering of the free surface as a result. The overall effect is that bumps are lowered and troughs are filled. In other words, the effect is to smoothen the longitudinal profile of the free surface.

Elementary solution

Solutions of the one-dimensional advection-diffusion equation have been derived in the classical literature for a range of initial and boundary conditions. Without derivation, we present just one of them here, for the case of the spreading of an initially concentrated mass in an infinitely long river reach. (The analogous case for heat diffusion would be the spreading of heat in a long conducting rod following a localized initial heating.)

The advection-diffusion equation is of first order in time and of second order in space. Therefore, one initial condition and two boundary conditions are required for a well-posed problem. We choose the following conditions:

Initial condition: Consider an initially uniform flow with depth d = constant = d_0 and flow velocity $U = U_0$, to which at time $t = 0$ a volume V is added abruptly, concentrated at the point $s = 0$. Note: addition of a volume V means addition of a volume per unit width equal to V/B. This has the meaning of an area in the longitudinal profile of the surface elevation.

Boundary conditions: For $s \to \pm\infty$, $d = d_0$ at all times.

For simplicity, we treat c_{HW} and K as given constants, equal to their initial values. That is acceptable to obtain an impression of the effects of the diffusion term.

The general solution of Equation (9.20) with the above stated initial- and boundary conditions is given by:

$$d(s,t) = d_0 + \frac{V/B}{\sqrt{2\pi}\,\sigma_s(t)}\ \exp\left(-\frac{(s - c_{HW}t)^2}{2{\sigma_s}^2(t)}\right) \tag{9.21}$$

in which

$$\sigma_s(t) = \sqrt{2K_0 t} \qquad \text{and} \qquad K_0 = \frac{Q_0}{2i_b B} = \frac{U_0 d_0}{2i_b}\,\frac{B_c}{B} \tag{9.22}$$

It can be shown through back substitution that these expressions satisfy Equation (9.20) as well as the initial- and boundary conditions. For a mathematical derivation and discussion see for instance Strauss [3].

The solution has been plotted for two instances $t = t_1$ and $t = t_2 = 4t_1$ in Figure 9.4. We note the following features of Equation (9.21), also shown in the Figure:

1. The first term in the right-hand side of Equation (9.21) is the undisturbed depth, the second term represents the flood wave. At any instant $t > 0$, the longitudinal profile of the flood wave is the classical bell-shaped Gauss curve, with total area V/B and 'standard deviation' (here: the distance from the location of the maximum to the locations of the inflection points) σ_s as specified in Equation (9.22).

2. σ_s increases in time proportional to $\sqrt{t}$: the wave elongates. At $t = t_2 = 4t_1$, we have $\sigma_s(t_2) = 2\sigma_s(t_1)$, so the 'length' of the wave is doubled compared to the situation at $t = t_1$.

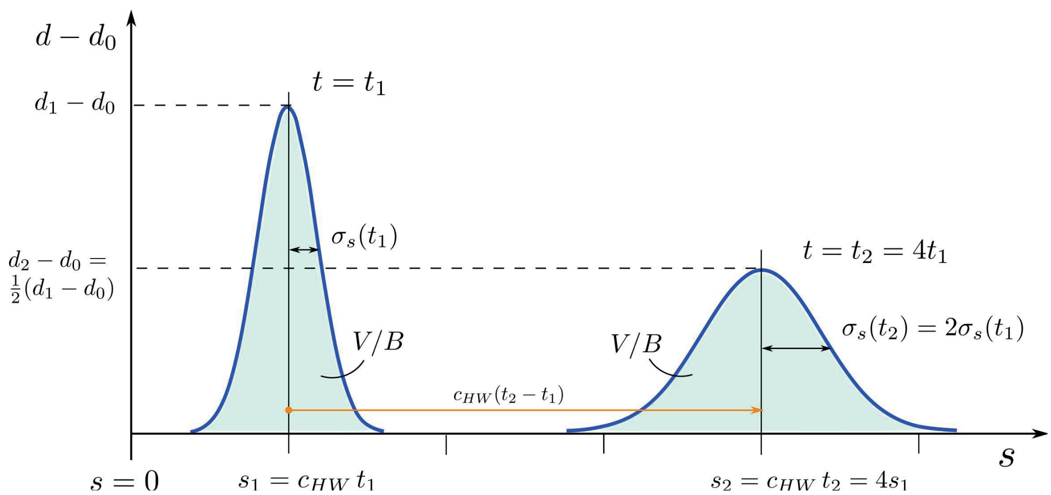

Figure 9.4: Elementary solution of the advection-diffusion equation

3. At an instant $t = t_0$, say, the spatially maximal depth occurs where $\partial d(s, t_0)/\partial s = 0$, i.e. at $s = c_{HW} t_0$, where the exp-function has its maximum value of unity. This shows that c_{HW} is the speed with which this maximum travels downriver.

4. The value of this spatial maximum decreases in time proportional to $1/\sigma_s$, or proportional to $1/\sqrt{t}$: the wave becomes lower. At $t = t_2 = 4t_1$, its maximum height is halved, compared to the situation at $t = t_1$. Note that the product of the height and the 'length' of the flood wave is constant.

5. At a fixed point $s = s_0$, say, the depth (or river stage) does not vary in time according to a Gauss curve. This is because the wave becomes lower and longer as it passes the point considered, so that the rising branch corresponds to a smaller value of σ_s than the falling branch. Therefore, the rise occurs faster than the fall.

6. The spatially maximal depth passes the fixed location $s = s_0$ at time $t = s_0/c_{HW}$, but since it is continually falling, it is preceded by higher values. This implies that the temporal maximum depth occurring at s_0 occurs earlier than this, and has a larger value than the spatial maximum at time $t = s_0/c_{HW}$ (this can be verified by solving for t from $\partial d(s_0, t)/\partial t = 0$).

Example

Figure 9.5 shows a number of plots of river stage versus time, measured in the river Rhine and one of its branches in The Netherlands (the Waal), following the bombardment in World War II (May 1943) by the RAF of some hydropower dams in the river Möhne in Germany (with the aim to harm German capacity of electricity production, needed in the war industry, see Brickhill [1]). As a result of this bombardment, dams failed and an amount of water of about 110 x 10^6 m^3 flowed from the Möhne into the Rhine in a short time, approximating the problem and its solution outlined above for some time after $t = 0$. (Natural flood waves usually are spread much more in time, with an irregular time variation, and therefore lend themselves not well for a direct comparison with the pulse-problem and its solution given above.)

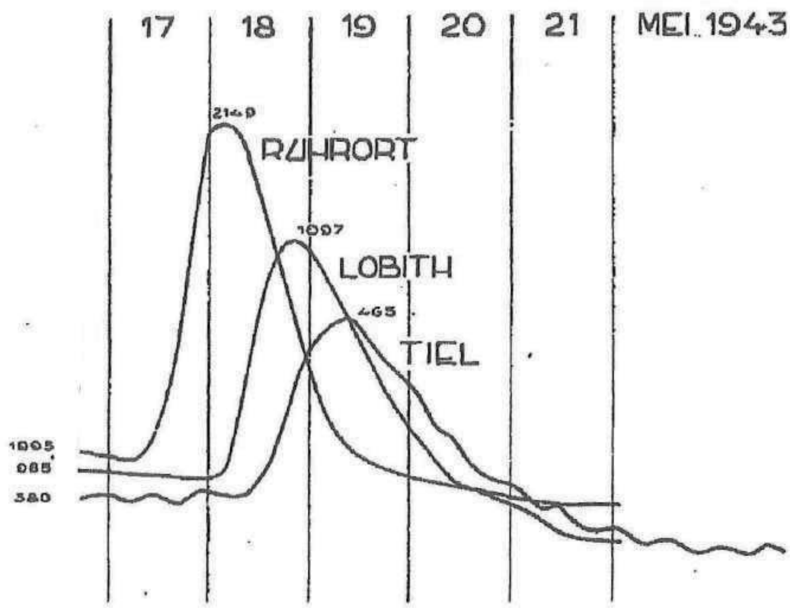

Figure 9.5: Water level recordings in the Rhine/Waal river following the collapse of the Möhne dam, source: Wemelsfelder [4]

The downstream progression of the flood wave, the lowering of the peak height and the asymmetry between the rising branch and the falling branch are clearly present in the measured data. The propagation speed determined from the observations varied somewhat per river section, but in all cases it was of the order of 1 m/s, in fact somewhat less than the flow velocity, due to the presence of groins. As a result, the debris, which resulted from the damage caused in the Möhne valley by the raging flood waters, and floating downstream with the main current, arrived in The Netherlands ahead of the high water! In fact, these observations led to the inception of the diffusive-wave model by Schönfeld [2].

9.5 Discussion

The analytical model described above is meant mainly to provide insight in the special features of the resistance-dominated flood waves in rivers, not so much as a tool for practical applications. We mention in particular the following aspects:

- the relatively low propagation speed (of the order of the flow velocity);

- the important influence of the ratio of storage width to conveyance width on the propagation speed (more than it is for inertia-dominated waves);
- decrease of the flood wave height and increase of the flood wave length during the propagation;
- the occurrence of hysteresis in the relation between the local discharge and surface elevation, i.e. for the same river stage a greater discharge when the water rises than when it falls;
- at a fixed location, the maximum discharge occurs ahead of the maximum surface elevation;
- asymmetry in the local variation of the river stage with time, the rising branche being steeper and (therefore) of shorter duration than the falling branche.

The classical flood wave model described above allows wave propagation in the downstream direction only, at a low speed, of the order of magnitude of the flow velocity. These are so-called kinematic waves.

The theory for kinematic flood waves rests on the assumption that the inertia is negligible compared to the resistance, but its predictions are partly in conflict with this assumption. Take the case of the pulse-type addition of a volume of water at one particular cross-section. The theory predicts a response in the form of a family of Gauss curves spreading in time. This implies an infinitely fast spreading of the wave (the tails of the Gauss curves), which in turn implies large accelerations, in conflict with the basic assumption that these would be negligible.

A more complete theory, in which inertia is not neglected, has positive and negative characteristics, corresponding to so-called dynamic waves which can travel both downstream and upstream (assuming subcritical flow) at the speed $U \pm \sqrt{gA_c/B}$. In case of a flood wave, these dynamic waves manifest themselves as a leading edge and a trailing edge. However, the mass associated with these is very small, in practice insignificant. The bulk of the water mass flows downstream with the much lower speed derived for the kinematic flood wave. Yet the dynamic waves cannot be ignored in numerical models because their speed is the speed at which information travels; numerical models should be able to deal with that.

Bibliography

[1] P. Brickhill. **The dam busters**. Evans Bros., London, 1951.

[2] J. C. Schönfeld. Voortplanting en verzwakking van hoogwatergolven op een rivier. **De Ingenieur**, 4:B1–B17, 1948. in Dutch.

[3] W. A. Strauss. **Partial differential equations**. John Wiley & Sons, Inc., 1992.

[4] P. Wemelsfelder. Hoogwatergolf doorbraak möhnetalsperre. **De Ingenieur**, 42:B103–B105, 1947. in Dutch.

Problems

1. What is the difference between the theories for so-called dynamic waves and kinematic waves?

2. What is the principal difference in the behaviour of these two categories of waves?

3. What is the so-called quasi-steady approximation?

4. What is the so-called quasi-uniform approximation?

5. Choose a few characteristic instants in the river stage records in Figure 3.4 or 9.1 and estimate the associated values of h and of $\partial h/\partial t$.

6. Estimate for these instances the value of the acceleration and verify the validity of the quasi-steady approximation, assuming uniform flow and a bed slope of $1/10^4$.

7. Verify for these instances the validity of the quasi-uniform flow approximation.

8. Prove that in the uniform-flow approximation the height and the length of the flood wave are constant as it propagates downstream.

9. Prove that in the uniform-flow approximation the flood wave deforms as it propagates downstream.

10. Explain why theoretically the crest of a flood wave decreases in height during propagation when the quasi-uniform flow approximation is not made.

11. What is the so-called hysteresis in flood waves? Explain why it occurs.

12. The propagation speed of a flood wave can be less than the flow velocity. What is the condition for this to happen?

13. Because of the failure of a dam, a volume of 10^6 m^3 of water is suddenly released in a river, at $t = 0$ in $s = 0$, say. Initially, the flow is uniform; the bed slope is $i_b = 1.5 \times 10^{-4}$, $c_f = 0.005, d = 3$ m, $B_c = B = 50$ m. Calculate:

- The value of the diffusivity K (using the initial values of the flow parameters). (Answer: $K = 8.9 \times 10^3$ m^2/s)
- The maximum height of the resulting flood wave at $t = 5$ hrs, and the location s_{max} where this occurs. (Answer: maximum height is 0.45 m, $s_{max} \simeq 25$ km)
- Explain why the maximum height of question (b) is less than the maximum height occurring in $s = s_{max}$ during the passage of the flood wave, and verify this with calculations for a few chosen instants near the time t = 5 hrs.